DEVELOPMENT AND PERFORMANCE ANALYSIS FOR PROCESS OPTIMIZATION OF PEDAL OPERATED CHAROLI NUT DESHELLER

A Thesis

Submitted for the award of the degree of

DOCTOR OF PHILOSOPHY

in

Mechanical Engineering

By

SHELARE SAGAR DNYANESHWAR

Registration no. 41700261

<table>
<tr><td>Supervised By</td><td>Co-Supervised by</td></tr>
<tr><td>Dr. Ravinder Kumar</td><td>Dr. Pravin B. Khope</td></tr>
</table>

LOVELY PROFESSIONAL UNIVERSITY
PUNJAB
2022

CANDIDATE'S DECLARATION

I hereby certify that the work which is being presented in this thesis, entitled **"DEVELOPMENT AND PERFORMANCE ANALYSIS FOR PROCESS OPTIMIZATION OF PEDAL OPERATED CHAROLI NUT DESHELLER"** for the fulfilment of the requirements for the award of the Degree of Doctor of Philosophy and submitted in the Department of Mechanical Engineering of Lovely Professional University, Punjab, India is an authentic record of my own work carried out under the supervision of Dr. Ravinder Kumar, Associate Professor, Department of Mechanical Engineering, Lovely Professional University, Punjab, India and Dr. Pravin B. Khope, Department of Mechanical Engineering, Priyadarshini College of Engineering, Nagpur, Maharashtra, India. The thesis is a unique piece of study that incorporates my results.

This thesis has not been submitted in part or in full for the granting of any other degree/diploma from this or any other Institute/University.

Date: 18/06/2022   **Mr. Shelare Sagar Dnyaneshwar.**

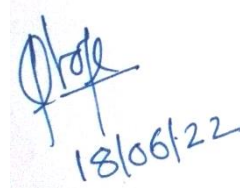Lovely Professional University,
Punjab.
(Regn. No. 41700261)

CERTIFICATE

This is to certify that the thesis entitled **"DEVELOPMENT AND PERFORMANCE ANALYSIS FOR PROCESS OPTIMIZATION OF PEDAL OPERATED CHAROLI NUT DESHELLER"**, being submitted by **Mr. Shelare Sagar Dnyaneshwar** (Reg. No. 41700261) to the Department of Mechanical, Lovely Professional University, Punjab, India for the award of Degree of 'Doctor of Philosophy' in Mechanical Engineering, is a bonafide research work carried out by him under my supervision and guidance. His thesis has reached the standard of fulfilling the requirements of regulations relating to degree.

The results presented have not been submitted in part or in full to any other University/Institute for the award of any other degree or diploma.

	Prof 18/06/22
Dr. Ravinder Kumar.	**Dr. Pravin B. Khope.**
Associate Professor,	Assistant Professor,
Mechanical Engineering Department,	Mechanical Engineering Department,
Lovely Professional University, Punjab, India	Priyadarshini College of Engineering, Nagpur, Maharashtra, India
Date:18/06/2022	Date:18/06/2022

ABSTRACT

Charoli (Buchanania lanzan) is an important multifunctional tree and plant for tribal and rural economies. Charoli has a sustainable economic potential due to its nutritional and medicinal values. The charoli tree provides fuel, food, timber, fodder, and medicine to the rural and tribal communities. It is a medicinally valuable tropical tree species and an essential cause of living for the bounded tribal community. Practically all the parts of this plant are used for the therapy of numerous disorders. The Charoli kernel has a high amount of protein (19.0 – 28.19 %) which is exceptionally nutritious. The kernel yields sweet oil (33.50 %), of which 1.90 % is unsaponifiable. Charoli oil is healthy and fit for the consumption of humans. The delicate piece of Charoli nut is the kernel that could be influenced by deshelling, its removal from a shell is the critical most practice. Damaging the kernels in de-shelling process decreases the demand cost of nuts. Preserving the quality and decreasing the losses of this kind of items is an important subject and has pulled numerous researchers in the field. In traditional ways, this Charoli kernel removal is made manually by using hammer and hands due to which there is lower efficiency with damaged and broken kernels. Hence, there is a demand to create an indigenous and sustainable Charoli nut desheller for improvement in Charoli nut processing efficiency and reducing the wastage occurring due to kernel damage.

In the past, minimal research has been done on some physical properties of Charoli nut and the work was carried out on the samples from the specified local region. It is essential to expand knowledge of the Charoli nut properties globally to produce an effective, efficient, and safe machine for kernel extraction, therefore the physical properties of Charoli nut was evaluated form various states/districts of India like Maharashtra, Madhya Pradesh, Chhattisgarh, Jharkhand, and Gujarat. On the basis of this physical properties Charoli nut deshelling machine was developed and tested using Taguchi's method of experimentation. For experimentation various independent parameters like feed rate (ψ), moisture content percent (M_c), clearance (C_d) between grinding disk, thickness of the grinding disk (t) and rotational speed of the flywheel (V_f) of three levels have been considered. Impact of the combinations of this

independent parameters was evaluated to check the response interms of Deshelling efficiency (η_d), Whole kernel recovery (η_w), Broken kernels (η_b), Partially Shelled / Unshelled nuts (η_u), (Γ_r)- Resistive Torque, and (T_p)- Processing time. Analysis and validation of the experimental data was done using the Taguchi's method of experimentation. Further, experimental data was compared with the mathematical and ANN simulation model for the individual responses.

Formulated experimental, mathematical model, and ANN Simulation model for Deshelling efficiency (η_d), Whole kernel recovery (η_w), Broken kernels (η_b), Partially Shelled / Unshelled nuts (η_u), Resistive Torque (Γ_r), and Processing time (T_p) follow the same pattern and are extremely similar to each other. They match with each other at a few points, indicating their closeness. As a result, the results of the actual experimentation, the mathematical model developed, and the projected values of the ANN Simulation are validated for all the responses. Also, to verify the mathematical & ANN Simulation model's proximity to the real-world process, a percentage error have been computed for all variables. The percentage error between mathematical and ANN values all follow the same pattern and are approximately equally distributed. The percentage error of values obtained from experimentation & mathematical model and experimentation & ANN simulation is below 5 %, also the average RMS Error is below 5 %. This shows that the ANN model and the mathematical model are in good agreement with one another. Furthermore, the positive agreement between mathematical and ANN model results with the experimental results suggests that both of the formulated models are capable of predicting the deshelling efficiency parameters instead of doing the actual experimental work.

Taguchi analysis shows, for the maximization of deshelling efficiency, clearance (PC=40.87%), feed rate (PC=30.23%), and moisture content percent (PC=25.77%) are significantly affecting on the process both physically and statistically. Whereas in case of whole kernel recovery, rotational speed of the flywheel is highly significant with contribution of 60.29 %, followed by clearance, feed rate and moisture content percent with contribution of 16.05 %, 11.91 %, and 10.25 % respectively. For minimization of the broken kernels, rotational speed of the flywheel plays the key role. Rotational speed of the flywheel (PC=96.89 %) is highly affecting the broken

kernels followed by the clearance (PC=1.27 %), feed rate (PC=0.93 %) & moisture content percent (PC=0.76 %). In case of partially shelled / unshelled nuts, clearance with contribution of 86.97 %, and moisture content percent with contribution of 9.04 % are the significantly affecting phenomena both physically and statistically. For the processing time, feed rate (PC = 91.89 %), moisture content percent (PC = 5.15 %), and clearance (PC = 1.52 %) are significantly affecting on the process both physically and statistically. Also, it is noted that none of the input variable found significant or significantly affecting the resistive torque. This may be due to the extraneous variable like vibrations in the machines which have not considered as a variable for the study.

Effect of individual input parameters on the output parameters was also calculated. Feed rate contribution is found highly significant in processing time (91.89%) followed by deshelling efficiency (30.23%), whole kernel recovery (11.91%), and broken kernels (0.93%) whereas moisture content percent contribution is highly significant in deshelling efficiency (25.77 %), whole kernel recovery (10.25%), partially shelled / unshelled nuts (9.04%), processing time (5.15%) and broken kernels (0.76%). In case of clearance, its contribution is highest in partially shelled / unshelled nuts (86.97%) followed by deshelling efficiency (40.87%), whole kernel recovery (16.05%), broken kernels (1.27 %), and processing time (1.52 %). Rotational speed of the flywheel significantly affects the broken kernels (96.89%) and whole kernel recovery (60.29%). Thickness of the grinding disk is not found too much significant in the to any response in the process of Charoli nut deshelling.

For finding the optimum set of parameters and levels for maximization of deshelling efficiency, whole kernel recovery, and minimization of broken kernels, % of partially shelled/unshelled nuts, resistive torque, processing time, the MCDM technique TOPSIS was used. As per this method, recorded output is 84.00%, 65.50%, 18.50%, 16.00%, 96364.49 N-mm and 74 seconds for deshelling efficiency, whole kernel recovery, broken kernels, percentage of partially shelled/unshelled nuts, resistive torque and processing time respectively was optimum.

As a result, the current study has clearly reflects the interaction of numerous independent factors. Percentage error of estimate for the anticipated / calculated

values of the dependent parameters is considered to be significantly lower. This confirms genuineness to the developed ANN and mathematical models. The patterns for the performance of the models shown by graphs, effect assessment, and Taguchi analysis were discovered to be complimentary. These tendencies have been shown to be genuinely warranted by certain conceivable phenomena physics. The optimum set of variable values, economic acceptability, and cheap cost of manufacturing will facilitate rural and tribal persons in establishing small-scale industries.

ACKNOWLEDGEMENTS

Finally, my heartfelt gratitude is owed to my father, Mr. Dnyaneshwar V. Shelare, my late mother Mrs. Vatsala D. Shelare, my brother Ajay D. Shelare, my wife Trupti Shelare and to my loving son Siddhant Shelare for patience, love, motivation and encouragement during this course of Ph.D. I owe entire of my academic achievements to my parents and family members, who have been incredibly supportive of me during my educational career and also my entire life.

Date: 18/06/2022   **Mr. Shelare Sagar Dnyaneshwar.**

Lovely Professional University,
Punjab.
(Regn. No. 41700261)

CONTENTS

LIST OF TABLES

LIST OF FIGURES

Abbreviations

Symbols	Meaning

Latin symbols/Greek symbols

φ	Sphericity
ϱ_b	Bulk density
ϱ_t	True density
ε	Porosity
μ	Coefficients of static friction
θ_f	Angle of repose
θ_e	Dynamic or emptying angle of repose
η_d	Deshelling efficiency
η_w	Whole kernel recovery
η_b	Broken kernels
η_u	Partially shelled / unshelled nuts
Υ_r	Resistive torque
ψ	Feed rate

Abbreviations

AC	Alternating current
ANOVA	Analysis of variance
ANN	Artificial neural network
ASAE	American Society of Agricultural Engineers
C_d	Clearance
d.b.	Dry basis
D_a	Arithmetic mean diameter
D_g	Geometric mean diameter
DOE	Design of experiment
HPFM	Human-powered flywheel motor
HPTLC	High Performance Thin Layer Chromatography

Symbols	Meaning
L	Length
M	Mass of each nut (kg)
M_c	Moisture content
M_f	Final moisture content of the sample
M_i	Initial moisture content of the sample
M_{1000}	Thousand nut mass
OA	Orthogonal array
PC	Pecentage contribution
Q	Amount of distilled water added (gms)
RPM	Revolutions per minute
SA	Surface area
S/N ratios	Signal to noise ratio
T	Thickness
t	Thickness of the grinding disk
T_p	Processing time (1000 nuts)
V	Volume displaced (m^3)
V_f	Rotational speed of the flywheel
V_t	Terminal velocity
w.b.	Wet basis
W_i	Initial sample mass (gms)
W	Width

INTRODUCTION

Indian forests have a very rich biodiversity. The different species of animals and plants have been recognized. The main produce of the forest is wood, but the non-wood species are also identified for some minor forest products which have medicinal, nutritional, and industrial importance [1]. India is ranked sixth among the world's twelve mega biodiversity zones. Two of these are found in our nation. India already accounts for 7.8 percent of the world's documented species while having just 2.5 percent of the land area [2]. As far as the diversity of major groups of plants and microorganisms is concerned it is estimated that in India there are 6500 species of Algae, 850 of the Virus and Bacteria, 2021 of Lichens, 14,500 of Fungi, 1200 of Pteridophytes, 2850 of Bryophytes, 17,500 of Angiosperms and 48 of Gymnosperms are found [3]. Most of these plant resources are found in the forest distributed in different geographical regions of the country. This rich floral wealth has a very important role in maintaining food, health, and livelihood security for an increasing population. About 200 million people depend directly or indirectly on the forest for their food, health, and livelihood security [3].

Forest contributes in varying degrees, either directly or indirectly, to food production both for human and livestock populations. Conventional and considerable reliance on biodiversity resources for feed, firewood, lumber, and minor forest output has been a recognized lifestyle for India's rural people, representing a sizable proportion of the country's population [4]. These supplementary sources of forest food may be in the form of fodder and grazing for livestock and a variety of edible fruits, flowers, nuts, tubers, and rhizomes for a rural and tribal population which not only augment supplier but also provide income and employment and nourishment to the poor during food scarcity[5].

The forest ecosystem maintains a life support system to biotic components. Furthermore, our abundant floral resources, particularly forest resources, have a significant impact on the country's and its people's environmental/ecological security and well-being because nature and humankind are an inseparable parts of the life support system since the beginning of time[6]. There is little information on the

contribution of forest foods to the diet of forest dwellers. Similarly, too little is known about methods of preparing these foods and storage systems used when available in excess during the season [6], [7].

About seven species of genus Buchanania occur in India. These species are B. lanzan Spreng, B. arborescens Blume, B. angustifolia Roxb, B. lanciolata Wight, B. barberi Gamble, B. lacifolia Roxb and B. platyneura Kurz (Anonymous, 1980). Among these B. axillaries (syn. agustifolia) and B. lanzan are the only species which produce edible fruits. It is the most significant and extensively dispersed species in India. It is native to the Indian subcontinent and may be found in India, Burma, Nepal, and a few more nations [8].

Charoli has a place with the family Anacardiaceae and mostly seen at deciduous forests overall India [2]. It is a smaller to medium tree with a diameter of 1.5 meters and a height of up to 18 m. The bark is dark grey or black, consistently split into tiny rectangular plates, suggesting crocodile hide on the outside and reddish on the inside. The plant expands on yellow sandy-topsoil and is regularly located inside the western, northern, and central India, notably inside the forest zone of Andhra Pradesh(AP), Bihar(BR), Chhattisgarh(CG), Gujarat(GJ), Jharkhand(JH), Maharashtra(MS), Madhya Pradesh(MP), and Uttar Pradesh(UP) [2],[9]. Along with India, this plant is also observed globally, like in Burma and Nepal [10].

The Charoli fruits grown-up in four to five months and are manually harvested in the summer season, generally in the month of April / May. Fully matured Charoli fruits become blackish after storage. This blackish skin must be expelled prior to deshelling. For expelling, fruits are kept in water for a night and scrubbed within palms or by a jute sack. Again this is washed with fresh water to get cleaned nuts. These nuts are then dried in solar light and put away for further processing, i.e., deshelling [11]. Figure 1.1. shows the Charoli tree with Charoli flower and fruit and Figure 1.2 shows the Charoli fruit at ripening stage

Figure 1.1. Charoli flower and fruit

Figure 1.2. Charoli ripening stage

It is a medicinally valuable tropical tree species and a fundamental cause of living for the bounded tribal community[2]. Practically all the parts of this plant are used for the therapy of numerous disorders. The Charoli kernel has a high amount of protein (19.0 - 28.19 %) which is exceptionally nutritious. The kernel yields sweet oil (33.50 %), of which 1.90 % is unsaponifiable. The 20.00 % of linolenic acid is found in the

saponifiable part. Charoli oil is healthy and fit for the consumption of humans [12]. Figure 1.3. (a) shows the Freshly harvested Charoli Fruits, and figure 1.3 (b) shows the Charoli nuts after expelling the skin.

| (a) | (b) |

Figure 1.3. (a) Freshly harvested Charoli Fruits, (b) Charoli nuts after expelling the skin.

1.1. Economic significance

Fresh fruit is consumed fresh and has a nice, sweetened, sub-acid flavor. It is enjoyed by locals and sold at the bazaar. Charoli is mostly known due to expensive and costly kernels [13]. In India, charoli kernels have flavor like almond and are consumed roasted or raw. They are utilized as a dry fruit in desserts and culinary spice, kheer, and meaty korma. Charoli seeds are high in minerals and have anti-inflammatory effects [14]. Charoli contains natural antioxidants, phenolics, minerals and fatty acids. Its oil is helpful to cure skin disorders and to eliminate facial spots and imperfections. Charoli provides a living for a tribal community all over India. Their economy is built on it. The population of Charoli has declined significantly in both forest and non-forest regions [15] (Singh et al., 2002), and it is now approaching extinction. It has a great potential in employment generation, particularly for forest dwellers. An estimate tells that the total potential of Charoli in undivided Madhya Pradesh yields about 5000 tonnes per annum that can generate 8 lakh man-days of employment [16]. On the basis of the species' economic potential, the Planning Commission adopted the species for enterprise development for central India under the 12th five years plan. The nutritional assessment of Charoli [17] is presented in table 1.1.

4

Table 1.1. Nutritional content in Charoli (per single unit of Kernel)

Nutrition	Value
Fat	59 g
Mineral like calcium	279 mg
Niacin	1.5 g
Oil	34-47 %
Phosphorus	528 mg
Protein	63-72 %
Riboflavin	0.53 g
Starch	12.1 %
Vitamin C	5.0 g
Vitamin like Thiamene	0.69 mg

1.2. Uses of Charoli tree/seeds

The Charoli tree/seeds have its uses in desserts baking. They are a good resource for protein, sugar, starch, minerals, and vitamins. They produce sweeter oil that is utilized as a supplement for olive oil and almond oil [15]. The major uses of Charoli tree/seeds are shown in Figure 1.4.
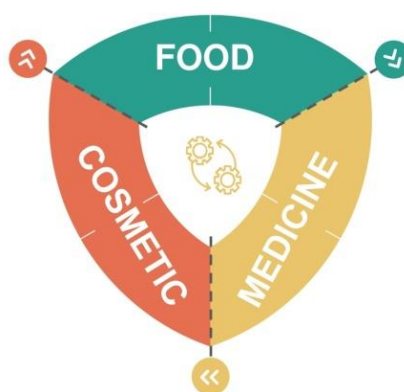
Figure 1.4. The major uses of Charoli tree/seeds

1.2.1 Food Charoli seeds are often used in Indian desserts (Charoli ka piyush, Barfi, kheer, shrikhand, and halwa), lamb pepper with Charoli, meaty kormas, Hyderabadi Haleem, Charoli mutton, Malai kofta, and as a flavoring for sauces and batters. Charoli seeds are nutritious and tasty and may be used as an alternative for almonds in

confectionery. The seeds are rich in lipid/fat, protein, starch/carbohydrate, fibre, minerals like iron, phosphorus, calcium, and vitamins like ascorbic acid/vitamin C, thiamine, niacin, riboflavin, and include fatty oil useful as an alternative for almond and olive oils [18].

1.2.2 Medicine All components of a tree, counting its fruits, bark, roots, nuts, leaves, and kernels, are used in Ayurvedic medicine to cure colds, intestinal problems, urinary incontinence, fever, and rheumatoid. Traditional treatment for diarrhea is the powdered roots and dried leaves combined with buttermilk as well as the gum derived from the bark of this tree [19]. In Andhra Pradesh traditional medicine, Charoli gum was combined with cow's milk to relieve rheumatic discomfort, and the leaves were used as a tonic to strengthen heart functions. The leaf powder was also used to promote faster wound healing. Externally, the oil is used to treat gland inflammations in the neck, both alone and in conjunction with several other natural oils [20]. Unani medicine uses the juice or decoction of Charoli leaves to detoxify the bloodstream, cure libido loss, infertility, and as a digestive tonic.

1.2.3 Cosmetic: Since ancient times, powdered seeds mixed with turmeric powder and milk have been used as a natural face pack in India to improve the skin's radiance, complexion, and suppleness. The oil produced by kernels is used for treatment of skin conditions and for geting rid of blemishes and spots on a face [21].

1.3. Various stages of Charoli nut processing
Kumar et al. (2012) [11] standardized the conventional process for preparing Charoli fruits and kernels. Its processing is broken down into three stages.

1.3.1. De-skinning: The collected nuts are steeped in water for a night. For large-scale processing, they are rubbed by a jute sack and palm. Decant the water containing fine skin. Nuts are washed in clean water to ensure that they are clean. The cleaned nuts are sun-dried about 2-3 days before being kept for deshelling.

1.3.2 Deshelling: This is the separation of the kernel from the husk. The dried nuts are rubbed with the help of a stone slab on an irregular surface of the stone for

smaller-scale processing. After that, the kernels are separated manually. On the other hand, high-scale deshelling is done using a parallel stone under a burr mill or runner. Abrasive forces and impact remove a rate coat of the kernel, causing it to fracture.

1.3.3 Grading: Grading is carried out to separate kernels from hulls and various diameters of kernels. A grader is used to sort the shelled or split kernels. Three oscillating screens of varying diameters are installed on the graders. The grader divides the fruit based on the size of its opening.

The systematic process of Charoli processing from the beginning is elaborated in figure 1.5.
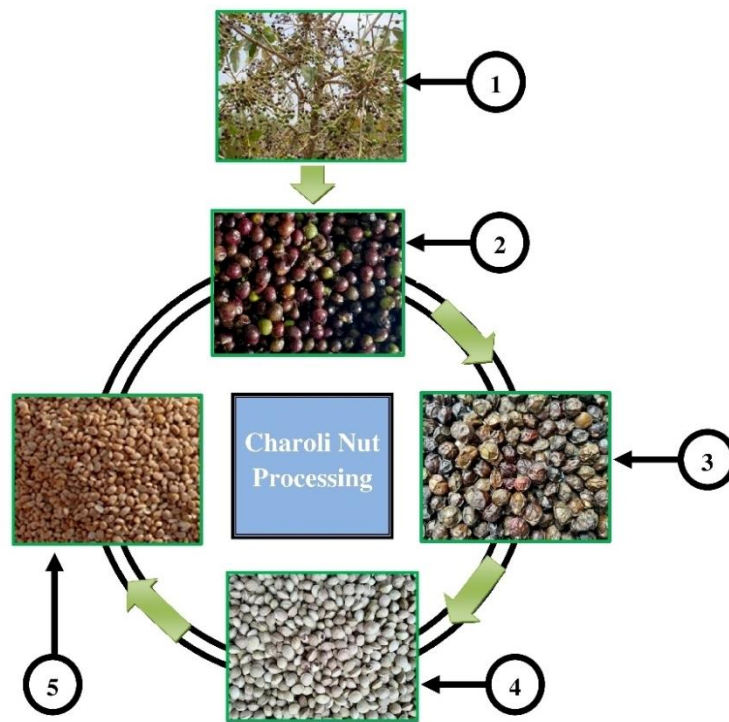
Figure 1.5. Systematic flow of Charoli Nut Processing

Note, 1: Full developed and matured Charoli fruits; 2: Freshly harvested Charoli fruit during month of April-May; 3: Charoli fruits after drying in Sun for 2-3 days; 4: Charoli nuts after soaking in water for one day then rubbed and then dried in Sun; and 5: Charoli kernels after deshelling ready to sell.

The delicate piece of Charoli nut is the kernel, which can be affected by deshelling. The procedure of removing it from the shells is the most crucial [11]. The selling price of nuts is reduced when the kernels are damaged during the de-shelling

process. Preserving the quality and decreasing the losses of this kind of item is an important subject and has drawn into numerous researchers in the field. In past research, there is limited literature reported regarding the physical, frictional, and aerodynamic properties of Charoli nut. Also, it is essential to expand knowledge of the Charoli nut properties to produce an effective, efficient, and safe machine for kernel extraction followed by separation and grading because these processes on Charoli nuts are still carried out manually in India [22].

In the past, minimal research has been done on some physical properties of Charoli nut and the work was carried out on the samples from the specified local region. The present research focused to contribute effectively in improvising the economic status and development of forest tribal communities in India whose livelihood depends on the products collected from forest by developing a machine that shall replace the traditional tedious methods of manual deshelling process of charoli nut, helping them to earn better income by selling finished product directly to the market. On the basis of this physical properties Charoli nut deshelling machine was developed and tested using Taguchi's method of experimentation. For experimentation various independent parameters like feed rate (ψ), moisture content percent (M_c), clearance (C_d) between grinding disk, thickness of the grinding disk (t) and rotational speed of the flywheel (V_f) of three levels have been considered. Impact of the combinations of this independent parameters was evaluated to check the response interms of Deshelling efficiency (η_d), Whole kernel recovery (η_w), Broken kernels (η_b), Partially Shelled / Unshelled nuts (η_u), (τ_r)- Resistive Torque, and (T_p)- Processing time. Analysis and validation of the experimental data was done using the Taguchi's method of experimentation. Further, experimental data was compared with the mathematical and ANN simulation model for the individual responses.

The development of the deshelling machine aims to simplify important processes and increase the productivity of the charoli processing for tribal communities and small businesses. As a result, the current study has clearly reflects the interaction of numerous independent factors. Percentage error of estimate for the anticipated / calculated values of the dependent parameters is considered to be significantly lower. This confirms genuineness to the developed ANN and

mathematical models. The patterns for the performance of the models shown by graphs, effect assessment, and Taguchi analysis were discovered to be complimentary. These tendencies have been shown to be genuinely warranted by certain conceivable phenomena physics. The optimum set of variable values, economic acceptability, and cheap cost of manufacturing will facilitate rural and tribal persons in establishing small-scale industries.

1.4 Organization of Thesis

The entire work carried out has been presented in this dissertation through **Chapter 1 to Chapter 8** as under:

Chapter 1 is "Introduction to present research." This chapter describes of the initiation of the present research work and an overview of the entire work.

Chapter 2 is "Literature review." In this chapter, the detailed literature review is carried out. The literature review on the basis of general features of charoli, its importance and related matters, deshelling techniques, process parameters/capabilities, the impact of process variables on performance, evaluation of hand-operated decorticator or sheller, evaluation of onload / pedal-operated decorticator or sheller, evaluation of human-powered flywheel motor, and evaluation of electrical or petrol operated decorticator or sheller has been done. The articles reviewed are from their aims and objectives, methodology adopted, important findings, and conclusions.

Chapter 3 is "Physical properties of Charoli (Buchanania Lanzan) nut." In this chapter, attempts have been undertaken to evaluate the physical properties of Charoli (Buchanania Lanzan) nut. Scientific information on physical, frictional, and aerodynamic properties collected by this study will be valuable to researchers/scientists in designing and developing equipment. This chapter determined various physical, frictional, and aerodynamic properties of Charoli (Buchanania lanzan) nut at increasing moisture content.

Chapter 4 is "Experimentation using design of experimentation" In this chapter details about the experimental set up is provided. Detailed experimentation variables, their test envelop, test sequence is discussed. In this chapter, experiments are performed as per Taguchi's L27 orthogonal array and experimental data is generated for its further analysis

Chapter 5 is " Analysis of experimental data ". In this chapter complete information about an approach for execution of experimentation, analysis of investigation by Taguchi method, and ANN model formulation. An analysis is performed as suggested by Taguchi, and ANN model is developed based on the experimental data.

Chapter 6 is "Optimization of parameters using a technique for order of preference similarity to ideal solution (TOPSIS)." In this chapter, optimization of the results of experimental data using TOPSIS is carried out. Using the technique of TOPSIS, a combination of optimum process parameters is determined and presented.

Chapter 7 is "Result and discussion." In this chapter, the validation of the results of experimental data, mathematical models, and ANN simulation has been done. The comparison of percentage error between experimental values & values obtained from mathematical model and ANN simulation model was done. Also, effect of various input parameters on the individual output parameters was studied and presented.

Chapter 8 is "Conclusions and future scope". In this chapter, the specific conclusions from the present investigation are given. Along to the findings, the limitations of the present investigation and suggestions for future work are reflected in this chapter.

The details of the publication based on the present investigation and the achievements are also mentioned in this thesis.

The bibliography is given at the end.

CHAPTER - 2
LITERATURE REVIEW

In this chapter, attempts have been undertaken to evaluate the kinds of literature relating to general features of charoli, its importance and related matters, deshelling techniques, process parameters/capabilities, the impact of process variables on performance, evaluation of hand-operated decorticator or sheller, evaluation of onload / pedal-operated decorticator or sheller, evaluation of human-powered flywheel motor, and evaluation of electrical or petrol operated decorticator or sheller. The collected information has been presented below:

2.1 General features of Charoli (Buchanania lanzan), its importance, and related matters.

Charoli, also known as Chironji (Buchanania lanzan Spreng), is outstanding agroforestry and community forest tree. It is very important in wasteland development and dry land horticulture because of its numerous applications and ability to endure difficult environmental situations. It is currently flourishing in the woodland as an under utilised fruit that provides monitory benefit to the nation's tribal people and appears to benefit them. It is an important species found across the nation, except the Indian Himalayas [23].

According to Das and Agrawal (1991) [18], Charoli fruits are digestive and utilized to alleviate fever, body burning and, thirst. Fruit kernels are seen like lotion in the treatment of skin disorders.

Tirky et al. (2004) [22] undertook an ethno-medicinal study in the tribal region of Chhattisgarh's Raigarh district, recording 24 therapeutic plants utilized in dyspepsia. They enlisted the assistance of the Oraon, Chamar, and Corwa tribes, who reside into the Raigarh district's woods of Jashpur, Kunkuri, Tapkara, Dharam-jaigarh, Gharghora, Lawakera, and Kansabel. They noticed that Buchanania lanzan was utilised in the treatment of Indigestion. Based on a survey of medicinal plants conducted in several locations of Jharkhand and Bihar, India.

Mehta, Mukherjee, and Jaiprakash (2010) [23] have examined the medicinal estimation of the leaves of Buchanania Lanzan (Anacardiaceae). Phyto compound screening, quantitative investigation, and subjective substance examinations were done utilizing HPTLC procedures. Discoveries acquired appoint another potential part of Buchanania Lanzan separate in human medicinal services. According to Patsnaik et al. (2011) [24], the Buchanania lanzan Spreng plant is widely recognised in Indian traditional medicine for its medicinal and therapeutic properties. They looked into the effects of methanolic extract of Buchanania lanzan Spreng, root on pain and acute inflammation. Their findings clearly show that Buchanania lanzan Spreng might be a viable source for anti-inflammatory and analgesic agents. According to Kumar et al. (2012) [11], kernel oil is primarily utilised in makeup production like a substitution for almond and olive oil, and kernels are utilized into sweeter-meal as an alternative for almonds kernels.

Chauhan et al. (2012) [8] reviewed on various uses of chironji. They concluded that chironji seeds are nutritious and may be used in place of almonds nuts. In many situations, these seeds are hurried to produce fine particles for flavorings or usage as spices into various Indian cuisines. Furthermore, charoli nuts can be used for thickening of stews and soups on occasion. The kernels are eaten raw or roasted and have a nice, subacidic flavour. Its kernel oil is beneficial in the treatment of glandular swellings of the neck. Charoli paste is a fantastic body moisturizer. Aside from the fruit, bark is utilised in natural tanning and varnish. Gum exudates derived from tree trunks are utilised in textile treatment. Gum can also be used to cure diarrhea, intercostal and rheumatism discomfort. The leaves are used to cure skin problems. Cough and asthma are treated with fruits. Cordiotonic characteristics are found in the leaves. Wounds are commonly treated using leaf powder. They are cow feed of the highest quality. The roots are abrasive, chilling, diaphoretic, and vasodilating, and can be used to cure diarrhea.

Watershed Programme (2012) [25] demonstrates the different employments of Charoli which is also called chironji. Different uses of seeds like flavors and desserts in India are also discussed. Charoli is additionally ground into powders to thicken tasty sauces and flavor player. Significance of Charoli seeds in Ayurveda and Unani

system of medicine was also discussed. Bandyopadhyay and Banerjee (2014) [26] examined the different substance constituents of strong medicinal estimation of Buchanania lanzan. Three most vital chemical constituent of intense medicinal value, to be specific vomicine, celidoniol, epinitol have been described from a natural extort of leaves. This examination attempts to current detailed efficient depiction of current and promising zones of research of Buchanania lanzan, especially towards phytomedicnes and pharmaceuticals. Kumar et al. (2016) [27] noted down the physical characteristics of Charoli nut as an element of moisture content, varying from 9.98 to 17.06% (d. b.). Different reasons for presence of moisture on physical parameter like nut width, nut length, nut thickness and geometric mean diameter additionally highlighted. Deshmukh et al. (2017) [28] decided the production parameters of Charoli nut and kernel to design a nut decorticator which would limit kernel breakage with proficient decortication. Study was completed for different moisture content, nut length, width and thickness. Author likewise computed properties like mass and true densities.

Charoli is a medicinally valuable tropical tree species and an essential cause of living for the bounded tribal community. Practically all the parts of this plant are used for the therapy of numerous disorders. The Charoli kernel is having a high amount of protein (19.0 - 28.19 %) which is exceptionally nutritious. The kernel yields sweet oil (33.50 %), of which 1.90 % is unsaponifiable. The 20.00 % of linolenic acid found in the saponifiable part. Charoli oil is healthy and fit for the consumption of humans [12].

Table 2.1 shows the approximate composition of Charoli, Sesame, Almond, Cashew, and Walnut kernels. As compared to other dried fruits Charoli kernels have significant content of fat, protein, ash, fiber, starch, and carbohydrate that is very significant for the human health.

Table 2.1. Some dried fruit kernels' approximate composition

Reference	Nut	Moisture (%)	Fat (%)	Protein (%)	Ash (%)	Fiber (%)	Starch / Carbohydrate (%)
Sahu, Tiwari, Naik, & Kariali, (2018); Hiwale, (2015); Banerjee & Jain, (1988); Dwivedi, Singh & Singh, (2012).	Charoli	2.86 - 3.12	50.72 - 61.91	19.0 - 28.19	5.63 - 6.59	3.8	10.87 - 12.25
Onsaard, (2012); Badifu & Akpagher, (1996)	Sesame	4.50 - 11.00	48.20- 56.30	19.10- 26.90	2.0- 5.59	2.5- 3.90	5.59-17.90
Ahrens, Venkatachalam, Mistry, Lapsley, & Sathe, (2005); Sze-Tao & Sathe, (2000)	Almond	2.84 - 5.86	43.3 - 56.05	16.42 - 23.30	2.69 - 4.56	1.98	23.6 - 27.0
Arogba, (1999); Alobo, Agbo, & Ilesanmi, (2009)	Cashew	9.30 - 12.40	45.17 - 51.0	20.23 - 36.0	0.3 - 6.96	4.54 - 4.56	3.4 - 11.39
Dogan, and Akgul, (2005); Sze-Tao & Sathe, (2000)	Walnut	3.00 - 3.62	66.75 - 67.15	16.23 - 17.47	1.81 - 2.26	----	65.0 - 70.0

2. 2 Deshelling techniques for nuts

Deshelling techniques generally utilized to dry horticultural materials. Deshelling machines apply mechanical power in the expulsion of the kernel from its casing to free it from any connection or confinement. The principle of operation of deshelling machines relies upon the nature of horticultural materials [29]. This includes the use of the different deshelling mechanism. Types of various deshelling techniques include the following:

2.2.1 Conventional techniques

Conventional techniques for deshelling are generally manual operations utilizing necessary tools as shown in figure 2.1. Proceeded with the utilization of such technique implies the presence of appropriate labor having correct abilities and costs; the deficiency of machine which could accomplish comparable outcomes; and then proceeding with demand for a costly, hand deshelled item [30].

Figure 2.1. Conventional techniques for deshelling

Contingent on the nature of the nuts, the deshelling has high profitability to the detriment of minor loss of entire kernel removal viability. For deshelling, two essential mechanical impacts could be utilized, first, the effect occurred due to the impact next to a harder object or second use of straight mechanical force to squash, slice or shear by a nut. In manual techniques, these activities can be accomplished by stones, basic presses, and so on [31].

Kumar et al. (2012) [12] worked on the processing and current practices of Charoli nut. Current strategy for deshelling with the assistance of hammer and couple of stone-slab taken after by parting of the kernel from the hull is specified. Some local artisan has created general mechanized nut cracking machine yet machines were not uniquely outlined, so they are again separating physically. So there is a need to develop an appropriate machine with separation unit. Singh, Mandal, and Das (2018) [31] examined the different technique and current practices of chironji nut processing in Chota Nagpur plateau region. The author highlighted the benefits of Charoli as elective host for Kusmi lac insect. It is additionally utilized as a fuel, nourishment, cosmetics things and cleansers. There is a broad utilization of Charoli but no processing of chironji nut machine. In some area, nearby artesian developed mechanized machines for breaking and separating however because of the absence of design it isn't working appropriately. So there is a scope to develop an appropriate machine with separation unit.

2.2.2 Centrifugal impact deshellers

Centrifugal impact deshellers comprises of two discs as shown in Fig. 2.2 (a) which are rotating and separated by several radial vanes [32]. Nuts are fed into a rotating impeller for its deshelling. By driving the impeller suitably, this vane produces radial acceleration on nuts. Nuts are released to a peripheral target to impact and tear open. The seriousness of a consequent effect is controlled by the impeller speed which is sufficiently more to crack the nut, yet not all that more as to do exorbitant harm to the kernel [33].
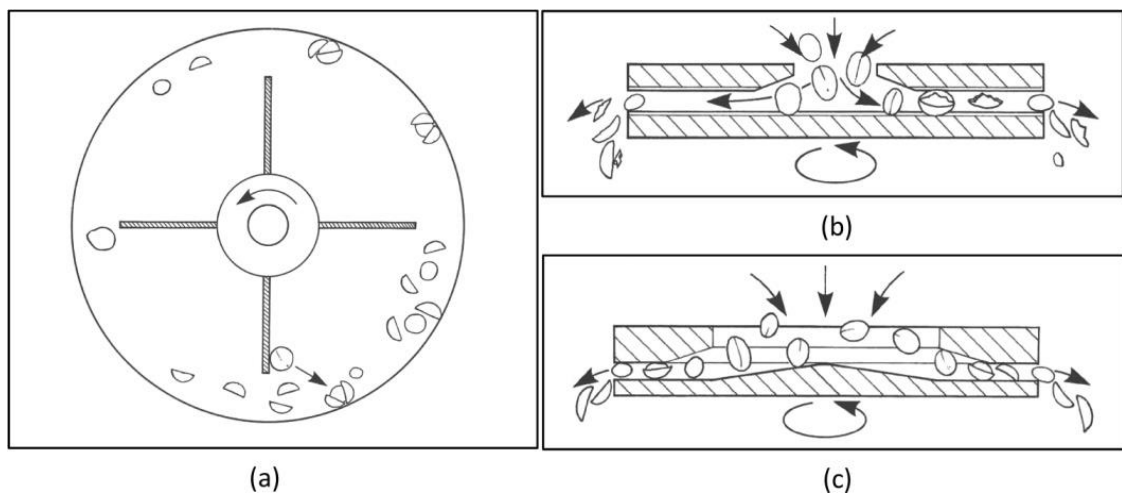
Figure 2.2. (a) Centrifugal impact de-sheller (b) Parallel gap disc desheller (c) Tapered gap disc desheller.

The evacuation of dust via air extraction is conceivable. The majority of the released material requires further preparation to divide the nuts and kernels further reprocess remaining unshelled nuts to cracking. Increasingly perplexing grading techniques permit the separation of the whole kernel from broken kernels.

2.2.3 Disc deshellers

2.2.3.1 Parallel gap disc deshellers.

Nuts having a circular section may need a minor rubbing and pressing for breaking the nuts. This impact can be accomplished by feeding nuts in the rotating disc, as shown in Fig. 2.2 (b).

The discs are having parallel gap continually, thus size evaluation of feed may wind up important. The discs surfaces are rough which helps in the deshelling. The cracking action is mostly dependent on disc rotational speed.

2. 2.3.2 Tapered gap disc deshellers

Exceptionally sensitive kernels need a still gentler activity for proficient deshelling, like manual hand deshelling. The tapered gap technique is the variety of a parallel gap technique which enables a shell to damage dynamically, as shown in Fig. 2c. In this, the key factors are the rotational speed, taper shape, and the surface texture of the disc [34].

2.2.4 Peg and drum deshellers

This type of desheller is a simple and powerful technique for cracking open weak-shelled nuts [35]. In this, a flood of nuts is put in speedily turning projections fixed to the curved portion of the rotor, as shown in Fig. 2.3 (a). This can create successful outcomes on nuts after reduction in the rotor speed. By restricting a flow around the drum by screen and liner, this projection strikes nuts and in a long run, cracks the shells and releases kernels, permitting just shell pieces and kernels are forwarded for discharge.
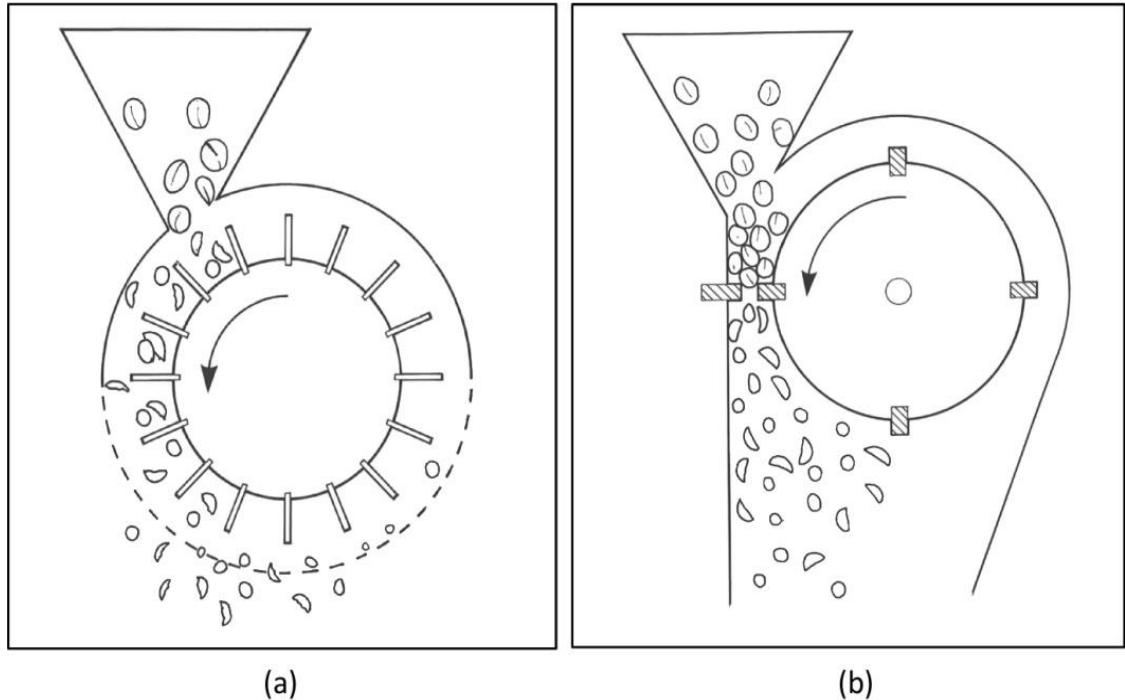
Figure 2.3. (a) Peg and drum desheller (b) Bar and drum desheller.

2.2.5 Bar and drum deshellers

Some nuts are unable to break due to toughness, an increasingly helpful technique of cracking the nut is necessary [36]. Bar and drum, knife deshellers, with sharp edges pivoting against predetermined edges at a pre-set clearance, can catch nuts for a moment and make a decisive cut into the nut with no fundamentally entering through to the kernel as shown in Fig. 2.3 (b).

With the brutal flow about a quickly turning rotor, keeping up the thorough arrangement is hard. The decision for right rotation speed isn't as vital as accomplishing the mainly suitable setting of the gap among stator and rotor. The gap is adjusted through altering the stationary blade and is operated as per nut dimensions. Too broad a gap results in inadequate penetration of the nuts and an abnormal state of unshelled nuts. Excessively small a gap prompts over the top harm of kernels. Every considerable size variation inside a nut feed will bring about the misfortune into deshelling effectiveness, size clumping or evaluating mandatory.

2.2.6 Reciprocating type deshellers

In the case of a reciprocating type of desheller, nuts are put in two parallel assemblies [37] as shown in Fig. 2.4 (a). The nuts move against the rotation, and the nut is broken gradually. The assembly on upper side is stirred back and forth, isolating a kernel and nuts to drop throughout a screen.
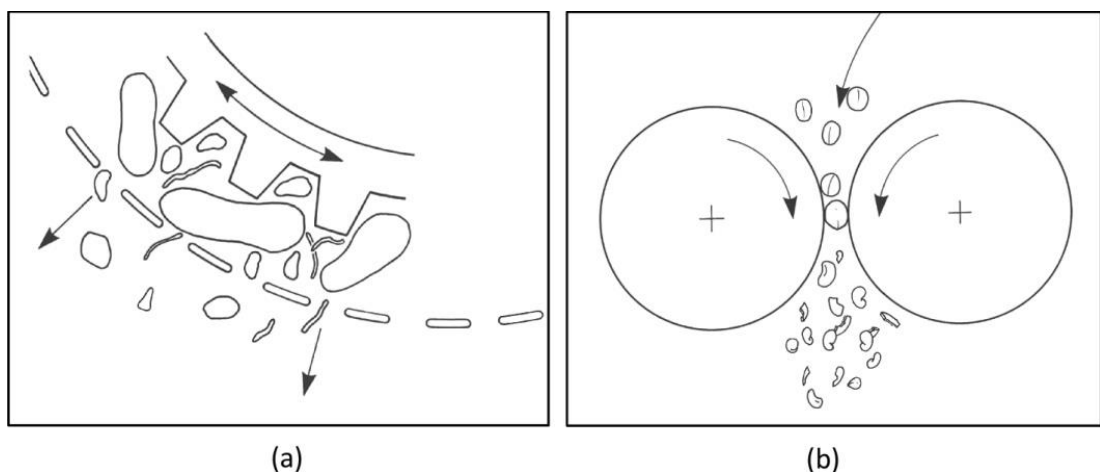
Figure 2.4. (a) Reciprocating action desheller (b) Parallel cylinder type desheller.

2.2.7 Parallel cylinder type desheller

In parallel cylinder type of deshelling technique, two contra-rotating parallel cylinders are set horizontally to get a junction to squeeze the weak nuts as shown in Fig. 2.4 (b). This technique is regularly utilized in mass production as one phase in an incorporated oil extraction task [37].

2.3 Process parameters / capabilities

Several quantitative terms are being used for illustration of the substantial behavior of any nut and to calculate the performance of the processing task [38]. There is no generalized standard to measure the performance of these; the formulae provided can give a guideline.

2.3.1 Whole kernel recovery

Whole kernel recovery is a percentage of the whole kernels obtained during the deshelling process. It gives the fraction of the kernel to that of the original nut. This percentage may depend on nut; varieties; and entity of nuts. The connection can be formulated as [39],

$$\text{Whole kernel recovery} = \frac{\text{Average weight of deshelled whole kernel}}{\text{Average weight of whole nut input}} \times 100 \%$$

The physical nature of the nuts determines the percentage of whole kernel recovery [40].

2.3.2 The kernel deshelling efficiency

It describes the percentage of all kernel obtained after deshelling. The weight of a possible kernel is expected from the percentage derived in the previous paragraph (2.3.1 Whole kernel recovery). The connection can be formulated as [41],

$$\text{The kernel deshelling efficiency} = \frac{\text{Weight of all recovered kernel}}{\text{Weight of potential kernel material}} \times 100 \%$$

Deshelling efficiency 100% reflects the most efficient operation [42].

2.3.3 **The proportion of broken kernel**

This incorporates the damaged and shriveled kernels. The connection can be formulated as [43]

$$\text{The proportion of broken kernel} = \frac{\text{Weight of particular substandard kernel}}{\text{Weight of all recovered kernel}} \times 100\%$$

The proportion of broken kernel 0% reflects the most resourceful process. Weight of a particular imperfect kernel is damaged or desiccated kernel subsequent to deshelling.

2.3.4 **The proportion of unshelled nuts**

This includes the weight of the nuts remaining unshelled after deshelling. The relationship can be formulated as [44],

$$\text{The proportion of unshelled nuts} = \frac{\text{Weight of nuts remaining unshelled}}{\text{Weight of original whole nut input}} \times 100\%$$

The proportion of unshelled nuts 0% reflects the most resourceful process. The weight of the initial whole nut input is a sample weight before deshelling.

2.3.5 **The kernel fraction recovery**

The kernel fraction recovery can be formulated as,

$$\text{The kernel fraction recovery} = \frac{\text{Weight of recovered whole kernel}}{\text{Weight of original whole nut input}} \times 100\%$$

The kernel fraction recovery increases with the alteration of the settings of the machine. The weight of the obtained whole kernel is an unspoiled kernel obtained subsequent to deshelling [45]. This relation can be used in experimentation to check the consequence on whole kernel recovery due to an alteration in machine settings, keeping remaining parameters constant.

2.3.6 The total recovery percentage

The total recovery percentage is a balance of mass of input to output material and can be formulated as,

$$\text{The total recovery percentage} = \frac{\text{Weight of all recovered products}}{\text{Weight of original whole nut input}} \times 100\ \%$$

The total recovery percentage must approach 100% for a reasonable trial. The weight of every single item incorporates dust, nuts, whole, and broken kernels. The whole nut input weight is the sample weight before deshelling [46] .

2.4 Impact of process variables on performance

It will be observed that the deshelling process and process variables that much consideration must be taken in choosing the exact process of deshelling that will be suitable for adapting the different properties of nut. After installation of a machine, it should be capable to work for a long period despite minor variations in the feed material [28]. Figure 2.5 shows the general aspects which should be considered for the performance of the machine.

01 Nature of the input nut

02 Physical properties of the input nut

Machine Performance

Machine setting and paired processes

Moisture content of the nut

04 03
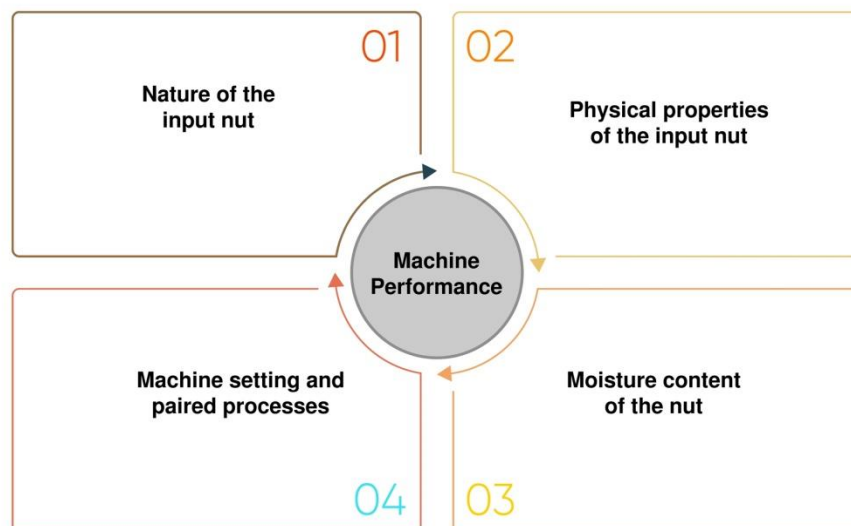
Figure 2.5. Aspects of the machine's overall performance.

2.4.1 Nature of the input nut

The input material should be enough dried, cleared, and dirt, stones free [47]. In several situations, it might be feasible to utilize cleaners and graders. Any endeavors at progress may, in any case, be unreasonable if, for example, long deferrals have just made an irreversible unfriendly alteration to the yield. Hence it is crucial to be particular in obtaining supplies.

2.4.2 Physical properties of the input nut

In numerous cases, the raw material quantity is originated by accessible stands of unchanged natural variety [48]. Then again, as recently cultivated zones are commonly planted by variety chosen as being ideal in nearby situations, reasonableness for productive deshelling is not an important measure, and subsequent yield is not perfectly related to an existing machine [49]. The range of varieties which may influence deshelling is significant, and the accompanying common features might have some impact [50]:

• Shape, strength, and size of the nuts and kernels;

• The extent of accessible kernel and strength between internal bonds

Any of the above features are probably needed a slightly different way for effective deshelling. In other words, a minor acclimation in machine setting can achieve higher results.

2.4.3 Moisture content of the nut

The moisture percentage in the nut is perpetually high when collected from the tree. In this condition, the deshelling promptly damages the kernel [51]. For delayed capacity and handling, this external layer of nut must be expelled prior to drying at a predetermined moisture level [51]. Proper drying is needed before deshelling as drying makes external layer brittle to break and generates a sufficient gap between the external layer of nut and kernel.

2.4.4 Setting of machine

There are various types of machine techniques, where adjustments in the machine are conceivable and essential [52]. As a common practice, the less distance in the settings shelled more nuts but in this case damage is also high. On the other hand, a delicate

setting will shell fewer nuts; however, minimize the percentage of broken kernels [53]. So, while setting up the machine, optimization must be there between efficiency and damage of kernels [54]. In practice, more significant budgetary pay can be gotten by the utilization of more tightly settings around significant limits, to detriment of just the marginally high broken kernels percentage [55].

2.4.5 Paired processes

There are several paired processes that need to be carried out before, during, and after the operation of deshelling as shown in figure 2.6.

2.4.5.1 Grading of size

When the nuts have a spherical shape, basic reciprocating screens, or turning drums can be utilized for accurate size grading [56]. Variation in shape decreases the grading accuracy of the machine of this kind, and a specific machine might be needed [57].
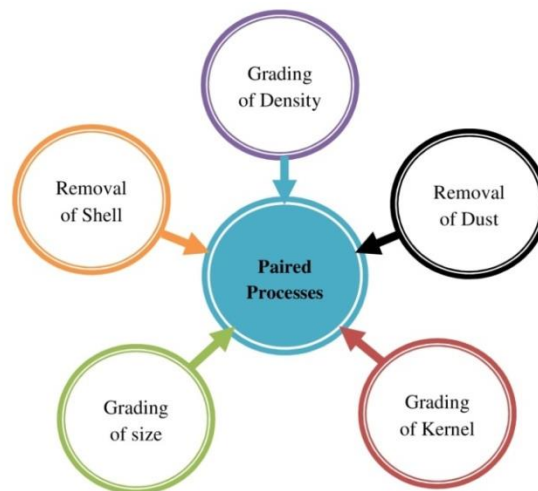
Figure 2.6. General paired processes before and after deshelling.

2.4.5.2. Grading of density

Using the simple or common type of size grading system does not produce the required output, it might be suitable to isolate the surge of feed material into parts dependent on density. Even though this kind of procedure is increasingly pertinent to nuts having lighter shells and kernels grading, it might be expected to meet better quality needs [57].

2.4.5.3 Removal of dust

Winnowing in circling air is adequate for separation of residue and material having lighter weight when a small scale situation is considered. While when mass production is considered, the utilization of a primary suction extraction machine comprising of an outward flow fan and a typhoon which used to gather the dust.

2.4.5.4 Removal of shell.

Even though shell removal by light air extraction is sufficient, excess shells are still there inside an air stream [58]. In this type of case, other techniques like sieving, even gravity tables or flotation in liquid may need to utilize.

2.4.5.5 Grading of kernel.

It is sensible to separate the different kernels grades by hand when considering the small scale enterprises. Unshelled nuts which also require shelling can also reuse likewise. These grading activities are probably going to be more dreary and tedious than the shelling itself, and specific machinery is required as the scale of activity increments.

2.5 Evaluation of Hand operated decorticator or sheller

As energy utilization over the world keeps on ascending, there is a solid need to grow new techniques for energy protection and power generation, especially approaches that have less ecological effects. There are promising application zones for human power in rising areas where electric power is either not accessible or not affordable. There is likewise undiscovered potential for tackling human power at most wellness facilities. Utilization of common fuel is expanded because of industrial improvement, its storage going to end. Since the 1980's, and still as of now, India has experienced a negative balance in overall energy utilization and creation. This has brought about the need to buy energy from outside the nation to supply and satisfy the requirements of the whole nation. Human power credits its significance looking for another source of energy as it fulfils the necessity of a renewable source of energy.

Too and Landwer (2003) [59] has gathered different biomechanical variables into one of three classes like natural variables, inner biomechanical variables, and outer

mechanical variables. The relations of diverse variables inside a group can be unpredictable, however, should be inspected and understand if extra efficient human-powered vehicles are to be produced. The author was engaged to look at the variables in every class, their connections. Pradhan et al. (2010) [60] has created and evaluated the execution parameters of small, consistent, hand-worked machine for decortications of Jatropha fruits. The machine comprises of a frame, container, decorticating space, inward strainer, rotating blades, release exit and separator which have a vibratory motion for detachment of seed and shell. The execution parameters were assessed at four individual moisture content with blends of concave clearance. Maximum efficiency was found at moisture presence of 7.97% d.b. at a clearance of 21 mm between the inward and the blade. A further modification is needed to improve separation efficiency.

Singh and Singh (2010) [61] designed, created, manufactured and assessed hand worked de-husker sheller for maize. The machine's output capacity was around 60 kg/h at a feed speed of 80 kg un-dehusked cob per h. At a peripheral cylinder speed of 5.6 ms^{-1}, the dehusking efficiency was 100 percent, the shelling efficiency was 98.8 percent, and the grain breakage was 0.3 percent. Both labourers might be relocated during the process to enhance activity continuity. Ojolo, Olatunji, and Orisaleye (2016) [62] concentrated on ergonomic assessment of a hand worked town level cashew nut shelling device. A physically worked cashew nut cracking machine was assessed. Poll for cashew nut cashew nut cracking machine was additionally surveyed. The examination indicated the importance of ergonomics in decreasing drudgery and enhancing user satisfaction and agreeableness in innovation improvement move in creating the nation. OLAOYE (2018) [63] has built up a Melon shelling and separating machine from the chaff on a small scale which is manual and electric engine driven. Impact method of shelling was utilized and comprises of a shelling drum, container, shelling plate and shelling vanes, chamber cover, outlet throat, AC motor, collector, bearing, belt and pulleys, manual working handle. Another separating unit comprises of the case cover, separator case, base and blower fan. Shelling efficiency discovered more at wet condition than a dry condition.

2.6 Evaluation of Onload / pedal operated decorticator or sheller

The normal effort rate of a human functioning constantly is identical to 0.13 h.p. The processing unit under 0.13 h.p. can be powered by man. Such man power-driven mechanized processes can be founded on this idea.

Barnes W.F, (1876) [64] discovered the first foot-powered tools based on bicycle innovation. The organization describes the advantage of the novel design in its 1880 list. Amateur Saw development of the limbs in running this saw is simple and as regular as in walking, and the operator can work consistently without weakness. Every muscle of the limbs are brought into healthful refreshing exercise, which ought to be an extraordinary thought while choosing a machine. All old style foot-powers do not have these points of interest of simplicity of activity and stimulating advancement of the muscles. An operator can't run one of them steadily without tiring and encountering an unnatural cramping of the muscles of the feet, lower legs and limbs. Wilson and Furber (1986) [65] have investigated, a man can produce four-times extra power (1/4 hp) as compared to hand with pedalling. At the rate of 1/4hp, constant pedalling is done in small time, about 10 minutes. Be that as it may, pedalling at a large portion of this power (1/8 hp) can be kept up for around 60 minutes. Chandurkar K.C, (1987) has built up the connection among the valuable torque created on a crank as a role of crank position through its rotation. Author additionally saw that out of 360° turn of a pedal crank, just from 30°-115° of crank position from TDC is helpful. The crank position up to 30° and between 115° to 162° isn't adequately utilized and between 162° to 360° is fully idle. Still when both the cranks are seen as the important driving point is seen to be 154°. Singh et al. (2008) [66] were planned and built up a pedal-operated paddy thresher at Uttrakhand region. The machine working was assessed for ideal design parameters, A cover for safety purpose was additionally given to ensure the worker according to standards and to save the grain losses throughout working. Due to the low generation and income, agriculturists can't manage the cost of expensive and high-capacity paddy threshers. Pedal- worked threshers are utilized for paddy crop.

Ajao et al. (2010) [67] have designed and developed bicycle pedal-powered soap mixer. The machine comprises of a chain drive and gear systems to turn impeller blades in an extensively treated steel holder, where soap contents are mixed. The machine was financially feasible, could be utilized by untrained labours, spare time generally used up in conventional blending and can be embraced for human-powered processing system which could have an irregular task with no affect upon the last outcome. Wu (2009) [68] has examined different elements to consider in designing and concentrated on experimental strategies that assist to optimize the power transmission of bicycle attachments. The author compares power transmission through different modes off of bicycles and suggested chain-driven attachments for design in developing nations. Zakiuddin and Modak (2010) [69] talked about the significance of human power from the most punctual occasions to the present and its future possibility. The utilization of common fuel is expanded because of industrial advancement, its storage going to end. There is a need to accompany alternating substitute of energy, which is none other than nonconventional energy. Human power its significance looking for a substitute source of energy as it satisfies the necessity of renewable energy source. Tiwari et al. (2011) [70] has concentrated on human muscle power for improvement of the socio-economical conditions of farmers internationally. Pedal power empowers the man for driving devices at more rate than hand turning with minimum exertion and exhaustion. Author has intended to control power production and pedaling rate meant for stationary farming activities. Physiological reactions of 12 males were examined upon computerized bicycle ergo meter for different power output levels at seven levels of pedalling rates. Examination demonstrates physiological reactions (pulse and oxygen utilization rate) were considerably influenced with output power and additionally pedalling rate. Physiological reactions expanded directly with output power were altogether extraordinary at various output powers.

Hussain et al. (2011) [71] planned and built up a bicycle integrated pipe bending mechanism. The machine comprises of a chain drive, compound gear train. It is worked by human energy with the course of action of irregular energy store at the flywheel. The bend angle of 90° was provided and only single bend intended in the

system. Waweru (2016) [72] has recommended human muscle power as a decent alternative to meet the energy necessities to defeat the socio-economic factors of creation in towns. Author has created pedal operated grain mill which comprises a roller shaft and a chain drive that turns the rotors in the process unit. The grains are crushed in the processing case to produce flour. The machine discovered financially reasonable, can be utilized by average citizens for time saving.

2.7 Evaluation of Human powered flywheel motor.

Modak and Bapat (1994) [73] have been produced a brick-making machine which runs manually. The machine comprises of three fundamental units: transmission in flywheel shaft, a pedal-driven flywheel motor; and the processing system, comprising of the various elements like cone, auger and die. The machine was basically created based on common mechanical design knowledge and perception. Regardless of this, it ended up being useful and cost-effectively workable. though, it was necessary to create it systematically. Modak J.P., (1998) [74] has exhibited two important characters in his report on brick-making in India. One is that human power can be utilized for undertakings that take, for a brief span, much more power than one individual can create. It can be done through energy storage, for this situation a flywheel. The second is that human-powered brick creation is financially feasible and socially desirable. Zakiuddin and Modak (2010) [75] have figured an exploratory information based ANN model for a Fodder Chopper which works on Human power to correct estimations of the response variables relating to a different estimations of the input variables. For the same, models have been formulated, approved and improved as per the recommended method. This is the best fit model based on the regression coefficient between the observed values and the values of the response variables registered by the ANN. Dhale and Modak (2012) [76] have built up a Human powered oil press which will extract oil from the oilseeds. Human power was observed sufficiently adequate to be changed over into work. Proposed innovation enhances the financial state of the rural population and furthermore decreases the gap amongst free market activity.

Zakiuddin and Modak (2012) [77] have examined the significance of human power from the initial era to the current and its upcoming extension. An effective mechanism for the utilization of human power was recommended. In bicycle innovation, the worker utilizes the pedal to work the machine which transmitted the power using the unit of crank, chain and freewheels. The proposed machine generally could be utilized to create electric power, to work an assortment of home apparatuses, various harvesting actions in agribusiness and for bodily wellness. Khope and Modak (2013) [78] have created human operated cutter for chaff devoid of any design information. The unit comprises of HPFM, Transmission into the process unit shaft and flywheel shaft, Processing entity i.e. chaff cutting. Point by point design of experimentation to be carried out to build exact correlation of chaff cutter phenomenon empowered by HPFM. Khope, Modak, and Singh (2014) [79] have built up a productive power unit for fodder cutting utilizing individual power as a supply of energy. The proposed fodder cutter driven by HPFM unit can substitute the electrical power driven cutting units. This fodder cutter can be worked with no fatigue and easily for the more drawn out period if manual fodder cutter replaced by the pedal operated. Additionally, the facts demonstrate that muscles in the hands are weaker than those in the legs.. This human-powered flywheel motor unit was tested under three studied variables to be specific gear ratio (1:2, 1:3 and 1:4), flywheel speed (300,400, 500 and 600 RPM) and the number of blades (2 and 3). Bhatkulkar and Modak (2014) [80] have endeavoured to create a blending machine and experimentally affirm its performance to appropriate extent. This blend was utilized as a fertilizer for the undersized size cultivated area. The developed machine plays out this blending work by human power. The purposeful achievability and cost-effective reasonability of nursery fertilizer blender are built up in this work.

Sonkhaskar, Asati, and Purohit (2015) [81] have reported a survey on the different process units empowered by Human Powered Flywheel Motor (HPFM) between the year 2010 to 2015. Literature gives an up and coming situation of the HPFM driven applications. The author finishes up a man can produce multiple times power by pedalling than by hand operated. On the off chance that a man pedals with his full limit then consistent pedalling should be possible for a just brief time of around 10

min. Undirwade, Singh, and Sakhale (2015) [82] have developed human powered bamboo sliver cutting which includes different factors influencing the responses of the dependent factors. The independent factors like length, width and bamboo split thickness, Elasticity Modulus of bamboo, angular speed, gear ratio and time necessary to accelerate the flywheel, etc. were influencing the performance of sliver cutting which influences the dependent factors responses like resistive torque, time required to process, and slivers numbers. At long last, the examination of experimental, ANN simulation and mathematical was looked at for output of a resistive torque, number of slivers and processing time.Undirwade, Singh, and Sakhale (2017) [83] have formulated sliver cutting models from with HPFM. It the plan of test work to be executed for setting up the inexact generalized observational model for responses of dependent factors like time required to process, slivers numbers and resistive torque using HPFM based on testing information picked, utilizing methodology of engineering experimentation. Detailing of the scientific model for handling time for bamboo sliver cutting is expounded totally in the work.Chandak, Lende, and Modak (2018) [84] have recommended a special technique for choosing ideal ANN design for a fitting capacity issue. Author has discovered reliability (96.68%) and coefficient of assurance for HPFM of the proposed ANN model (0.95). Undirwade (2018) [85] has clarified the advancement of the test information based mathematical models for slivers cutting by means of HPFM. It the plan of test work to be executed for setting up the inexact generalized observational model for responses of dependent factors like time required to process, slivers numbers and resistive torque using HPFM based on testing information picked, utilizing methodology of engineering experimentation. Detailing of the scientific model for handling time for bamboo sliver cutting is expounded totally in the work.

2.7.1 Agricultural application of flywheel

Several researchers used flywheel for the storage of human energy. Dr. J. P. Modak and his team have developed several machines for agricultural mechanization. Machines which was also called as a processing unit works on the pedaling unit which mainly comprises of bicycle unit and flywheel. In this pedaling unit, flywheel stores the energy which has generated by the peddler and utilizes the same for the working

of various agricultural machines. The various authors like Bhatkulkar et. al, Dhale et. al, Ganorkar et. al, Ghuge et. al, Khope et. al, Moghe and team, Nimbarte et. al, Sonawane et. al, Sonde et. al, Undirwade et. al, and Waghmare et. al, have been developed the process units like Nursery Fertilizer Mixer, Oil press, Water Pump, Novel Gearbox, Chaff cutting machine, Forge Cutter, Ice-cream Making Machine, Turmeric Polishing Machine, Garlic Peeling Machine, Sugar Cane Sprout Cutter Machine, Wood Chipper Cutter, Sliver cutting machine, and Stirrup Making Machine respectively.

The various flywheel assisted machines for agricultural purpose are given below in table 2.2

Table 2.2. Various agricultural machines assisted by a flywheel.

S.N.	Agricultural Machine	Specification/ Significance/ Limitations	Reference
1	Chaff cutting machine	Developed chaff cutting machine to overcome uncertainly of electricity. The developed machine is worked with the help of HPFM. The machine is proper for marginal farmers having 2 to 3 cattle.	Khope and team. [37]-[38]
2	Forge Cutter	A newer cutter is made-up which different than other fodder cutters that will work on the non-conventional energy source. The machine runs with the help of flywheel energy.	Khope and team. [39]
3	Garlic Peeling Machine	Developed Garlic Peeling Machine assisted by a flywheel. The machine is cost-effective and useful for human-operated machines having intermitted working.	Nimbarte and team. [42]
4	Machine for Ice-cream Making	A flywheel aided human-powered ice cream manufacturing machine was developed. In a wooden machine containing a combination of ice and salt, ice cream components are swirled and mixed using flywheel energy.	Khope and team. [40]
5	Novel Gearbox	Developed a novel gearbox for the HPFM. Gearbox runs smoothly with the help of flywheel.	Ghuge and team.[35]-[36]
6	Nursery Fertilizer Mixer	Developed human-powered nursery fertilizer mixer assisted by flywheel (HPFM). The machine is economically feasible, can be used by a normal worker and it minimizes the time.	Bhatkulkar and team. [31]-[32]
7	Oil press	Developed an approximate generalized data-based model by varying independent variables for an oil press. The recognized database will be helpful for lower to medium output oil press.	Dhale and team.[33]
8	Sliver cutting machine	Designed and developed a sliver cutting machine assisted by a flywheel. The operation of the	Undirwade and team.[45]-[47]

31

		machine is successful and highly reliable.	
9	Stirrup Making Machine	Developed a human-powered flywheel motor for stirrup making machine. The machine is cost-effective and useful for human-operated machines having intermitted working. The efficiency of the machine finds higher at low input.	Waghmare and team. [48]
10	Sugar Cane Sprout Cutter Machine	The machine is useful for cutting a sugarcane bud that is helpful for sugarcane sown. The machine reduces economic loss and human effort.	Sonawane and team. [43]
11	Turmeric Polishing Machine	Designed and developed a turmeric polishing Machine. Machine work well with flywheel energy.	Moghe and team. [41]
12	Water Pump	Developed human-powered water pump assisted by a flywheel. The machine can lift a moderate amount of water at a considerable height.	Ganorkar and team. [34]
13	Wood Chipper Cutter	Developed wood chipper cutter assisted by a flywheel. The machine is cost-effective and useful for human-operated machines having intermitted working.	Sonde and team. [44]

The above machine found cost-effective, can be used for human-operated process machines having intermitted working. The efficiency of the machine finds higher at low input.

2.8 Evaluation of electrical or petrol operated decorticator or sheller

Oluwole, Aviara, and Haque (2004) [86] have planned, built, tested and evaluated the performance of shea nut cracker. The cracker, which comprises of a container fitted with a breaking unit, power system, a flow rate control device, and winnowing unit. Impact of moisture content on performance was contemplated. Radial vane arrangement gave the greatest percentage effective cracking at zero breakage.

Atiku, Aviara, and Haque (2004) [87] has planned, built and tested roller mechanism for Bambara groundnut processing. Performance tests on machine demonstrate that the presence of moisture, nut feed rate and the contact among them had extensive impact on the amount of shelled, unshelled and incompletely shelled nut. The relationship between the sheller performance records, pod moisture content and feed rate were built up with the assistance of regression models. There is nonappearance of separation mechanism, so further need manual screening. Oluwole, Abdulrahim, and Oumarou (2007) [88] have various uses of the in the various fields are discussed in

couple of papers planned, developed and evaluated a centrifugal Bambara groundnut sheller driven by the electric motor with belt and pulley arrangement. The machine comprises a feed container along a device to control feed, shelling unit, arranging unit and power unit. Examination at three different pod moisture contents was completed with the assistance of nine unique impellers. Impeller slot angulations, Moisture content, contact and number of impeller slots statistically influenced the centrifugal Bambara groundnut sheller performance. Change in separating unit expected to expand the winnowing efficiency of the machine.

Ogunsina, Koya, and Adeosun (2008) [89] have composed a machine which is helpful for cracking of dika nut. The toggle instrument comprises of the slider and a fixed block in which nut is fed physically by hand. The experimentation was done on sun-dried dika nut at 6.6 % M.C. (w.b), 100 % breaking efficiency along with 24 % kernel breakage is observed. The machine discovered reasonable and powerful for secure dika kernel removal. Sharifian, Didar, and Derafshi (2017) [90] had designed a walnut fruit breaking machine based on neighbourhood walnut mechanical properties which were gotten from an Instron test machine. The designed machine has proficient to apply variable deformation according to the flexibility of the walnut fruit. The scope of shell deformation required to crack, as per the testing machine, appeared to be in the range 1.75 and 3.15 mm. The highest breaking load and power necessary was figured to be 797 N and 1.99 Watt respectively. The high flexibility, the lesser is the harmed fruits in the breaking process. The machine is fit for sizing and breaking process at the same time within 6 cone-shaped breaking units. The time important for the breaking technique was evaluated at 6 seconds. A separating system is needed to separate kernels out of shells. Jarimopas, Niamhom, and Terdwongworakul (2009) [91] have created and experimented the model for betel nut husking machine. Machine was contained two equivalent husking wheels mounted in series of material rubber tyre and a steel bars concave sieve built. The dried betel nut was placed between the running tyre and the husking system's sieve surface. The optimal machine settings were described by a tyre pressure and betel nut fruit moisture content. Ideal setting demonstrates a production gain of 76.9 % with broken nuts (15.2 %), husked full nuts (64.4 %); and unhusked nuts (20.5 %).

Wesley et al. (2010) [92] were developed a groundnut thresher that may be used to decorticate castor and groundnut pods. The main concave, cylinder, and sieves for separation of kernel were changed on the groundnut thresher, and it was tested for a new variety of groundnut. Ojolo et al. (2010) [93] have explored the mechanical and physical qualities of the roasted cashew. The examination was completed by fluctuating impact loading testing at various orientations. Acquired load value was interrelated with general nut mass, shell/kernel moisture content level, to decide the required projection speed to accomplish this force. Shelling efficiency was 95 %; Machine throughput capacity was found as 15.57 kg/h and Whole kernel recovery was 70 %. Enhancing the pre-treatment method upon nuts reflects the change in whole kernel recovery. Improvement in the machine is expected to enhance the manufacturing cost the and whole recovery kernel. Ishola et al. (2011) [94] have composed and built up a motorized Prosopis Africana pod thresher. The thresher comprises of the threshing unit, casing, container and cleaning fan. Optimum arrangement of 30 kg/h feed rate, 1200 rpm fan speed, 1200 rpm cylinder speed, and 16 % wb moisture content gives greatest threshing / cleaning efficiency with least seed loss and mechanical harm index. A cylinder and fan speed combination with a comparable minimum % grain loss must be obtained. TING et al. (2012) [95] have designed and created jatropha sheller which comprises mainframe, a transmission unit, fixed cylinder and revolving cylinder. Clearance, moisture content, and roller speed considered as input variables while recovery, energy utilization of sheller, shelling capacity, bulk density factor, oil recovery, energy use by extruder and whole kernel recovery considered as a dependent parameter. Effect of different independent parameters was assessed. Optimization demonstrates the working situation of 9.5 % w.b. moisture content, a roller speed of 750 rpm at a clearance of 6 mm. To enhance the efficiency of the sheller, future examination belt slippage, low whole kernels recovery, Clogging resulting in low recovery and adjustment in the discharged system.

Kumar, Lokesh, and Sandeep (2012) [96] have built up a mango stone decorticator and assessed its performance. Decorticator comprises of the primary casing, cylinder

assembly, feeding chute, concave, kernel and shell exit, blower and a drive unit. Execution assessment was completed by differing moisture content (10, 15 and 18% d.b.), feed rate (150, 200 and 250 kg/h), and cylinder speed (200, 250 and 300 rpm). Decortications efficiency and kernel breakage of 93.91 and 68.12 per cent were found at optimum working conditions of 10 per cent moisture content, 200 kg/h and 250 rpm. Decortication efficiency and kernel breakage were determined to be 93.91 and 68.12 percent, respectively, for the machine. Kareem, Owolarafe, and Ajayi (2012) [97] were planned, created and assessed a kolanut peeling machine for the post-harvest seed processing. The machine predominantly includes a peeling unit, standing frame, and container. The execution of the kolanut peeling machine was assessed at various moisture content (53.0, 57.6, 61.4 % w.b.) and speeds of activity of the machine. The outcome additionally demonstrates that the peeling effectiveness of the machine is directly proportional to moisture content and inversely proportional to the machine speed. The highest effectiveness was discovered 60.3 % at a speed of 40 rpm and M.C of 61.4 % w.b. Lim et al. (2014) [98] have assessed the performance of a Jatropha fruit shelling machine which fundamentally comprises a breaking unit with compression rollers and a separation unit with a vibratory sifter. The investigation appears; the vibratory sifter has unable to totally separate the shells from seeds. Separation efficiency acquired was 91.25 %. Jatropha fruits' particles created have unequal shape and size, which influences the separation through the vibratory sifter. Author has recommended expansion of a blower to for proper separation system. Ojolo, Ogundare, and Adegbiji (2015) [99] has built up an electrical motor driven uneven size nut cracking and parting machine tested to enhance the effectiveness of shelling activity. The shelling operation alongside partition of the shell from the nut was performed with the assistance of a created machine. The machine primarily comprises of a casing, container, rectangular box housing with compression plate and cracking drum and two phases unsettled separating tray. Palm kernel was tested with the machine. The machine working is sufficient with entire kernel recovery to an exceptional value of 87%.

Karthickumar, Karpoora, and Pandian (2015) [100] has built up a constant type tamarind deseeder. The machine comprises of a seed separation unit with separate

exists for the seeds and deseeded fruits. Impact and simultaneous shearing force from pegs set on the wooden roller finished the fruit breaking. The assessment was done at a various moisture content of tamarind fruit and varying wooden roller speed, feed rate and horizontal clearance. Proposed deseeder unit recorded the greatest deseeding efficiency of 89.15% at 74.9 % saving in working cost and 93.34 % saving in time. Aremu, Adeniyi, and Fadele (2015) [101] were created engine operated jatropha seed shelling machine and assessed the performance based on moisture content. The machine comprised of the frame, container, concave, blower with discharge units and shelling chamber. The shelling efficiency of the machine was discovered directly proportional to seed % moisture content; whole kernel recovered and inversely proportional to the partially shelled seed. The maximum percentage of the whole kernel recovered (23.23%) and shelling efficiency (73.95%) was gotten at the optimum working condition of the 8.00% w.b moisture content. For separation of the seed shell from a kernel-shell mixture, blower was utilized. Sobowale, Adebiyi, and Adebo (2016) [102] were designed and built gasoline-powered melon seed sheller. Different parameters like percentage seed shelled and damaged, shelling efficiency along with machine capacity was assessed. Melon seed sheller essentially comprises of a cleaning and shelling unit, container, frame, prime mover and chutes. Shelling operation was conveyed at three distinctive moisture contents with variable speed of 2,500 and 1,500 rpm. Additionally, work ought to be completed utilizing other moisture contents and speed combinations. Kheiralla et al. (2015) [103] were concentrated on plan, advancement and assessment of a small-scale Jatropha seeds shelling machine which would be valuable for the bio-fuel generation in rural areas. Different designing properties for Jatropha seeds and kernel were assessed. Different geometric dimensions of Jatropha seeds and kernel were assessed. The created machine was fueled with a 1.0 hp motor and had a measurement (LHW) of 1100 x1150x450 mm comprises of a casing, fan, container, drum, kernels and shells delivery. Results of the developed shelling machine indicated most extreme the shelling efficiency up to 100%. Air blower was utilized to separates the chaff from the shelled seeds (kernels).

Manjunath, Ahmed, and Sreepathi (2016) [104] were designed and manufactured a small scale Pongamia pinnata decorticator powered through electrical engine for bio-fuel creation in rural areas. Pongamia pinnata decorticator machine powered utilizing a 1 Hp motor through the belt drives and for the most part comprises of the container, frame, de-shelling chamber, blower and outlet tray. The de-shelling of Pongamia pinnata happens because of a combination of a variety of forces like shear, compressive and impact which were applied by a series of bolts arranged in the shaft assembly inside the deshelling chamber. The assessment was done by changing the position and orientation of bolts. The result of the assessment demonstrates an average de-shelling efficiency of 97.95 percent could be accomplished with seed damage up to 28.75 percent. Pradeep and Sasikala (2016) [105] were created cashew nut shelling machine suited for cashew nuts assimilating another shell component in which handling was bulky, expensive, foreign-made and additionally require regular maintenance. The machine allows the operators to watch and sort any issues or fault through the shelling process. Inverse slider crank mechanism was utilized to activate the oscillator unit that drives the scrapper. The machine was assessed, and the shelling effectiveness was seen to be 70%. Ibrahim et al. (2016) [106] have investigated the conventional shelling procedure of Sheanut (Butyrospernum paradoxum) in Nigeria which was generally done physically by rural peoples. The author had determined the mechanical and physical properties of sheanut. The mean values of different diameters i.e major, intermediate, minor, geometric mean, arithmetic mean and angle of repose were found for the physical properties at 25% (wb) moisture content. In view of these properties, an electrical powered sheanut shelling machine was produced which was fit for a shell, clean and separate sheanuts. The outcome of the execution assessment indicated enhanced efficiency and use. The highest value of cleaning efficiency was discovered 69.56% produces the extent of work on cleaning mechanism. Kumar, Chandra, and Sabyasachi (2016) [107] have planned and created Sal (Shorea robusta) seed decorticator with separation system and assessed for its performance. The assessment was done by changing clearance from 10 to 19 mm and M.C. from 10.49- 21.95% (d.b). The execution parameters like kernel percentage and machine and decorticating efficiency were found in terms of seed moisture content and concave clearance. Response surface approach was utilized to optimize the

parameters to get the connotation between the dependent and independent factors. Decorticator yields 62.71% of kernels with the machine efficiency up to 93.62%. In spite of the fact that the separation mechanism was there, it additionally requires manual screening.

Fadele and Aremu (2016) [108] have planned and built moringa seed shelling machine which basically comprises screen, tangential impact shelling device, container, compartment for fan and exists for both the shells and kernels. The machine was evaluated by assessed by fluctuating the moisture content 8.43% to 34.59% (w.b.) from and different dependent variables such as machine capability, % whole kernel, shelling efficiency, and broken recovered, overall machine efficiency +% whole seeds were observed. The result indicates the considerable effect of variation in moisture content on the performance of the machine. Math et al. (2016) [109] have designed, created and evaluated small, annatto (Bixa Orellana L.) seeds separation machine. The machine essentially contains concentric cylinders and mixers having variety in pitch of 40/45/50 mm and a 800 mm length of the shafts. Most extreme bixin contents were seen to be held at an optimum speed of 300 rpm. Chengmao et al. (2017) [110] were produced a mechanical nut test bed to precisely quantify the power, energy, force, and watch the generating process of nutshell. The system was put to the test using pecans, and the results show that the test bed is capable of determining the implementation of nuts as well as data gathering and analysis. The techniques and data may be used to provide theoretical direction for the modeling and evaluation of shell-breaking devices, as well as a reduction in the kernel-breaking rate. Fadele and Aremu (2017) [111] were discussed about the principle of operations of threshing, shelling, decorticating and de-hulling machines and additional factors influencing their efficiencies. The author also concentrated on shelling, threshing, de-hulling, and decorticating machine management and routine maintenance. Adejugbe et al. (2017) [112] were designed a palm kernel processing (Separating and Cracking) unit The machine's efficiency was determined to be 98 percent, with a 95 nuts per second processing rate. This is a significant improvement over the current standard palm kernel equipment, which operates at 90% effectiveness and processes 87 nuts per sec without segregation.

A low-cost almond (Prunus dulcis) kernel extraction machine was built, produced, and tested by Ajav and Mankinde (2015) [113]. The designed machine's performance was assessed in terms of cracking efficiency, machine productivity, particular energy needs and kernel breakage. The 16 mm rollers clearance resulted in the lower values of energy demand, machine productivity, and extraction cost for all roller speeds and casing materials. The greatest values of cracking efficiency were obtained with a clearance between rollers of 14 mm.

2.9 Summary of literature review

Thus the whole literature review is carried out separately on following sections:

- General features of Charoli (Buchanania lanzan), its importance and related matters.

- Deshelling techniques for nuts

- Process parameters / capabilities

- Impact of process variables on performance

- Evaluation of Hand operated decorticator or sheller

- Evaluation of Onload / pedal operated decorticator or sheller

- Evaluation of Human powered flywheel motor.

- Evaluation of electrical or petrol operated decorticator or sheller

At the beginning of this section i.e., in "General features of Charoli (Buchanania lanzan), its importance and related matters" an introduction to Charoli (Buchanania lanzan), its processing, properties and importance are discussed. The important species and their uses in the various fields were discussed in couple of papers. Few author shared the information about the uses of complete tree of charoli like kernel oil, Charoli paste, charoli bark, gum exudates derived from tree trunks, leaves of tree, tree wounds and the roots. Various causes of moisture content on physical parameters

like nut width, nut length, nut thickness and geometric mean diameter also studied. The uses of Charoli in daily eaten items like spices, sweets, sauces and flavour batter is observed by few papers. Few papers explained the importance of Charoli seeds in Ayurveda and Unani system of medicine. Few papers compared the various approximate composition of Charoli nut with the various dry fruits. Charoli is having a rich composition as good as Sesame, Almond, Cashew, and Walnut still no considerable attention has been given on this food and its standardize processing.

In another section, the conventional method of Charoli deshelling is discussed. In the conventional method of Charoli deshelling, all the kernel recovery is done manually by labour using stones and breaking the nut, in which because of little size of nuts the kernel gets damaged yielding approx. 13 % of the kernel recovery and rest kernels are obtained in either broken or dust forms. The kernel costs right around 2 to 3 times as the cost of nut alone and thus even single kernel damage reduces the economic value and productivity. The need of mechanization to deshell the Charoli is observed in this section.

Next section provides the information about human power credits its importance in search of an alternative source of energy. Few hand powers operated successful operating machines like decortications machine for Jatropha fruits, maize de-husker sheller, cashew nut sheller, melon shelling and separating machines are clarified extensively.

Other section concentrated on improvement of pedal operated deshelling machines as hand muscles are weaker than the leg muscle. Various pedal operated deshelling machines are studied in this section.

Further, the review is carried out in detail on the concept of human-powered machines and human-powered flywheel motor (HPFM). The detailed literature review on HPFM enlightens how the researchers have made the efforts since long back to use human power.

The last section focused on the advancement of electrically or petrol operated deshelling machines. Various electrically or petrol operated deshelling machines are contemplated in this section.

2.10 Research Gap Identification / Identification of Problem

Based on the literature review, following the research gap and problems are observed, which need to overcome in the research

1.   Traditional deshelling with stone and hammer leads to damage to the kernels, so kernels are obtained in either broken or dust forms which degrade its value. (J. Kumar et al. 2012)

2.   Traditional deshelling takes more time, labour intensive and drudgery having low deshelling efficiency. (J. Kumar et al. 2012)

3.   Motorized deshelling machines have good efficiency but required power, but in the rural and tribal area, there is a huge scarcity of electricity.

4.   Unshelled Charoli nuts have very low market potential as compared to shelled kernel as there is a long chain of commission agents in between.

5.   Most of the machines were designed for only deshelling, and no mechanism was provided for separations of kernels and shell. (Aremu et al. 2015)

6.   Some of the machines are available with separation mechanism but separation percentage is very low, it further requires manual separation/screening to make it marketable. (Oluwole, Abdulrahim, et al. 2007)

7.   Most of the manual deshelling machines are designed for hand-operated only, but it is proven by literature hand muscles are weaker than the leg muscle. (Modak and Bapat 1994)

2.11. RESEARCH OBJECTIVES

The following are the broad objectives of the research:

1.   To provide the mechanization by developing the Charoli nut desheller.

2.   To establish the experimental data based mathematical model for process parameters.

3.   To evaluate the performance of the machine based on the output parameters.

4.   To validate the developed mathematical model by ANN Simulation.

5.   To perform a sensitivity analysis for determining the most sensitive (critical) parameter (s).

6.   To optimize the process parameters for maximizing/minimizing the response variables.

2.12. METHODOLOGY ADOPTED: Methodologies to be adopted for carrying out the present research work is

i)   The physical design and development of the Charoli nut desheller.

ii)   Pilot experimentation to identify dependant, independent and extraneous variables affecting the phenomenon.

iii)   Deciding variable levels and ranges by performing pilot experimentations.

iv)   Selection of the best suitable method for Design of Experimentation.

v)   Experimentation on the developed experimental setup.

vi)   Establishment of the experimental data based mathematical model based on the data collected.

vii)   Validation of the mathematical model by ANN Simulation

viii)   Sensitivity analysis for determining a most sensitive (critical) parameter (s)

ix)   Optimization of the process parameters for maximizing/minimizing the response variables.

x)   Results and Discussions

xi)   Conclusions

CHAPTER 3
PHYSICAL PROPERTIES OF CHAROLI NUT

In this chapter, attempts have been undertaken to evaluate the physical properties of Charoli (Buchanania Lanzan) nut. The insufficiency of systematic research on physical, frictional, and aerodynamic properties is a fundamental cause behind less popularity Charoli nut. Scientific information on physical, frictional, and aerodynamic properties collected by this study will be valuable to researchers/scientists in designing and developing equipment. This chapter determined various physical, frictional, and aerodynamic properties of Charoli (Buchanania lanzan) nut at increasing moisture content. The collected information has been presented below:

3.1   Sample Preparation

Charoli nuts used in the study were procured from the nearby markets of various states/districts of India like Maharashtra, Madhya Pradesh, Chhattisgarh, Jharkhand, and Gujarat during April 2019 for the purpose of randomization. The Charoli nuts were typically soaked overnight in plain water and scoured against the rough surface of the jute bag to remove the skin. Then the nuts were rewashed with clean water and dried in sunlight [12]. These dried, cleaned nuts were used for further experimentation. Figure 3.1   (a) shows the Freshly harvested Charoli Fruits, and figure 3.1 shows (b) Charoli nuts after expelling the skin.

(a)   (b)

Figure 3.1: (a) Freshly harvested Charoli Fruits, (b) Charoli nuts after expelling the skin.

3.2   Moisture content

Primarily experiments were conducted for moisture content determination of dried Charoli nut. The experiments were performed at the Metallurgical lab of the Mechanical Engineering Department, Priyadarshani College of Engineering, Nagpur, Maharashtra, India. Drying in the oven (hot air oven; Universal, New Delhi, India) method was adopted to find the moisture content of Charoli nuts. The nuts were kept in oven at 105°C for 6 hrs as per the ASAE standard [115]. The moisture content of dried Charoli nut was observed as 9.06 % (db) and was considered as base moisture level for other experiments. The moisture content was varied from 09.06 to 17.86 % (d.b) for an examination. The required moisture level of Charoli nuts was obtained by the addition of a specific amount (Equation 1) of distilled water and packing into the isolated polyethylene packets. For consistency of moisture, Charoli nut samples were stored at 5^0 C in the fridge around 15 days. Prior to each test of nuts, the required Charoli nut samples were brought out of fridge and kept in room temperature [116] . The distilled water amount to be added to achieve the required moisture content was computed by following relation (1) [117].

$$Q = \frac{W_i\ (M_f - M_i)}{(100 - M_f)} \qquad\qquad (1)$$

Where, W_i- initial sample mass (gms); M_i- initial moisture content of the sample (% d.b.); M_f- final moisture content of the sample (% d.b.); and Q- amount of distilled water added (gms).

3.3   Measurement of dimensional properties

Dimensional properties of a samples were assessed on five levels of moisture content, namely 9.06, 10.92, 12.51, 15.29, and 17.86 % d.b. To determine the dimensions of the Charoli nut, 100 nuts of five moisture content levels were picked randomly from the sample [118]. The axial dimensions like length (L), width (W) and thickness (T) of a nuts as shown in figure 3.2 were measured using digital micrometer screw guage (Mitutoyo, Japan) having accuracy of ± 0.001 mm [119].
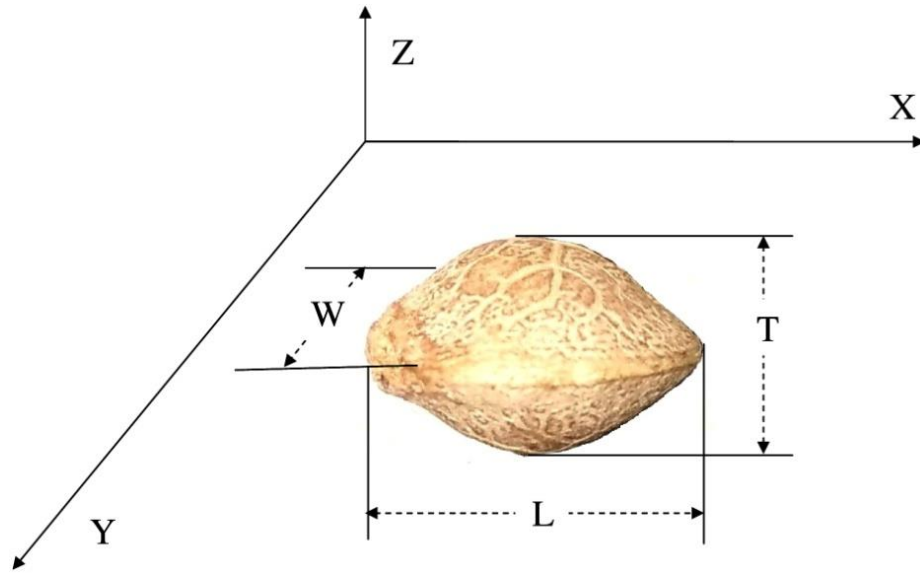
Figure 3.2: Axis and dimensions of Charoli Nut.

Geometric (D_g) and arithmetic (D_a) mean diameter were calculated through relations (2)–(3) [120]-[121].

$$D_g = (L+W+T)^{1/3} \tag{2}$$

$$D_a = \frac{(L+W+T)}{3} \tag{3}$$

The sphericity (φ) and surface area (S) of the Charoli nut were found through the relationship as in Equation (4)–(5) [122].

$$\varphi = \frac{D_g}{L} \tag{4}$$

$$S = \pi \, (D_g)^2 \tag{5}$$

Table 3.1 shows the various mean ± SD values of various dimensional properties of Charoli nut. Dimensional properties of nut help in the design process of sorting, deshelling, and separating equipments.

Table 3.1. Moisture content dependent mean ± SD values of various dimensional properties of Charoli nut.

Moisture Content	Length (mm)	Width (mm)	Thickness (mm)	Geo. mean dia. (mm)	Surface area (mm²)	Sphericity (%)
9.06	7.5844 ± 0.6601	7.7543 ± 0.6740	4.7608 ± 0.3462	6.5318 ± 0.3974	134.53 ± 16.07	86.427 ± 4.936
10.92	8.8725 ± 0.6615	8.7765 ± 0.6477	6.0136 ± 0.3247	7.7575 ± 0.3959	189.54 ± 19.08	87.662 ± 4.227
12.51	9.7811 ± 0.6202	9.5680 ± 0.6291	6.8819 ± 0.3482	8.6291 ± 0.3929	234.41 ± 21.11	88.379 ± 3.602
15.29	11.141 ± 0.629	10.678 ± 0.643	7.7786 ± 0.3562	9.7389 ± 0.4101	298.49 ± 24.98	88.428 ± 3.012
17.86	11.962 ± 0.579	11.583 ± 0.595	8.5923 ± 0.3853	10.593 ± 0.378	352.98 ± 25.12	88.643 ± 2.780

Fig. 3.3 (a) show the bar chart for the variation in mean dimensions like length (L), width (W), thickness (T) and geometric mean diameter (D_g) of Charoli nut for individual moisture level. It can be seen from Fig. 3.3 (a), dimensions of L, W, T and D_g increases by an increment in moisture from 9.06 to 17.86%. The dimensions of nut thickness significantly lower than the other two dimensions (length and width). Fig. 3.3 (b) shows a linear dimension for variation in mean dimensions at an individual moisture content of Charoli nut. The dimensions of nut length were mostly recorded more than the width, while in few cases, the nut widths were found more than the length.
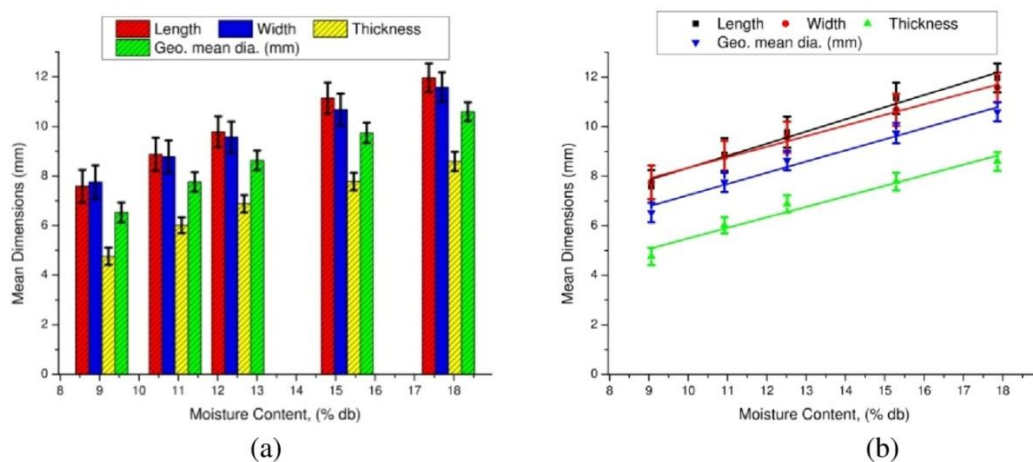
Figure 3.3. (a) Bar chart and (b) linear dimension for variation in mean dimensions at individual moisture content of Charoli nut.

The L, W, T and D_g of the Charoli nuts varied linearly from 7.58 to 11.96 mm, 7.75 to 11.58 mm, 4.76 to 8.59 mm, and 6.53 to 10.59 mm, respectively by varying moisture level between 9.06 to 17.86% on dry basis. The extension in length and width were seen as very closer than the thickness, which could be because of a cellular arrangement of Charoli nuts. The percentage increment in L, W, T and Dg dimensions are 57.72, 49.37, 80.47, and 62.17 %, respectively. Comparative patterns in the measurements were also found for Jamun (Syzgium cuminii) seed with respect to dimensions of L, B, T, and Dg within the moisture level within 11.54 – 26% d.b. [116]. The moisture content (M_C) dependent relationship of the L, B, T, and Dg dimensions are shown in Equations (6), (7), (8) and (9)

$$L = 0.4953 \ M_C + 3.367 \ (R^2 = 0.9809) \qquad (6)$$
$$B = 0.4309 \ M_C + 4.015 \ (R^2 = 0.9914) \qquad (7)$$
$$T = 0.4211 \ M_C + 1.278 \ \ (R^2 = 0.9678) \qquad (8)$$
$$Dg = 0.4532 \ M_C + 2.700 \ (R^2 = 0.9798) \qquad (9)$$

Mean values for the sphericity (φ) of Charoli nuts were 86.42, 87.66, 88.37, 88.42, and 88.64 %, respectively, with varying moisture content between 9.06 to 17.86% on a dry basis. Fig. 3.4 (a) shows the bar chart, and Fig. 3.4 (b) shows the linear dimension for the variation in sphericity of Charoli nut for individual moisture level.

(a)   (b)
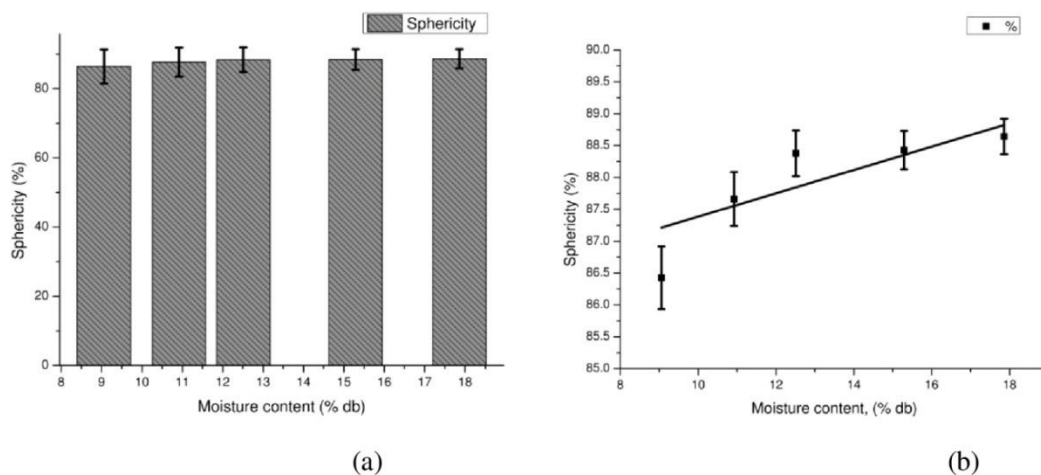
Figure 3.4. (a) Bar chart and (b) linear dimension for variation in sphericity at individual moisture content of Charoli nut.

This indicates that average values of sphericity increased with increment in moisture content, which depicts nut's becoming more spherical. This result gives confirmation with results of Arjun et al. (2017) for makhana and Vilche et al. (2003) for hemp seeds [124]. The higher value shows the tendency of rolling than sliding upon the surface. Therefore while designing the transfer, transport and sorting systems, make nut roll rather than slide. The moisture content effect on the sphericity of Charoli nuts is represented by regression equation (10).

$$\varphi = 0.2226 \ M_C + 84.99 \ (R^2 = 0.7367) \tag{10}$$

The moisture content effect on the surface area of Charoli nuts is shown in Fig. 3.5 (a) and (b).
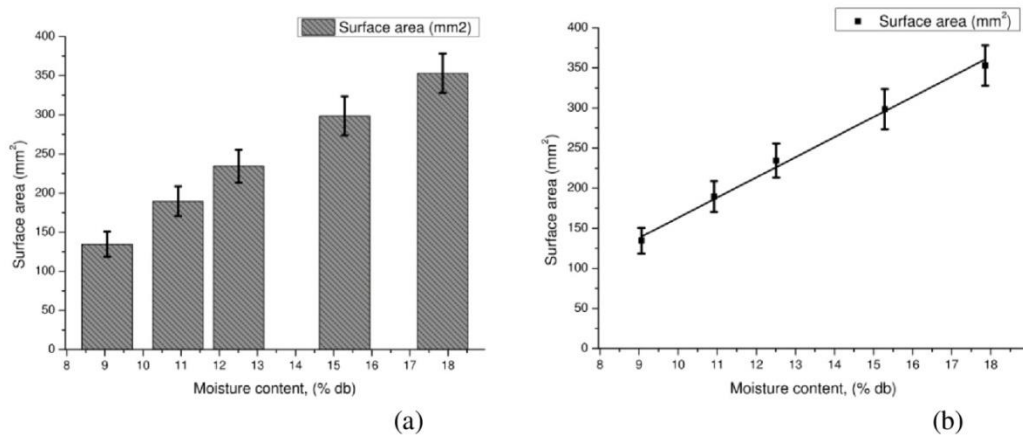
Figure 3.5. (a) Bar chart and (b) variation in surface area at individual moisture content of Charoli nut.

The surface area (SA) of the Charoli nuts varied between 134.52 and 352.97 mm^2. Values show a notable increment in surface area by means of increment of moisture content.

A similar linear increasing trend found in work done by Gharibzahedi et al. (2011) for castor seeds; and Malik and Saini (2016) for sunflower seeds [124]. The surface area plays a significant function in sizing systems design. Apart from this, surface areas are utilized to model material and heat transfer while freezing or drying nuts

[125]. Equation (11) shows the moisture content effect on the surface area of Charoli nuts

$$SA = 24.66\, M_C - 81.7\ (R^2 = 0.9948) \tag{11}$$

3.4 Measurement of gravimetric properties
1.4.1 Thousand nut mass (M_{1000})

Thousand unit masses were obtained by an electronic balance of 0.001g accuracy. 100 nuts of cleaned sample were randomly picked and weighed in the balance. Output was multiplied with 10 to get 1000 nuts mass. The measurements were replicated ten times for individual moisture content [126]-[127].

1.4.2 Bulk density

The bulk density (ϱ_b) was calculated by pouring nuts from 15 cm height into an empty 50 ml graduated cylinder [126]. For achieving the throughout consistency, the cylinder was stabbed ten times to consolidate the nuts. Similar process were performed ten times individually for five moisture content level and the bulk density was computed using the formula (12) [127]

$$\varrho_b = \frac{W_s}{V_s} \tag{12}$$

Where, W_s- nut weight (kg); and V_s- Occupied Volume by nuts (m^3)

1.4.3 True density

True density (ϱ_t) can be calculated by toluene displacement method. Toluene (C_7H_8) have low absorptivity as compared to water, hence it was used [128]. Due to the property of low surface tension, it occupies the fills shallow dips of the nuts. Sample of nuts was immersed in toluene of a measuring cylinder with 0.1 ml accuracy. The graduated scale of cylinder shows the amount of displaced toluene. For true density

value of samples, similar process was performed ten times (Thakur & Nanda, 2018). The true density was computed using the formula (13)

$$\varrho_t = \frac{M}{V} \qquad\qquad (13)$$

Where, M- mass of each nut (kg); and V- volume displaced (m^3)

1.4.4 Porosity

Porosity (ε) indicates a number of pores into sample at given moisture content. It was computed by true and bulk density values and appears into the percentage. The porosity was determined by the use of given formula (14). [129].

$$\epsilon = \frac{(\varrho_t - \varrho_b)}{\varrho_t} \times 100 \qquad\qquad (14)$$

Where, ϱ_t- true density of nut (kg/m^3); and ϱ_b- bulk density (kg/m^3).

Table 3.2 shows the mean $\pm$ SD values of various gravimetric properties of Charoli nut. In contrast, variation in a thousand Nut Mass of Charoli nut by the moisture content is illustrated in Fig. 3.6 (a) and (b). A result indicates the linear increment in mean value from 0.134 kg to 0.421 kg with moisture content.

Table 3.2. Moisture content dependent mean $\pm$ SD values of various gravimetric properties of Charoli nut.

Moisture Content (%db)	Thousand gram Weight (kg)	Bulk Density (kg/m^3)	True Density (kg/m^3)	Porocity (%)
9.06	0.1342 $\pm$ 0.01579	657.23 $\pm$ 15.30	917.94 $\pm$ 43.9	28.25249 $\pm$ 3.84
10.92	0.196667 $\pm$ 0.0364	638.99 $\pm$ 10.01	898.43 $\pm$ 41.3	28.77164 $\pm$ 2.671
12.51	0.2765 $\pm$ 0.01893	616.58 $\pm$ 13.35	883.25 $\pm$ 45.7	30.04625 $\pm$ 3.46
15.29	0.3524 $\pm$ 0.02210	599.32 $\pm$ 19.87	874.65 $\pm$ 46.5	31.3178 $\pm$ 4.07
17.86	0.4215 $\pm$ 0.02371	578.32 $\pm$ 14.93	851.21 $\pm$ 46.9	31.9583 $\pm$ 2.050
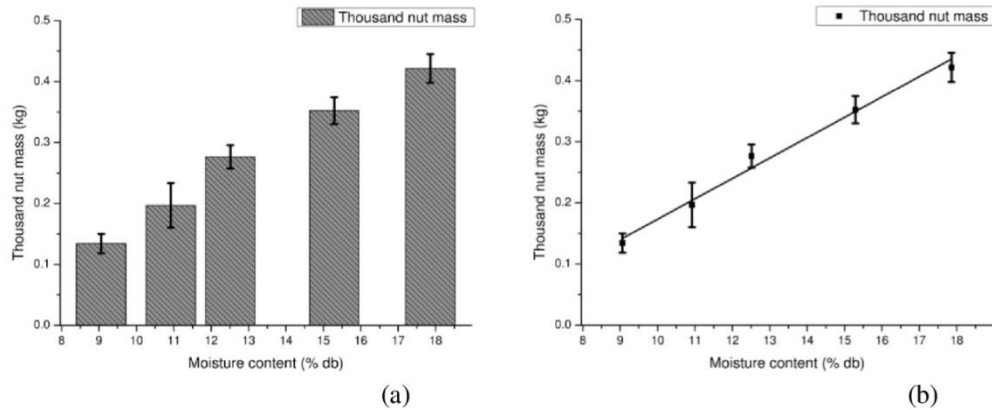
Figure 3.6. (a) Bar chart and (b) variation in thousand nuts mass at individual moisture content of Charoli nut.

The increase in thousand nuts mass illustrates the considerable moisture absorption by the Charoli nut for increase in moisture range. The nut mass is the important parameter while considering the flow rate of the equipment, therefore, deciding Charoli nut mass for acknowledgement of the impact of moisture content on increment of each nut weight.

Similar incremental tendency for thousand Nut mass were observed by Izli [130] and Sacilik [131] for rapeseeds and hemp seed respectively. The variation of the thousand nut mass (kg) is mathematically expressed as in equation (15)

$$M_{1000} = 0.03285\,M_C - 0.1550\,(R^2 = 0.9874) \qquad (15)$$

Because of moisture content increment in nuts, bulk and true density values are significantly reduced from 657.23 to 578.32 kg m^{-3} and 917.94 to 851.21 kg m^{-3}. The bulk and true density relationship of Charoli nut is illustrated in Fig. 3.7 (a) and (b).

Bulk and true density consideration is very important while designing different devices for cleaning, separation, and conveyance systems of nut. The mass of the nut increased because of moisture gaining of Charoli nuts ultimately decreased the bulk density. A similar trend of contrary connection between moisture content and bulk density has been concluded by Ghosh [132] for Jamun seed and Pradhan [133] for Karanja kernel. Bulk density and moisture content relationship of Charoli nut has expressed as in equation (16)

$$\rho_b = -8.864 \, M_C + 734.46 \, (R^2 = 0.9834) \tag{16}$$
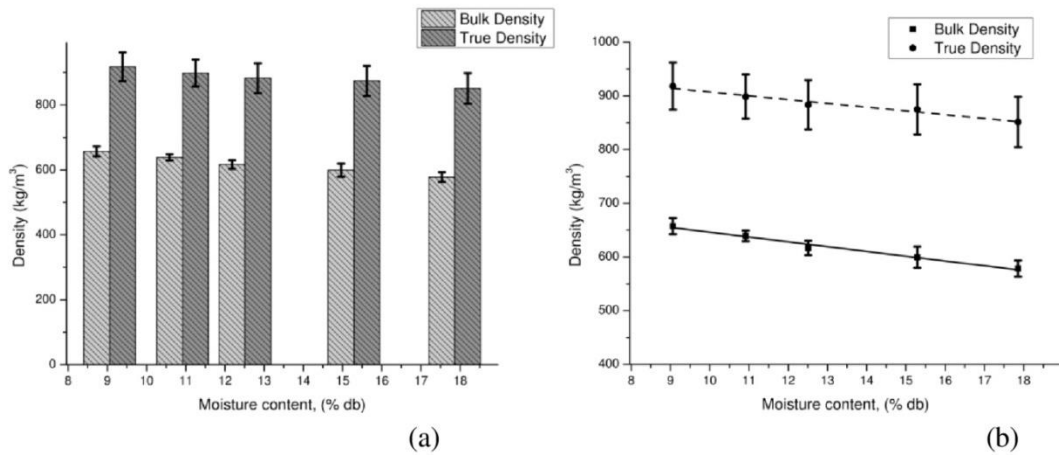
Figure 3.7. (a) Bar chart and (b) variation in bulk and true density at individual moisture content of Charoli nut.

The true density is a real mass of Charoli nuts with excluding a pores / empty spaces. Decrease in true density might be because of a higher true volume. The true density signifies the nuts are heavy in weight and will not float on water. Similar trend of contrary connection between moisture content and true density has been reported for pistachio nuts (Kashaninejad et al. 2005) [134]; sorghum (Mwithiga and Sifuna 2006) [135]; and spinach seeds (Kilickan et al. 2010) [136]. The variation in true density have been expressed as in equation (17)

$$\rho_t = -7.056 \, M_C + 977.7 \, (R^2 = 0.9666) \tag{17}$$

Porosity (ε) % value communicates the inter–granular to a total occupied space of the nut. Porosity dependency on a bulk and true density is diverse for individual nut with moisture content increment. A slight increment in porosity value of Charoli nut was observed with increment in moisture content. Porosity of Charoli nuts increased from 28.40% to 32.05% with moisture content increment from 9.06% to 17.86% (d.b.). A moisture content effect on porosity is shown in Fig. 3.8 (a) and (b).
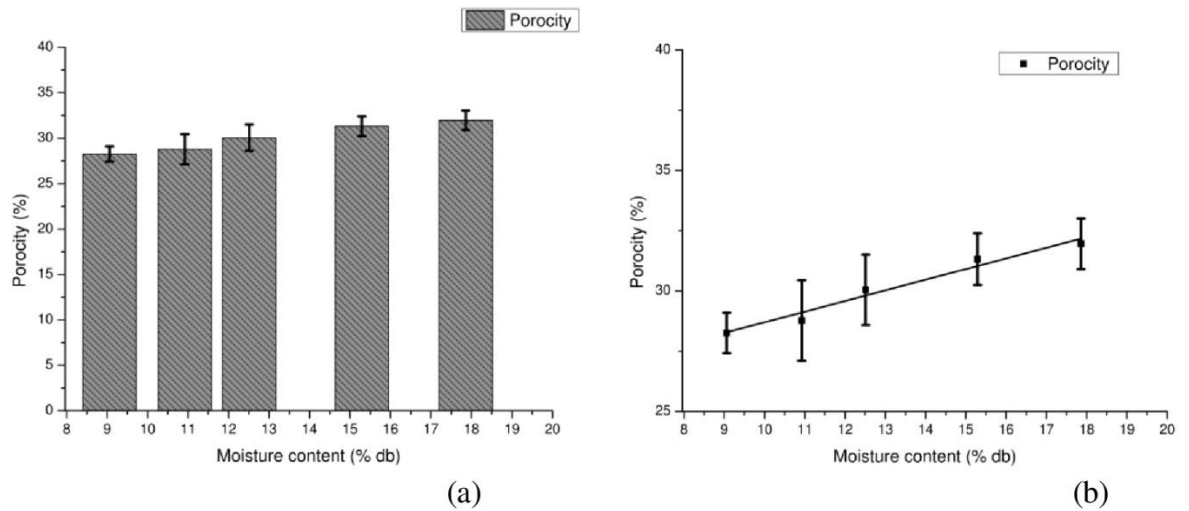
Figure 3.8. (a) Bar chart and (b) variation in porosity at individual moisture content of Charoli nut.

The porosity of nuts provides the significance of the resistance to the air flow at aeration or drying. A similar linear increment in porosity has been found for gram [137] (Chowdhury et al. 2001); chickpea seed (Konak et al. 2002) [138]; and Brachystegia Eurycoma seed (Aviara et al. 2014) [139]. Morphological characteristics play an important role in increase or decrease of porosity of nuts observed by the result. The linear correlation was observed in porosity and moisture content of nuts, and it can be shown by a regression equation (18):

$\varepsilon = 0.4461\, M_C + 24.345$ $(R^2 = 0.9654)$ (18)

3.5 Measurement of frictional properties

1.5.1 Coefficients of static friction

Coefficients of static friction (μ) of Charoli nut at five moisture contents was estimated for distinct frictional surfaces specifically aluminium, plywood, and rubber [140]. The samples were kept in open-ended wooden container of 150 x 150 x 50 mm size and the container was kept on the adjustable friction material tilting surface [141]. Schematic of the arrangement is as shown in Figure 3.9. A friction material surface was inclined slowly until a container begins sliding on the surface and the tilting angle was recorded with the help of a graduated scale provided near surface. A

coefficient of static friction (μ) was determined with Equation (19).

μ = tan θ $\qquad$ (19)

Where, μ- coefficient of static friction and θ- tilt angle (degree).
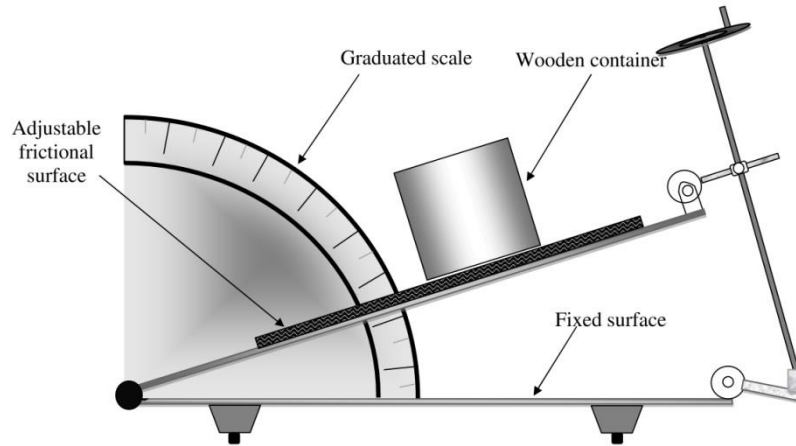
Figure 3.9 Schematic of the arrangement for measurement of coefficient of static friction of Charoli nut.

The result of the coefficient of static friction (μ) of Charoli nut having different moisture contents (9.06, 10.92, 12.51, 15.29, and 17.86 % db) on three frictional surfaces as aluminium, plywood, and rubber is presented into Fig. 3.10 (a) and (b). A value of μ increased significantly with moisture content. The μ increases linearly from 0.367 to 0.495, 0.381 to 0.512, and 0.432 to 0.585 for aluminium, plywood, and rubber respectively within the moisture range between 9.06–17.86% (d.b.).
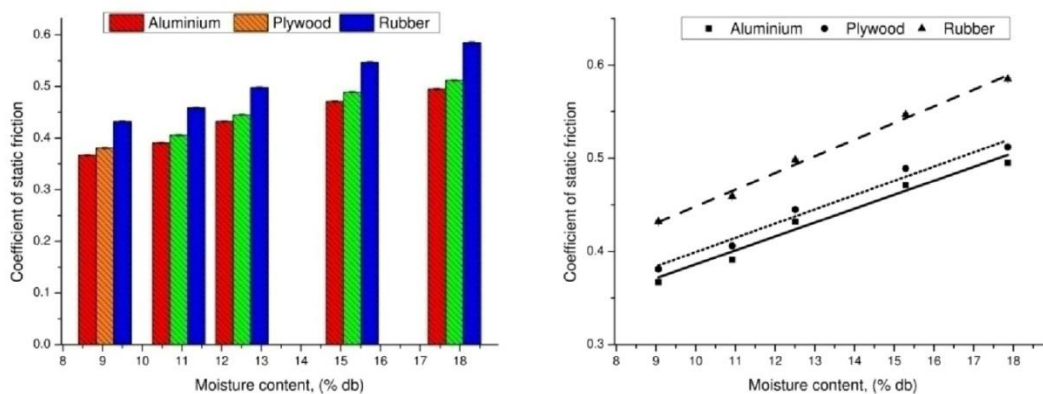
Figure 3.10 (a) Bar chart and (b) variation in coefficients of static friction at individual moisture content of Charoli nut.

The value of coefficient of static friction varies linearly with increment in moisture content. A highest value of (μ) found at high moisture content in all of three surfaces. An increment in value of (μ) may be because of an increment in cohesive force between Charoli nut and contact surfaces. Nut becomes rough with increase in moisture content which ultimately reduces its sliding characteristics. Coefficient of friction results were similarly stated by Mirzabe et al. (2017) [142] for cucumber seeds and Tabatabaeefar (2003) for wheat [143].

The correlation in coefficient of static friction with moisture content of aluminium, plywood, and rubber are presented in equations. (20), (21), and (22), respectively:

$$\mu_{al} = 0.01509 \ M_C + 0.2331 \quad (R^2 = 0.9766) \quad (20)$$

$$\mu_{ply} = 0.01552 \ M_C + 0.2428 \quad (R^2 = 0.9790) \quad (21)$$

$$\mu_{ru} = 0.017847 \ M_C + 0.2699 \quad (R^2 = 0.9944) \quad (22)$$

1.5.2 Static and dynamic angle of repose

Cylinder having 150 mm diameter and 250 mm height was used to find a static or filling angle of repose. The cylinder was filled by Charoli nut kept on middle portion of the circular plate. Then the cylinder was then removed gradually until nut sample formed of the cone shape on the circular plane [144]. The cone height and diameter was measured to calculate an angle of repose (θ_f) utilizing a formula (23).

$$\theta_f = \tan^{-1} \left(\frac{2H}{D} \right) \quad (23)$$

Where, D and H are the cone diameter and height, respectively.

A fiberglass box of dimension $200 \times 200 \times 200$ mm was utilized for finding a dynamic or emptying angle of repose. Complete box was filled by Charoli nut and front panel of the box was immediately slid upwards. Because of this sudden slid the sample nuts were flow outside and form a heap. Samples height between two points (b1, b2) in the sloping Charoli nut heap and a horizontal dimensions at different point (a1, a2) were noted. A dynamic or emptying angle of repose (θ_e) was determined with a relationship (24) [120].

$$\theta_e = \tan^{-1} \left[\frac{(b2-b1)}{(a2-a1)} \right] \qquad (24)$$

Dynamic and static angle of repose plays key role while designing a hoppers for Charoli nuts where bulk of the materials are in motion [145].

Variations of the static and dynamic angle of repose of Charoli nut within moisture range of 9.06–17.86% (db) are presented in Fig. 3.11 (a) and (b). A value of static and dynamic angle of repose increased significantly by 16.52º to 22.31º and 27.91º to 33.23º respectively with respect to moisture content ranging from 9.06–17.86% (db).
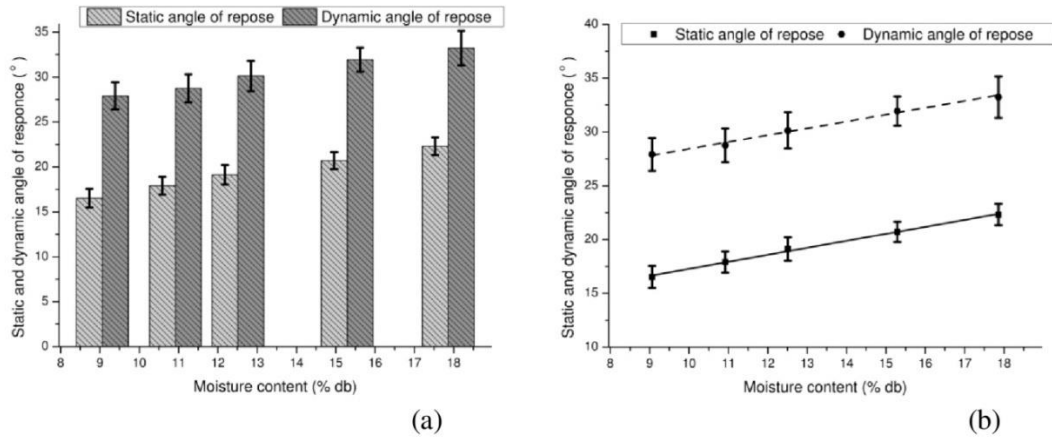
Figure 3.11. (a) Bar chart and (b) variation in coefficients of angle of repose at individual moisture content of Charoli nut.

The angle of repose indicates the nuts flow–ability. It is also characteristic indicating the cohesion between nut and the surface layer of moisture of nut. With increase in moisture content, surface of nut becomes rough. Therefore, for easier flow–ability of nut, hopper angle must be more than 35º.

The relationship between static and dynamic angle of repose of Charoli nut with respect to moisture content is represented in equation 25 and 26.

$$\theta_s = 0.6503\ M_C + 10.777\ (R^2 = 0.9965 \qquad (25)$$
$$\theta_d = 0.6274\ M_C + 22.156\ (R^2 = 0.9928 \qquad (26)$$

3.6   Measurement of aerodynamic properties

Terminal velocity of Charoli nut was measured by air column at 9.06, 10.92, 12.51, 15.29, and 17.86 % db moisture content. Schematic of the arrangement for measurement of terminal velocity is as shown in Figure 3.12. During the test, Charoli nut sample was dropped inside stream of air from upper side of the air column [146]. Then flow of air was increased gradually until nut sample got suspended into stream of air. The digital anemometer (least count 0.1 m/s) was utilized for measurement of air velocity near nut suspension point.
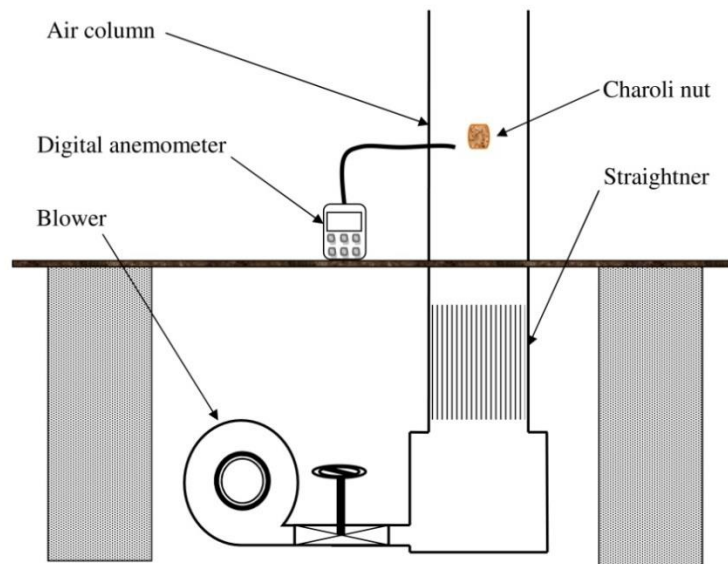
Figure 3.12. Schematic of the arrangement for measurement of terminal velocity of Charoli nut.

An experimental result for variations of the terminal velocity (V_t) of Charoli nut with respect to moisture content ranging from 9.06–17.86% (db) are shown in Fig. 3.13 (a) and (b). With increment in moisture content (9.06–17.86% (db)), increment into terminal velocity noted from 13.21 to 14.94 m/s.

An increment into terminal velocity with respect to moisture content is due to an increment in frontal area mass of a nut offered to a stream of air. Terminal velocity data may be useful for various post-harvest operations like separation from impurities, cleaning and transportation. The relationship between the terminal velocity of Charoli nut with respect to moisture content is represented in equation 27.
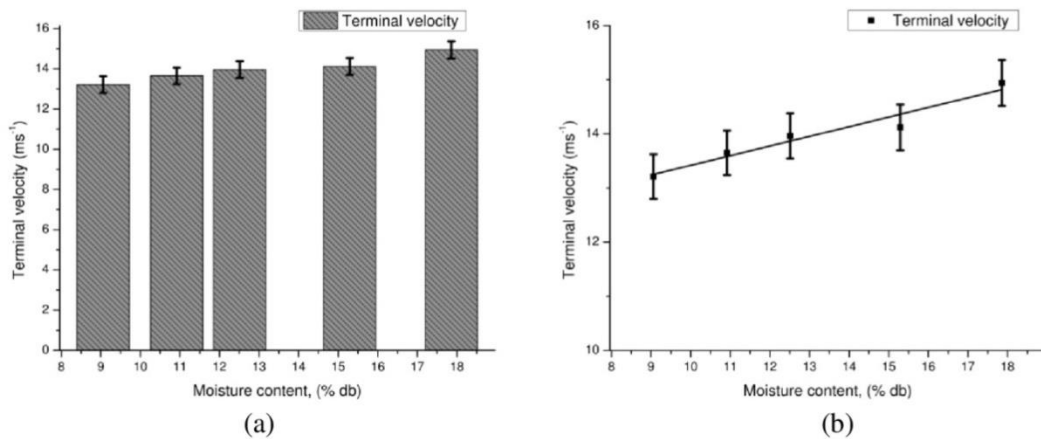
Figure 3.13. (a) Bar chart and (b) variation in terminal velocity at individual moisture content of Charoli nut.

$$V_t = 0.1784 \, M_C + 11.634 \; (R^2 = 0.9465) \qquad (27)$$

Present study has been conducted to find various characteristics like physical, frictional and aerodynamic characteristics of nut. The results of this study indicated moisture content significantly influences and modifies the physical, frictional and aerodynamic properties. Following major conclusions are obtained by the study.

1. In all properties, only the true and bulk densities decreased with increment in moisture content whereas remaining properties were increased. Increments in the properties are attributed mostly to the cellular arrangements and water absorption by the nut.

2. The mean values for the sphericity of nuts were increased from 86.42 to 88.64 % with moisture content which shows the tendency of rolling than sliding upon the surface. This is helpful while designing handling and sorting systems for the nuts.

3. The surface area increased from 134.52 and 352.97 mm^2 which shows more attention needs to take while designing of sizing system. The nuts having higher moisture content needs more space for heat transfer while freezing or drying.

4. The gravimetric properties such as thousand nut mass and porosity increased linearly from 0.134 kg to 0.421 kg and 28.40% to 32.05%, respectively, whereas bulk and true density decreased. Decrease in a bulk density was noted because of increase

of mass due to gaining of moisture. Whereas the true density signifies the nuts are heavy in weight and will not float on water.

5. The coefficient of static friction increased with moisture content and found highest in case of rubber as compared to aluminium and plywood. An increment in the value of (μ) is because of cohesive force increment.

6. The static and dynamic angle of repose increased significantly from 16.52^{o} to 22.31^{o}, and 27.91^{o} to 33.23^{o}. Therefore, for easier flow–ability of nut, hopper angle must be more than 35°.

7. Terminal velocity of nut increased in linear manner from 13.21 to 14.94 m/s. This terminal velocity data may be useful in different post–harvest operations like separation from impurities, cleaning and transportation.

These results provide valuable information to various scientists, technologists, and engineers having keen interest for development of sustainable mechanization for postharvest processing of Charoli nut.

CHAPTER 4

EXPERIMENTATION USING DESIGN OF EXPERIMENTATION

Chapter 4 comprises details about the experimental set up. Detailed experimentation variables, their test envelop, test sequence is discussed. In this chapter, experiments are performed as per Taguchi's L27 orthogonal array and experimental data is generated for its further analysis.

4.1 Experimental Set-up

It is important to develop an experimental setup that includes provisions for setting test points, modifying test sequences, carrying out suggested experimental plans, and providing instruments for recording responses and independent variables. The experimental setup is built with different physical features of its parts in mind. For example, if it involves a gear, it must be developed using the gear design method. From the perspective of strength, there is scope for further improvement in this experiment in terms of Charoli nut desheller design. The remaining parameters of the Charoli nut desheller are developed based on past mechanical design expertise and practise, with the assumption that the process would operate at the specified feed condition. This is due to the fact that just that data is available.

The experimental setup is intended to meet the aforementioned conditions, so that the predetermined test points may be appropriately placed inside the test envelope given in the experimental plan. The method for designing the experimental apparatus, on the other hand, cannot be completely followed in the field experimentation. This is because in the field trial, the available ranges of the numerous independent variables to estimate the value of the dependent variable were used.

Experimental set up comprises of three units [78], [79], [83]:

1. **Pedeling Unit:** Pedeling Unit mainly comprises of Bicycle, Chain Sprocket, Pedal , Chain, Freewheel , Bearings for bicycle side and Speed amplification gear pair.

2.   Energy Unit: Energy Unit mainly comprises of Flywheel, Torque amplification gear pair, bearings and Clutch

3.   Process Unit Process Unit mainly comprises of Pair of Abrasive stone disc, Cross plate, Pair of Shaft, pair of bevel gear, 3 layer screens with reducing grade size and Cam System
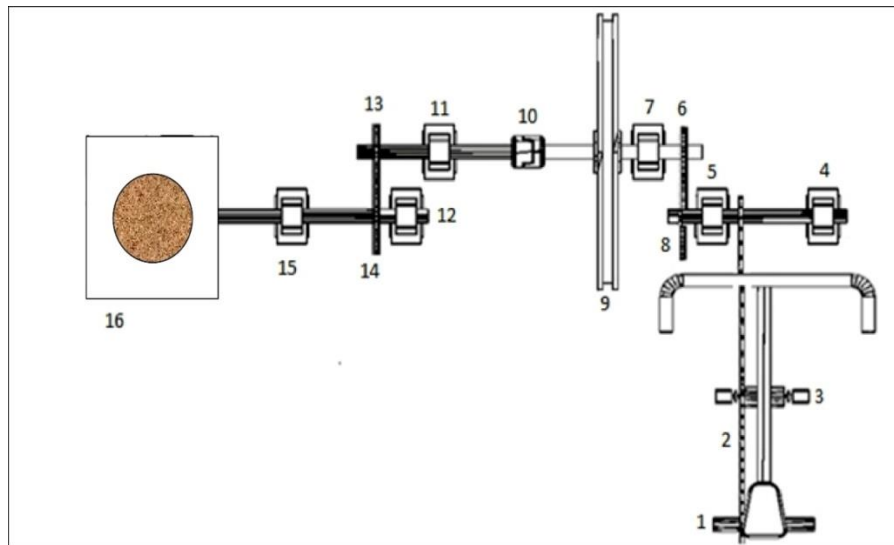
Figure 4.1: Line diagram of experimental set up [78], [79], [83]

1 - Chain Sprocket, 2 - Chain, 3 - Pedal, 4 & 5 - Bearing for bicycle, 6 - Gear I, 7 - Bearing Flywheel Shaft, 8 - Gear – II, 9 – Flywheel, 10 – Clutch, 11 - Bearing for flywheel shaft, 12 - Bearing for Process Unit Shaft, 13 - Gear – III, 14 - Gear – IV, 15 - Bearing for Process Unit Shaft, 16 - Process Unit.

Figure 4.2: Pictorial view of complete fabricated set-up

Figure 4.3: Pictorial view 2 of complete fabricated set-up

In this experimental work, the peddling process of bicycle mechanism transmits the human energy to the kinetic energy of the flywheel [78]. The stored energy of the flywheel will be utilized as per need for the actual deshelling process. So, operations

could be performed intermittently. Modak [79] reports on the functional feasibility and financial viability of bicycle operated mechanism. A driver peddles pedal and converts the oscillatory motion into the rotational motion of flywheel, thereby increasing speed. The inertia required to the flywheel provided by the legs of the rider is only. The rider needs to store the energy in the flywheel as per his/her capacity. Thus, with the help of this human mechanism, human muscular strength gets converted into the rotational kinetic energy of the flywheel. It was essential to develop the energy unit of a similar kind for Charoli desheller scientifically.

4.2 Identification of process variables

Variables are used in a very broad meaning to refer to any physical quantity that changes. An independent variable is one that may be modified independently of the other values. If a physical quantity varies as a result of the modification of one or more variables, it is referred to be a dependant or response variable. Table 4.1. shows the various variables considered for study, their corresponding symbols and units

Table 4.1. Variables considered for study, their corresponding symbols and units

Type of Variable	Description of Variables	Symbol	Unit
Dependent	Deshelling efficiency	η_d	%
	Whole kernel recovery	η_w	%
	Broken kernels	η_b	%
	Partially shelled / unshelled nuts	η_u	%
	Resistive torque	T_r	N-mm
	Processing time (1000 nuts)	T_p	Sec
Independent	Feed rate	ψ	kg/hr
	Moisture content	M_c	% d.b
	Clearance	C_d	mm
	Thickness of the grinding disk	t	mm
	Rotational speed of the flywheel	V_f	rpm

4.3 Test Planning of Experiment

Test planning or test plan of experiment refers to the process of determining the test envelope, test points, test sequence, and experimental plan for a derived set of dimensional equations [83].

4.3.1 Determination of Test Envelope

The test envelope comprised of deciding the end points or limitations, and it is the apparent and best approach to pick or fix the test points. The test envelope includes all of these test points. As a result, it is clear to determine the full range throughout which the entire experiment is carried out.

4.3.2 Determination of Test Points

The spacing of the independent variables in a specified and most effective method will result in an efficient and compact experimental plan. Ideally the every part of the curve should be represented by test points but in actual situation it has got the constraints imposed by experimental set up, and research funds. As a result, the idea of correct spacing of test points has given way to acceptable spacing of test points. The decided test points for Charoli nut deshelling machines are as shown in Table 4.2.

4.3.3 Determination of Test Sequence

The test sequence is chosen by reversible or irreversible nature of experiments [83]. Basically all the tests are irreversible in sense; no apparatus can be brought to the original state of configuration after use. If the changes imposed by testing are below the level of detection such tests can be assumed as reversible. In current research, test sequence has been decided as per Taguchi method. Because the bulk of engineering experiments employ a somewhat randomised design, it is used to test the phenomena.

Table 4.2. Test envelop and test point for experimentation

S.N.	Description of Variables	Test envelop	Test points
1	Feed rate (ψ)	15 kg/hr – 25 kg/hr	15 – 20 – 25 kg/hr
2	Moisture content (M_c)	9 % d.b – 17 % d.b	09 – 13 – 17 % d.b
3	Clearance (C_d)	6 mm – 10 mm	06 – 08 – 10 mm
4	Thickness of the grinding disk (t)	19 mm – 32 mm	19 – 25 – 32 mm
5	Rotational speed of the flywheel (V_f)	400 rpm – 600 rpm	400 – 500 – 600 rpm

4.4 Experimental Procedure

The detailed procedure of performance of the test as per the experimental plan prepared for this test is stated here. The test involves subdivisions as given below.

• Measurement of rotational speed (before engagement of clutch) of the flywheel.

• Measurement of speed (after engagement of clutch) of the process unit

• Measurement of time (after engagement of the clutch) of the process unit.

• Calculation of the Resistive Torque

• Setting up the disk and clearance between the disk of the charoli nut desheller as per the plan.

4.4.1 Measurement of Speed of the Flywheel before Engagement of Clutch

A tachometer is used to measure the speed of the flywheel. Before engaging the clutch, the selected speed of the flywheel is determined by trial. When the necessary speed is reached, the clutch is engaged to power the process unit.

4.4.2 Measurement of Time of the Process Unit after Engagement of the Clutch.

When the flywheel achieves the appropriate speed, the clutch is engaged to the process unit, and the time required to deshell the nut is monitored using a smart watch during experimentation. These readings are recorded and noted for reference.

4.4.3 Calculation of the Resistive Torque

When energy of the flywheel is communicated to the process unit by means of engagement of clutch, the torque is estimated. The values of the resisting torque are calculated by formula given b equation 28, 29

$$\text{Resisting Torque} = \frac{I_T}{g} \propto \qquad (28)$$

$$\text{where } I_T = I_{F(EQ)} + I_C \qquad (29)$$

Where I_T is the Moment of Inertia of cutter shaft with respect to flywheel shaft α is angular retardation of cutter shaft, I_F is equivalent moment of inertia of flywheel, I_C is moment of inertia of chaff cutter and g is acceleration due to gravity

4.4.4 Setting up the disk and disk clearence for deshelling as per the Plan.

The abrasive stone disk is fabricated for the experimentation so as to set the thickness of the disk as per the experimental plan. The experimental setup is provided with arrangement of changing the disk as per requirement. Disk clearance is adjusted by the nut arrangement provided therein.

4.5 Procedure of experimentation

The schematic diagram of an experimental setup is shown in Figure 4.2 and Figure 4.3. An unskilled operator of slim stature and middle height operates system similar to bicycle by pedaling thereby spinning the flywheel. Chain drive used in bicycle is required to be irreversible, which is achieved by conventional bicycle drive having a free wheel.

When flywheel attends the pre-decided speed, the clutch is engaged. A double jaw spiral clutch is used here. Clutch drives the cutter through gears. Gear ratio of 1:3 has been used for attending the maximum process time. Angular velocity of output shaft and flywheel shaft is to be measured.

Five (05) people between the ages of 30 and 40 were chosen to perform the experiments. All of the experiments began at 11 a.m. (8th – 26th February 2021) at our workshop at Priyadarshini College of Engineering in Nagpur, Maharashtra, India,

where the room temperature ranged from 30-35 degrees Celsius. The rider controls the device in the same way as a bicycle does by pedalling the pedals and spinning the flywheel at the desired speed for a particular time, storing energy in the flywheel. After attaining the specific speed of the flywheel, peddling is stopped and flywheel shaft is connected to processing unit through spiral jaw clutch and energizes the Charoli nut desheller.

Samples of Charoli nut with 09, 13, & 17 % d.b moisture have been prepared for the experiments. The 1000 samples of the nuts were fed into the deshelling chamber via a hopper as per the experimental plan. The clearance between the disk is adjusted by nut bolt arrangement provided therein as per experimental plan. Feed rate is adjusted via feed adjusting plate provided at the bottom of the hopper. After the clutch engagement the desheller starts deshelling the nuts and gets speed getting retarded after some time. Time taken for deshelling the nuts was recorded with the help of real time mobile clock. The unshelled and partially shelled nuts are then counted manually to obtain the deshelling efficiency. Further for obtaining the whole kernel percentage, the whole kernels are counted manually and on the basis of this data, broken kernels are counted. The same process is repeated for all 27 numbers of runs as per Taguchi's design.

4.6 Design of Experimentation

Because there are so many governing processing factors, systematic experimentation and analysis might be challenging. A single parameter modification will have a complicated impact on the process. Thus, for identifying the patterns of variation in process, the numerous elements impacting the process must be understood. Statistical and analytical approaches are utilized to identify the best combination of process variables for maximum performance. Unfortunately, relating the input process variables to responses metrics is quite difficult.

Experiments may be used to model a process, and they're also a good method to get around the tiresome challenge of connecting process parameters to performance measurements. As a result, in order to organise trials with meaningful outcomes, a scientific methodology is required. The statistical design of experiments allows for the

collection and analysis of suitable data using statistical methods, resulting in reliable and objective findings. When dealing with data that has been exposed to experimental error, statistical technique is the sole objective way of analysis. Thus, an experimental problem has two components: the design of the trials and the statistical analysis of the results. These two aspects are inextricably linked since the technique of analysis is directly dependent on the design of experiments used. There are several benefits to utilising the design of experiment technique:

- Determination of the impact of process factors on performance measures.
- Substantial decrease in the number of trials to be carried out.
- It is possible to precisely anticipate the optimal combination of parameters.
- It is possible to calculate the experimental error.
- Parameters can be estimated qualitatively.

4.6.1 Design of Experimentation Using Taguchi Method

Taguchi techniques are a systematic and effective strategy to improve design performance, quality, and cost. In industries like as cars and consumer electronics, Taguchi techniques have been utilised effectively in United States and Japan to create dependable, higher-quality products at cheap costs [147]. Taguchi's methodologies, rather than advanced statistical tools, emphasise the successful implementation of technical concepts. It encompasses both upstream and downstream quality engineering. Upstream techniques employ small-scale trials to decrease variability while being cost-effective, as well as strong designs for large-scale manufacturing and market place. Shop-floor procedures give low-cost, real-time solutions for monitoring and sustaining production quality.

Taguchi's technique to variable design gives an ensure effective and efficient way for obtaining near-optimal design requirements for cost and performance to the design engineer [148]. The Taguchi approach uses orthogonal arrays (OA) from design of experiments theory to evaluate a large number of parameters with a small number of tests. The "OA" s are Graeco-Latin squares that have been generalised. Selecting the most relevant OA and assigning the variables and interactions of concern to the proper columns is the first step in designing an experiment. Taguchi

suggests using linear graphs and triangle tables to make variable allocation easier. The array compels all investigators to create tests that are almost similar.

The Taguchi approach analyses experiment data in order to achieve several of the following goals [149]:

- To determine the right or most ideal conditions for a product or procedure.

- The contribution of individual factors and interactions must be estimated.

- To calculate the responses under ideal conditions

By examining the major effects of each of the factors, the ideal situation is discovered. The major impacts show the overall trends of each parameter's influence. The ability to determine the contribution of various factors is crucial in determining the type of control that should be implemented on a manufacturing process. The analysis of variance (ANOVA) is the statistical method most often used for determination of percent contribution of every parameter against a specified degree of confidence in the findings of experiments. The ANOVA table for a particular analysis may be used to determine which parameters need to be controlled [149].

There are mainly four phases in Taguchi's Method,
1. Planning for experiments
2. Conduction of experiments
3. Analysis of experiments, and
4. Validation

Various steps involved in different phases are shown in Figure 4.4.
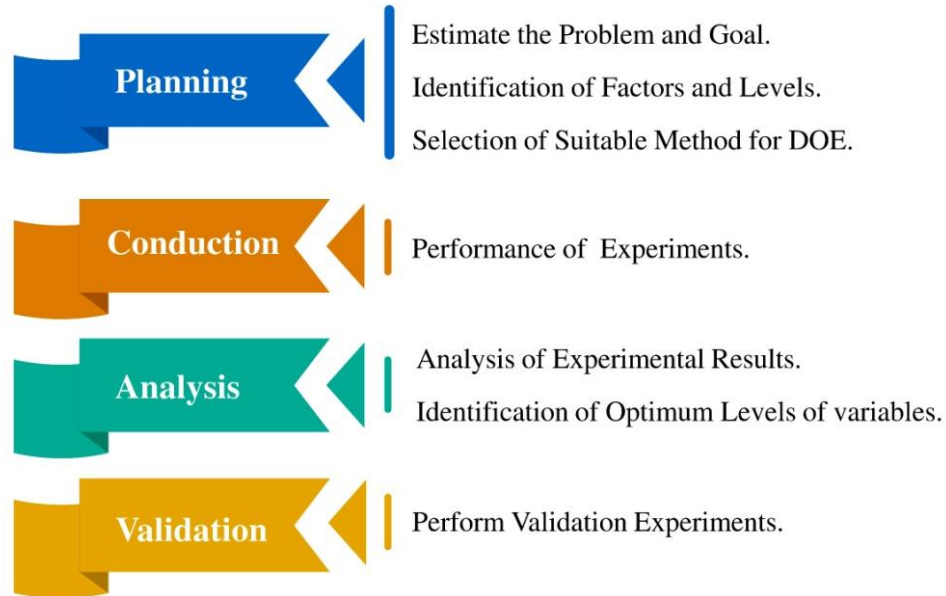
Figure 4.4. Various phases and steps concerned in Taguchi process.

The experiment has been carried out using five factors and three-level process variables. The process variables include feed rate, moisture content percent, clearance, thickness of the grinding disk and rotational speed of the flywheel. The selected process variables with corresponding levels are shown in Table 4.3.

Table 4.3 : Process variables with corresponding levels

Column	Factors	Level 1	Level 2	Level 3
A	Feed rate (ψ) in (kg/hr)	15	20	25
B	Moisture content (M_c) in (% d.b)	9	13	17
C	Clearance (C_d) in (mm)	6	8	10
D	Thickness of the grinding disk (t) in (mm)	19	25	32
E	Rotational speed of the flywheel (V_f) in (rpm)	400	500	600

A complete factorial design typically necessitates $3^5 = 243$ experimental runs. Carrying out a design with 243 trials necessitates unnecessary work and incurs a large experimental cost, making it unfeasible to implement.

Table 4.4: L27 (3^5) OA of the experimental runs

Experiment no. / Factors	A	B	C	D	E
	(ψ) (kg/hr)	(M_c) (% d.b)	(C_d) (mm)	(t) (mm)	(V_f) (rpm)
1	15	9	6	19	400
2	15	9	8	25	500
3	15	9	10	32	600
4	15	13	6	25	500
5	15	13	8	32	600
6	15	13	10	19	400
7	15	17	6	32	600
8	15	17	8	19	400
9	15	17	10	25	500
10	20	17	6	19	500
11	20	17	8	25	600
12	20	17	10	32	400
13	20	9	6	25	600
14	20	9	8	32	400
15	20	9	10	19	500
16	20	13	6	32	400
17	20	13	8	19	500
18	20	13	10	25	600
19	25	13	6	19	600
20	25	13	8	25	400
21	25	13	10	32	500
22	25	17	6	25	400
23	25	17	8	32	500
24	25	17	10	19	600
25	25	9	6	32	500
26	25	9	8	19	600
27	25	9	10	25	400

Where, (ψ) - Feed rate, (M_c)- Moisture content, (C_d)- Clearance between disks,

(V_f)- Rotational speed of the flywheel and (t)- Thickness of the grinding disk

In this work, the 5 processing parameters were studied using 27 experimental runs based on the OA L27 (3^5) as indicated in Table 4.4. For studying the effects of feed rate, moisture content percent, clearance, thickness of the grinding disk and

rotational speed of the flywheel on the deshelling efficiency, whole kernel recovery, broken kernels, partially shelled / unshelled nuts, resistive torque and processing time (1000 nuts), the Charoli nuts were deshelled using the machine as per Taguchi L27 array. For determination of the response variables, trials were conducted by deshelling the 1000 nuts. After conduction of each test the deshelled nuts, whole kernels, broken kernels, unshelled nuts, partially shelled nuts were measured manually and the responses were computed using the standard equation. Table 4.5 shows the experimentation results. The experimental data are analyzed using the software MINITAB 17 specially used for the design of experiment applications.

Table 4.5: L27 (3^5) OA of the experimental runs and responses

Expt. no. / Responses	(η_d) (%)	(η_w) (%)	(η_b) (%)	(η_u) (%)	(T_r) (N-mm)	(T_p) (Sec)
1	84	65.5	18.5	16	96364.488	74
2	82.1	65.6	16.5	17.9	129916.95	75
3	79.8	68.6	11.2	24.4	123945.45	76
4	83.2	66.5	16.7	14.7	104410.36	80
5	82.6	71	11.6	18.8	109014.2	77
6	79.8	62.2	17.6	27.5	130280.15	77
7	80.8	69.4	11.4	16.9	125714.17	85
8	79.5	62	17.5	22.8	135984.9	80
9	77.1	61.6	15.5	28.4	112077.33	82
10	79.4	63.5	15.9	18.5	104356.05	71
11	77	66.2	10.8	21.4	116254.85	69
12	75.2	58.6	16.6	28.5	112538	67
13	82.1	70.6	11.5	10.8	116492.71	67
14	79.9	62.3	17.6	17.6	95916.216	65
15	77	61.6	15.4	25.7	105850.27	64
16	81.2	63.3	17.9	12.4	124754.95	67
17	79.7	63.7	16	19.6	110508.38	64
18	77.5	66.6	10.9	26.8	126730.54	65
19	81	69.6	11.4	12.6	146322.31	58
20	79.2	61.7	17.5	18.8	118791.27	56
21	77.6	62	15.6	27.6	123293.51	55
22	77.8	60.6	17.2	17.3	121341.73	61
23	75.1	60	15.1	20.9	119725.16	58

24	72.9	62.6	10.3	29	136359.54	57
25	80.2	64.1	16.1	11.2	115339.06	56
26	77.8	66.9	10.9	17.4	138207.55	54
27	75.7	59	16.7	26.5	104198.86	53

Where, (η_d)- Deshelling efficiency, (η_w)- Whole kernel recovery, (η_b)- Broken kernels, (η_u)- Partially Shelled / Unshelled nuts, (τ_r)- Resistive Torque, (T_p)- Processing time (1000 nuts)

CHAPTER - 5
ANALYSIS OF EXPERIMENTAL DATA

Chapter 5 comprises information about approach for analysis of experimentation by Taguchi method and ANN model formulation. In this chapter, experiments are performed as per Taguchi's L27 orthogonal array. Analysis is performed as suggested by Taguchi and ANN model is developed based on the experimental data.

In this work, the 5 processing parameters were studied using 27 experimental runs based on the OA L27 (3^5) as indicated in Table 5.1. For studying the effects of feed rate, moisture content percent, clearance, thickness of the grinding disk and rotational speed of the flywheel on the deshelling efficiency, whole kernel recovery, broken kernels, partially shelled / unshelled nuts, resistive torque and processing time (1000 nuts), the Charoli nuts were deshelled using the machine as per Taguchi L27 array [150]. For determination of the response variables, trials were conducted by deshelling the 1000 nuts. After conduction of each test the deshelled nuts, whole kernels, broken kernels, unshelled nuts, partially shelled nuts were measured manually and the responses were computed using the standard equation. The experimental data are analyzed using the software MINITAB 17 specially used for the design of experiment applications [151].

Table 5.1: L27 (3^5) OA of the experimental runs and responses

Expt. no. / Responses	(η_d) (%)	(η_w) (%)	(η_b) (%)	(η_u) (%)	(τ_r) (N-mm)	(T_p) (Sec)
1	84.0	65.5	18.5	16	96364.488	74
2	82.1	65.6	16.5	17.9	129916.95	75
3	79.8	68.6	11.2	24.4	123945.45	76
4	83.2	66.5	16.7	14.7	104410.36	80
5	82.6	71	11.6	18.8	109014.2	77
6	79.8	62.2	17.6	27.5	130280.15	77
7	80.8	69.4	11.4	16.9	125714.17	85
8	79.5	62	17.5	22.8	135984.9	80
9	77.1	61.6	15.5	28.4	112077.33	82

10	79.4	63.5	15.9	18.5	104356.05	71
11	77	66.2	10.8	21.4	116254.85	69
12	75.2	58.6	16.6	28.5	112538	67
13	82.1	70.6	11.5	10.8	116492.71	67
14	79.9	62.3	17.6	17.6	95916.216	65
15	77	61.6	15.4	25.7	105850.27	64
16	81.2	63.3	17.9	12.4	124754.95	67
17	79.7	63.7	16	19.6	110508.38	64
18	77.5	66.6	10.9	26.8	126730.54	65
19	81	69.6	11.4	12.6	146322.31	58
20	79.2	61.7	17.5	18.8	118791.27	56
21	77.6	62	15.6	27.6	123293.51	55
22	77.8	60.6	17.2	17.3	121341.73	61
23	75.1	60	15.1	20.9	119725.16	58
24	72.9	62.6	10.3	29	136359.54	57
25	80.2	64.1	16.1	11.2	115339.06	56
26	77.8	66.9	10.9	17.4	138207.55	54
27	75.7	59	16.7	26.5	104198.86	53

Where, (η_d)- Deshelling efficiency, (η_w)- Whole kernel recovery, (η_b)- Broken kernels, (η_u)- Partially Shelled / Unshelled nuts, (τ_r)- Resistive Torque, (T_p)- Processing time (1000 nuts)

5.1 Analysis for deshelling efficiency

Taguchi suggests using the signal-to-noise (S/N) ratio, which is determined because of deviations of features by the intended values. S/N ratios are calculated using Taguchi technique experimental data [152-155] For maximizing the deshelling efficiency of the Charoli nut, the ''the higher the better'' quality feature was used in this study. The Taguchi characteristic "the higher the better" is as follows (30):

$$S/_N = -10 \log \frac{1}{n}\left(\sum \frac{1}{y_i{}^2}\right) \qquad (30)$$

where S/N- deshelling efficiency signal-to-noise ratio, y_i-outcome of the i-th test for each experiment, and n-number of runs repeated. The S/N ratio change shown above

is appropriate for maximizing the deshelling efficiency. The S/N ratio variable analysis is utilized to determine statistical significant variables.

Table 5.2 shows the L27 (3^5) OA of the experimental runs, results, S/N ratio for deshelling efficiency

Table 5.2: L27 (3^5) OA of the experimental runs, results, S/N ratio for deshelling efficiency

Expt no. / Factors	A (ψ) (kg/hr)	B (M_c) (% d.b)	C (C_d) (mm)	D (t) (mm)	E (V_f) (rpm)	(η_d)	S/N ratio (db)
1	15	9	6	19	400	84	38.49
2	15	9	8	25	500	82.1	38.29
3	15	9	10	32	600	79.8	38.04
4	15	13	6	25	500	83.2	38.40
5	15	13	8	32	600	82.6	38.34
6	15	13	10	19	400	79.8	38.04
7	15	17	6	32	600	80.8	38.15
8	15	17	8	19	400	79.5	38.01
9	15	17	10	25	500	77.1	37.74
10	20	17	6	19	500	79.4	38.00
11	20	17	8	25	600	77	37.73
12	20	17	10	32	400	75.2	37.52
13	20	9	6	25	600	82.1	38.29
14	20	9	8	32	400	79.9	38.05
15	20	9	10	19	500	77	37.73
16	20	13	6	32	400	81.2	38.19
17	20	13	8	19	500	79.7	38.03
18	20	13	10	25	600	77.5	37.79
19	25	13	6	19	600	81	38.17
20	25	13	8	25	400	79.2	37.97
21	25	13	10	32	500	77.6	37.80
22	25	17	6	25	400	77.8	37.82

23	25	17	8	32	500	75.1	37.51
24	25	17	10	19	600	72.9	37.25
25	25	9	6	32	500	80.2	38.08
26	25	9	8	19	600	77.8	37.82
27	25	9	10	25	400	75.7	37.58

Where, (η_d) – Deshelling efficiency, (ψ) - Feed rate, (M_c)- Moisture content, (C_d)- Clearance between disks, (V_f)- Rotational speed of the flywheel and (t)- Thickness of the grinding disk.

Table 5.2 shows that for each input set of parameters, a separate set of output results for deshelling efficiency was achieved. The greatest and lowest percentages for deshelling efficiency were 84.00 and 72.90 percent, respectively. The responses in Table 5.3 were generated with Minitab software with respect to input variables.

A S/N ratio response table was used to analyze the effect of every control variables (feed rate, moisture content percent, clearance, thickness of the grinding disc, and rotating speed of the flywheel) on deshelling efficiency. Table 5.3 shows S/N ratio response table for deshelling efficiency. They display the S/N ratio for every level of a control variables and changes as the levels of every control variable are adjusted through one level to the next.

Table 5.3 S/N ratios response table (higher-is-better) for deshelling efficiency.

Level	(ψ)	(M_c)	(C_d)	(t)	(V_f)
1	38.17	38.04	38.18	37.95	37.96
2	37.92	38.08	37.97	37.96	37.95
3	37.78	37.75	37.72	37.97	37.95
Delta	0.39	0.33	0.45	0.02	0.01
Rank	2	3	1	4	5

Where, (ψ)- Feed rate, (M_c)- Moisture content, (C_d)- Clearance between disks, (V_f)- Rotational speed of the flywheel and (t)- Thickness of the grinding disk

The influence of five parameters for S/N ratio on deshelling efficiency is graphically illustrated in Figure 5.1 on the basis the S/N ratio. According to Table 5.3 and Figure 5.1, variables of the processes with greater S/N ratio values will provide

the optimised variable variants. The findings show that a feed rate of 15 kg/hr, a moisture content of 13% d.b, a clearance of 6 mm, a thickness of the grinding disc of 32 mm, and a rotating speed of the flywheel of 400 rpm result in the best deshelling efficiency. In addition, the most significant variables may be identified based on the rank in this table, that are clearance between disks, then feed rate, moisture content, thickness of the grinding disk and rotational speed of the flywheel. The optimum variable variant's levels are A_1, B_2, C_1, D_3, E_1, which indicates that the first factor on first level, second factor on second level, third factor on first level, fourth factor on third level, and fifth factor on first level. The interactions of parameters feed rate and clearance between disks, on all levels for deshelling efficiency is given in Figure 5.3
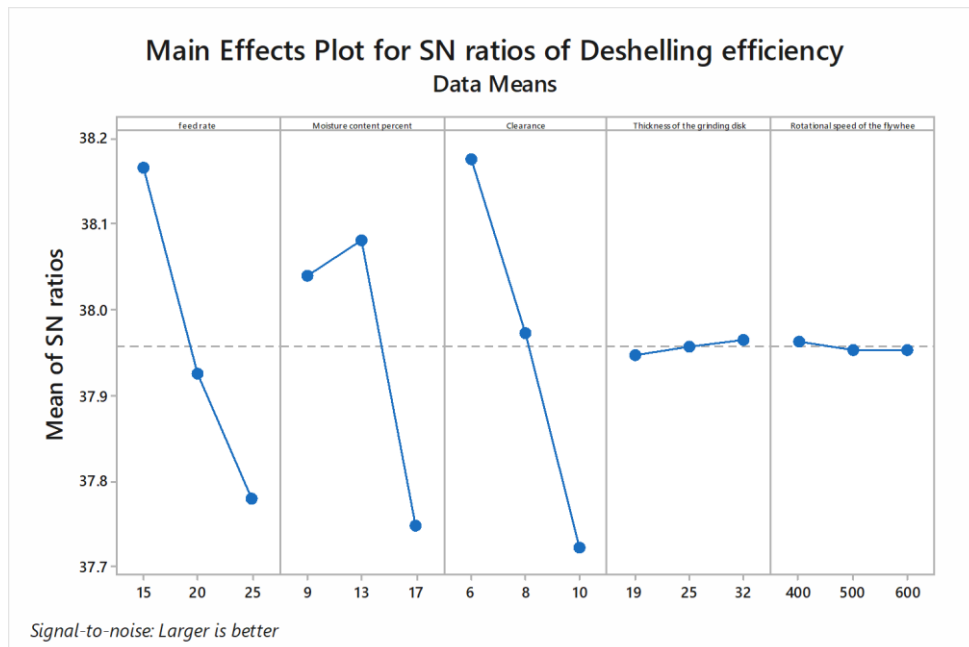
Fig. 5.1 Plot of main effect for S/N ratio of deshelling efficiency

The line slope connecting the levels in the S/N ratio influences graphs (Figs.5.1) evidently illustrates the strength of impact of each control variable. Specifically, the clearance between disk, followed by feed rate and moisture content, has been found to have a significant impact on deshelling efficiency and S/N ratios. The narrow slope of the lines indicates that the thickness of the grinding disks and the rotating speed of the flywheel have a smaller influence on deshelling efficiency.
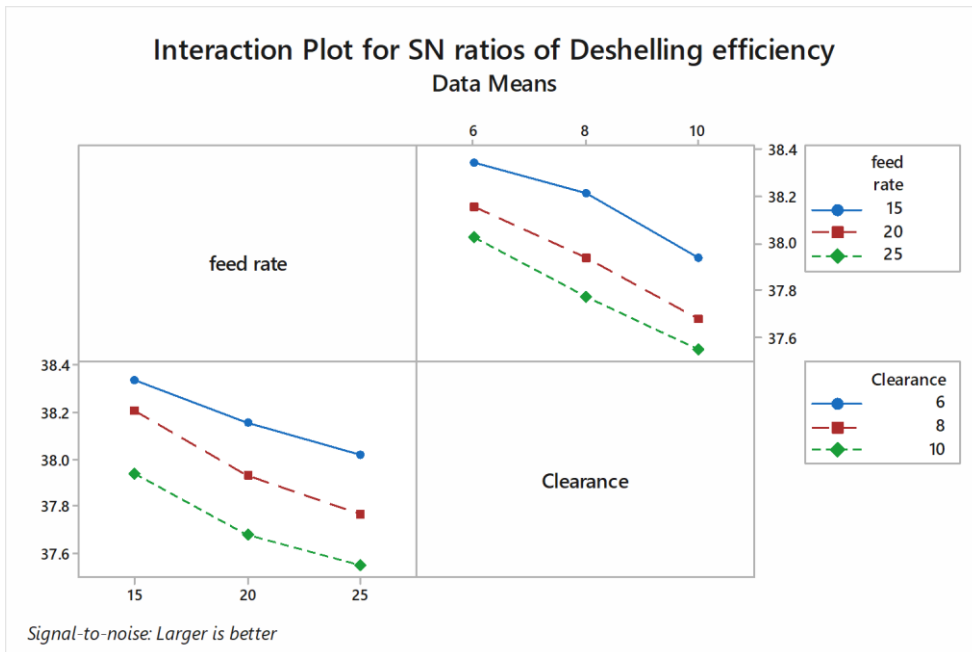
Fig. 5.2 Plot of main effect for S/N ratio of Effects of feed rate and clearance interactions on deshelling efficiency

Moreover, it can be seen in Fig. 5.2 that plot of interactions between feed rate and clearance that feed rate at 15 kg/hr and The changes of the thickness of the clearance of 6 mm gave the maximum deshelling efficiency.
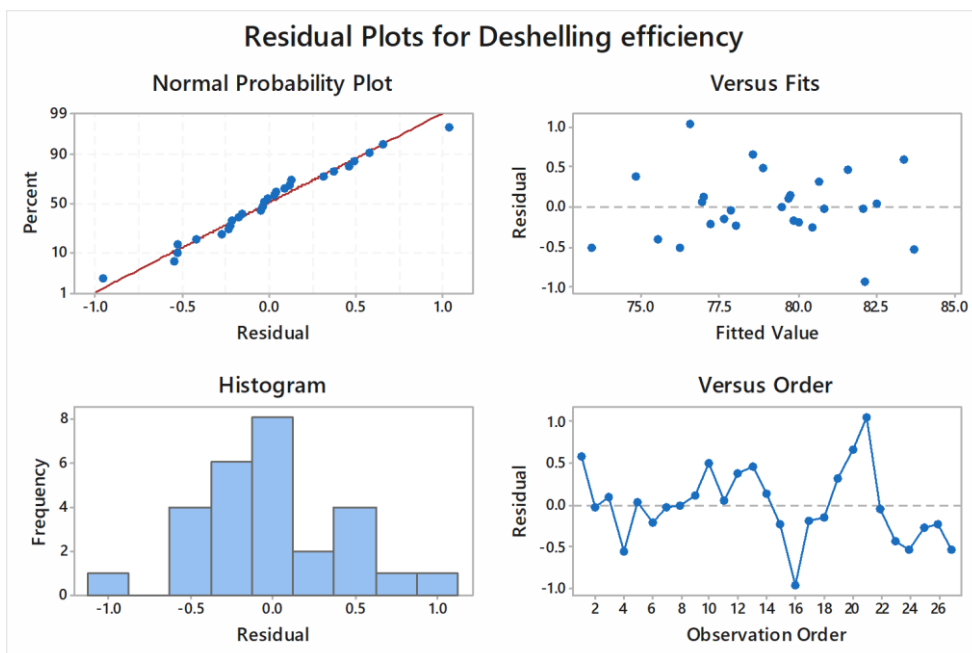
Figure 5.3: Residual plot for deshelling efficiency

Figure 5.3 depicts the residual plot for deshelling efficiency, which comprises a normality plot, a histogram, a fitted vs predicted plot, and a residual against observation order plot.

The normality plot demonstrates that almost the residuals follow a straight line, suggesting that the suggested model is fit. A histogram display shows a bell-shaped curve, suggesting that the data is normal. The residual vs fitted plot shows the randomized allotment on both sides of the reference line of all residuals.

Additionally, there is no pattern in the residual versus observation order plot, which is required for significant ANOVA. This confirms that the suggested model will have a good future outcome if all four tests are satisfied.

It is preferable to create the analysis of variance (ANOVA) for discovering the important factors to comprehend the impact of the different control variables upon the response of experimental data. To analyze the significant and non-significant process parameters, the ANOVA approach is utilized. ANOVA shows the effect of the every control variable on the result. The F and P values emphasize the significance of an input process variable on the output response. A greater F value or a lower P value signifies the significance of process variables on the output variable. To maintain the specific process variable significant at the 95 % confidence interval, the value of P must be less than 0.05. The lack of fit was found to be negligible for all responses, indicating that the model is capable of predicting the output values for every combinations of the process variables evaluated in the range [34].

Table 5.4 shows the results of analysis of variance (ANOVA) for deshelling efficiency. From the analysis, it is noted that clearance (PC = 40.87 %), feed rate (PC = 30.23 %), and moisture content percent (PC = 25.77 %) are the significantly affecting the deshelling efficiency. Among these factors effect of Clearance followed by feed rate and moisture content percent are highly significant both physically and statistically. The changes due to the thickness of the grinding disk, rotational speed of the flywheel and interaction of feed rate and clearance in the ranges given in Table 5.4

have minimal impacts on deshelling efficiency, both statistically and physically. As a result of ANOVA and S/N analysis, the best process variables for deshelling efficiency are A_1, B_2, C_1, D_3, E_1 i.e., feed rate (ψ) = 15 kg/hr, moisture content (C_d) = 13 % d.b, clearance between disks (C_d) = 6 mm, thickness of the grinding disk (t) = 32 mm and rotational speed of the flywheel (V_f) = 400 (rpm).

Table 5.4 Analysis of Variance for deshelling efficiency.

Source	DF	Adj SS	Adj MS	F-Value	P-Value	PC (%)
Feed rate	2	56.721	28.3604	70.80	0.000	30.23 %
Moisture content percent	2	48.359	24.1793	60.36	0.000	25.77 %
Clearance	2	76.694	38.3470	95.73	0.000	40.87 %
Thickness of the grinding disk	2	0.094	0.0470	0.12	0.890	0.05 %
Rotational speed of the flywheel	2	0.054	0.0270	0.07	0.935	0.03 %
Feed rate*Clearance	4	0.913	0.2281	0.57	0.690	0.49 %
Error	12	4.807	0.4006			2.56 %
Total	26	187.641				
R-sq = 97.44%%; R-sq (adj)= 94.45%; R-sq (pred)= 87.03%						

Minitab software (Version 17) is used to create a multiple linear regression model. By establishing the regression equation, this model provides the ratio of input to output . A regression equation created in this manner creates a connection between significant conditions discovered through ANOVA analysis, i.e. feed rate, moisture content percent, clearance, thickness of the grinding disk and rotational speed of the flywheel. The regression equation developed for deshelling efficiency is given as follow in equation (31)

Deshelling efficiency,

(η_d) = 96.59 - 0.251 ψ - 0.3306 M_c - 0.781 C_d + 0.0111 t - 0.00044 V_f - 0.0125 ψ * C_d

(31)

5. 2 Analysis for Whole kernel recovery

For maximizing the whole kernel recovery of the Charoli nut, the ''the higher the better" quality feature was used in this study.

Taguchi characteristic "the higher the better" is as follows equation (32):

$$S/N = -10 \log \frac{1}{n}\left(\sum \frac{1}{y_i^2}\right) \qquad (32)$$

where S/N- whole kernel recovery signal-to-noise ratio, y_i-outcome of the i-[th] test for each experiment, and n-number of runs repeated. The S/N ratio change shown above is appropriate for maximizing the whole kernel recovery. The S/N ratio variable analysis is utilized to determine statistical significant variables.

Table 5.5 shows the L27 (3^5) OA of the experimental runs, results, S/N ratio for whole kernel recovery

Table 5.5: L27 (3^5) OA of the experimental runs, results, S/N ratio for whole kernel recovery

Expt no. / Factors	A (ψ) (kg/hr)	B (M_c) (% d.b)	C (C_d) (mm)	D (t) (mm)	E (V_f) (rpm)	(η_w)	S/N ratio (db)
1	15	9	6	19	400	65.5	36.32
2	15	9	8	25	500	65.6	36.34
3	15	9	10	32	600	68.6	36.73
4	15	13	6	25	500	66.5	36.46
5	15	13	8	32	600	71	37.03
6	15	13	10	19	400	62.2	35.88
7	15	17	6	32	600	69.4	36.83
8	15	17	8	19	400	62	35.85
9	15	17	10	25	500	61.6	35.79
10	20	17	6	19	500	63.5	36.06
11	20	17	8	25	600	66.2	36.42
12	20	17	10	32	400	58.6	35.36
13	20	9	6	25	600	70.6	36.98
14	20	9	8	32	400	62.3	35.89

15	20	9	10	19	500	61.6	35.79
16	20	13	6	32	400	63.3	36.03
17	20	13	8	19	500	63.7	36.08
18	20	13	10	25	600	66.6	36.47
19	25	13	6	19	600	69.6	36.85
20	25	13	8	25	400	61.7	35.81
21	25	13	10	32	500	62	35.85
22	25	17	6	25	400	60.6	35.65
23	25	17	8	32	500	60	35.56
24	25	17	10	19	600	62.6	35.93
25	25	9	6	32	500	64.1	36.14
26	25	9	8	19	600	66.9	36.51
27	25	9	10	25	400	59	35.42

Where, (η_w) – Whole kernel recovery, (ψ) - Feed rate, (M_c)- Moisture content, (C_d)-
Clearance between disks, (V_f)- Rotational speed of the flywheel and (t)- Thickness
of the grinding disk.

Table 5.5 shows that for each input set of parameters, a separate set of output results
for whole kernel recovery was achieved. The greatest and lowest percentages for
whole kernel recovery were 71.00 and 58.60 percent, respectively. The output
response values in Table 5.5 were generated using Minitab software in terms of input
variables.

A S/N ratio response table was used to analyze the effect of every control variables
(feed rate, moisture content percent, clearance, thickness of the grinding disc, and
rotating speed of the flywheel) on whole kernel recovery. Table 5.6 shows S/N ratio
response table for whole kernel recovery. They display the S/N ratio for every level of
a control variables and changes as the levels of every control variable are adjusted
through one level to the next.

Table 5.6 S/N ratios response table (higher-is-better) for whole kernel recovery.

Level	(ψ)	(M_c)	(C_d)	(t)	(V_f)
1	36.36	36.23	36.37	36.14	35.80
2	36.12	36.27	36.16	36.15	36.01
3	35.97	35.94	35.91	36.16	36.64
Delta	0.39	0.33	0.46	0.01	0.84
Rank	3	4	2	5	1

Where, (ψ)- Feed rate, (M_c)- Moisture content, (C_d)- Clearance between disks,

(V_f)- Rotational speed of the flywheel and (t)- Thickness of the grinding disk

The influence of five parameters for S/N ratio on whole kernel recovery is graphically illustrated in Figure 5.4 on the basis the S/N ratio. According to Table 5.6 and Figure 5.4, variables of the processes with greater S/N ratio values will provide the optimised variable variants. The findings show that a feed rate of 15 kg/hr, a moisture content of 13% d.b, a clearance of 6 mm, a thickness of the grinding disc of 32 mm, and a rotating speed of the flywheel of 600 rpm result in the best whole kernel recovery. In addition, the most significant variables may be identified based on the rank in this table, that are rotational speed of the flywheel, clearance between disks, then feed rate, moisture content, and thickness of the grinding disk. The optimum variable variant's levels are A_1,B_2,C_1,D_3,E_3, which indicates that the first factor on first level, second factor on second level, third factor on first level, fourth factor on third level, and fifth factor on third level.
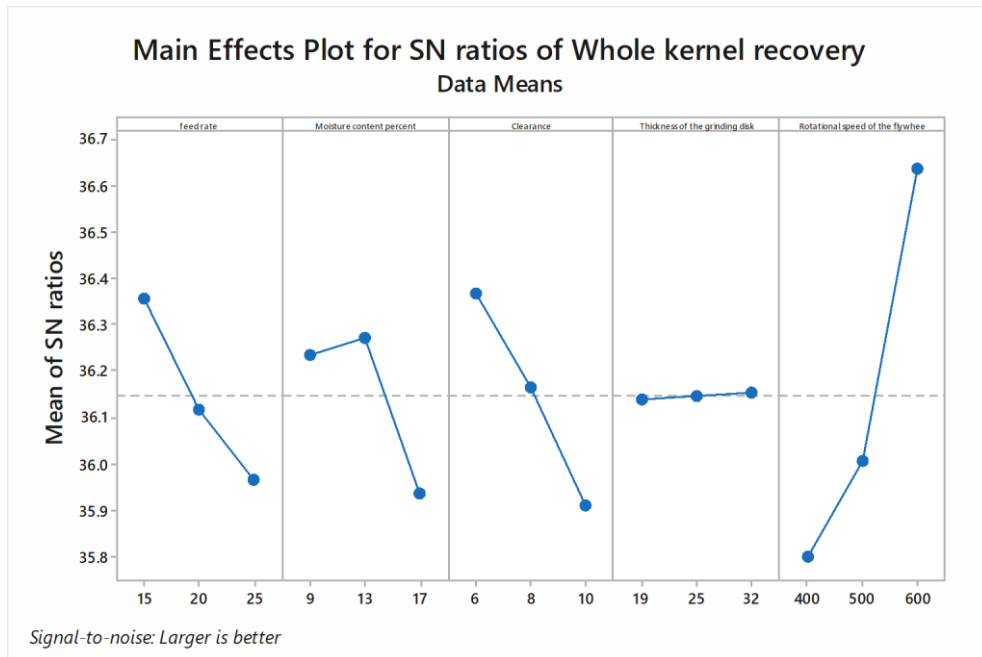
Fig. 5.4 Plot of main effect for S/N ratio of whole kernel recovery

The line slope connecting the levels in the S/N ratio influences graphs (Figs. 5.4) evidently illustrates the strength of impact of each control variable. Specifically, the rotational speed of the flywheel, clearance between disks, feed rate, and moisture content, has been found to have a significant impact on whole kernel recovery and S/N ratios. The narrow slope of the lines indicates that the thickness of the grinding disks have a smaller influence on whole kernel recovery.

The interactions of parameters feed rate and clearance between disks, on all levels for whole kernel recovery is given in Figure 5.5
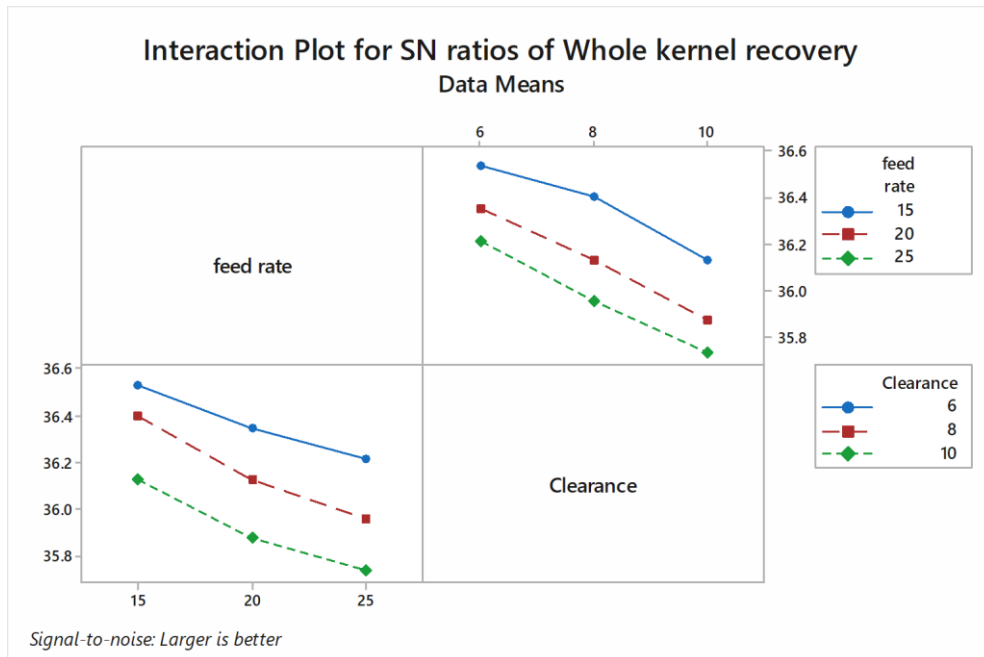
Fig. 5.5 Plot of main effect for S/N ratio of Effects of feed rate and clearance interactions on whole kernel recovery.

Moreover, it can be seen in Fig. 5.5 that plot of interactions between feed rate and clearance that feed rate at 15 kg/hr and clearance of 6 mm gave the largest whole kernel recovery.

Figure 5.6 depicts the residual plot for whole kernel recovery, which comprises a normality plot, a histogram, a fitted vs predicted plot, and a residual against observation order plot.
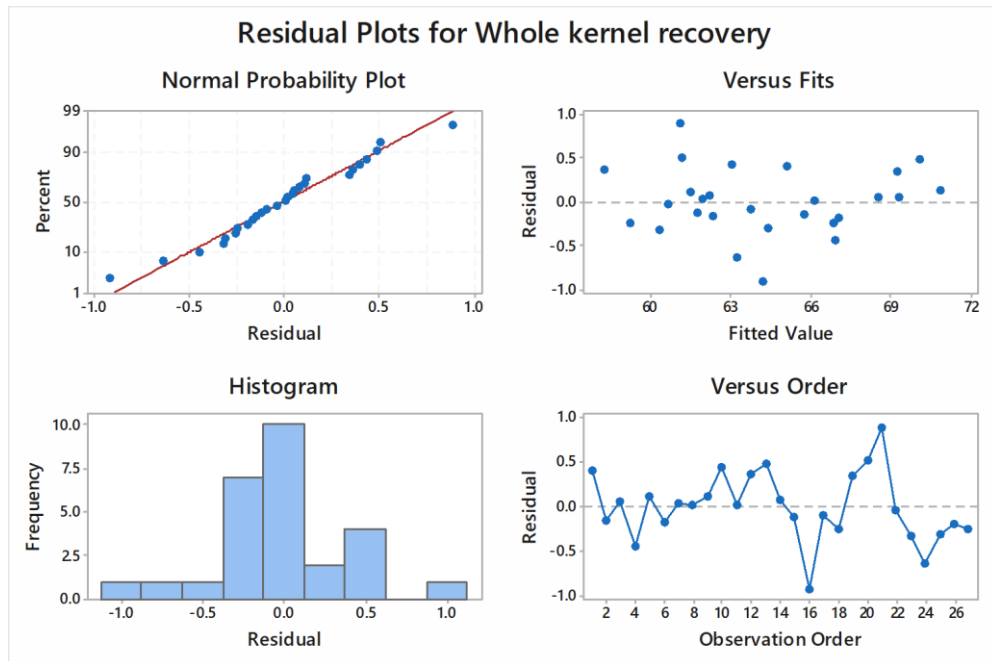
Figure 5.6: Residual plot for whole kernel recovery

The normality plot demonstrates that almost the residuals follow a straight line, suggesting that the suggested model is fit. A histogram display shows a bell-shaped curve, suggesting that the data is normal. The residual vs fitted plot shows the randomized allotment on both sides of the reference line of all residuals.. Additionally, there is no pattern in the residual versus observation order plot, which is required for significant ANOVA. This confirms that the suggested model will have a good future outcome if all four tests are satisfied.

Table 5.7 shows the results of analysis of variance (ANOVA) for whole kernel recovery. From the analysis, it is noted that rotational speed of the flywheel (PC = 60.29 %), clearance (PC = 16.05 %), feed rate (PC = 11.91 %), and moisture content percent (PC = 10.25 %) are the significantly affecting the whole kernel recovery. Among these factors effect of rotational speed of the flywheel, followed by clearance feed rate and moisture content percent are highly significant both physically and statistically. The changes due to the thickness of the grinding disk, and interaction of feed rate and clearance in the ranges given in Table 5.7 have minimal impacts on whole kernel recovery, both statistically and physically. As a result of ANOVA and S/N analysis, the best process variables for whole kernel recovery are A_1, B_2, C_1, D_3, E_3

i.e., feed rate (ψ) = 15 kg/hr, moisture content (C_d) = 13 % d.b, clearance between disks (C_d) = 6 mm, thickness of the grinding disk (t) = 32 mm and rotational speed of the flywheel (V_f) = 600 (rpm).

Table 5.7 Analysis of Variance for whole kernel recovery.

Source	DF	Adj SS	Adj MS	F-Value	P-Value	PC (%)
Feed rate	2	37.956	18.9781	59.72	0.000	11.91 %
Moisture content percent	2	32.676	16.3381	51.41	0.000	10.25 %
Clearance	2	51.161	25.5804	80.50	0.000	16.05 %
Thickness of the grinding disk	2	0.161	0.0804	0.25	0.781	0.05 %
Rotational speed of the flywheel	2	192.210	96.1048	302.43	0.000	60.29 %
Feed rate*Clearance	4	0.819	0.2048	0.64	0.641	0.26 %
Error	12	3.813	0.3178			1.20 %
Total	26	318.796				100.00 %
R-sq = 98.80%; R-sq(adj)= 97.41%; R-sq(pred)= 93.94%						

Minitab software is used to create a multiple linear regression model. A regression equation created in this manner creates a connection between significant conditions discovered through ANOVA analysis, i.e. feed rate, moisture content percent, clearance, thickness of the grinding disk and rotational speed of the flywheel. The regression equation developed for whole kernel recovery is given as follow in equation (33)

Whole kernel recovery,
(η_w) = 62.04 - 0.174 ψ - 0.2736 M_c - 0.558 C_d + 0.0145 t + 0.03128 V_f - 0.0142 ψ * C_d

$$(33)$$

5. 3 Analysis for broken kernel

For minimizing the broken kernel of the Charoli nut, the ''the smaller the better" quality feature was used in this study.

The Taguchi characteristic "the smaller the better" is as follows equation (34):

$$S/N = -10 \log \frac{1}{n} \left(\sum y_i^2 \right) \qquad (34)$$

88

where S/N- broken kernel signal-to-noise ratio, y_i-outcome of the i-th test for each experiment, and n-number of runs repeated. The S/N ratio change shown above is appropriate for minimizing the broken kernel. The S/N ratio variable analysis is utilized to determine statistical significant variables.

Table 5.8 shows the L27 (3^5) OA of the experimental runs, results, S/N ratio for broken kernel.

Table 5.8: L27 (3^5) OA of the experimental runs, results, S/N ratio for broken kernel

Expt no. / Factors	A	B	C	D	E	(η_b)	S/N ratio (db)
	(ψ) (kg/hr)	(M_c) (% d.b)	(C_d) (mm)	(t) (mm)	(V_f) (rpm)		
1	15	9	6	19	400	18.5	-25.34
2	15	9	8	25	500	16.5	-24.35
3	15	9	10	32	600	11.2	-20.98
4	15	13	6	25	500	16.7	-24.45
5	15	13	8	32	600	11.6	-21.29
6	15	13	10	19	400	17.6	-24.91
7	15	17	6	32	600	11.4	-21.14
8	15	17	8	19	400	17.5	-24.86
9	15	17	10	25	500	15.5	-23.81
10	20	17	6	19	500	15.9	-24.03
11	20	17	8	25	600	10.8	-20.67
12	20	17	10	32	400	16.6	-24.40
13	20	9	6	25	600	11.5	-21.21
14	20	9	8	32	400	17.6	-24.91
15	20	9	10	19	500	15.4	-23.75
16	20	13	6	32	400	17.9	-25.06
17	20	13	8	19	500	16	-24.08
18	20	13	10	25	600	10.9	-20.75
19	25	13	6	19	600	11.4	-21.14
20	25	13	8	25	400	17.5	-24.86
21	25	13	10	32	500	15.6	-23.86

22	25	17	6	25	400	17.2	-24.71
23	25	17	8	32	500	15.1	-23.58
24	25	17	10	19	600	10.3	-20.26
25	25	9	6	32	500	16.1	-24.14
26	25	9	8	19	600	10.9	-20.75
27	25	9	10	25	400	16.7	-24.45

Where, (η_b) – Broken kernel, (ψ) - Feed rate, (M_c)- Moisture content, (C_d)- Clearance between disks, (V_f)- Rotational speed of the flywheel and (t)- Thickness of the grinding disk.

Table 5.8 shows that for each input set of parameters, a separate set of output results for broken kernel was achieved. The greatest and lowest percentages for broken kernel were 18.50 and 10.30 percent, respectively. The output response values in Table 5.8 were generated using Minitab software in terms of input variables.

A S/N ratio response table was used to analyze the effect of every control variables (feed rate, moisture content percent, clearance, thickness of the grinding disc, and rotating speed of the flywheel) on broken kernel. Table 5.9 shows S/N ratio response table for broken kernel. They display the S/N ratio for every level of a control variables and changes as the levels of every control variable are adjusted through one level to the next.

Table 5.9 S/N ratios response table (smaller-is-better) for broken kernel.

Level	(ψ)	(M_c)	(C_d)	(t)	(V_f)
1	-23.46	-23.32	-23.47	-23.24	-24.83
2	-23.21	-23.38	-23.26	-23.25	-24.01
3	-23.08	-23.05	-23.02	-23.26	-20.91
Delta	0.38	0.33	0.45	0.03	3.92
Rank	3	4	2	5	1

Where, (ψ)- Feed rate, (M_c)- Moisture content, (C_d)- Clearance between disks,

(V_f)- Rotational speed of the flywheel and (t)- Thickness of the grinding disk

The influence of five parameters for S/N ratio on broken kernel is graphically illustrated in Figure 5.7 on the basis the S/N ratio. According to Table 5.9 and Figure 5.7, variables of the processes with greater S/N ratio values will provide the optimised variable variants. The findings show that a feed rate of 25 kg/hr, a moisture content of 17% d.b, a clearance of 10 mm, a thickness of the grinding disc of 19 mm, and a rotating speed of the flywheel of 600 rpm result in the lowest broken kernel. In addition, the most significant variables may be identified based on the rank in this table, that are rotating speed of the flywheel, clearance between disks, then feed rate, moisture content, and thickness of the grinding disk. The optimum variable variant's levels are A_3,B_3,C_3,D_1,E_3, which indicates that the first factor on third level, second factor on third level, third factor on third level, fourth factor on first level, and fifth factor on third level.

The line slope connecting the levels in the S/N ratio influences graphs (Figs. 5.8) evidently illustrates the strength of impact of each control variable. Specifically, the rotating speed of the flywheel, clearance between disk, followed by feed rate and moisture content, has been found to have a significant impact on broken kernel and S/N ratios. The narrow slope of the lines indicates that the thickness of the grinding disks have a smaller influence on broken kernel.
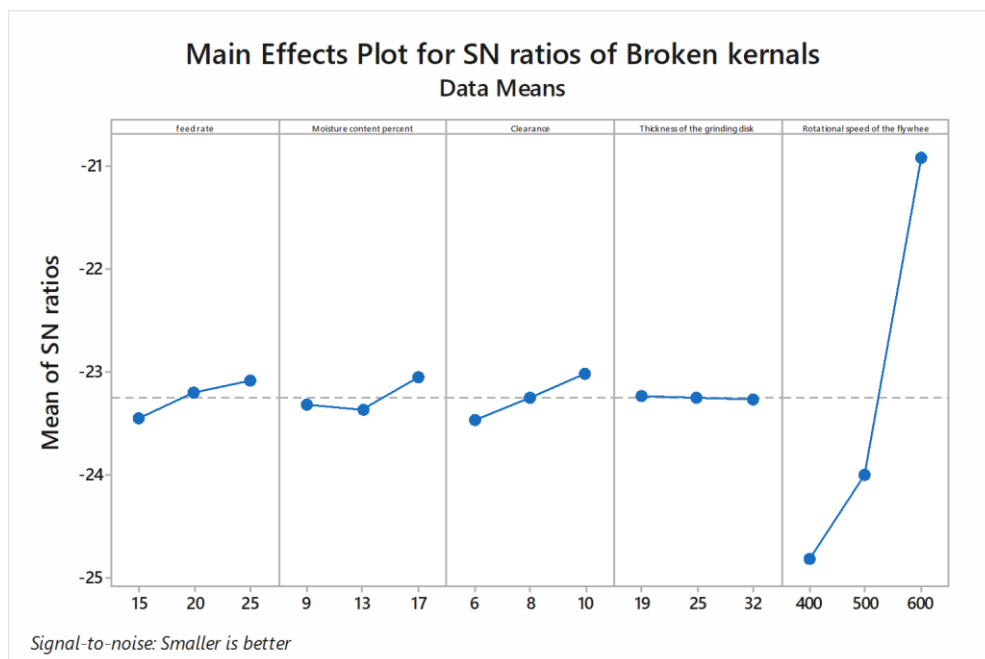
Fig. 5.7 Plot of main effect for S/N ratio of broken kernel

91

The interactions of parameters feed rate and clearance between disks, on all levels for broken kernel is given in Figure 5.8
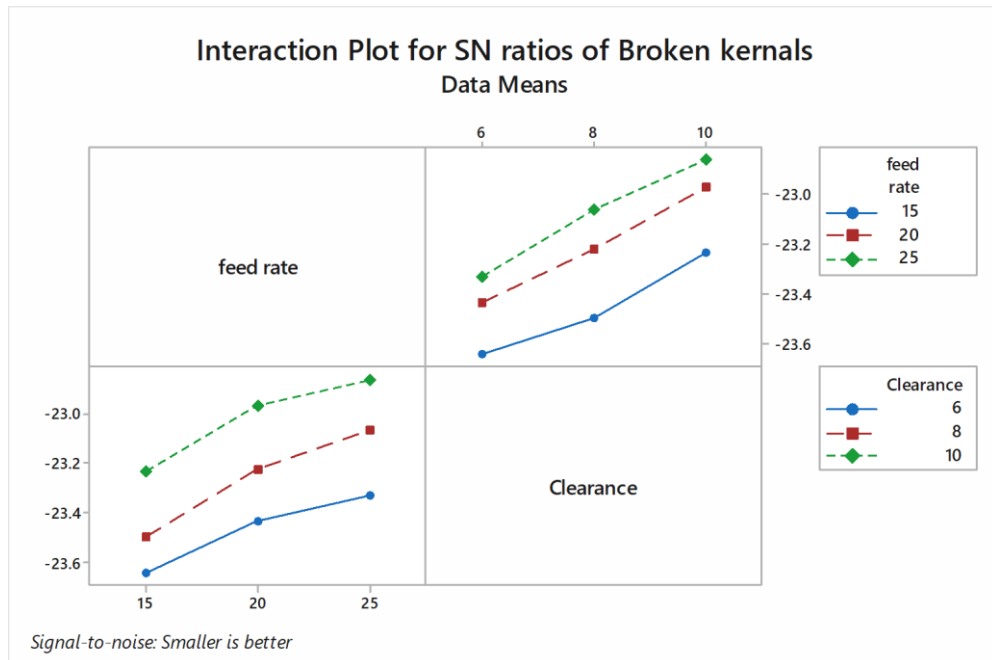
Fig. 5.8 Plot of main effect for S/N ratio of Effects of feed rate and clearance interactions on broken kernel.

Moreover, it can be seen in Fig. 5.8 that plot of interactions between feed rate and clearance that feed rate at 25 kg/hr and clearance of 10 mm gave the lowest broken kernel.

Figure 5.9 depicts the residual plot for broken kernel, which comprises a normality plot, a histogram, a fitted vs predicted plot, and a residual against observation order plot.
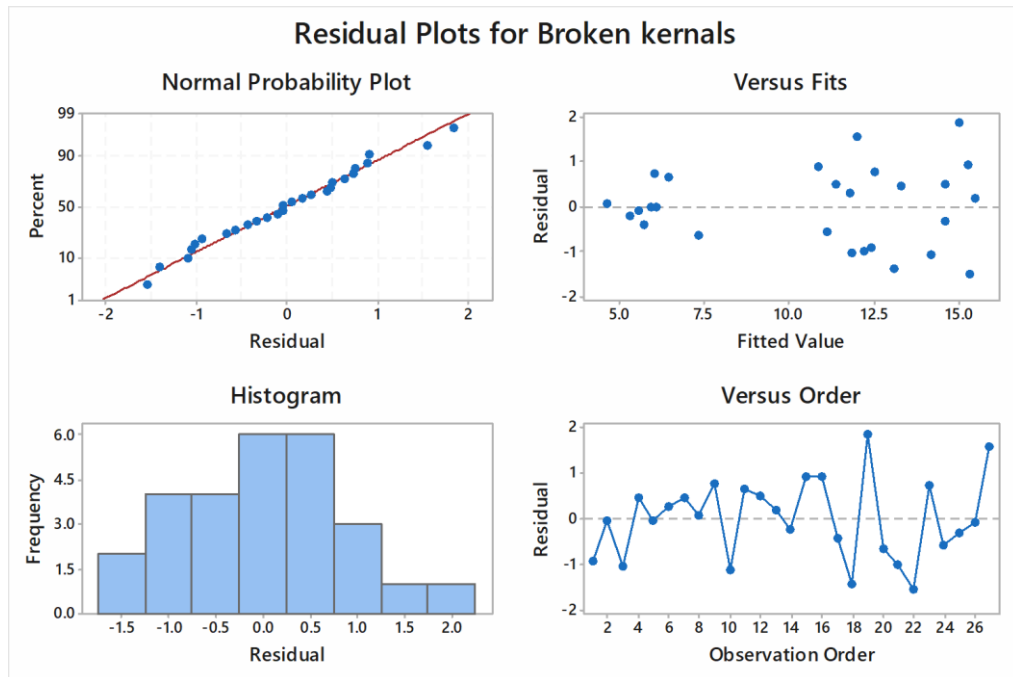
Figure 5.9: Residual plot for broken kernel.

The normality plot demonstrates that almost the residuals follow a straight line, suggesting that the suggested model is fit. A histogram display shows a bell-shaped curve, suggesting that the data is normal. The residual vs fitted plot shows the randomized allotment on both sides of the reference line of all residuals.. Additionally, there is no pattern in the residual versus observation order plot, which is required for significant ANOVA. This confirms that the suggested model will have a good future outcome if all four tests are satisfied.

Table 5.10 shows the results of analysis of variance (ANOVA) for broken kernel. From the analysis, it is noted that rotational speed of the flywheel (PC = 96.89 %), clearance (PC = 1.27 %), feed rate (PC = 0.93 %), and moisture content percent (PC = 0.76 %) are the significantly affecting the broken kernel. Among these factors effect of rotational speed of the flywheel followed by clearance, feed rate and moisture content percent are highly significant both physically and statistically. The changes of the thickness of the grinding disk, and interaction of feed rate and clearance in the ranges given in Table 5.10 have minimal impacts on broken kernel., both statistically and physically. As a result of ANOVA and S/N analysis, the best process variables for deshelling efficiency are A_3,B_3,C_3,D_1,E_3, i.e., feed rate (ψ) = 25 kg/hr, moisture

content (C_d) = 17 % d.b, clearance between disks (C_d) = 10 mm, thickness of the grinding disk (t) = 19 mm and rotational speed of the flywheel (V_f) = 600 (rpm).

Table 5.10 Analysis of Variance for broken kernel.

Source	DF	Adj SS	Adj MS	F-Value	P-Value	PC (%)
Feed rate	2	1.887	0.9433	44.68	0.000	0.93 %
Moisture content percent	2	1.536	0.7678	36.37	0.000	0.76 %
Clearance	2	2.576	1.2878	61.00	0.000	1.27 %
Thickness of the grinding disk	2	0.009	0.0044	0.21	0.813	0.00 %
Rotational speed of the flywheel	2	196.176	98.0878	4646.26	0.000	96.89 %
Feed rate*Clearance	4	0.031	0.0078	0.37	0.827	0.02 %
Error	12	0.253	0.0211			0.12 %
Total	26	202.467				100 %
R-sq = 92.09%; R-sq(adj)= 89.72%; R-sq(pred)= 85.50%						

Minitab software is used to create a multiple linear regression model. A regression equation created in this manner creates a connection between significant conditions discovered through ANOVA analysis, i.e. feed rate, moisture content percent, clearance, thickness of the grinding disk and rotational speed of the flywheel. The regression equation developed for broken kernel.is given as follow in equation (35)

Broken kernels,
(η_b) = 34.54 - 0.077 ψ - 0.0569 M_c - 0.222 C_d - 0.0034 t - 0.03172 V_f + 0.0017 ψ * C_d
(35)

5.4 Analysis for partially shelled / unshelled nuts

For minimizing the partially shelled / unshelled nuts of the Charoli nut, the ''the smaller the better" quality feature was used in this study.

The Taguchi characteristic "the smaller the better" is as follows (36):

$$S/N = -10 \log \frac{1}{n} \left(\sum y_i^2 \right) \qquad (36)$$

where S/N- partially shelled / unshelled nuts signal-to-noise ratio, yi-outcome of the i-th test for each experiment, and n-number of runs repeated. The S/N ratio change shown above is appropriate for minimizing the partially shelled / unshelled nuts. The S/N ratio variable analysis is utilized to determine statistical significant variables.

Table 5.11 shows the L27 (3^5) OA of the experimental runs, results, S/N ratio for partially shelled / unshelled nuts

Table 5.11: L27 (3^5) OA of the experimental runs, results, S/N ratio for partially shelled / unshelled nuts

Expt no. / Factors	A	B	C	D	E	(η_u)	S/N ratio (db)
	(ψ) (kg/hr)	(M_c) (% d.b)	(C_d) (mm)	(t) (mm)	(V_f) (rpm)		
1	15	9	6	19	400	16	-24.08
2	15	9	8	25	500	17.9	-25.06
3	15	9	10	32	600	24.4	-27.75
4	15	13	6	25	500	14.7	-23.35
5	15	13	8	32	600	18.8	-25.48
6	15	13	10	19	400	27.5	-28.79
7	15	17	6	32	600	16.9	-24.56
8	15	17	8	19	400	22.8	-27.16
9	15	17	10	25	500	28.4	-29.07
10	20	17	6	19	500	18.5	-25.34
11	20	17	8	25	600	21.4	-26.61
12	20	17	10	32	400	28.5	-29.10
13	20	9	6	25	600	10.8	-20.67
14	20	9	8	32	400	17.6	-24.91
15	20	9	10	19	500	25.7	-28.20
16	20	13	6	32	400	12.4	-21.87
17	20	13	8	19	500	19.6	-25.85
18	20	13	10	25	600	26.8	-28.56
19	25	13	6	19	600	12.6	-22.01
20	25	13	8	25	400	18.8	-25.48

21	25	13	10	32	500	27.6	-28.82
22	25	17	6	25	400	17.3	-24.76
23	25	17	8	32	500	20.9	-26.40
24	25	17	10	19	600	29	-29.25
25	25	9	6	32	500	11.2	-20.98
26	25	9	8	19	600	17.4	-24.81
27	25	9	10	25	400	26.5	-28.46

Where, (η_μ) – Partially shelled / unshelled nuts, (ψ) - Feed rate, (M_c)- Moisture content, (C_d)- Clearance between disks, (V_f)- Rotational speed of the flywheel and (t)- Thickness of the grinding disk.

Table 5.11 shows that for each input set of parameters, a separate set of output results for Partially shelled / unshelled nuts was achieved. The greatest and lowest percentages for Partially shelled / unshelled nuts were 29.00 and 10.80 percent, respectively. The output response values in Table 5.11 were generated using Minitab software in terms of input variables.

A S/N ratio response table was used to analyze the effect of every control variables (feed rate, moisture content percent, clearance, thickness of the grinding disc, and rotating speed of the flywheel) on Partially shelled / unshelled nuts. Table 5.12 shows S/N ratio response table for Partially shelled / unshelled nuts. They display the S/N ratio for every level of a control variables and changes as the levels of every control variable are adjusted through one level to the next.

Table 5.12 S/N ratios response table (lower-is-better) for Partially shelled / unshelled nuts.

Level	(ψ)	(M_c)	(C_d)	(t)	(V_f)
1	-26.14	-24.99	-23.07	-26.16	-26.07
2	-25.68	-25.58	-25.75	-25.78	-25.90
3	-25.66	-26.92	-28.67	-25.54	-25.52
Delta	0.48	1.92	5.60	0.62	0.55
Rank	5	2	1	3	4

Where, (ψ)- Feed rate, (M_c)- Moisture content, (C_d)- Clearance between disks,

(V_f)- Rotational speed of the flywheel and (t)- Thickness of the grinding disk

The influence of five parameters for S/N ratio on Partially shelled / unshelled nuts is graphically illustrated in Figure 5.10 on the basis the S/N ratio. According to Table 5.12 and Figure 5.10, variables of the processes with greater S/N ratio values will provide the optimised variable variants. The findings show that a feed rate of 20 kg/hr, a moisture content of 9% d.b, a clearance of 6 mm, a thickness of the grinding disc of 32 mm, and a rotating speed of the flywheel of 600 rpm result in the best Partially shelled / unshelled nuts. In addition, the most significant variables may be identified based on the rank in this table that are clearance between disks, moisture content, thickness of the grinding disk, rotational speed of the flywheel and feed rate. The optimum variable variant's levels are A_2, B_1, C_1, D_3, E_3, which indicates that the first factor on second level, second factor on first level, third factor on first level, fourth factor on third level, and fifth factor on third level.

The line slope connecting the levels in the S/N ratio influences graphs (Figs. 5.10) evidently illustrates the strength of impact of each control variable. Specifically, the moisture content, and clearance between disks, has been found to have a significant impact on deshelling efficiency and S/N ratios. The narrow slope of the lines indicates that the thickness of the grinding disk, rotational speed of the flywheel and feed rate have a smaller influence on Partially shelled / unshelled nuts.
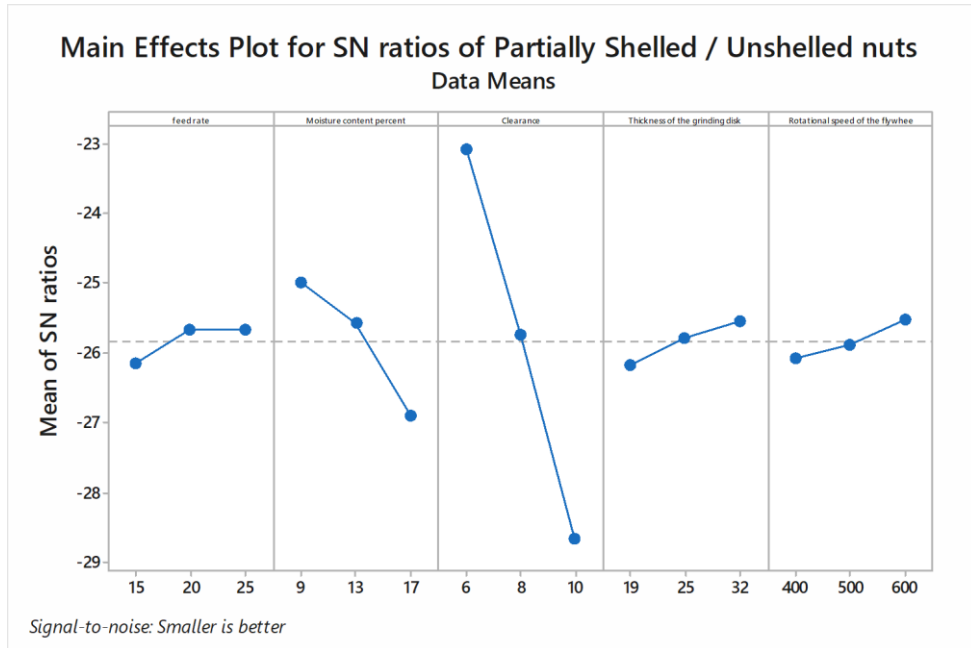
Fig. 5.10 Plot of main effect for S/N ratio of Partially shelled / unshelled nuts

The interactions of parameters feed rate and clearance between disks, on all levels for Partially shelled / unshelled nuts is given in Figure 5.11.
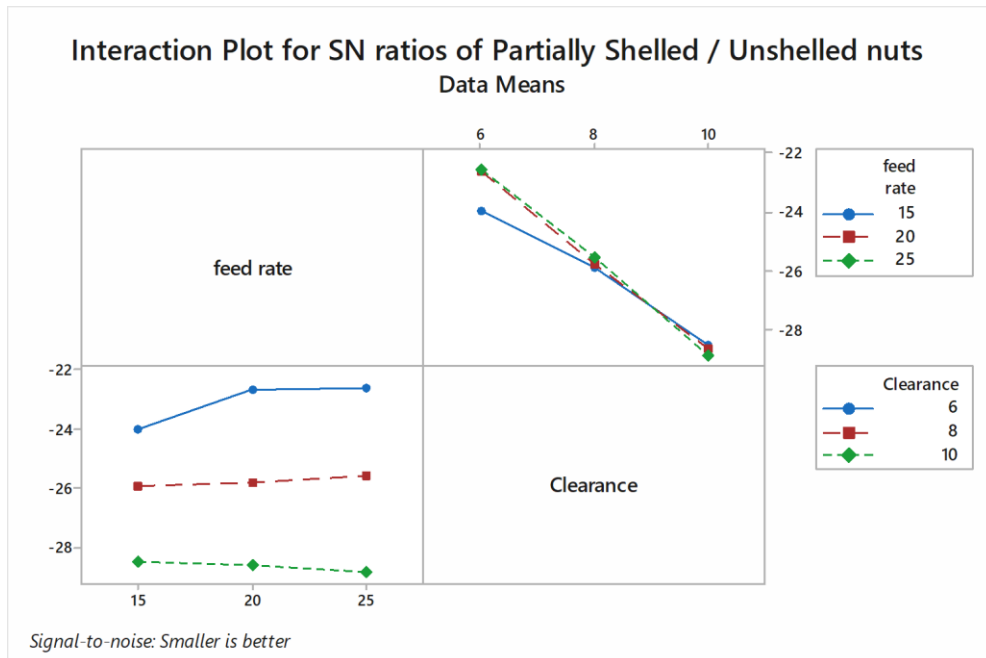
Fig. 5.11 Plot of main effect for S/N ratio of Effects of feed rate and clearance interactions on Partially shelled / unshelled nuts

Moreover, it can be seen in Fig. 5.11 that plot of interactions between feed rate and clearance that feed rate at 25 kg/hr and clearance of 6 mm gave the lowest Partially shelled / unshelled nuts.

Figure 5.12 depicts the residual plot for Partially shelled / unshelled nuts, which comprises a normality plot, a histogram, a fitted vs predicted plot, and a residual against observation order plot.
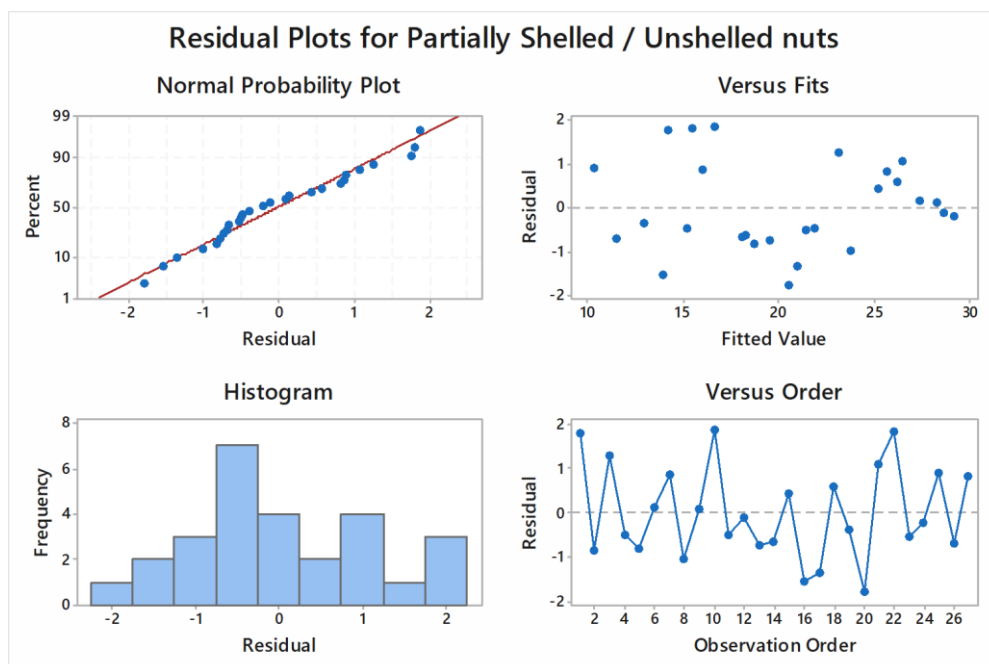
Figure 5.12: Residual plot for Partially shelled / unshelled nuts

The normality plot demonstrates that almost the residuals follow a straight line, suggesting that the suggested model is fit. A histogram display shows a bell-shaped curve, suggesting that the data is normal. The residual vs fitted plot shows the randomized allotment on both sides of the reference line of all residuals.. Additionally, there is no pattern in the residual versus observation order plot, which is required for significant ANOVA. This confirms that the suggested model will have a good future outcome if all four tests are satisfied.

Table 5.13 shows the results of analysis of variance (ANOVA) for Partially shelled / unshelled nuts. From the analysis, it is noted that clearance (PC = 86.97 %), and moisture content percent (PC = 9.04 %) are the significantly affecting the Partially

shelled / unshelled nuts. Among these factors effect of clearance followed by moisture content percent are highly significant both physically and statistically. The changes of the feed rate, thickness of the grinding disk, rotational speed of the flywheel and interaction of feed rate and clearance in the ranges given in Table 5 have minimal impacts on deshelling efficiency, both statistically and physically. As a result of ANOVA and S/N analysis, the best process variables for deshelling efficiency are A_2, B_1, C_1, D_3, E_3, i.e., feed rate (ψ) = 20 kg/hr, moisture content (C_d) = 13 % d.b, clearance between disks (C_d) = 6 mm, thickness of the grinding disk (t) = 25 mm and rotational speed of the flywheel (V_f) = 600 (rpm).

Table 5.13 Analysis of Variance for Partially shelled / unshelled nuts.

Source	DF	Adj SS	Adj MS	F-Value	P-Value	PC (%)
Feed rate	2	2.756	1.378	1.50	0.262	0.33 %
Moisture content percent	2	76.227	38.114	41.49	0.000	9.04 %
Clearance	2	733.025	366.513	398.95	0.000	86.97 %
Thickness of the grinding disk	2	6.570	3.285	3.58	0.061	0.78 %
Rotational speed of the flywheel	2	5.032	2.516	2.74	0.105	0.60 %
Feed rate*Clearance	4	8.241	2.060	2.24	0.125	0.98 %
Error	12	11.024	0.919			1.31 %
Total	26	842.876				100.00 %
R-sq = 98.69%; R-sq(adj)= 97.17%; R-sq(pred)= 93.38%						

Minitab software is used to create a multiple linear regression model. By establishing the regression equation, this model provides the ratio of input to output. A regression equation created in this manner creates a connection between significant conditions discovered through ANOVA analysis, i.e. feed rate, moisture content percent, clearance, thickness of the grinding disk and rotational speed of the flywheel. The regression equation developed for Partially shelled / unshelled nuts is given as follow in equation (37)

Partially shelled / unshelled nuts,

$$(\eta_u) = 7.16 - 0.688\ \psi + 0.5028\ M_c + 1.617\ C_d - 0.0916\ t - 0.00517\ V_f + 0.0775\ \psi * C_d$$

$$(37)$$

5. 5 Analysis for Resistive Torque

For minimizing the resistive torque of the Charoli nut, the ''the smaller the better" quality feature was used in this study.

The Taguchi characteristic "the smaller the better" is as follows equation (38):

$$S/N = -10 \log \frac{1}{n} \left(\sum y_i{}^2 \right) \qquad (38)$$

where S/N- resistive torque signal-to-noise ratio, yi-outcome of the i-th test for each experiment, and n-number of runs repeated. The S/N ratio change shown above is appropriate for minimizing the resistive torque. The S/N ratio variable analysis is utilized to determine statistical significant variables.

Table 5.14 shows the L27 (3^5) OA of the experimental runs, results, S/N ratio for resistive torque

Table 5.14: L27 (3^5) OA of the experimental runs, results, S/N ratio for resistive torque

Expt no./ Factors	A (ψ) (kg/hr)	B (M_c) (% d.b)	C (C_d) (mm)	D (t) (mm)	E (V_f) (rpm)	(T_r)	S/N ratio (db)
1	15	9	6	19	400	96364.488	-99.68
2	15	9	8	25	500	129916.95	-102.27
3	15	9	10	32	600	123945.45	-101.86
4	15	13	6	25	500	104410.36	-100.37
5	15	13	8	32	600	109014.2	-100.75
6	15	13	10	19	400	130280.15	-102.30
7	15	17	6	32	600	125714.17	-101.99
8	15	17	8	19	400	135984.9	-102.67
9	15	17	10	25	500	112077.33	-100.99
10	20	17	6	19	500	104356.05	-100.37
11	20	17	8	25	600	116254.85	-101.31
12	20	17	10	32	400	112538	-101.03

13	20	9	6	25	600	116492.71	-101.33
14	20	9	8	32	400	95916.216	-99.64
15	20	9	10	19	500	105850.27	-100.49
16	20	13	6	32	400	124754.95	-101.92
17	20	13	8	19	500	110508.38	-100.87
18	20	13	10	25	600	126730.54	-102.06
19	25	13	6	19	600	146322.31	-103.31
20	25	13	8	25	400	118791.27	-101.50
21	25	13	10	32	500	123293.51	-101.82
22	25	17	6	25	400	121341.73	-101.68
23	25	17	8	32	500	119725.16	-101.56
24	25	17	10	19	600	136359.54	-102.69
25	25	9	6	32	500	115339.06	-101.24
26	25	9	8	19	600	138207.55	-102.81
27	25	9	10	25	400	104198.86	-100.36

Where, (T_r) – resistive torque, (ψ) - Feed rate, (M_c)- Moisture content, (C_d)- Clearance between disks, (V_f)- Rotational speed of the flywheel and (t)- Thickness of the grinding disk.

Table 5.14 shows that for each input set of parameters, a separate set of output results for resistive torque was achieved. The greatest and lowest percentages for resistive torque were 146322.31 and 95916.21 N-mm, respectively. The output response values in Table 5.14 were generated using Minitab software in terms of input variables.

A S/N ratio response table was used to analyze the effect of every control variables (feed rate, moisture content percent, clearance, thickness of the grinding disc, and rotating speed of the flywheel) on resistive torque. Table 5.15 shows S/N ratio response table for resistive torque. They display the S/N ratio for every level of a control variables and changes as the levels of every control variable are adjusted through one level to the next.

Table 5.15 S/N ratios response table (lower-is-better) for resistive torque.

Level	(ψ)	(M_c)	(C_d)	(t)	(V_f)
1	-101.4	-101.1	-101.3	-101.7	-101.2
2	-101.0	-101.7	-101.5	-101.3	-101.1
3	-101.9	-101.6	-101.5	-101.3	-102.0
Delta	0.9	0.6	0.2	0.4	0.9
Rank	2	3	5	4	1

Where, (ψ)- Feed rate, (M_c)- Moisture content, (C_d)- Clearance between disks, (V_f)- Rotational speed of the flywheel and (t)- Thickness of the grinding disk

The influence of five parameters for S/N ratio on resistive torque is graphically illustrated in Figure 5.13 on the basis the S/N ratio. According to Table 5.15 and Figure 5.13, variables of the processes with greater S/N ratio values will provide the optimised variable variants. The findings show that a feed rate of 20 kg/hr, a moisture content of 9% d.b, a clearance of 6 mm, a thickness of the grinding disc of 25 mm, and a rotating speed of the flywheel of 500 rpm result in the best resistive torque. In addition, the most significant variables may be identified based on the rank in this table, that are rotational speed of the flywheel, feed rate, moisture content, thickness of the grinding disk and then clearance between disks. The optimum variable variant's levels are A_2, B_1, C_1, D_2, E_2, which indicates that the first factor on second level, second factor on first level, third factor on first level, fourth factor on second level, and fifth factor on second level.

The line slope connecting the levels in the S/N ratio influences graphs (Figs. 5.13) evidently illustrates the strength of impact of each control variable. None of the variables found significant impact on the resistive torque. This may be due to the some extraneous parameters impact on the machine.
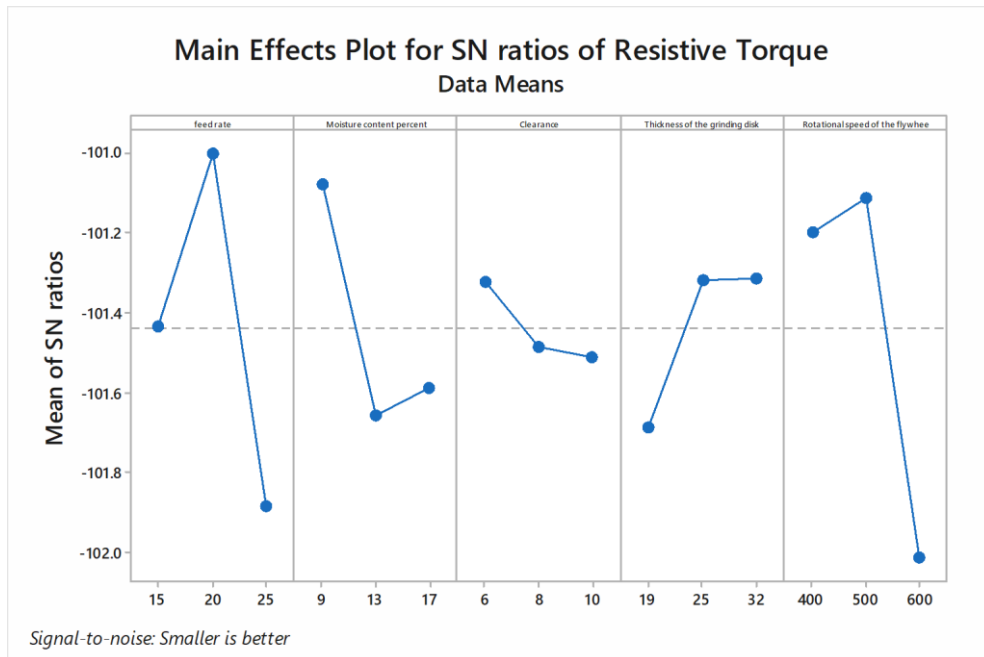
Fig. 5.13 Plot of main effect for S/N ratio of resistive torque

The interactions of parameters feed rate and clearance between disks, on all levels for resistive torque is given in Figure 5.14.
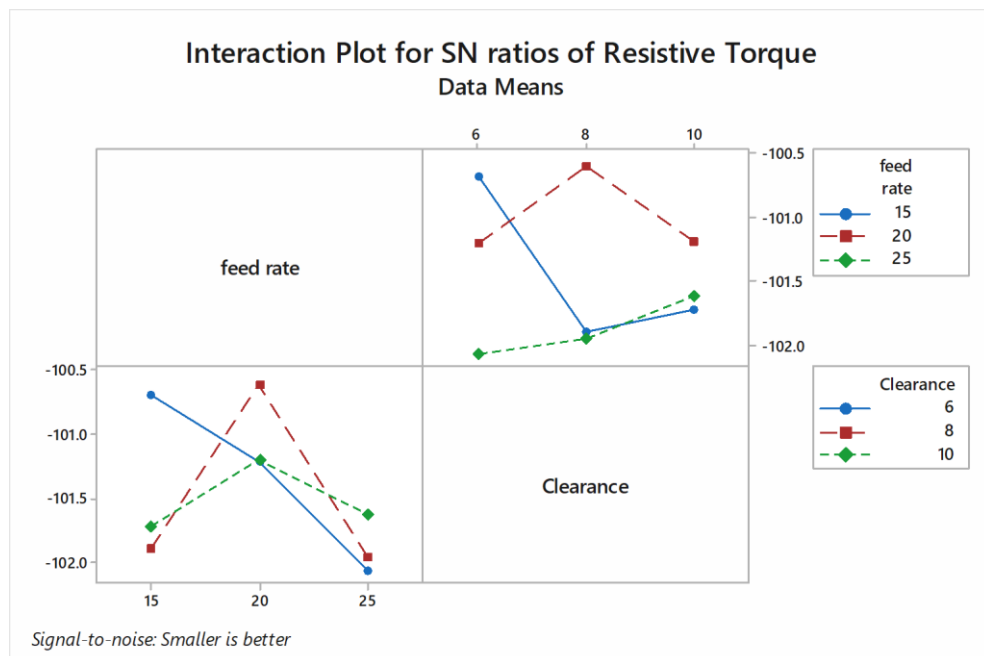
Fig. 5.14 Plot of main effect for S/N ratio of Effects of feed rate and clearance interactions on resistive torque

Moreover, it can be seen in Fig. 5.14 that plot of interactions between feed rate and clearance that feed rate at 20 kg/hr and clearance of 8 mm gave the lowest resistive torque.

Figure 5.15 depicts the residual plot for resistive torque, which comprises a normality plot, a histogram, a fitted vs predicted plot, and a residual against observation order plot.
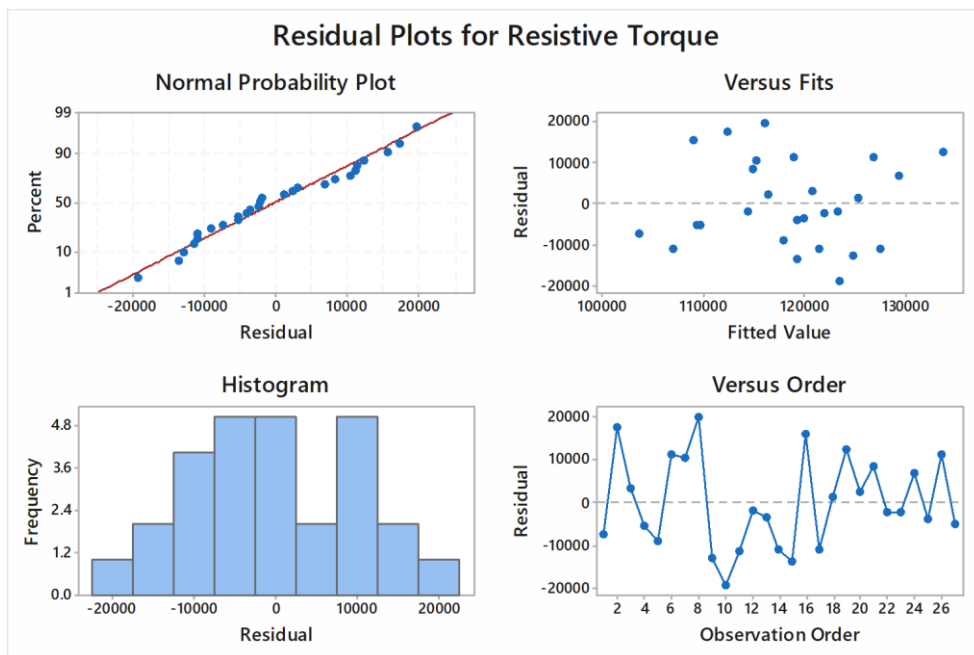
Figure 5.15: Residual plot for resistive torque

The normality plot demonstrates that almost the residuals follow a straight line, suggesting that the suggested model is fit. A histogram display shows a bell-shaped curve, suggesting that the data is normal. The residual vs fitted plot shows the randomized allotment on both sides of the reference line of all residuals.. Additionally, there is no pattern in the residual versus observation order plot, which is required for significant ANOVA. This confirms that the suggested model will have a good future outcome if all four tests are satisfied.

Table 5.16 shows the results of analysis of variance (ANOVA) for resistive torque. From the analysis, it is noted that rotational speed of the flywheel (PC = 19.76 %), feed rate (PC = 15.72 %), moisture content percent (PC = 6.98 %), and thickness of

the grinding disk (PC = 5.04 %) are the affecting the resistive torque. As a result of ANOVA and S/N analysis, the best process variables for resistive torque are A_2, B_1, C_1, D_2, E_2 i.e., feed rate (ψ) = 20 kg/hr, moisture content (C_d) = 9 % d.b, clearance between disks (C_d) = 6 mm, thickness of the grinding disk (t) = 25 mm and rotational speed of the flywheel (V_f) = 500 (rpm).

Table 5.16 Analysis of Variance for resistive torque.

Source	DF	Adj SS	Adj MS	F-Value	P-Value	PC (%)
Feed rate	2	674432938	337216469	2.48	0.125	15.72 %
Moisture content percent	2	299258926	149629463	1.10	0.364	6.98 %
Clearance	2	28800137	14400069	0.11	0.900	0.67 %
Thickness of the grinding disk	2	216047837	108023918	0.80	0.474	5.04 %
Rotational speed of the flywheel	2	847709846	423854923	3.12	0.081	19.76 %
Feed rate*Clearance	4	594053030	148513258	1.09	0.403	13.85 %
Error	12	1628993853	135749488			37.98 %
Total	26	4289296567				100.00 %
R-sq = 62.02%; R-sq(adj)= 17.71%; R-sq(pred)= 0.00%						

A regression equation created in this manner creates a connection between significant conditions discovered through ANOVA analysis, i.e. feed rate, moisture content percent, clearance, thickness of the grinding disk and rotational speed of the flywheel. The regression equation developed for resistive torque is given as follow in equation (39)

Resistive Torque,
(T_r) = -3417 + 4552 ψ + 807 M_c + 10388 C_d - 449 t + 54.9 V_f - 491 ψ * C_d

(39)

5.6 Analysis for processing time for 1000 nuts

For minimizing the Processing time for 1000 nuts of the Charoli nut, the ''the smaller the better" quality feature was used in this study.

The Taguchi characteristic "the smaller the better" is as follows (40):

$$S/N = -10 \log \frac{1}{n} \left(\sum y_i^2 \right) \qquad (40)$$

where S/N- Processing time for 1000 nuts signal-to-noise ratio, y_i-outcome of the i-th test for each experiment, and n-number of runs repeated. The S/N ratio change shown above is appropriate for minimizing the Processing time for 1000 nuts. The S/N ratio variable analysis is utilized to determine statistical significant variables.

Table 5.17 shows the L27 (3^5) OA of the experimental runs, results, S/N ratio for Processing time for 1000 nuts

Table 5.17: L27 (3^5) OA of the experimental runs, results, S/N ratio for Processing time for 1000 nuts

Expt no. / Factors	A (ψ) (kg/hr)	B (M_c) (% d.b)	C (C_d) (mm)	D (t) (mm)	E (V_f) (rpm)	(Tp)	S/N ratio (db)
1	15	9	6	19	400	74	-37.38
2	15	9	8	25	500	75	-37.50
3	15	9	10	32	600	76	-37.62
4	15	13	6	25	500	80	-38.06
5	15	13	8	32	600	77	-37.73
6	15	13	10	19	400	77	-37.73
7	15	17	6	32	600	85	-38.59
8	15	17	8	19	400	80	-38.06
9	15	17	10	25	500	82	-38.28
10	20	17	6	19	500	71	-37.03
11	20	17	8	25	600	69	-36.78
12	20	17	10	32	400	67	-36.52
13	20	9	6	25	600	67	-36.52
14	20	9	8	32	400	65	-36.26
15	20	9	10	19	500	64	-36.12
16	20	13	6	32	400	67	-36.52
17	20	13	8	19	500	64	-36.12
18	20	13	10	25	600	65	-36.26
19	25	13	6	19	600	58	-35.27
20	25	13	8	25	400	56	-34.96

21	25	13	10	32	500	55	-34.81
22	25	17	6	25	400	61	-35.71
23	25	17	8	32	500	58	-35.27
24	25	17	10	19	600	57	-35.12
25	25	9	6	32	500	56	-34.96
26	25	9	8	19	600	54	-34.65
27	25	9	10	25	400	53	-34.49

Where, (Tp) – Processing time for 1000 nuts, (ψ) - Feed rate, (M_c)- Moisture content, (C_d)- Clearance between disks, (V_f)- Rotational speed of the flywheel and (t)- Thickness of the grinding disk.

Table 5.17 shows that for each input set of parameters, a separate set of output results for Processing time for 1000 nuts was achieved. The greatest and lowest percentages for Processing time for 1000 nuts were 85 and 53 seconds, respectively. The output response values in Table 2 were generated using Minitab software in terms of input variables.

A S/N ratio response table was used to analyze the effect of every control variables (feed rate, moisture content percent, clearance, thickness of the grinding disc, and rotating speed of the flywheel) on Processing time for 1000 nuts. Table 5.18 shows S/N ratio response table for processing time for 1000 nuts. They display the S/N ratio for every level of a control variables and changes as the levels of every control variable are adjusted through one level to the next.

Table 5.18 S/N ratios response table (lower-is-better) for processing time for 1000 nuts.

Level	(ψ)	(M_c)	(C_d)	(t)	(V_f)
1	-37.88	-36.17	-36.67	-36.39	-36.40
2	-36.46	-36.38	-36.37	-36.51	-36.46
3	-35.03	-36.82	-36.33	-36.48	-36.50
Delta	2.86	0.65	0.35	0.12	0.10
Rank	1	2	3	4	5

Where, (ψ)- Feed rate, (M_c)- Moisture content, (C_d)- Clearance between disks,

(V$_f$)- Rotational speed of the flywheel and (t)- Thickness of the grinding disk

The influence of five parameters for S/N ratio on processing time is graphically illustrated in Figure 5.16 on the basis the S/N ratio. According to Table 5.18 and Figure 5.16, variables of the processes with greater S/N ratio values will provide the optimised variable variants. The findings show that a feed rate of 25 kg/hr, a moisture content of 9% d.b, a clearance of 10 mm, a thickness of the grinding disc of 19 mm, and a rotating speed of the flywheel of 400 rpm result in the best Processing time. In addition, the most significant variables may be identified based on the rank in this table, that are feed rate, moisture content, clearance between disks, thickness of the grinding disk and rotational speed of the flywheel. The optimum variable variant's levels are A_3,B_1,C_3,D_1,E_1, which indicates that the first factor on third level, second factor on first level, third factor on third level, fourth factor on first level, and fifth factor on first level.

The line slope connecting the levels in the S/N ratio influences graphs (Figs. 5.17) evidently illustrates the strength of impact of each control variable. Specifically, the feed rate, followed by moisture content and clearance between disk has been found to have a significant impact on processing time for 1000 nuts and S/N ratios. The narrow slope of the lines indicates that the thickness of the grinding disks and the rotating speed of the flywheels have a smaller influence on processing time for 1000 nuts.
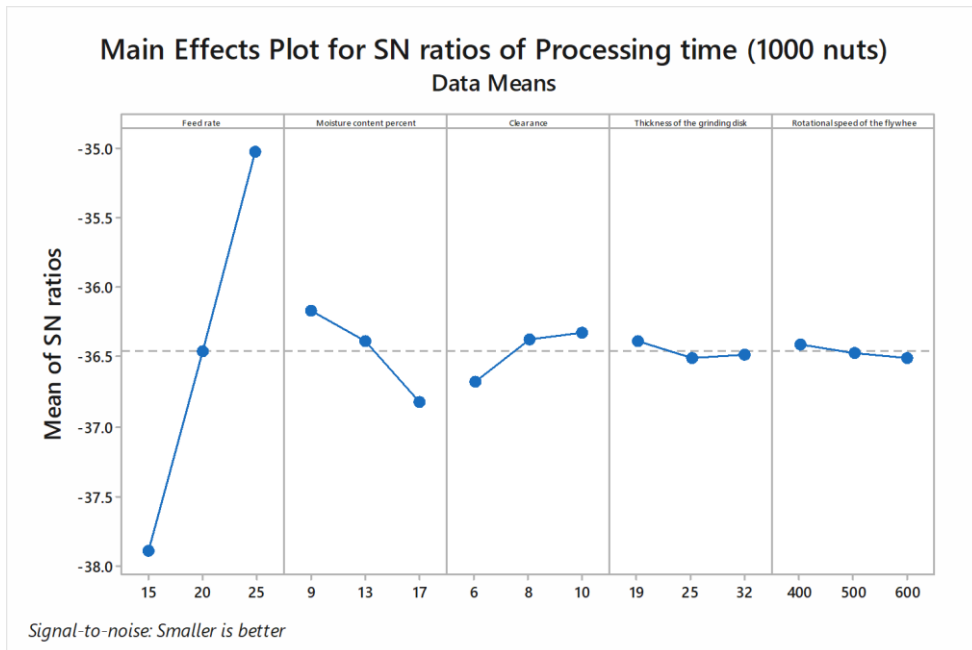
Fig. 5.16 Plot of main effect for S/N ratio of processing time for 1000 nuts

The interactions of parameters feed rate and clearance between disks, on all levels for processing time is given in Figure 5.17.
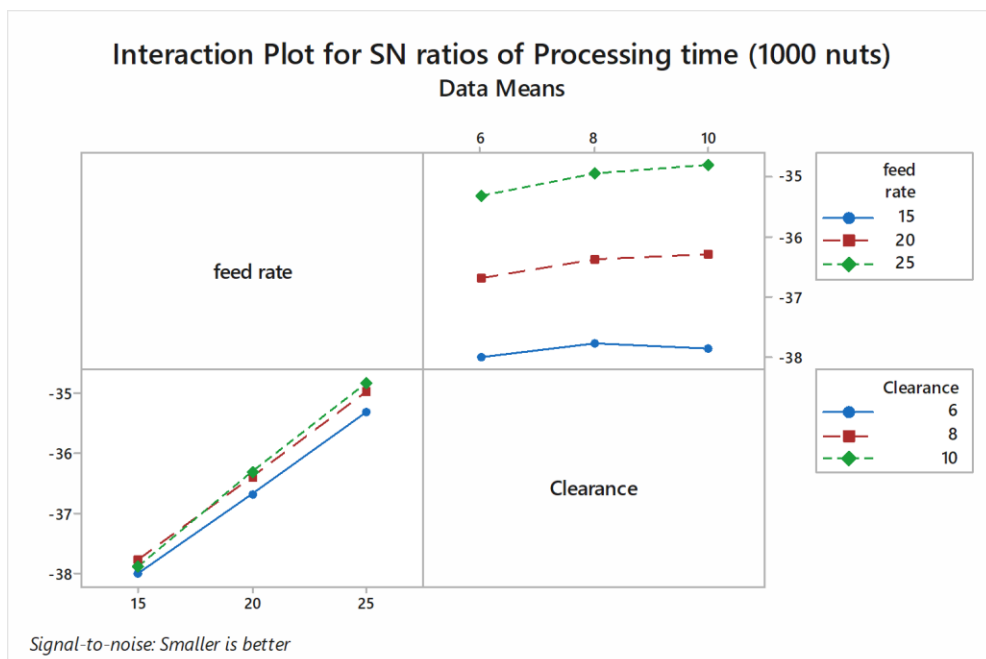
Fig. 5.17 Plot of main effect for S/N ratio of Effects of feed rate and clearance interactions on processing time for 1000 nuts

Moreover, it can be seen in Fig. 5.17 that plot of interactions between feed rate and clearance that feed rate at 25 kg/hr and clearance of 10 mm gave the largest processing time for 1000 nuts.

Figure 5.18 depicts the residual plot for processing time for 1000 nuts, which comprises a normality plot, a histogram, a fitted vs predicted plot, and a residual against observation order plot.
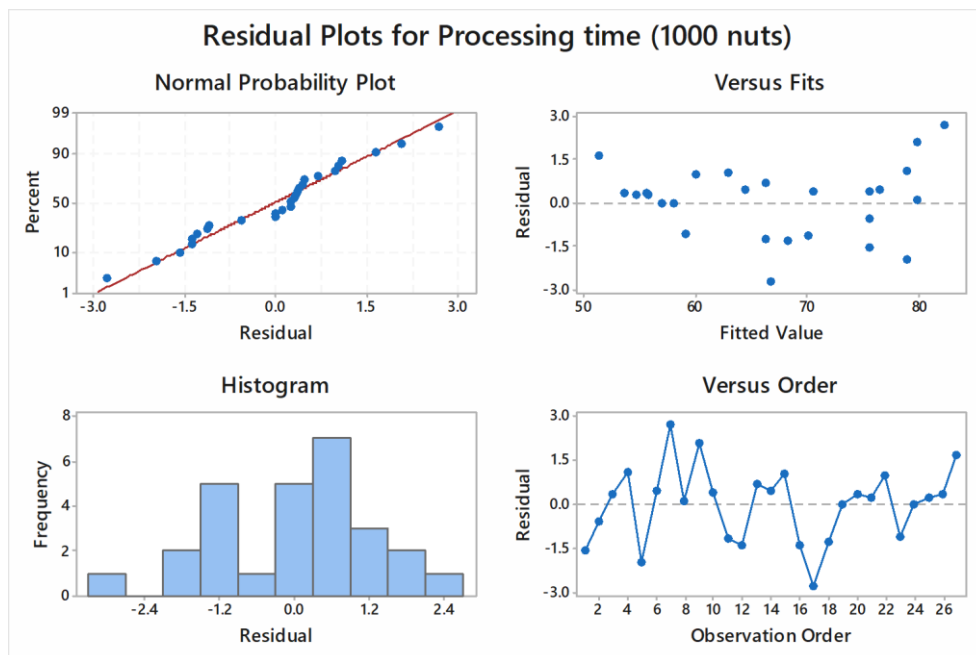
Figure 5.18: Residual plot for processing time for 1000 nuts

The normality plot demonstrates that almost the residuals follow a straight line, suggesting that the suggested model is fit. A histogram display shows a bell-shaped curve, suggesting that the data is normal. The residual vs fitted plot shows the randomized allotment on both sides of the reference line of all residuals. Additionally, there is no pattern in the residual versus observation order plot, which is required for significant ANOVA. This confirms that the suggested model will have a good future outcome if all four tests are satisfied.

Table 5.19 shows the results of analysis of variance (ANOVA) for processing time for 1000 nuts. From the analysis, it is noted that feed rate (PC = 91.88 %), moisture content percent (PC = 5.14 %) and clearance (PC = 1.51%) are the significantly

affecting the processing time. Among these factors effect of feed rate followed by moisture content percent and clearance feed are highly significant both physically and statistically. The changes of the thickness of the grinding disk, rotational speed of the flywheel and interaction of feed rate and clearance in the ranges given in Table 21 have minimal impacts on processing time, both statistically and physically. As a result of ANOVA and S/N analysis, the best process variables for processing time are A_3, B_1, C_3, D_1, E_1 i.e., feed rate (ψ) = 25 kg/hr, moisture content (C_d) = 9 % d.b, clearance between disks (C_d) = 10 mm, thickness of the grinding disk (t) = 19 mm and rotational speed of the flywheel (V_f) = 400 (rpm).

Table 5.19 Analysis of Variance for processing time for 1000 nuts.

Source	DF	Adj SS	Adj MS	F-Value	P-Value	PC (%)
Feed rate	2	2182.74	1091.37	620.36	0.000	91.89%
Moisture content percent	2	122.30	61.15	34.76	0.000	5.19%
Clearance	2	36.07	18.04	10.25	0.003	1.59%
Thickness of the grinding disk	2	4.96	2.48	1.41	0.282	0.21%
Rotational speed of the flywheel	2	3.63	1.81	1.03	0.386	0.15%
Feed rate*Clearance	4	4.59	1.15	0.65	0.636	0.19%
Error	12	21.11	1.76			
Total	26	2375.41				
R-sq = 98.26%; R-sq(adj)= 97.73%; R-sq(pred)= 96.68%						

A regression equation created in this manner creates a connection between significant conditions discovered through ANOVA analysis, i.e. feed rate, moisture content percent, clearance, thickness of the grinding disk and rotational speed of the flywheel. The regression equation developed for processing time for 1000 nuts is given as follow in equation (41)

Processing time (1000 nuts),
$$(T_p) = 96.28 - 1.800 \, \psi + 0.6389 \, M_c + 0.361 \, C_d + 0.0573 \, t + 0.00444 \, V_f - 0.0500 \, \psi * C_d \tag{41}$$

5.7 Development of artificial neural network simulation

Artificial Neural Network (ANN) Simulation is used to validate the experimentation conducted and mathematical model formed. The data base modeling has been achieved based on observed data for the two output parameters. In such complex phenomenon involving non-linear function wherein the validation of mathematical models is not in close proximity, it becomes necessary to formulate Artificial Neural Network (ANN) simulation of the observed data. Simulation consists of three layers. First layer is known as input layer. Number of neurons in input layer is equal to the number of input parameters. Second layer is known as hidden layer. It consists of ten numbers of neurons. The third layer is output layer. It contains six neurons equal to the number of dependent variables. Levenberg-Marquardt back-propagation topology is decided for the network.

Figure 5.19 shows a simple artificial neural network model [37]
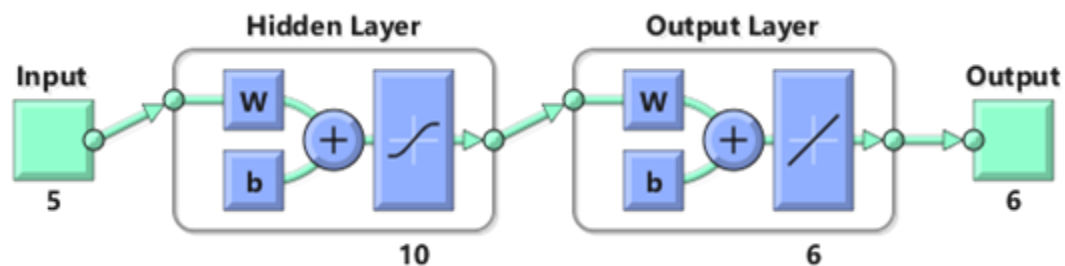
Fig. 5.19: artificial neural network model.

5.7.1 Procedure for Model Formation in ANN

The ANN Model is created using the MATLAB R2021a programme. The following are the stages that were taken in designing the algorithm that resulted in ANN.

1. The experiment's observed data is divided into two parts: input data and output data. The input and output data are loaded into the application separately.

2. The prestd function (standard neural network function which is used to preprocess the training set data) reads and properly sizes the input and output data.

3.   The input and output data are standardised using mean and standard deviation during the pre-processing stage.

4.   Based on the data pattern, a feed forward back propagation neural network is chosen.

5.   The training data is then used to train this network. The network is simulated after the computational errors in the actual and target data are calculated.
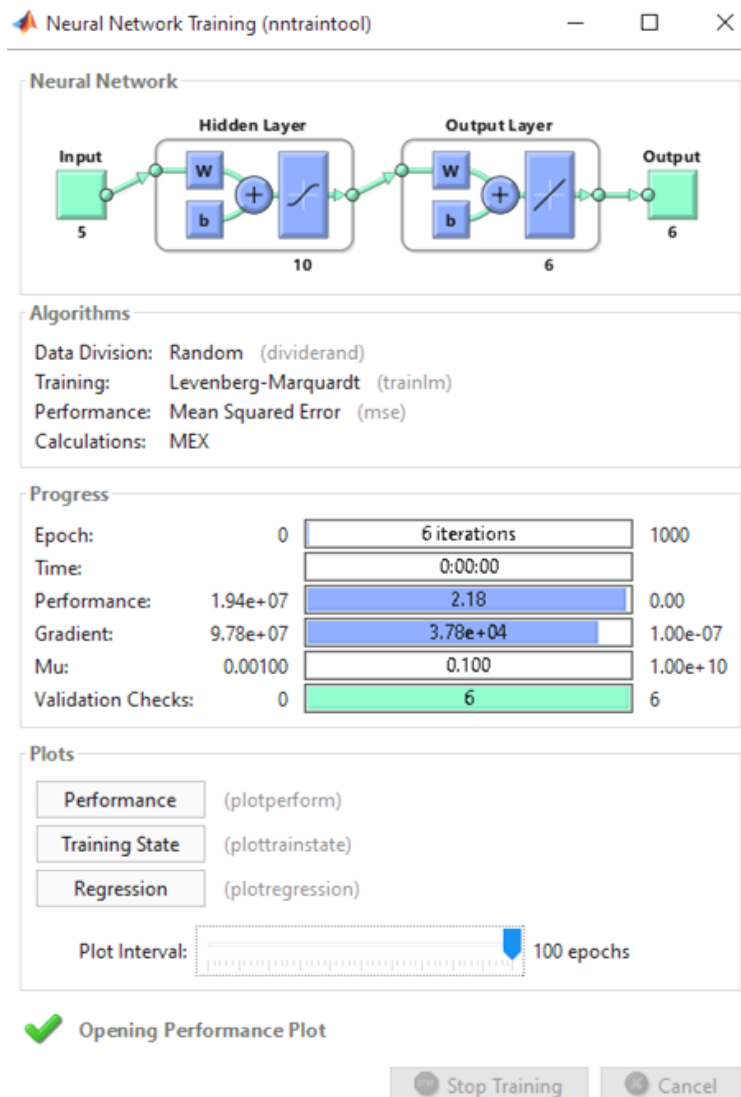
Figure 5.20: ANN Training Network (Levenberg-Marquardt back-propagation)
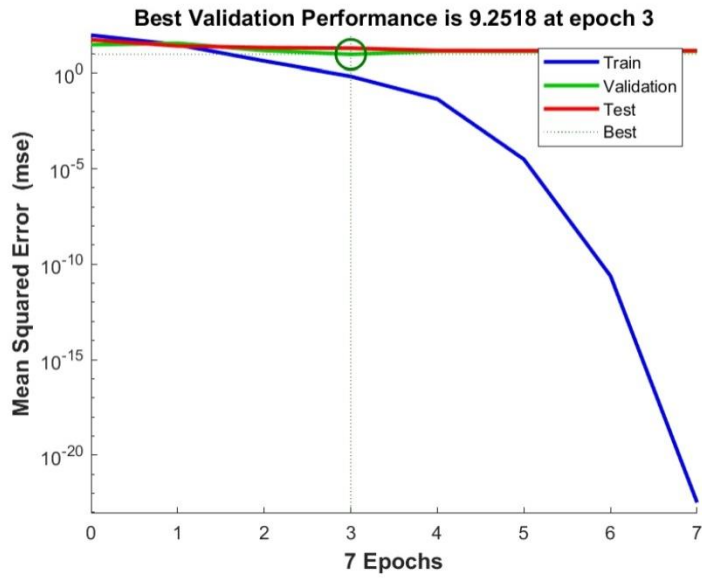
Figure 5.21: Network Training to Predict Output
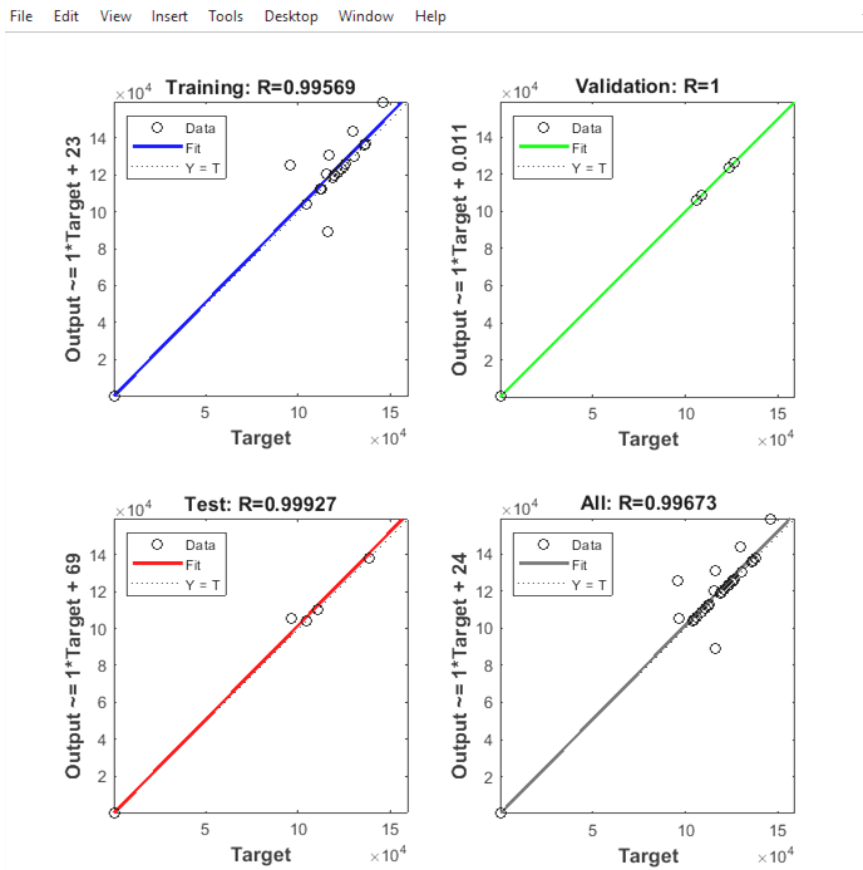
Figure 5.22: Line of Best Fit and Correlation Coefficient between Actual and Predicted values for Training, Validation, Testing and overall Performance

Table 5.20: Summary of ANN Simulation

Network Toolbox	NNSTARTTOOL
Network Type	Feed Forward Back Propagation
Network Training Function	TrainLM (Levenberg-Marquardt Algorithm)
Learning Function	LEARMGDM (Gradient descent with momentum back propagation method)
Transfer Function	LOGSIG (Logistic Sigmoid)
Learning Scheme	Supervised Learning
Learning Rule	Gradient descent Rule
Number of neuron in Input Layer	Five (Number of Input Parameters)
Number of neuron in output Layer	Six (Number of Output Parameters)
Data Division Method	DIVIDERAND (Random)
Sample Data Division	70 % for Training, 15 % for Testing, 15 % for Validation
Performance Function	MSE (Mean Squared Error)
Minimum Performance Gradient	1.00e-10
Maximum Mu	1.00e+10
Maximum Epochs (Cycles)	1000
Best Validation Performance of MSE	9.2518 at 3 Epochs
Correlation Coefficient (R) values	0.99569 (Training), 0.1 (Validation), 0.99927 (Testing), 0.99673 (Overall)

CHAPTER - 6

Optimization of Parameters Using Technique for Order of Preference Similarity to Ideal Solution (TOPSIS)

This chapter presents the optimization of the results of experimental data using Technique for Order of Preference by Similarity to Ideal Solution (TOPSIS).Using the technique of TOPSIS a combination of optimum process parameters is determined and presented in this chapter.

6.1 Multi-Criteria Decision Making (MCDM) methods

Multi criterion decision making methods (MCDM) are frequently used in engineering design and production to select the best solution from a finite multitude of alternatives. MCDM techniques can assist decision makers in reaching an effective agreement with such a scenario and making appropriate design selections to generate an optimal design. As there are several extant MCDM approaches, selecting the most appropriate methods is essential, because the use of inappropriate methods is frequently the source of inaccurate decision making. Nonetheless, the collection of MCDM techniques is a complicated MCDM challenge that must be properly carried out [156]. TOPSIS is an MCDM technique for dealing with numerous criteria. The idea behind this technique is to select the ideal alternatives with the smallest distance from the positive solution and the greatest distance from the negative solution[157]. These hypothetical solutions correlate to the database's maximum and minimum attribute values that compose acceptable solutions[158]. To find the optimal solutions, the nearest hypothetical best and furthest hypothetical worst are utilised. TOPSIS quickly analyses the tangible qualities as well as the quantity of options. TOPSIS uses the following steps to choose the right solution [159]-[160].

6.2 Steps in TOPSIS

Step 1: The objective and essential assessment attributes are established. For this particular problem deshelling efficiency and whole kernel recovery are considered as a beneficial attribute (maximization) and broken kernels,   partially   shelled   /

117

unshelled nuts, resistive torque, and processing time for 1000 nuts are considered non beneficial attributes (minimization).

Step 2: A decision matrix is used to represent all of the available information.

Step 3: Determination of the normalized decision matrix using the following formula (42)

$$r_{ij} = x_{ij} \sqrt{\sum_{i-1}^{m} x_{ij}^2} \quad i = 1, 2, ..., m \text{ and } j = 1, 2, ..., n. \qquad (42)$$

Step 4: The weighted normalised decision matrix is generated using the weighted normalised value v_{ij}, which is computed as follows (43).

$$v_{ij} = r_{ij} \times w_j \qquad i = 1, 2, ..., m \text{ and } j = 1, 2, ..., n. \qquad (43)$$

Where, w_j is the weight of the jth criterion or attribute and $\sum_{j=1}^{n} w_j = 1$.

Step 5: Determination of the positive ideal solution (A*) and the negative ideal solution (A⁻) using the equations (44) & (45) given below.

$$A^* = \{(\max_i v_{ij} \mid j \in C_b), (\min_i v_{ij} \mid j \in C_c)\} = \{v_j^* \mid j = 1,2,...,m\} \qquad (44)$$

$$A^- = \{(\min_i v_{ij} \mid j \in C_b), (\max_i v_{ij} \mid j \in C_c)\} = \{v_j^- \mid j = 1,2,...,m\} \qquad (45)$$

Step 6: The m-dimensional Euclidean distance is used to calculate the separation measurements. The distance between each alternative and the positive ideal one is determined by (46):

$$S_i^* = \sqrt{\sum_{j=1}^{m} (v_{ij} - v_j^*)^2}, j = 1,2,...,m \qquad (46)$$

The distance between each alternative and the negative ideal one is determined by (47)

$$S_{\bar{i}} = \sqrt{\sum_{j=1}^{m} (v_{ij} - v_{\bar{j}})^2}, j = 1,2,...,m \qquad (47)$$

Step 7: Determination of the relative closeness is of the alternative to the ideal solution (48).

$$RC_i^* = \frac{S_i^-}{S_i^* + S_i^-} \qquad i = 1, 2, ..., m \qquad (48)$$

The greater the RC_i^* value, the superior the performance of the solutions..

Step 8: Ranking of the relative preference order.

Figure 6.1 depicts the flowchart used to compute the ranking by using the TOPSIS approach.
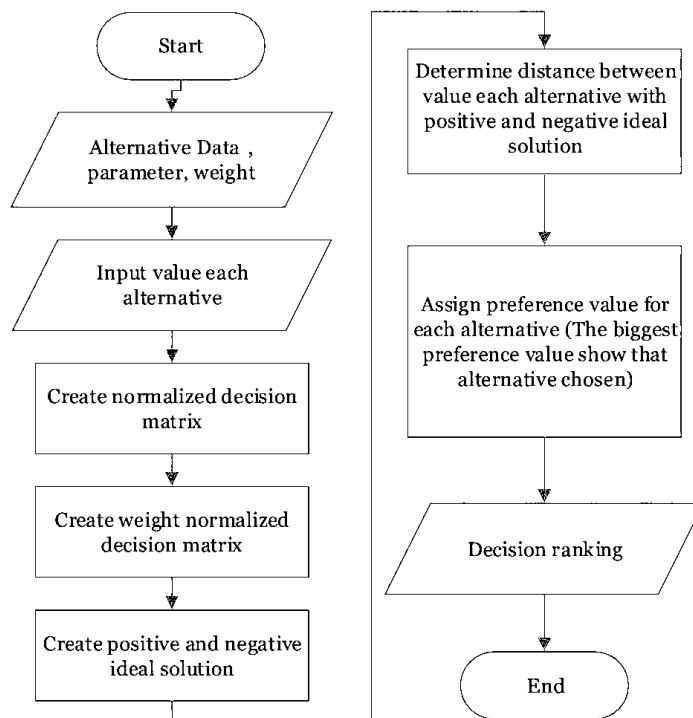
Figure 6.1. Flowchart TOPSIS process

119

6.3 Optimization using the proposed TOPSIS methodology

In this study, the response variables are deshelling efficiency, whole kernel recovery broken kernels, partially shelled / unshelled nuts, resistive torque, and processing time for 1000 nuts. The experimental observations of these responses are shown in Table 6.1.

Table 6.1. The experimental observations of the responses

Expt. No	Deshelling efficiency (%)	Whole kernel recovery (%)	Broken kernels (%)	Partially Shelled / Unshelled nuts (%)	Resistive Torque (N-mm)	Processing time (1000 nuts)
Expt. 1	84.0	65.5	16.5	16	96364.49	74
Expt. 2	79.8	65.6	14.2	17.9	129916.95	75
Expt. 3	80.9	68.6	12.3	20.2	123945.45	76
Expt. 4	83.5	66.5	17	16.8	104410.36	80
Expt. 5	83	71	12	17.4	109014.20	77
Expt. 6	75.2	62.2	13	20.2	130280.15	77
Expt. 7	84.4	69.4	15	19.2	125714.17	85
Expt. 8	79.5	62	17.5	20.5	135984.90	80
Expt. 9	77.1	61.6	15.5	22.9	112077.33	82
Expt. 10	78	63.5	14.5	20.6	104356.05	71
Expt. 11	77	66.2	10.8	23	116254.85	69
Expt. 12	75.2	58.6	16.6	24.8	112538.00	67
Expt. 13	86.8	70.6	16.2	17.9	116492.71	67
Expt. 14	76.8	62.3	14.5	20.1	95916.22	65
Expt. 15	74.4	61.6	12.8	23	105850.27	64
Expt. 16	80.5	63.3	17.2	18.8	124754.95	67
Expt. 17	76.1	63.7	12.4	20.3	110508.38	64
Expt. 18	79.8	66.6	13.2	22.5	126730.54	65
Expt. 19	86.4	69.6	16.8	19	146322.31	58
Expt. 20	73.8	61.7	12.1	20.8	118791.27	56
Expt. 21	75.1	62	13.1	22.4	123293.51	55
Expt. 22	74.8	60.6	14.2	22.2	121341.73	61
Expt. 23	75.1	60	15.1	24.9	119725.16	58

Expt. 24	72.9	62.6	10.3	27.1	136359.54	57
Expt. 25	80.2	64.1	16.1	19.8	115339.06	56
Expt. 26	80.5	66.9	13.6	22.2	138207.55	54
Expt. 27	71.5	59	12.5	24.3	104198.86	53

The normalized experimental observations of responses are shown in Table 6.2

Table 6.2. The normalized matrix for experimental observations

Expt. No	Deshelling efficiency (%)	Whole kernel recovery (%)	Broken kernels (%)	Partially Shelled / Unshelled nuts (%)	Resistive Torque (N-mm)	Processing time (1000 nuts)
Expt. 1	0.201	0.196	0.221	0.146	0.155	0.210
Expt. 2	0.195	0.196	0.190	0.163	0.209	0.213
Expt. 3	0.198	0.205	0.164	0.184	0.200	0.216
Expt. 4	0.204	0.199	0.227	0.153	0.168	0.227
Expt. 5	0.203	0.212	0.160	0.159	0.176	0.219
Expt. 6	0.184	0.186	0.174	0.184	0.210	0.219
Expt. 7	0.207	0.208	0.200	0.175	0.203	0.241
Expt. 8	0.195	0.185	0.234	0.187	0.219	0.227
Expt. 9	0.189	0.184	0.207	0.209	0.181	0.233
Expt. 10	0.191	0.190	0.194	0.188	0.168	0.202
Expt. 11	0.188	0.198	0.144	0.210	0.187	0.196
Expt. 12	0.184	0.175	0.222	0.226	0.181	0.190
Expt. 13	0.212	0.211	0.217	0.163	0.188	0.190
Expt. 14	0.188	0.186	0.194	0.183	0.155	0.185
Expt. 15	0.182	0.184	0.171	0.210	0.171	0.182
Expt. 16	0.197	0.189	0.230	0.172	0.201	0.190
Expt. 17	0.186	0.190	0.166	0.185	0.178	0.182
Expt. 18	0.195	0.199	0.176	0.205	0.204	0.185
Expt. 19	0.211	0.208	0.225	0.173	0.236	0.165
Expt. 20	0.181	0.184	0.162	0.190	0.192	0.159
Expt. 21	0.184	0.185	0.175	0.204	0.199	0.156
Expt. 22	0.183	0.181	0.190	0.203	0.196	0.173

Expt. 23	0.184	0.179	0.202	0.227	0.193	0.165
Expt. 24	0.178	0.187	0.138	0.247	0.220	0.162
Expt. 25	0.196	0.192	0.215	0.181	0.186	0.159
Expt. 26	0.197	0.200	0.182	0.203	0.223	0.153
Expt. 27	0.175	0.176	0.167	0.222	0.168	0.150

The weighted normalized decision matrix for experimental observations is shown in Table 6.3.

Table 6.3. The weighted normalized decision matrix for experimental observations

Expt. No	Deshelling efficiency (%)	Whole kernel recovery (%)	Broken kernels (%)	Partially Shelled / Unshelled nuts (%)	Resistive Torque (N-mm)	Processing time (1000 nuts)
Expt. 1	0.040	0.049	0.033	0.022	0.016	0.032
Expt. 2	0.039	0.049	0.028	0.025	0.031	0.032
Expt. 3	0.040	0.051	0.025	0.028	0.030	0.032
Expt. 4	0.041	0.050	0.034	0.023	0.025	0.034
Expt. 5	0.041	0.053	0.024	0.024	0.026	0.033
Expt. 6	0.037	0.046	0.026	0.028	0.032	0.033
Expt. 7	0.041	0.052	0.030	0.026	0.030	0.036
Expt. 8	0.039	0.046	0.035	0.028	0.033	0.034
Expt. 9	0.038	0.046	0.031	0.031	0.027	0.035
Expt. 10	0.038	0.047	0.029	0.028	0.025	0.030
Expt. 11	0.038	0.049	0.022	0.031	0.028	0.029
Expt. 12	0.037	0.044	0.033	0.034	0.027	0.029
Expt. 13	0.042	0.053	0.032	0.025	0.028	0.029
Expt. 14	0.038	0.047	0.029	0.028	0.023	0.028
Expt. 15	0.036	0.046	0.026	0.031	0.026	0.027
Expt. 16	0.039	0.047	0.034	0.026	0.030	0.029
Expt. 17	0.037	0.048	0.025	0.028	0.027	0.027
Expt. 18	0.039	0.050	0.026	0.031	0.031	0.028
Expt. 19	0.042	0.052	0.034	0.026	0.035	0.025
Expt. 20	0.036	0.046	0.024	0.028	0.029	0.024

Expt. 21	0.037	0.046	0.026	0.031	0.030	0.023
Expt. 22	0.037	0.045	0.028	0.030	0.029	0.026
Expt. 23	0.037	0.045	0.030	0.034	0.029	0.025
Expt. 24	0.036	0.047	0.021	0.037	0.033	0.024
Expt. 25	0.039	0.048	0.032	0.027	0.028	0.024
Expt. 26	0.039	0.050	0.027	0.030	0.033	0.023
Expt. 27	0.035	0.044	0.025	0.033	0.025	0.023

The positive ideal (A^*) and negative ideal (A^-) solutions are determined using Equations (44) and (45). The results are shown in Table 6.4.

Table 6.4. The positive ideal (A^*) and negative ideal (A^-) ideal solutions

Solution	Deshelling efficiency (%)	Whole kernel recovery (%)	Broken kernels (%)	Partially Shelled / Unshelled nuts (%)	Resistive Torque (N-mm)	Processing time (1000 nuts)
Positive ideal V+	0.0425	0.0531	0.0206	0.0219	0.0155	0.0226
Negative ideal V-	0.0350	0.0438	0.0351	0.0371	0.0353	0.0362

The separation of each alternative solution is calculated using Equations (46) and (47). The computed values are shown in Table 6.5.

Table 6.5. The distance from positive ideal solution (Si+) and distance from negative ideal solution (Si-)

Expt. No	Distance from Positive Ideal Solution (Si+)	Distance from Negative Ideal Solution (Si-)
Expt. 1	0.01603	0.02653
Expt. 2	0.02088	0.01674
Expt. 3	0.01911	0.01786
Expt. 4	0.02054	0.0194
Expt. 5	0.01551	0.02255
Expt. 6	0.0223	0.01442
Expt. 7	0.02275	0.01649

123

Expt. 8	0.02716	0.01069
Expt. 9	0.02358	0.01149
Expt. 10	0.0177	0.01666
Expt. 11	0.01826	0.01873
Expt. 12	0.02439	0.01191
Expt. 13	0.01849	0.02032
Expt. 14	0.01592	0.01907
Expt. 15	0.01807	0.01741
Expt. 16	0.02233	0.01572
Expt. 17	0.01602	0.01913
Expt. 18	0.01975	0.01616
Expt. 19	0.02422	0.01944
Expt. 20	0.01791	0.01988
Expt. 21	0.01977	0.01797
Expt. 22	0.02075	0.01531
Expt. 23	0.02294	0.01449
Expt. 24	0.02498	0.01912
Expt. 25	0.01881	0.01875
Expt. 26	0.02133	0.0185
Expt. 27	0.01946	0.02012

The result of the ranking of approaches is derived using Equations (48) i.e by determining the relative closeness. For this particular problem deshelling efficiency and whole kernel recovery are considered as a beneficial attribute (maximization) and broken kernels, partially shelled / unshelled nuts, resistive torque, and processing time for 1000 nuts are considered non beneficial attributes (minimization). Table 6.6 shows the relative correlation coefficient and ranking of the experimental run based on its performance.

Table 6.6. The relative closeness and ranking based on it

Expt. No	Relative closeness (RC_i^*)	Ranking
Expt. 1	0.01603	1
Expt. 2	0.02088	18

Expt. 3	0.01911	13
Expt. 4	0.02054	11
Expt. 5	0.01551	2
Expt. 6	0.0223	23
Expt. 7	0.02275	21
Expt. 8	0.02716	27
Expt. 9	0.02358	26
Expt. 10	0.0177	12
Expt. 11	0.01826	8
Expt. 12	0.02439	25
Expt. 13	0.01849	6
Expt. 14	0.01592	3
Expt. 15	0.01807	10
Expt. 16	0.02233	22
Expt. 17	0.01602	4
Expt. 18	0.01975	16
Expt. 19	0.02422	17
Expt. 20	0.01791	5
Expt. 21	0.01977	14
Expt. 22	0.02075	20
Expt. 23	0.02294	24
Expt. 24	0.02498	19
Expt. 25	0.01881	9
Expt. 26	0.02133	15
Expt. 27	0.01946	7

From Table 6.6, based on the relative correlation coefficient and ranking of the experimental run based on its performance; Expt.1 combinations gives the optimum output followed by Expt.5, Expt.14, Expt.17 & Expt.20 for top five combinations.

CHAPTER - 7

RESULTS AND DISCUSSION

This chapter presents the validation of the results of experimental data, mathematical models and ANN simulation. The comparison of percentage error between experimental values & values obtained from mathematical model and ANN simulation model was done. Also, effect of various input parameters on the individual output parameters was studied and presented.

7.1 Validation of the output of Experimental Data, Mathematical Models and ANN Simulation

Table 7.1 shows the output values obtained from experimentation, mathematical model and ANN simulation for deshelling efficiency (η_d). Output obtained from ANN Model is compared with output obtained from experimentation and output calculated from mathematical model for deshelling efficiency (η_d). The maximum deshelling efficiency obtained by experimentation, mathematical model and ANN Model is 84 %, 84.07 % and 81.96 % respectively. Whereas minimum deshelling efficiency of 72.9 %, 73.71 and 72.87 are obtained by experimentation, mathematical model and ANN Model respectively.

Table 7.1: Comparison between Experimental Data, Mathematical Models and ANN Simulation of Deshelling Efficiency

Trial No.	(ψ) (kg/hr)	(M_c) (% d.b)	(C_d) (mm)	(t) (mm)	(V_f) (rpm)	Deshelling Efficiency (η_d) (%)		
						Experimental (η_d) (%)	Mathematical (η_d) (%)	ANN Simulation (η_d) (%)
1	15	9	6	19	400	84	84.07	81.95927
2	15	9	8	25	500	82.1	82.16	81.0579
3	15	9	10	32	600	79.8	80.26	79.61863
4	15	13	6	25	500	83.2	82.77	83.16116
5	15	13	8	32	600	82.6	80.87	82.67335
6	15	13	10	19	400	79.8	78.88	79.66149
7	15	17	6	32	600	80.8	81.49	81.00033

8	15	17	8	19	400	79.5	79.49	79.81281
9	15	17	10	25	500	77.1	77.58	76.52437
10	20	17	6	19	500	79.4	79.75	79.82386
11	20	17	8	25	600	77	77.72	74.88231
12	20	17	10	32	400	75.2	75.82	75.53596
13	20	9	6	25	600	82.1	82.42	78.78779
14	20	9	8	32	400	79.9	80.53	77.8113
15	20	9	10	19	500	77	78.28	76.78516
16	20	13	6	32	400	81.2	81.27	81.18554
17	20	13	8	19	500	79.7	79.02	79.45757
18	20	13	10	25	600	77.5	76.98	77.949
19	25	13	6	19	600	81	79.40	78.76792
20	25	13	8	25	400	79.2	77.37	78.83065
21	25	13	10	32	500	77.6	75.22	77.14962
22	25	17	6	25	400	77.8	78.24	77.53313
23	25	17	8	32	500	75.1	76.08	75.35134
24	25	17	10	19	600	72.9	73.71	72.86657
25	25	9	6	32	500	80.2	80.91	77.23401
26	25	9	8	19	600	77.8	78.54	77.6982
27	25	9	10	25	400	75.7	76.51	76.2496

It is observed from Figure 7.1 that Output produced by experimentation, mathematical model and ANN Simulation is very close to each other. At few point they match with each other shows their closeness is quite high. Similar kind of trend was noticed for output produced by experimentation, mathematical model and ANN Simulation for various agricultural products [69], [76]. Hence the values of actual experimentation conducted, mathematical model formed and predicted values of ANN Simulation is validated.
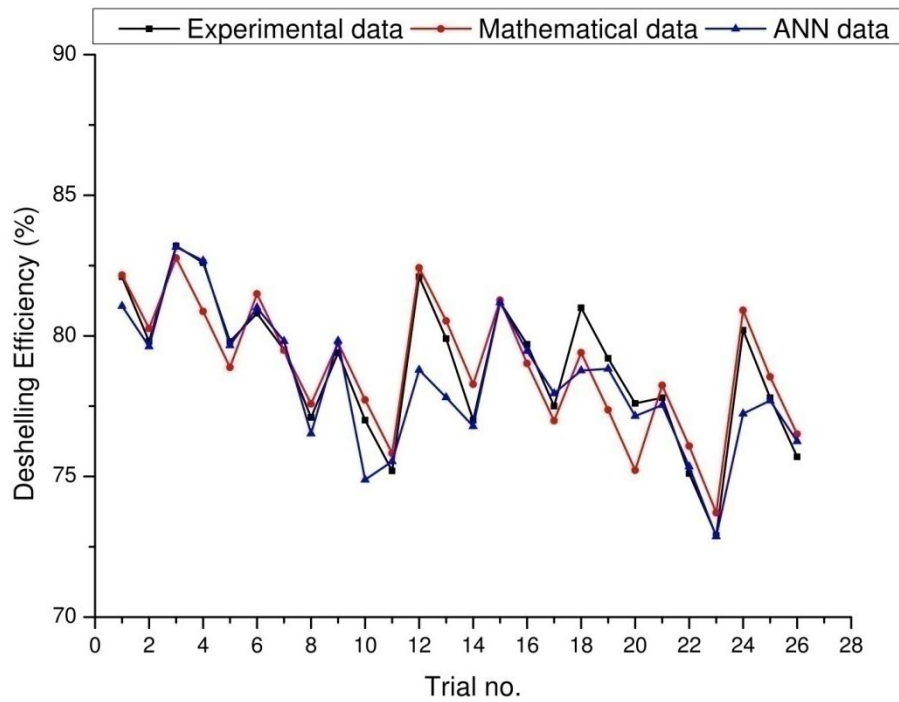
Figure 7.1: Comparison of output obtained from Experimentation, Mathematical Model and ANN Model for Deshelling Efficiency

Table 7.2 shows the output values obtained from experimentation, mathematical model and ANN simulation for Whole kernel recovery (η_w). Output obtained from ANN Model is compared with output obtained from experimentation and output calculated from mathematical model for Whole kernel recovery (η_w). The maximum whole kernel recovery obtained by experimentation, mathematical model and ANN Model is 71 %, 70.18 % and 71.08 % respectively. Whereas experimental, mathematical model, and ANN model achieve minimal whole kernel recovery of 58.6 %, 58.46 %, and 58.58 %, respectively.

Table 7.2: Comparison between Experimental Data, Mathematical Models and ANN
Simulation of Whole kernel recovery

Trial No.	(ψ) (kg/hr)	(M_c) (% d.b)	(C_d) (mm)	(t) (mm)	(V_f) (rpm)	Whole kernel recovery ($η_w$) (%)		
						Experimental ($η_w$) (%)	Mathematical ($η_w$) (%)	ANN Simulation ($η_w$) (%)
1	15	9	6	19	400	65.5	65.13	64.36
2	15	9	8	25	500	65.6	66.80	68.80
3	15	9	10	32	600	68.6	68.49	68.49
4	15	13	6	25	500	66.5	67.25	66.39
5	15	13	8	32	600	71	68.94	71.08
6	15	13	10	19	400	62.2	60.95	62.13
7	15	17	6	32	600	69.4	69.38	69.44
8	15	17	8	19	400	62	61.40	62.10
9	15	17	10	25	500	61.6	63.07	61.64
10	20	17	6	19	500	63.5	64.77	63.57
11	20	17	8	25	600	66.2	66.30	62.99
12	20	17	10	32	400	58.6	58.46	58.58
13	20	9	6	25	600	70.6	70.18	67.11
14	20	9	8	32	400	62.3	62.34	60.40
15	20	9	10	19	500	61.6	63.59	61.85
16	20	13	6	32	400	63.3	62.93	63.31
17	20	13	8	19	500	63.7	64.18	63.59
18	20	13	10	25	600	66.6	65.71	66.48
19	25	13	6	19	600	69.6	67.70	70.13
20	25	13	8	25	400	61.7	59.70	61.94
21	25	13	10	32	500	62	61.11	62.06
22	25	17	6	25	400	60.6	60.44	60.39
23	25	17	8	32	500	60	61.84	59.97
24	25	17	10	19	600	62.6	62.95	60.26
25	25	9	6	32	500	64.1	65.85	62.49
26	25	9	8	19	600	66.9	66.97	66.88
27	25	9	10	25	400	59	58.97	58.87

Figure 7.2 shows that whole kernel recovery (w) obtained by experimental, mathematical model, and ANN Simulation all follow the same pattern and are extremely similar to each other. They match with each other at a few points, indicating their closeness. Similar kind of closeness was noticed for output produced by experimentation, mathematical model and ANN Simulation for various agricultural products [78], [82]. As a result, the results of the actual experimentation, the mathematical model developed, and the projected values of the ANN Simulation are validated for whole kernel recovery.
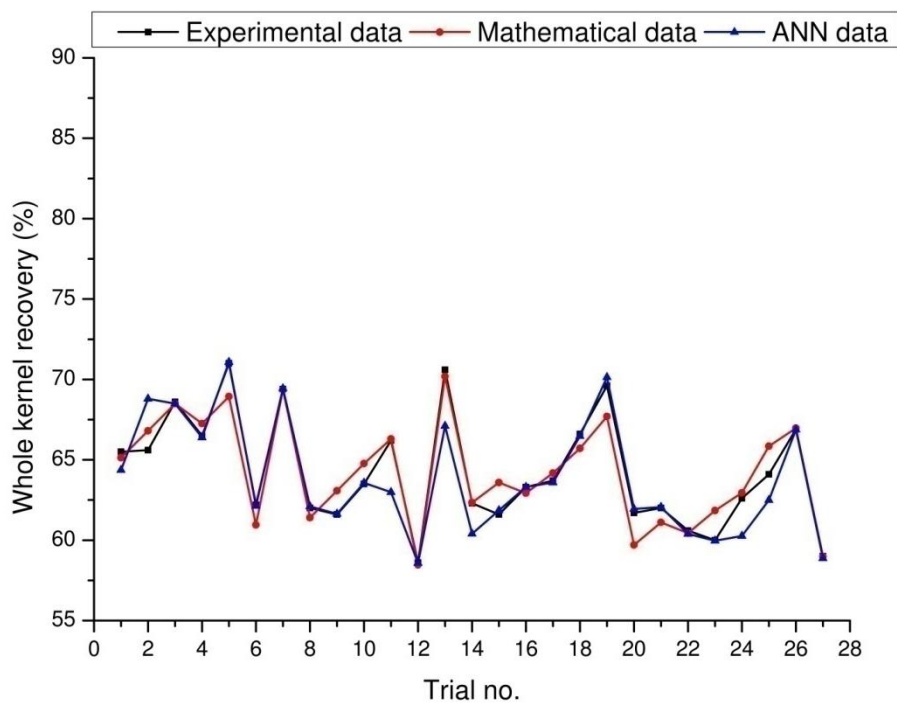
Figure 7.2: Comparison of output obtained from Experimentation, Mathematical Model and ANN Model for Whole kernel recovery

Table 7.3 shows the output values obtained from experimentation, mathematical model and ANN simulation for broken kernels (η_b). Output obtained from ANN Model is compared with output obtained from experimentation and output calculated from mathematical model for broken kernels. The maximum broken kernels obtained by experimentation, mathematical model and ANN Model is 18.5 %, 18.94 % and 18.39 % respectively. While, experimentation, mathematical modelling, and ANN modelling provide minimal broken kernels of 10.3 %, 10.76 %, and 10.28 %, respectively.

130

Table 7.3: Comparison between Experimental Data, Mathematical Models and ANN
Simulation of Broken Kernel

Trial No.	(ψ) (kg/hr)	(M_c) (% d.b)	(C_d) (mm)	(t) (mm)	(V_f) (rpm)	Broken Kernel (η_b) (%)		
						Experimental (η_b) (%)	Mathematical (η_b) (%)	ANN Simulation (η_b) (%)
1	15	9	6	19	400	18.5	18.94	18.39
2	15	9	8	25	500	16.5	17.10	16.11
3	15	9	10	32	600	11.2	11.66	11.12
4	15	13	6	25	500	16.7	15.96	16.82
5	15	13	8	32	600	11.6	11.93	11.63
6	15	13	10	19	400	17.6	17.93	17.51
7	15	17	6	32	600	11.4	11.90	11.55
8	15	17	8	19	400	17.5	18.09	17.70
9	15	17	10	25	500	15.5	14.81	14.87
10	20	17	6	19	500	15.9	15.58	16.28
11	20	17	8	25	600	10.8	11.11	10.28
12	20	17	10	32	400	16.6	17.36	16.96
13	20	9	6	25	600	11.5	11.98	12.06
14	20	9	8	32	400	17.6	18.19	17.32
15	20	9	10	19	500	15.4	14.68	14.92
16	20	13	6	32	400	17.9	18.34	17.83
17	20	13	8	19	500	16	15.73	15.91
18	20	13	10	25	600	10.9	11.26	11.36
19	25	13	6	19	600	11.4	11.70	11.91
20	25	13	8	25	400	17.5	17.67	16.92
21	25	13	10	32	500	15.6	15.11	15.10
22	25	17	6	25	400	17.2	17.80	17.10
23	25	17	8	32	500	15.1	14.39	15.34
24	25	17	10	19	600	10.3	10.76	10.57
25	25	9	6	32	500	16.1	15.56	16.59
26	25	9	8	19	600	10.9	11.17	10.80
27	25	9	10	25	400	16.7	17.53	17.40

Figure 7.3 shows that broken kernels generated via experimental, mathematical modelling, and ANN Simulation all follow the same pattern and are extremely similar. They match at a few points, indicating a high degree of closeness. Similar kind of trend was noticed for output produced by experimentation, mathematical model and ANN Simulation for various agricultural products [79], [83]. As a result, for broken kernels, the results of the actual experimentation, the mathematical model developed, and the projected values of the ANN Simulation are all valid.

Figure 7.3: Comparison of output obtained from Experimentation, Mathematical Model and ANN Model for Broken kernels

Table 7.4 shows the output values obtained from experimentation, mathematical model and ANN simulation for partially shelled / unshelled nuts (η_u). Output obtained from ANN Model is compared with output obtained from experimentation and output calculated from mathematical model for partially shelled / unshelled nuts. The maximum partially shelled / unshelled nuts obtained by experimentation, mathematical model and ANN Model is 29.0 %, 29.21 % and 28.62 % respectively. Whereas minimum partially shelled / unshelled nuts of 10.8 %, 10.85 % and 10.94 % are obtained by experimentation, mathematical model and ANN model respectively.

Table 7.4: Comparison between Experimental Data, Mathematical Models and ANN
Simulation of Partially Shelled / Unshelled nuts

Trial No.	(ψ) (kg/hr)	(M_c) (% d.b)	(C_d) (mm)	(t) (mm)	(V_f) (rpm)	Partially Shelled / Unshelled nuts (η_u) (%)		
						Experimental (η_u) (%)	Mathematical (η_u) (%)	ANN Simulation (η_u) (%)
1	15	9	6	19	400	16	15.23	16.55
2	15	9	8	25	500	17.9	18.73	18.74
3	15	9	10	32	600	24.4	23.23	24.13
4	15	13	6	25	500	14.7	15.18	14.67
5	15	13	8	32	600	18.8	19.58	18.85
6	15	13	10	19	400	27.5	27.36	27.44
7	15	17	6	32	600	16.9	16.13	17.05
8	15	17	8	19	400	22.8	23.82	23.01
9	15	17	10	25	500	28.4	28.31	28.22
10	20	17	6	19	500	18.5	17.62	18.82
11	20	17	8	25	600	21.4	21.89	21.96
12	20	17	10	32	400	28.5	28.62	28.62
13	20	9	6	25	600	10.8	11.14	10.94
14	20	9	8	32	400	17.6	18.26	18.43
15	20	9	10	19	500	25.7	25.27	25.77
16	20	13	6	32	400	12.4	12.98	12.42
17	20	13	8	19	500	19.6	20.55	19.19
18	20	13	10	25	600	26.8	26.21	26.79
19	25	13	6	19	600	12.6	12.98	12.02
20	25	13	8	25	400	18.8	19.57	18.58
21	25	13	10	32	500	27.6	26.53	27.65
22	25	17	6	25	400	17.3	16.75	17.17
23	25	17	8	32	500	20.9	21.43	20.78
24	25	17	10	19	600	29	29.21	27.90
25	25	9	6	32	500	11.2	10.85	11.30
26	25	9	8	19	600	17.4	18.08	17.67
27	25	9	10	25	400	26.5	25.67	26.67

It is observed from figure 7.4 that partially shelled / unshelled nuts produced by experimentation, mathematical model and ANN Simulation is follow the same pattern and is very close to each other. At few point they match with each other shows their closeness is quite high. Similar kind of closeness was noticed for output produced by experimentation, mathematical model and ANN Simulation for various agricultural products [84]-[85]. Hence the values of actual experimentation conducted, mathematical model formed and predicted values of ANN Simulation is validated for partially shelled / unshelled nuts.
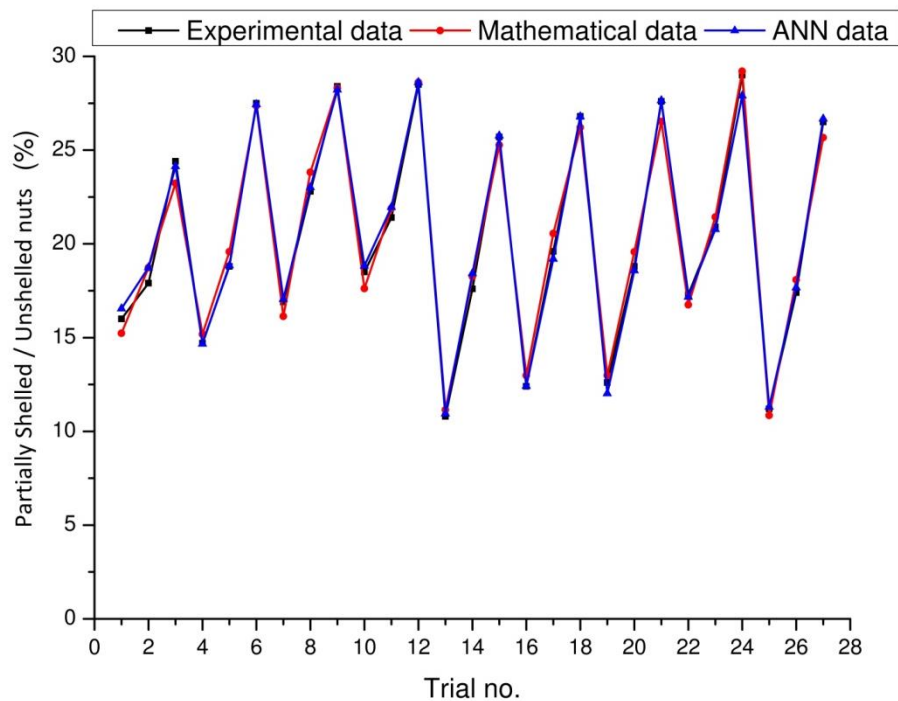
Figure 7.4: Comparison of output obtained from Experimentation, Mathematical Model and ANN Model for Partially Shelled / Unshelled nuts

Table 7.5 shows the output values obtained from experimentation, mathematical model and ANN simulation for resistive torque (Ʈr). Output obtained from ANN Model is compared with output obtained from experimentation and output calculated from mathematical model for resistive torque. The maximum resistive torque experienced by experimentation, mathematical model and ANN Model is 1466322 N-mm, 144195 N-mm and 149305 N-mm respectively. Whereas minimum resistive torque of 95916 N-mm, 100022 N-mm and 95555 N-mm are experienced by experimentation, mathematical model and ANN model respectively.

Table 7.5: Comparison between Experimental Data, Mathematical Models and ANN
Simulation of Resistive Torque

Trial No.	(ψ) (kg/hr)	(M_c) (% d.b)	(C_a) (mm)	(t) (mm)	(V_f) (rpm)	Resistive Torque (Ʈr) (N-mm)		
						Experimental (Ʈr) (N-mm)	Mathematical (Ʈr) (N-mm)	ANN Simulation (Ʈr) (N-mm)
1	15	9	6	19	400	96364.488	103693	100284.1
2	15	9	8	25	500	129916.95	122535	123841.6
3	15	9	10	32	600	123945.45	120928	129946.4
4	15	13	6	25	500	104410.36	109717	108410.3
5	15	13	8	32	600	109014.2	116110	119014.6
6	15	13	10	19	400	130280.15	139013	139279.8
7	15	17	6	32	600	125714.17	133292	129714.2
8	15	17	8	19	400	135984.9	144195	127984.6
9	15	17	10	25	500	112077.33	117037	119077.6
10	20	17	6	19	500	104356.05	110669	109355.7
11	20	17	8	25	600	116254.85	119601	109039.3
12	20	17	10	32	400	112538	114614	120537.6
13	20	9	6	25	600	116492.71	120009	110875.8
14	20	9	8	32	400	95916.216	100022	95555.98
15	20	9	10	19	500	105850.27	111485	109850.5
16	20	13	6	32	400	124754.95	119114	129754.5
17	20	13	8	19	500	110508.38	115577	117508.3
18	20	13	10	25	600	126730.54	125509	119730.6
19	25	13	6	19	600	146322.31	139961	149305.4
20	25	13	8	25	400	118791.27	116513	122791.6
21	25	13	10	32	500	123293.51	115086	133293.1
22	25	17	6	25	400	121341.73	123515	125341.7
23	25	17	8	32	500	119725.16	122088	121725.1
24	25	17	10	19	600	136359.54	129641	136530.6
25	25	9	6	32	500	115339.06	119406	120532.1
26	25	9	8	19	600	138207.55	129959	131207.3
27	25	9	10	25	400	104198.86	109511	109199.2

Figure 7.5 shows that the resistive torque experienced by experimental, mathematical model, and ANN Simulation all follow the same pattern, but the values are not too close to each other. At a few points, they match, indicating that their closeness is still present. Similar kind of trend was noticed for output produced by experimentation, mathematical model and ANN Simulation for various agricultural products [84]-[85]. As a result, the results of the actual experimentation, the mathematical model developed, and the projected values of the ANN Simulation are validated for resistive torque.
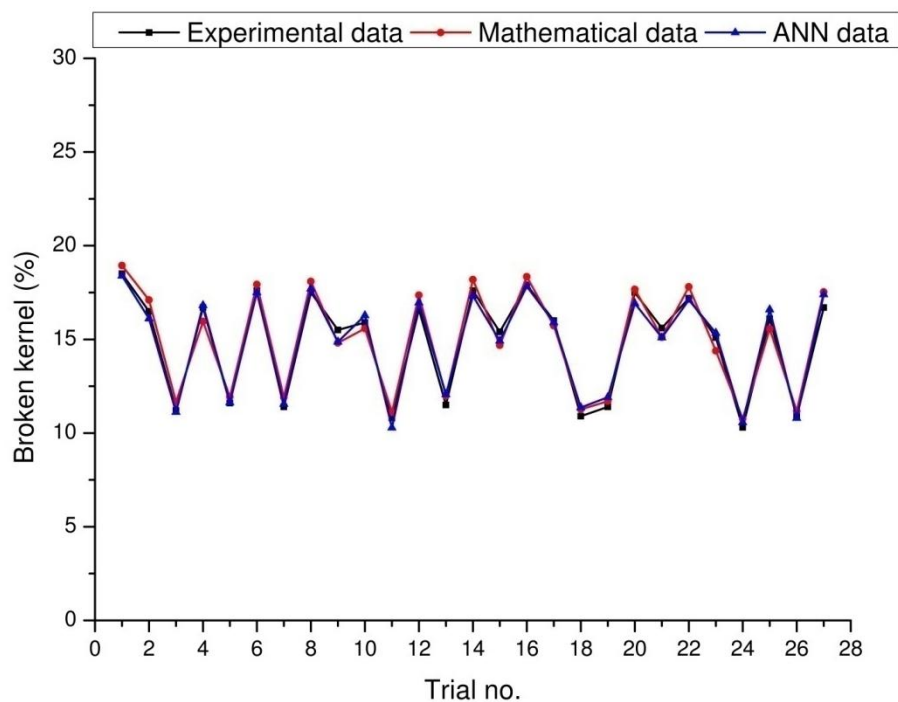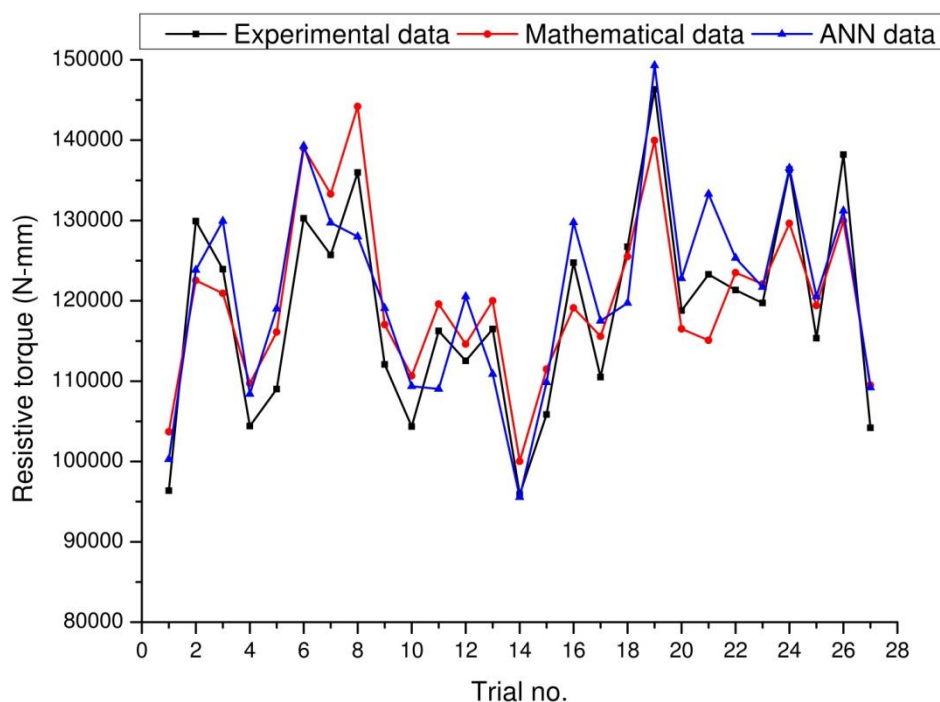

Figure 7.5: Comparison of output obtained from Experimentation, Mathematical Model and ANN Model for Resistive torque

Table 7.6 shows the output values obtained from experimentation, mathematical model and ANN simulation for processing time (1000 nuts) (Tp). Output obtained from ANN Model is compared with output obtained from experimentation and output calculated from mathematical model for processing time. The maximum processing time obtained by experimentation, mathematical model and ANN Model is 85 seconds, 82.30 seconds and 85.01 seconds respectively. Whereas minimum

processing time of 53 seconds, 51.35 seconds and 53.09 seconds are obtained by experimentation, mathematical model and ANN model respectively.

Table 7.6: Comparison between Experimental Data, Mathematical Models and ANN Simulation of Processing time (1000 nuts)

Trial No.	(ψ) (kg/hr)	(M_c) (% d.b)	(C_d) (mm)	(t) (mm)	(V_f) (rpm)	Processing time (1000 nuts) (Tp) (%)		
						Experimental (Tp) (Sec.)	Mathematical (Tp) (Sec.)	ANN Simulation (Tp) (Sec.)
1	15	9	6	19	400	74	75.56	73.71
2	15	9	8	25	500	75	75.57	74.88
3	15	9	10	32	600	76	75.64	75.99
4	15	13	6	25	500	80	78.90	80.02
5	15	13	8	32	600	77	78.97	77.03
6	15	13	10	19	400	77	76.56	76.99
7	15	17	6	32	600	85	82.30	85.01
8	15	17	8	19	400	80	79.89	80.04
9	15	17	10	25	500	82	79.90	81.85
10	20	17	6	19	500	71	70.62	71.02
11	20	17	8	25	600	69	70.13	67.23
12	20	17	10	32	400	67	68.36	67.08
13	20	9	6	25	600	67	66.29	64.08
14	20	9	8	32	400	65	64.53	67.83
15	20	9	10	19	500	64	62.95	63.96
16	20	13	6	32	400	67	68.36	66.99
17	20	13	8	19	500	64	66.78	63.95
18	20	13	10	25	600	65	66.29	65.15
19	25	13	6	19	600	58	58.00	55.59
20	25	13	8	25	400	56	55.68	56.05
21	25	13	10	32	500	55	54.75	54.82
22	25	17	6	25	400	61	60.02	60.90
23	25	17	8	32	500	58	59.08	58.14
24	25	17	10	19	600	57	57.00	58.95

25	25	9	6	32	500	56	55.75	54.19
26	25	9	8	19	600	54	53.67	53.91
27	25	9	10	25	400	53	51.35	53.09

Figure 7.6 shows that processing time generated by experimental, mathematical model, and ANN Simulation all follow the same trend and are extremely similar. They match at a few points, indicating that they are fairly near. Similar kind of trend was noticed for output produced by experimentation, mathematical model and ANN Simulation for various agricultural products [69], [76]. As a result, the results of the actual experiment, the mathematical model that was created, and the projected values of the ANN Simulation were all validated for processing time.
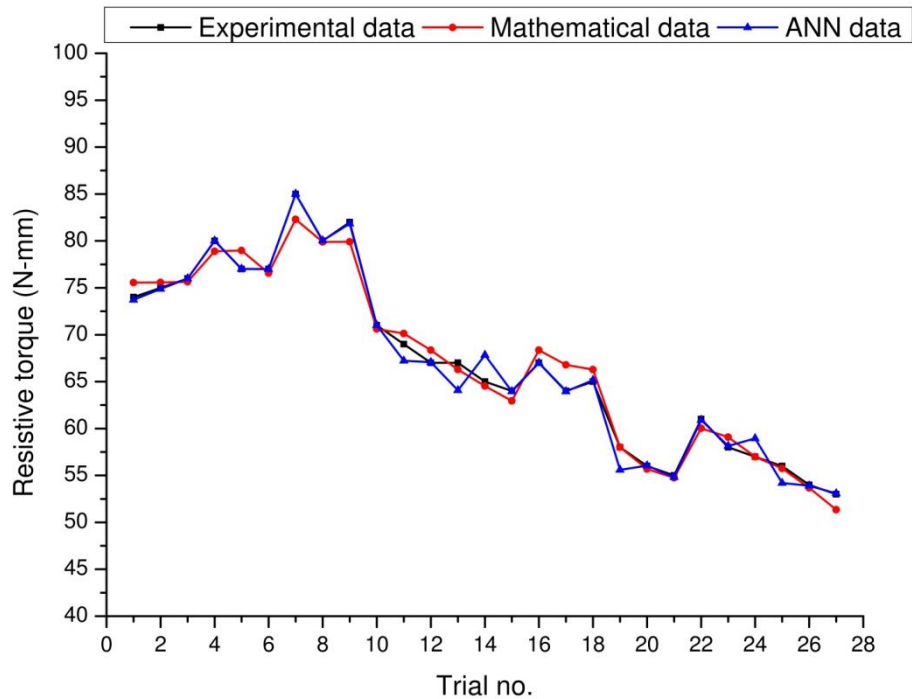
Figure 7.6: Comparison of output obtained from Experimentation, Mathematical Model and ANN Model for Processing time

7.2 Percentage Error Test

The experimental values of independent variables are entered into mathematical models to produce a set of dependent values. The deviation between the values derived from the mathematical model and the actual experimental values of dependent parameters demonstrates the mathematical model's proximity to the real-world process. The closer the value, the more accurate the mathematical model to utilise. The deviation of the numbers can be expressed as a percentage error. The lower the percentage inaccuracy, the greater the closeness. The following mathematical connection will calculate the percentage inaccuracy between actual and mathematical values.

$$Percentage\ Error = \frac{Y_{Actual} - Y_{mathematical}}{Y_{Actual}} \times 100$$

Percentage error between experimental values and values obtained from mathematical model for Deshelling Efficiency (η_d) is obtained as

$$Percentage\ Error = \frac{Y_{Experimental} - Y_{mathematical}}{Y_{Experimental}} \times 100$$

For observation No.1, $Percentage\ Error = \frac{84 - 84.07}{84} \times 100 = 0.09\ \%$

For observation No. 11, $Percentage\ Error = \frac{77 - 77.72}{77} \times 100 = 0.93\ \%$

For observation No. 27, $Percentage\ Error = \frac{75.7 - 76.51}{75.7} \times 100 = 1.06\ \%$

Similarly, Percentage error between experimental values and ANN values for Deshelling Efficiency (η_d) is obtained.

Similar procedure can be adapted to determine percentage error between experimental values, values from mathematical model and ANN values for Deshelling efficiency, Whole kernel recovery, Broken kernels, Partially Shelled / Unshelled nuts, Resistive Torque and Processing time (1000 nuts). Collective data sheet is formed with same procedure and tabulated in Table 7.7 to 7.12.

7.2.1 Percentage Error for Deshelling Efficiency (η_d)

Table 7.7 shows the percentage error of values obtained from experimentation & mathematical model and experimentation & ANN simulation for deshelling efficiency (η_d). From Table 7.7, it can be seen that percentage error between experimental values and values from mathematical model for deshelling efficiency ranges from –1.66% to 3.07% and average RMS Error is 1.196%. Similarly, percentage error between experimental values and ANN values for deshelling efficiency ranges from –1.31% to 4.03 % and average RMS Error is 1.558%.

Table 7.7: Comparison Percentage Error of Deshelling Efficiency (η_d) between Experimental Data, Mathematical Models and ANN Simulation

Sr. No	Deshelling Efficiency (η_d) (%)			Percentage Error	
	Experimental (η_d) (%)	Mathematical (η_d) (%)	ANN Simulation (η_d) (%)	Experimental & Mathematical Model	Experimental & ANN Simulation
1	84	84.07	81.95927	-0.09	2.43
2	82.1	82.16	81.0579	-0.07	1.27
3	79.8	80.26	79.61863	-0.57	0.23
4	83.2	82.77	83.16116	0.51	0.05
5	82.6	80.87	82.67335	2.09	-0.09
6	79.8	78.88	79.66149	1.16	0.17
7	80.8	81.49	81.00033	-0.85	-0.25
8	79.5	79.49	79.81281	0.01	-0.39
9	77.1	77.58	76.52437	-0.62	0.75
10	79.4	79.75	79.82386	-0.45	-0.53
11	77	77.72	74.88231	-0.93	2.75
12	75.2	75.82	75.53596	-0.82	-0.45
13	82.1	82.42	78.78779	-0.39	4.03
14	79.9	80.53	77.8113	-0.78	2.61
15	77	78.28	76.78516	-1.66	0.28
16	81.2	81.27	81.18554	-0.08	0.02
17	79.7	79.02	79.45757	0.86	0.30
18	77.5	76.98	77.949	0.68	-0.58
19	81	79.40	78.76792	1.97	2.76

20	79.2	77.37	78.83065	2.31	0.47
21	77.6	75.22	77.14962	3.07	0.58
22	77.8	78.24	77.53313	-0.56	0.34
23	75.1	76.08	75.35134	-1.31	-0.33
24	72.9	73.71	72.86657	-1.11	0.05
25	80.2	80.91	77.23401	-0.89	3.70
26	77.8	78.54	77.6982	-0.95	0.13
27	75.7	76.51	76.2496	-1.06	-0.73
Maximum				3.07	4.03
Minimum				-1.66	-1.30
Mean Square Error				1.431605	2.427086
Root Mean Square Error				**1.196 %**	**1.558 %**

Figure 7.7 shows the percentage error of values obtained from experimentation & mathematical model and experimentation & ANN simulation for deshelling efficiency.
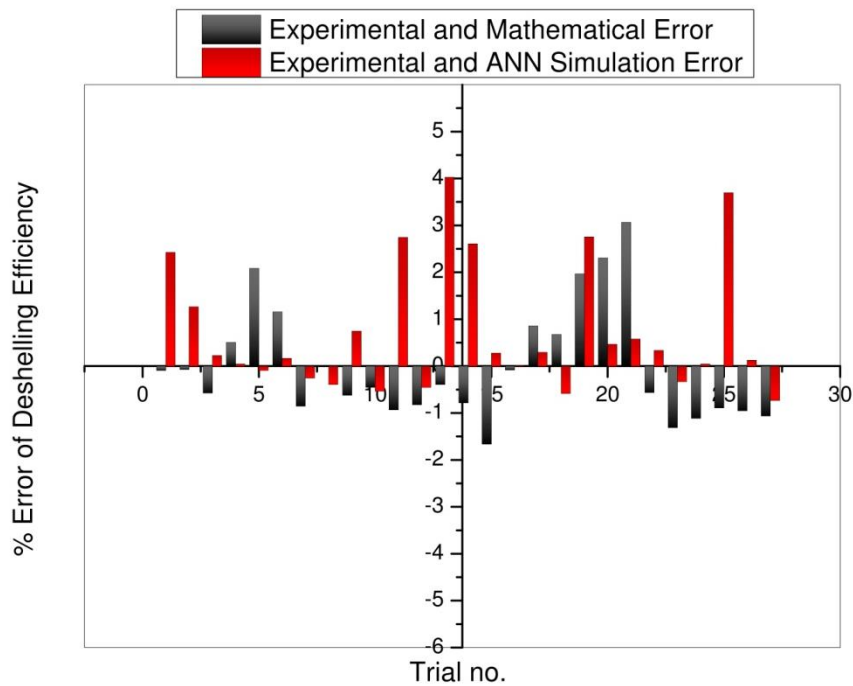
Figure 7.7: Comparison of Percentage Error between Experimental &Mathematical Model, and Experimental & ANN Simulation for Deshelling Efficiency

From figure 7.7, it can be seen that, percentage error between experimental values and ANN values all follow the same pattern and are approximately equally distributed. The percentage error of values obtained from experimentation & mathematical model and experimentation & ANN simulation is below 5 %, also the average RMS Error is below 5 %. This shows that the ANN model and the mathematical model are in good agreement with one another. Furthermore, the positive agreement between the mathematical model model results and the ANN model results with the experimental results suggests that both of the formulated models are capable of predicting the deshelling efficiency parameters instead of doing the actual experimental work.

7.2.2 Percentage Error for Whole kernel recovery (η_w)

Table 7.8 shows the percentage error of values obtained from experimentation & mathematical model and experimentation & ANN simulation for Whole kernel recovery (η_w).

Table 7.8: Comparison Percentage Error of Whole kernel recovery (η_w) between Experimental Data, Mathematical Models and ANN Simulation

Sr. No	Whole kernel recovery (η_w) (%)			Percentage Error	
	Experiment al (η_d) (%)	Mathematical (η_d) (%)	ANN Simulation (η_d) (%)	Experimental & Mathematical Model	Experimental & ANN Simulation
1	65.5	65.13	64.36	0.57	1.74
2	65.6	66.80	68.80	-1.83	-4.87
3	68.6	68.49	68.49	0.16	0.17
4	66.5	67.25	66.39	-1.13	0.16
5	71	68.94	71.08	2.91	-0.12
6	62.2	60.95	62.13	2.01	0.12
7	69.4	69.38	69.44	0.02	-0.05
8	62	61.40	62.10	0.97	-0.16
9	61.6	63.07	61.64	-2.39	-0.07
10	63.5	64.77	63.57	-2.00	-0.12
11	66.2	66.30	62.99	-0.16	4.85
12	58.6	58.46	58.58	0.23	0.03
13	70.6	70.18	67.11	0.60	4.94

14	62.3	62.34	60.40	-0.06	3.05
15	61.6	63.59	61.85	-3.24	-0.41
16	63.3	62.93	63.31	0.59	-0.02
17	63.7	64.18	63.59	-0.76	0.17
18	66.6	65.71	66.48	1.33	0.18
19	69.6	67.70	70.13	2.73	-0.76
20	61.7	59.70	61.94	3.24	-0.39
21	62	61.11	62.06	1.44	-0.10
22	60.6	60.44	60.39	0.27	0.34
23	60	61.84	59.97	-3.06	0.05
24	62.6	62.95	60.26	-0.56	3.74
25	64.1	65.85	62.49	-2.74	2.51
26	66.9	66.97	66.88	-0.10	0.02
27	59	58.97	58.87	0.05	0.23
Maximum				3.24	4.94
Minimum				-3.23	-4.88
Mean Square Error				2.922049	3.911889
Root Mean Square Error				**1.709 %**	**1.978 %**

From Table 7.8, it can be seen that percentage error between experimental values and values from mathematical model for Whole kernel recovery ranges from –3.23% to 3.24% and average RMS Error is 1.709%. Similarly, percentage error between experimental values and ANN values for Whole kernel recovery ranges from –4.88% to 4.94 % and average RMS Error is 1.978%.

Figure 7.8 shows the percentage error of values obtained from experimentation & mathematical model and experimentation & ANN simulation for Whole kernel recovery.

Figure 7.8: Comparison of Percentage Error between Experimental &Mathematical Model, and
Experimental & ANN Simulation for Whole kernel recovery

From figure 7.8, it can be seen that, percentage error between experimental values and ANN values all follow the same pattern and are approximately equally distributed. The percentage error of values obtained from experimentation & mathematical model and experimentation & ANN simulation is below 5 %, also the average RMS Error is below 5 %. This shows that the ANN model and the mathematical model are in good agreement with one another. Furthermore, the positive agreement between the mathematical model model results and the ANN model results with the experimental results suggests that both of the formulated models are capable of predicting the Whole kernel recovery parameters instead of doing the actual experimental work.

7.2.3 Percentage Error for Broken kernel (η_b)

Table 7.9 shows the percentage error of values obtained from experimentation & mathematical model and experimentation & ANN simulation for broken kernel (η_b).

Table 7.9: Comparison Percentage Error of Broken kernel (η_b) between Experimental Data, Mathematical Models and ANN Simulation

Sr. No	Broken kernel (η_b) (%)			Percentage Error	
	Experimental (η_b) (%)	Mathematical (η_b) (%)	ANN Simulation (η_b) (%)	Experimental & Mathematical Model	Experimental & ANN Simulation
1	18.5	18.94	18.39	-2.39	0.60
2	16.5	17.10	16.11	-3.64	2.39
3	11.2	11.66	11.12	-4.11	0.73
4	16.7	15.96	16.82	4.43	-0.72
5	11.6	11.93	11.63	-2.87	-0.29
6	17.6	17.93	17.51	-1.86	0.52
7	11.4	11.90	11.55	-4.39	-1.34
8	17.5	18.09	17.70	-3.39	-1.13
9	15.5	14.81	14.87	4.45	4.05
10	15.9	15.58	16.28	2.01	-2.41
11	10.8	11.11	10.28	-2.87	4.86
12	16.6	17.36	16.96	-4.55	-2.17
13	11.5	11.98	12.06	-4.17	-4.88
14	17.6	18.19	17.32	-3.34	1.61
15	15.4	14.68	14.92	4.65	3.14
16	17.9	18.34	17.83	-2.43	0.38
17	16	15.73	15.91	1.69	0.59
18	10.9	11.26	11.36	-3.33	-4.25
19	11.4	11.70	11.91	-2.65	-4.44
20	17.5	17.67	16.92	-0.95	3.31
21	15.6	15.11	15.10	3.14	3.23
22	17.2	17.80	17.10	-3.48	0.57
23	15.1	14.39	15.34	4.70	-1.61
24	10.3	10.76	10.57	-4.43	-2.65
25	16.1	15.56	16.59	3.35	-3.04
26	10.9	11.17	10.80	-2.48	0.96
27	16.7	17.53	17.40	-5.00	-4.20

Maximum	4.70	4.81
Minimum	-4.97	-4.87
Mean Square Error	12.40827	7.161825
Root Mean Square Error	**3.523 %**	**2.676 %**

From Table 7.9, it can be seen that percentage error between experimental values and values from mathematical model for broken kernel ranges from –4.97% to 4.70% and average RMS Error is 3.523%. Similarly, percentage error between experimental values and ANN values for broken kernel ranges from –4.87% to 4.81 % and average RMS Error is 2.676%.

Figure 7.9 shows the percentage error of values obtained from experimentation & mathematical model and experimentation & ANN simulation for broken kernel.

Figure 7.9: Comparison of Percentage Error between Experimental &Mathematical Model, and Experimental & ANN Simulation for Broken kernel

From figure 7.9, it can be seen that, percentage error between experimental values and ANN values all follow the same pattern and are approximately equally distributed. The percentage error of values obtained from experimentation & mathematical model and experimentation & ANN simulation is below 5 %, also the average RMS Error is below 5 %. This shows that the ANN model and the mathematical model are in good agreement with one another. Furthermore, the positive agreement between the

mathematical model model results and the ANN model results with the experimental results suggests that both of the formulated models are capable of predicting the broken kernel parameters instead of doing the actual experimental work.

7.2.4 Percentage Error for Partially Shelled / Unshelled nuts (η_u)

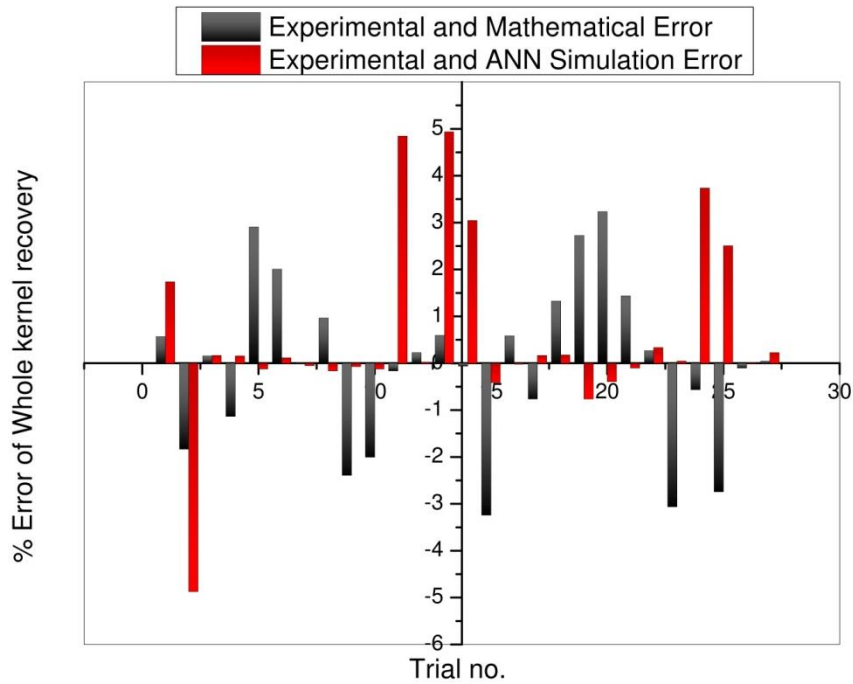Table 7.10 shows the percentage error of values obtained from experimentation & mathematical model and experimentation & ANN simulation for partially shelled / unshelled nuts (η_u).

Table 7.10: Comparison Percentage Error of Partially Shelled / Unshelled nuts (η_u) between Experimental Data, Mathematical Models and ANN Simulation

Sr. No	Partially Shelled / Unshelled nuts (η_u) (%)			Percentage Error	
	Experimental (η_u) (%)	Mathematical (η_u) (%)	ANN Simulation (η_u) (%)	Experimental & Mathematical Model	Experimental & ANN Simulation
1	16	15.23	16.55	4.81	-3.42
2	17.9	18.73	18.74	-4.62	-4.71
3	24.4	23.23	24.13	4.80	1.10
4	14.7	15.18	14.67	-3.25	0.17
5	18.8	19.58	18.85	-4.14	-0.29
6	27.5	27.36	27.44	0.50	0.21
7	16.9	16.13	17.05	4.56	-0.88
8	22.8	23.82	23.01	-4.45	-0.90
9	28.4	28.31	28.22	0.33	0.62
10	18.5	17.62	18.82	4.76	-1.73
11	21.4	21.89	21.96	-2.30	-2.61
12	28.5	28.62	28.62	-0.42	-0.41
13	10.8	11.14	10.94	-3.15	-1.33
14	17.6	18.26	18.43	-3.76	-4.74
15	25.7	25.27	25.77	1.67	-0.26
16	12.4	12.98	12.42	-4.68	-0.19
17	19.6	20.55	19.19	-4.85	2.07
18	26.8	26.21	26.79	2.19	0.04
19	12.6	12.98	12.02	-3.02	4.57

20	18.8	19.57	18.58	-4.10	1.18
21	27.6	26.53	27.65	3.89	-0.17
22	17.3	16.75	17.17	3.18	0.78
23	20.9	21.43	20.78	-2.52	0.58
24	29	29.21	27.90	-0.72	3.80
25	11.2	10.85	11.30	3.13	-0.86
26	17.4	18.08	17.67	-3.90	-1.58
27	26.5	25.67	26.67	3.12	-0.66
Maximum				4.81	4.60
Minimum				-4.85	-4.72
Mean Square Error				12.38927	4.339445
Root Mean Square Error				**3.520 %**	**2.083 %**

From Table 7.10, it can be seen that percentage error between experimental values and values from mathematical model for partially shelled / unshelled nuts ranges from –4.85% to 4.81% and average RMS Error is 3.520%. Similarly, percentage error between experimental values and ANN values for partially shelled / unshelled nuts ranges from –4.72% to 4.60 % and average RMS Error is 2.83%.

Figure 7.10 shows the percentage error of values obtained from experimentation & mathematical model and experimentation & ANN simulation for partially shelled / unshelled nuts. From figure 7.10, it can be seen that, percentage error between experimental values and ANN values all follow the same pattern and are approximately equally distributed. The percentage error of values obtained from experimentation & ma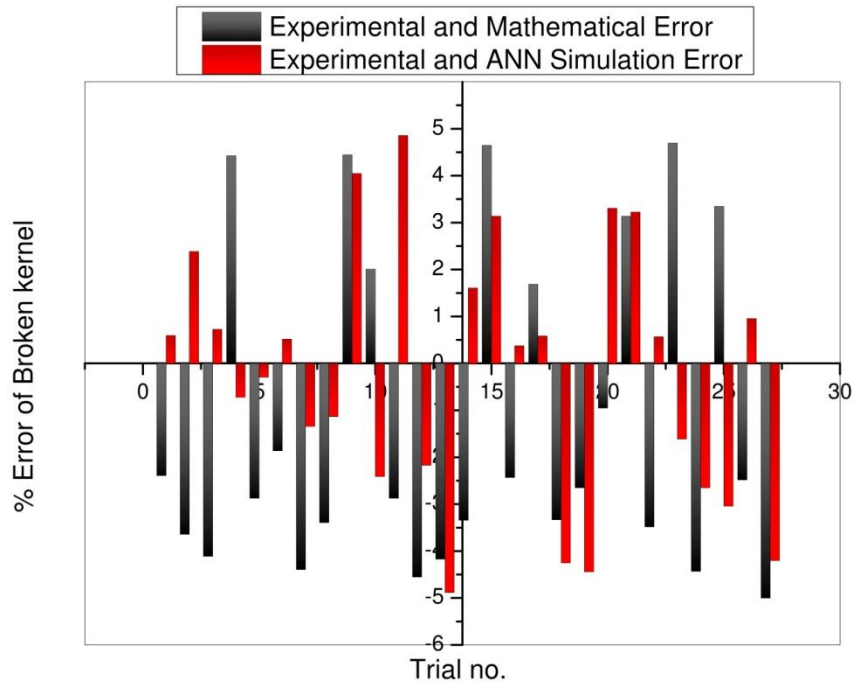thematical model and experimentation & ANN simulation is below 5 %, also the average RMS Error is below 5 %. This shows that the ANN model and the mathematical model are in good agreement with one another. Furthermore, the positive agreement between the mathematical model results and the ANN model results with the experimental results suggests that both of the formulated models are capable of predicting the partially shelled / unshelled nuts parameters instead of doing the actual experimental work.

Figure 7.10: Comparison of Percentage Error between Experimental &Mathematical Model, and
Experimental & ANN Simulation for Partially Shelled / Unshelled nuts

7.2.5 Percentage Error for Resistive torque (Ʈr)

Table 7.11 shows the percentage error of values obtained from experimentation &
mathematical model and experimentation & ANN simulation for resistive torque (Ʈr).

Table 7.11: Comparison Percentage Error of Resistive torque (Ʈr) between
Experimental Data, Mathematical Models and ANN Simulation

Sr. No	Resistive torque (Ʈr) (%)			Percentage Error	
	Experimental (Ʈr) (%)	Mathematical (Ʈr) (%)	ANN Simulation (Ʈr) (%)	Experimental & Mathematical Model	Experimental & ANN Simulation
1	96364.488	103693	100284.1	-7.60	-4.07
2	129916.95	122535	123841.6	5.68	4.68
3	123945.45	120928	129946.4	2.43	-4.84
4	104410.36	109717	108410.3	-5.08	-3.83
5	109014.2	116110	119014.6	-6.51	-9.17
6	130280.15	139013	139279.8	-6.70	-6.91
7	125714.17	133292	129714.2	-6.03	-3.18
8	135984.9	144195	127984.6	-6.04	5.88

9	112077.33	117037	119077.6	-4.43	-6.25
10	104356.05	110669	109355.7	-6.05	-4.79
11	116254.85	119601	109039.3	-2.88	6.21
12	112538	114614	120537.6	-1.84	-7.11
13	116492.71	120009	110875.8	-3.02	4.82
14	95916.216	100022	95555.98	-4.28	0.38
15	105850.27	111485	109850.5	-5.32	-3.78
16	124754.95	119114	129754.5	4.52	-4.01
17	110508.38	115577	117508.3	-4.59	-6.33
18	126730.54	125509	119730.6	0.96	5.52
19	146322.31	139961	149305.4	4.35	-2.04
20	118791.27	116513	122791.6	1.92	-3.37
21	123293.51	115086	133293.1	6.66	-8.11
22	121341.73	123515	125341.7	-1.79	-3.30
23	119725.16	122088	121725.1	-1.97	-1.67
24	136359.54	129641	136530.6	4.93	-0.13
25	115339.06	119406	120532.1	-3.53	-4.50
26	138207.55	129959	131207.3	5.97	5.06
27	104198.86	109511	109199.2	-5.10	-4.80
Maximum				6.66	6.21
Minimum				-7.60	-9.17
Mean Square Error				22.9752	25.64525
Root Mean Square Error				**4.793 %**	**5.064 %**

From Table 7.11, it can be seen that percentage error between experimental values and values from mathematical model for resistive torque ranges from –7.60% to 6.66% and average RMS Error is 4.793%. Similarly, percentage error between experimental values and ANN values for resistive torque ranges from –9.17% to 6.21 % and average RMS Error is 5.064%.

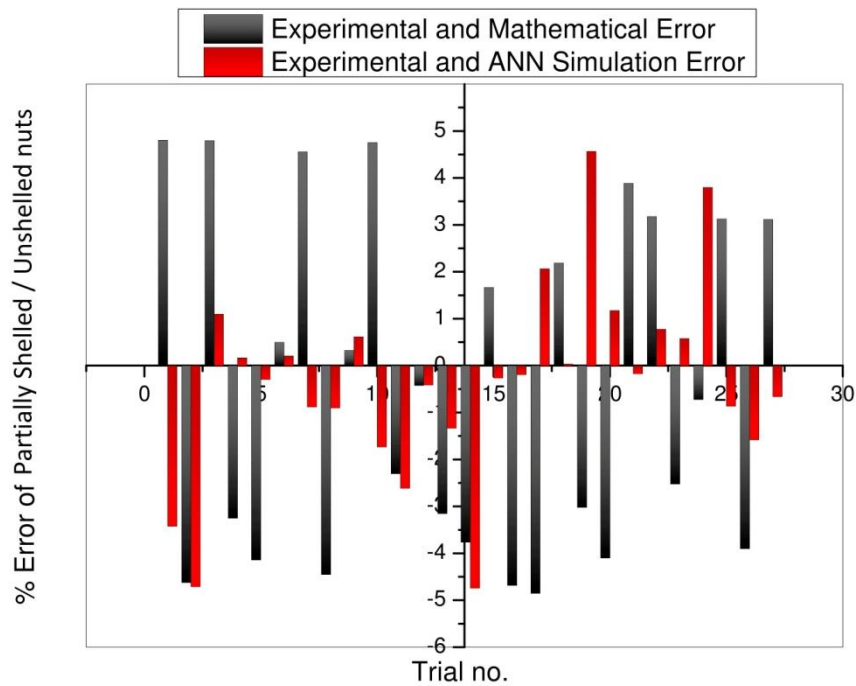Figure 7.11 shows the percentage error of values obtained from experimentation & mathematical model and experimentation & ANN simulation for resistive torque.

Figure 7.11: Comparison of Percentage Error between Experimental &Mathematical Model, and Experimental & ANN Simulation for Resistive torque

From figure 7.11, it can be seen that, percentage error between experimental values and ANN values all follow the same pattern and are approximately equally distributed. This shows that the ANN model and the mathematical model are in good agreement with one another. Furthermore, the positive agreement between the mathematical model results and the ANN model results with the experimental results suggests that both of the formulated models are capable of predicting the resistive torque parameters instead of doing the actual experimental work.

7.2.6 Percentage Error for Processing time (1000 nuts) (P_T)

Table 7.12 shows the percentage error of values obtained from experimentation & mathematical model and experimentation & ANN simulation for processing time for 1000 nuts (P_T). From Table 7.12, it can be seen that percentage error between experimental values and values from mathematical model for processing time ranges from –4.34% to 3.18% and average RMS Error is 1.783%. Similarly, percentage error between experimental values and ANN values for processing time ranges from – 4.35% to 4.36 % and average RMS Error is 1.769%.

Table 7.12: Comparison Percentage Error of Processing time (1000 nuts) (P_T) between Experimental Data, Mathematical Models and ANN Simulation

Sr. No	Processing time (1000 nuts) (P_T) (Seconds)			Percentage Error	
	Experimental (P_T) (%)	Mathematical (P_T) (%)	ANN Simulation (P_T) (%)	Experimental & Mathematical Model	Experimental & ANN Simulation
1	74	75.56	73.71	-7.60	0.39
2	75	75.57	74.88	5.68	0.16
3	76	75.64	75.99	2.43	0.02
4	80	78.90	80.02	-5.08	-0.03
5	77	78.97	77.03	-6.51	-0.04
6	77	76.56	76.99	-6.70	0.02
7	85	82.30	85.01	-6.03	-0.01
8	80	79.89	80.04	-6.04	-0.05
9	82	79.90	81.85	-4.43	0.18
10	71	70.62	71.02	-6.05	-0.02
11	69	70.13	67.23	-2.88	2.57
12	67	68.36	67.08	-1.84	-0.12
13	67	66.29	64.08	-3.02	4.36
14	65	64.53	67.83	-4.28	-4.36
15	64	62.95	63.96	-5.32	0.05
16	67	68.36	66.99	4.52	0.02
17	64	66.78	63.95	-4.59	0.07
18	65	66.29	65.15	0.96	-0.24
19	58	58.00	55.59	4.35	4.15
20	56	55.68	56.05	1.92	-0.09
21	55	54.75	54.82	6.66	0.33
22	61	60.02	60.90	-1.79	0.16
23	58	59.08	58.14	-1.97	-0.24
24	57	57.00	58.95	4.93	-3.43
25	56	55.75	54.19	-3.53	3.23
26	54	53.67	53.91	5.97	0.17
27	53	51.35	53.09	-5.10	-0.18

Maximum	3.18	4.36
Minimum	-4.34	-4.35
Mean Square Error	3.180592	3.129602
Root Mean Square Error	**1.783 %**	**1.769 %**

Figure 7.12 shows the percentage error of values obtained from experimentation & mathematical model and experimentation & ANN simulation for processing time.
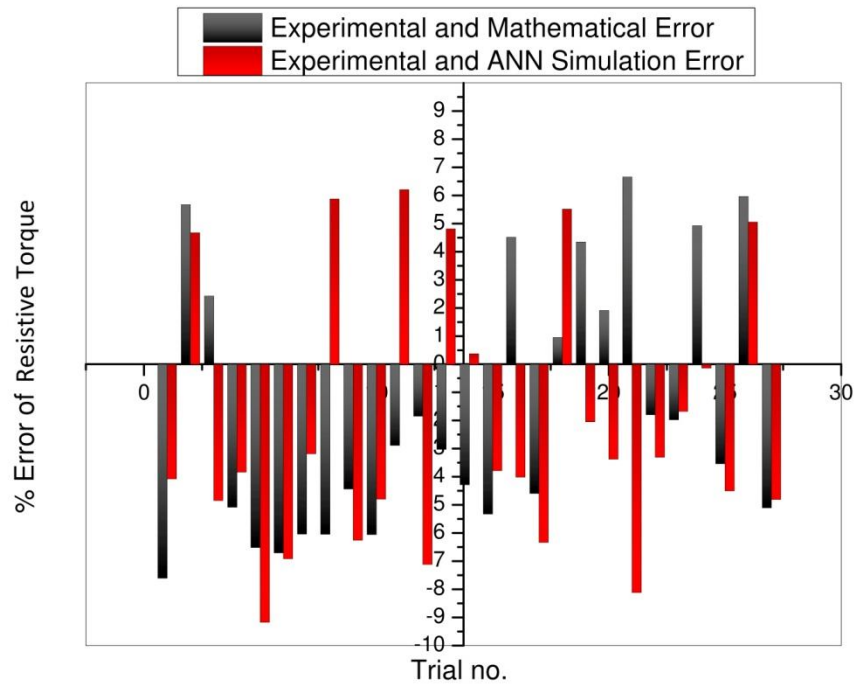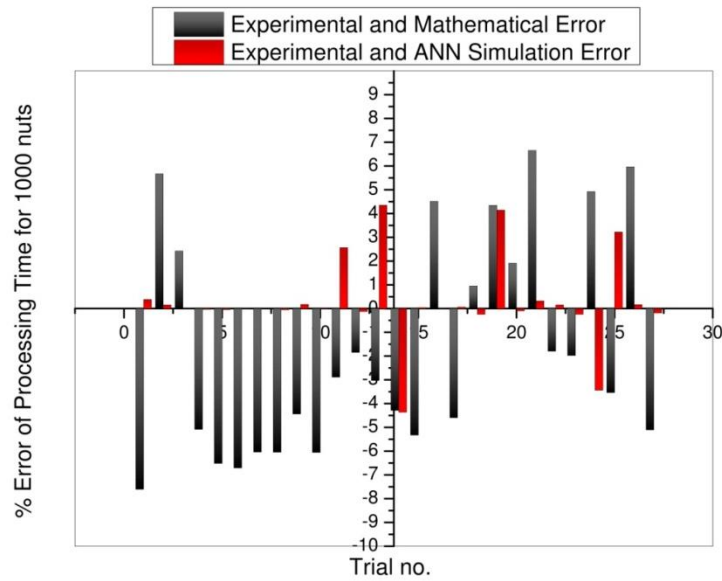

Figure 7.12: Comparison of Percentage Error between Experimental &Mathematical Model, and Experimental & ANN Simulation for Processing time

From figure 7.12, it can be seen that, percentage error between experimental values and ANN values all follow the same pattern and are approximately equally distributed. The percentage error of values obtained from experimentation & mathematical model and experimentation & ANN simulation is below 5 %, also the average RMS Error is below 5 %. This shows that the ANN model and the mathematical model are in good agreement with one another. Furthermore, the positive agreement between the mathematical model results and the ANN model results with the experimental results suggests that both of the formulated models are capable of predicting the processing time parameters instead of doing the actual experimental work.

7.3 Effect of various input parameters on the individual output parameters

7.3.1. Influence of various input parameters on the deshelling efficiency:

Figure 7.13 shows the effect of feed rate, moisture content (% d.b), clearance, thickness of the grinding disk and rotational speed of the flywheel on the deshelling efficiency.

It can be seen from figure 7.13, deshelling efficiency decreases from 84.0% to 72.9% by increasing the feed rate (15 kg/hr to 25 kg/hr); moisture content percent from (9 % d.b to 17 % d.b); the clearance (6 mm to 10 mm); the thickness of the grinding disk from (19 mm to 32 mm); and the rotational speed of the flywheel (400 rpm to 600 rpm).
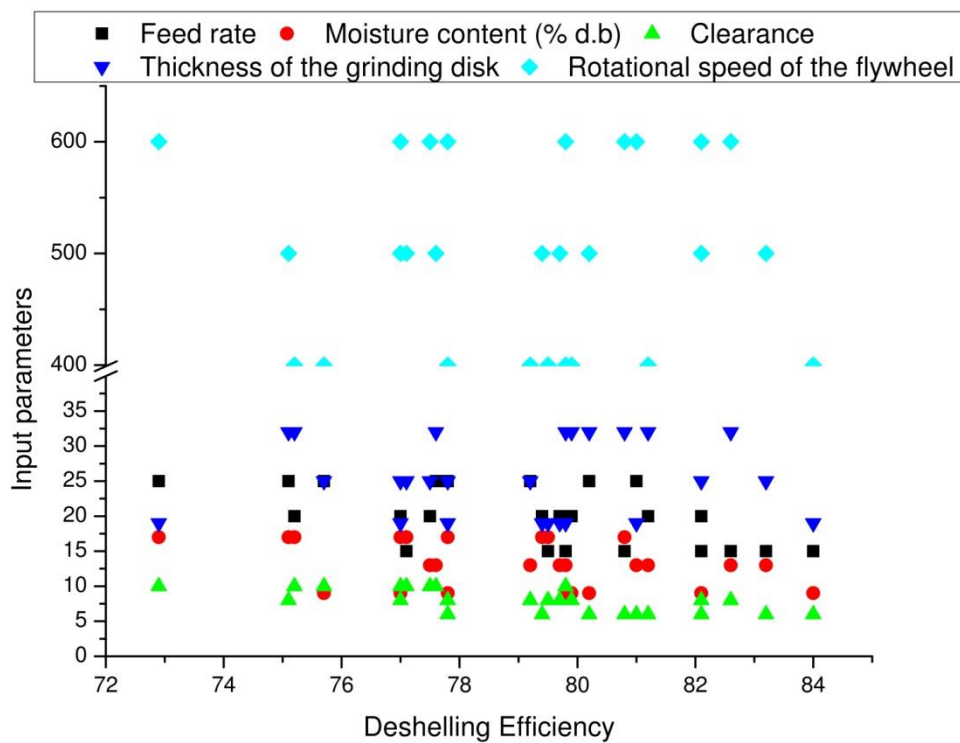
Figure 7.13 shows the effect of individual feed rate and moisture content on the deshelling efficiency.

Figure 7.14 shows the effect of feed rate and moisture content on the deshelling efficiency.

154

From figure 7.14 (a) it can be seen that deshelling efficiency received at a feed rate of 15 kg/hr, 20 kg/hr and 25 kg/hr varies between 84.0 to 77.0 %, 79.4 to 77.50 % and 81.0 to 72.9% respectively. The highest deshelling efficiency obtained was 84.0, 82.1, & 81.0 at a feed rate of 15 kg/hr, 20 kg/hr and 25 kg/hr respectively. Whereas the lowest deshelling efficiency obtained was 77.1% for feed rate of 15 kg/hr, 75.20% for feed rate of 20 kg/hr, & 72.9% for feed rate of 25 kg/hr. The highest deshelling efficiency was observed 84.0 % at a feed rate of 15 kg/hr; whereas the lowest deshelling efficiency was observed 72.9% for feed rate of 25 kg/hr.

A value of deshelling efficiency decreased considerably from 84 % to 72.9 % with increase in feed rate. By this behavior, it can conclude that, feed rate is inversely proportion to deshelling efficiency. The low deshelling efficiency at higher feed was mainly due to the reduction in the residence time. The high deshelling efficiency at lower feed rate was because of Charoli nut has got enough time to be impacted. Also, as per Taguchi analysis, feed rate affects significantly with second highest contribution 30.23% on the deshelling efficiency.
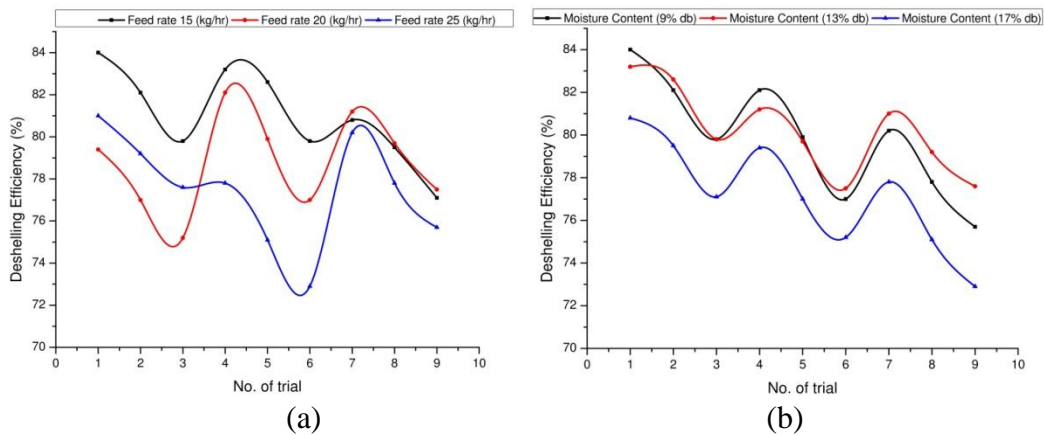
Figure 7.14 Influence of individual feed rate and moisture content on the deshelling efficiency.

From figure 7.14 (b) it can be seen that deshelling efficiency obtained at a moisture content percent of 9 (% d.b), 13 (% d.b) and 17 (% d.b) varies between 84.0 to 75.7 %, 83.2 to 77.60 % and 80.8 to 72.9 % respectively. The highest deshelling efficiency obtained was 84.0%, 83.2%, & 80.8% at a moisture content percent of 9 (% d.b), 13

(% d.b) and 17 (% d.b) respectively. Whereas the lowest deshelling efficiency obtained was 75.7 % for a moisture content percent of 9 (% d.b), 77.50 % for a moisture content percent of 13 (% d.b), & 72.9 % for a moisture content percent of 13 (% d.b). The highest deshelling efficiency was observed 84.0 % at a moisture content percent of 9 (% d.b); whereas the lowest deshelling efficiency was observed 72.9% for a moisture content percent of 17 (% d.b).

The value of deshelling efficiency decreased significantly with increasing moisture content percent, from 84 % to 72.9 %. It can conclude from this trend that moisture content % is inversely proportional to deshelling efficiency. This implies that the deshelling efficiency is great when Charoli nut is dry. This is related to the brittleness when nut dry & softening ability of the nuts as moisture level rises. It is more recommended to deshell nut at lower moisture level in order to prevent formation of mould in kernel. Furthermore, according to Taguchi analysis, moisture content percent has a significant impact on deshelling efficiency, with third highest contribution of 25.77 %.

Figure 7.15 shows the effect of clearance & thickness of the grinding disk on the deshelling efficiency. From figure 7.15 (a) it can be seen that deshelling efficiency obtained at a clearance of 6 mm, 8 mm and 10 mm varies between 84.0 to 77.8 %, 82.1 to 77.10 % and 79.8 to 72.9% respectively. The highest deshelling efficiency obtained was 84.00%, 82.6%, & 79.8% at clearance of 6 mm, 8 mm and 10 mm respectively. Whereas the lowest deshelling efficiency obtained was 77.8% for clearance of 6 mm, 75.10% for clearance of 8 mm, & 72.9% for clearance of 10 mm. The highest deshelling efficiency was observed 84.0 % at clearance of 6 mm; whereas the lowest deshelling efficiency was observed 72.9% for clearance of 10 mm.

The value of deshelling efficiency decreased considerably with increase in clearance from 84 % to 72.9 %. By this behavior, it can conclude that, clearance is inversely proportion to deshelling efficiency. The highest deshelling efficiency is obtained at lower clearance. This is due to the fact that at lower clearance there is more contact between nut & disc due to which machine developed more force & hence more nuts

are deshelled. Furthermore, according to Taguchi analysis, moisture content percent has a significant impact on deshelling efficiency, with highest contribution of 40.87 %.

From figure 7.15 (b) it can be seen that deshelling efficiency obtained at a thickness of grinding disk of 19 mm, 25 mm and 32 mm varies between 84.0 to 77.8 %, 82.1 to 75.70 % and 79.8 to 82.6% respectively. The highest deshelling efficiency obtained was 84.00%, 83.2%, & 82.6% at disk thickness of 19 mm, 25 mm and 32 mm respectively. Whereas the lowest deshelling efficiency obtained was 72.90% for disk thickness of 19 mm, 75.70% for disk thickness of 25 mm, & 75.1% for disk thickness of 32 mm. The highest deshelling efficiency was observed 84.0 % at disk thickness of 19 mm; whereas the lowest deshelling efficiency was observed 72.9% for disk thickness of 32 mm.

(a)   (b)
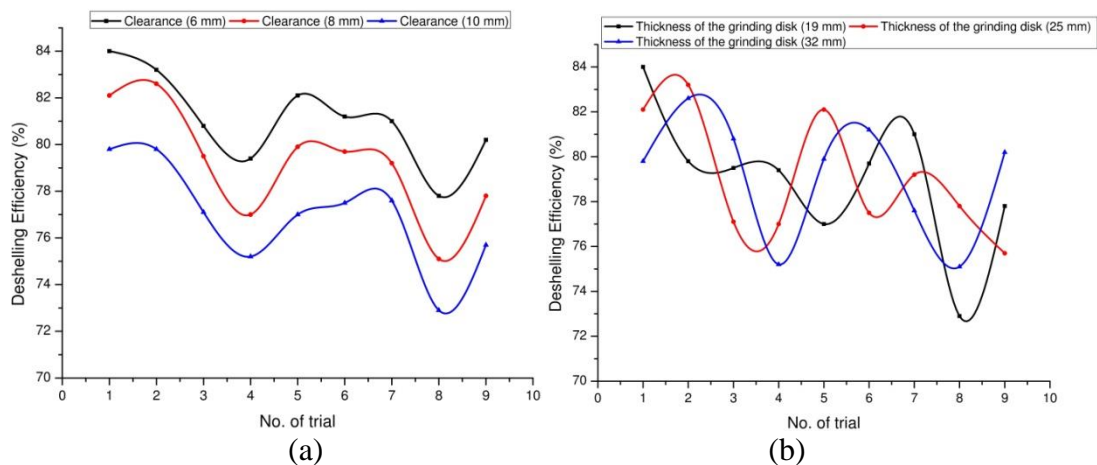
Figure 7.15 Influence of individual clearance and thickness of grinding disk on the deshelling efficiency.

The value of deshelling efficiency decreased considerably with increase in disk thickness from 84 % to 75.1 %. Furthermore, according to Taguchi analysis, disk thickness has not a significant impact on deshelling efficiency, and have a least contribution of 0.05 %.

Figure 7.16 shows the effect of rotational speed of the flywheel on the deshelling efficiency. From figure 7.16 it can be seen that deshelling efficiency obtained at a rotational speed of the flywheel of 400 rpm, 500 rpm and 600 rpm varies between

84.0 to 75.5 %, 82.1 to 80.20 % and 79.8 to 77.8% respectively. The highest deshelling efficiency obtained was 84.00%, 83.2%, & 82.6% at rotational speed of 400 rpm, 500 rpm and 600 rpm respectively. Whereas the lowest deshelling efficiency obtained was 75.20% for rotational speed of 400 rpm, 75.10% for rotational speed of 500 rpm, & 72.9% for rotational speed of 600 rpm. The highest deshelling efficiency was observed 84.0 % at rotational speed of 400 rpm; whereas the lowest deshelling efficiency was observed 72.9% for rotational speed of 600 rpm.
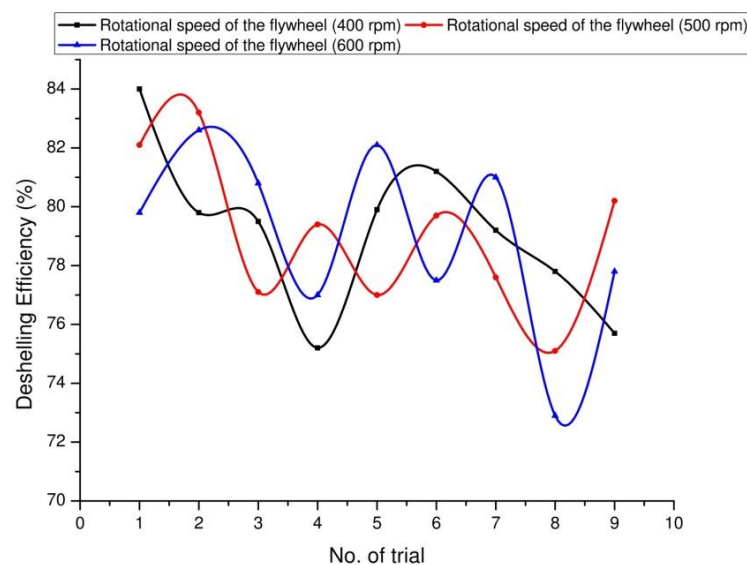
Figure 7.16 Influence of individual rotational speed of the flywheel on the deshelling efficiency.

The value of deshelling efficiency shows the complex behavior with the rotational speed of the flywheel. The highest deshelling efficiency is obtained at a speed of 400 rpm. This is due to the fact that at highest speed nuts try to get away because of centrifugal force. Furthermore, according to Taguchi analysis, rotational speed of the flywheel does not contribute significantly on deshelling efficiency, and have a least contribution of 0.03 %.

Interaction effect of feed rate and clearance also have considered in study to find out its impact on the deshelling efficiency. As per Taguchi analysis, Interaction effect of feed rate and clearance has a not a significant impact on deshelling efficiency, and have a least contribution of 0.49 % only. That means, though the feed rate and

clearance have significant effect on deshelling efficiency but their interactions doesn't have any significant contribution on deshelling efficiency.

From the Taguchi analysis, it is noted that clearance with contribution of 40.87 %, feed rate with contribution of 30.23 %, and moisture content percent with contribution of 25.77 % were affecting significantly on the deshelling efficiency. Among these factors effect of Clearance followed by feed rate and moisture content percent are highly significant both physically and statistically. The changes of the thickness of the grinding disk, rotational speed of the flywheel and interaction of feed rate and clearance have minimal impacts on deshelling efficiency, both statistically and physically. Therefore, for maximum efficiency, more attention needs to be focused on clearance followed by feed rate and moisture content percent.

7.3.2. Influence of various input parameters on the whole kernel recovery:

Figure 7.17 shows the effect of feed rate, moisture content, clearance, thickness of the grinding disk and rotational speed of the flywheel on the whole kernel recovery.
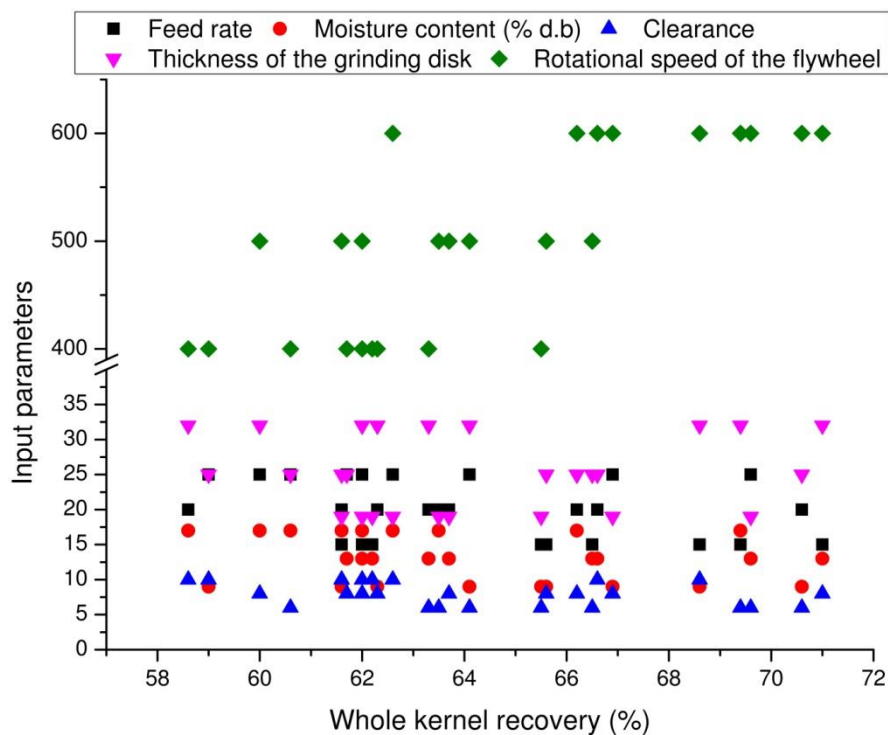
Figure 7.17 effects of feed rate, moisture content, clearance, thickness of the grinding disk and rotational speed on the whole kernel recovery.

It can be seen from figure 7.17, whole kernel recovery decreases from 71.0% to 58.6% by increasing the feed rate (15 kg/hr to 25 kg/hr); moisture content percent from (9 % d.b to 17 % d.b); the clearance (6 mm to 10 mm); the thickness of the grinding disk from (19 mm to 32 mm); and the rotational speed of the flywheel (400 rpm to 600 rpm).

Figure 7.18 shows an influence of feed rate and moisture content on the whole kernel recovery.

From figure 7.18 (a) it can be seen that whole kernel recovery received at a feed rate of 15 kg/hr, 20 kg/hr and 25 kg/hr varies between 65.50 to 61.60%, 63.50 to 66.60 % and 69.60 to 59.0% respectively. The highest whole kernel recovery obtained was 71.00, 70.60, & 69.60 at a feed rate of 15 kg/hr, 20 kg/hr and 25 kg/hr respectively. Whereas the lowest whole kernel recovery obtained was 61.6 % for feed rate of 15 kg/hr, 66.6% for feed rate of 20 kg/hr, & 59.0% for feed rate of 25 kg/hr. The highest whole kernel recovery was observed 71.0 % at a feed rate of 15 kg/hr; whereas the whole kernel recovery was observed 59.0% for feed rate of 25 kg/hr.

A value of whole kernel recovery decreased considerably from 71.0 % to 59.0 % with increase in feed rate. The lower whole kernel recovery with higher feed rate was due to lower residence time due to which lower surface contact. The high whole kernel recovery with Lower feed rate was because of Charoli nut has got enough time to be impacted. Also, as per Taguchi analysis, feed rate affects significantly with second highest contribution 11.91% on the whole kernel recovery.
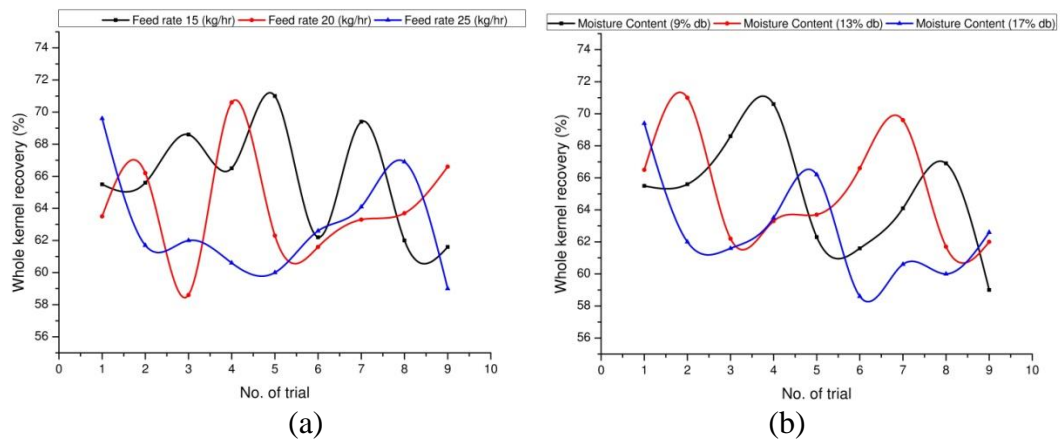
Figure 7.18 Influence of individual feed rate and moisture content on the whole kernel recovery.

From figure 7.18 (b) it can be seen that whole kernel recovery received at a moisture content percent of 9 (% d.b), 13 (% d.b) and 17 (% d.b) varies between 65.5 to 59.0 %, 66.5 to 62.00 % and 69.4 to 62.6 % respectively. The highest whole kernel recovery obtained was 70.60%, 71.00%, & 69.40% at a moisture content percent of 9 (% d.b), 13 (% d.b) and 17 (% d.b) respectively. Whereas the lowest whole kernel recovery obtained was 59.0 % for a moisture content percent of 9 (% d.b), 61.70 % for a moisture content percent of 13 (% d.b), & 58.6 % for a moisture content percent of 17 (% d.b). The highest whole kernel recovery was observed 71.0 % at a moisture content percent of 13 (% d.b); whereas the lowest whole kernel recovery was observed 58.60% for a moisture content percent of 17 (% d.b).

The value of whole kernel recovery varies significantly with increasing moisture content percent, from 70.60 % to 58.60 %. The percentage of whole kernel recovery tends to increased first with increase with moisture content. Further it slightly decreases with further increase moisture content. Because of the nut's flexible nature when the kernel has a greater moisture level, the percentage of entire kernel recovery rose as moisture content increased. Furthermore, according to Taguchi analysis, moisture content percent has a significant impact on whole kernel recovery, with forth highest contribution of 10.25 %.

161

Figure 7.19 shows the effect of clearance & thickness of the grinding disk on the whole kernel recovery. From figure 7.19 (a) it can be seen that whole kernel recovery obtained at a clearance of 6 mm, 8 mm and 10 mm varies between 65.5 to 64.1 %, 65.6 to 66.90 % and 68.6 to 59.0% respectively. The highest whole kernel recovery obtained was 70.60%, 71.00%, & 68.6% at clearance of 6 mm, 8 mm and 10 mm respectively. Whereas the lowest whole kernel recovery obtained was 60.60% for clearance of 6 mm, 60.00% for clearance of 8 mm, & 58.60% for clearance of 10 mm. The highest whole kernel recovery was observed 71.0 % at clearance of 8 mm; whereas the lowest whole kernel recovery was observed 58.60% for clearance of 10 mm.

The value of whole kernel recovery varies considerably with increase in clearance from 71.00 % to 58.6 %. The trend of the increasing/decreasing the whole kernel recovery with clearance is found complex. But there is a significant variation in the whole kernel recovery. At a clearance of 10 mm, percentage of whole kernel recovery was significantly changed from 68.6 to 58.6 %. The whole kernel recovery percentage significantly affected by the clearance. This indicates at higher clearance whole kernel recovery decreases constantly. The effect of clearance represents the optimum gap between stationary disc & rotating disc. This is because of optimum pressure created at this point of clearance to nuts & kernels. Furthermore, according to Taguchi analysis, clearance has a significant impact on whole kernel recovery, with second highest contribution of 16.05 %.

(a)   (b)
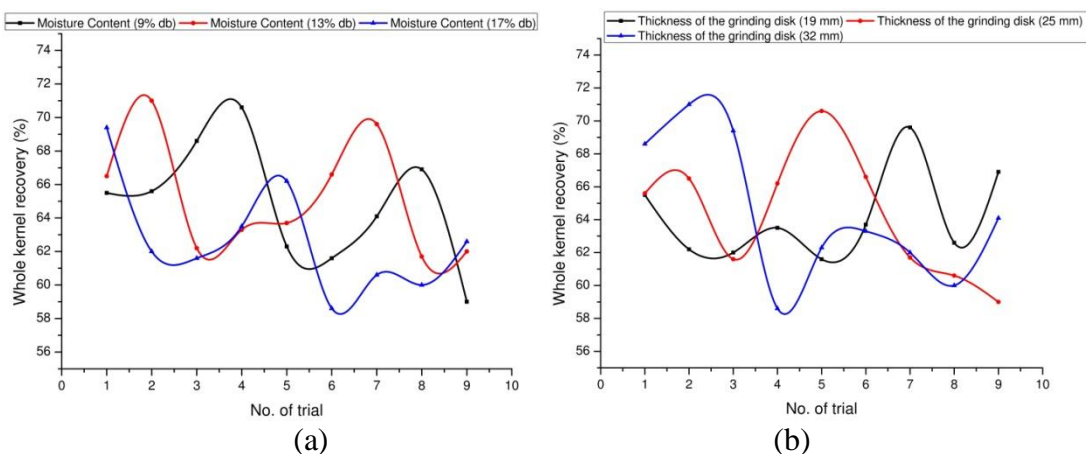
Figure 7.19 Influence of individual clearance and thickness of grinding disk on the whole kernel recovery.

From figure 7.19 (b) it can be seen that whole kernel recovery obtained at a thickness of grinding disk of 19 mm, 25 mm and 32 mm varies between 65.5 to 66.9 %, 65.6 to 59.00 % and 68.6 to 64.1.6% respectively. The highest whole kernel recovery obtained was 69.60%, 70.6%, & 71.0% at disk thickness of 19 mm, 25 mm and 32 mm respectively. Whereas the lowest whole kernel recovery obtained was 61.60% for disk thickness of 19 mm, 59.00% for disk thickness of 25 mm, & 58.60% for disk thickness of 32 mm. The highest whole kernel recovery was observed 71.0 % at disk thickness of 32 mm; whereas the lowest whole kernel recovery was observed 58.6% for disk thickness of 32 mm.

The value of whole kernel recovery varies considerably with increase in disk thickness from 69.6 % to 58.6 %. The trend of the increasing/decreasing the whole kernel recovery with clearance is found complex. But there is a significant variation in the whole kernel recovery. Furthermore, according to Taguchi analysis, disk thickness has not a significant impact on whole kernel recovery, and have a least contribution of 0.05 %.
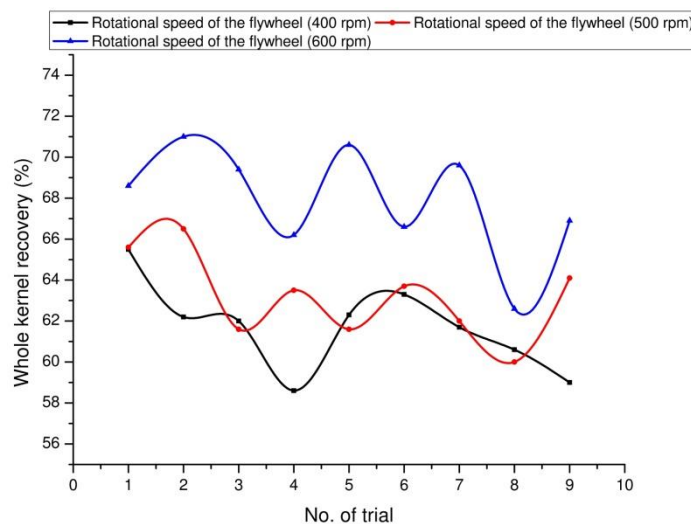
Figure 7.20 Influence of individual rotational speed of the flywheel on the whole kernel recovery.

From figure 7.20 it can be seen that whole kernel recovery obtained at a rotational speed of the flywheel of 400 rpm, 500 rpm and 600 rpm varies between 65.5 to 59.0 %, 65.6 to 64.10 % and 68.6 to 66.9% respectively. The highest whole kernel recovery obtained was 65.50%, 66.50%, and 71.00% at rotational speed of 400 rpm,

500 rpm and 600 rpm respectively. Whereas the lowest whole kernel recovery obtained was 58.60% for rotational speed of 400 rpm, 60.00% for rotational speed of 500 rpm, & 62.60.9% for rotational speed of 600 rpm. The highest whole kernel recovery was observed 71.0 % at rotational speed of 600 rpm; whereas the lowest whole kernel recovery was observed 58.6% for rotational speed of 400 rpm.

The value of whole kernel recovery increase significantly with increasing with the rotational speed of the flywheel. The trend of the increasing the whole kernel recovery with increasing rotational speed is found. At a rotational speed of 600 rpm, percentage of whole kernel recovery was significantly changed from 71.0 to 62.6 %. This indicates at higher rotational speed whole kernel recovery is maximum. The low whole kernel recovery at minimum speed may be due to the low impact force applied on ma Charoli nut. On the other hand, whole kernel recovery higher at higher speed is due to increase of impact force on Charoli nut at higher speed. Furthermore, according to Taguchi analysis, rotational speed of the flywheel has a significant impact on whole kernel recovery, with highest contribution of 60.29 %.

Interaction effect of feed rate and clearance also considered in study to find out its impact on the whole kernel recovery. As per Taguchi analysis, Interaction effect of feed rate and clearance have not a significant impact on whole kernel recovery, and have a least contribution of 0.26 % only. That means, though the feed rate and clearance have significant effect on whole kernel recovery but their interactions doesn't have any significant contribution on whole kernel recovery.

From the Taguchi analysis, it is noted that rotational speed of the flywheel with contribution of 60.29 %, clearance with contribution of 16.05 %, feed rate with contribution of 11.91 %, and moisture content percent with contribution of 10.25 % are the significantly affecting the whole kernel recovery. Among these factors effect of rotational speed of the flywheel followed by clearance, feed rate and moisture content percent are highly significant both physically and statistically. The changes of the thickness of the grinding disk and interaction of feed rate and clearance have minimal impacts on whole kernel recovery, both statistically and physically.

Therefore, for maximum whole kernel recovery, more attention needs to be focused on rotational speed of the flywheel followed by clearance, feed rate and moisture content percent.

7.3.3. Influence of various input parameters on the broken kernels:

Figure 7.21 shows the effect of feed rate, moisture content, clearance, thickness of the grinding disk and rotational speed of the flywheel on the broken kernels.
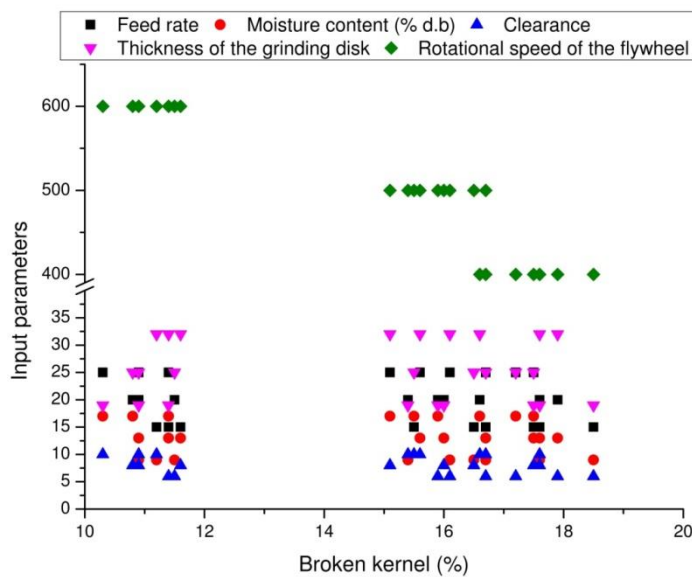
Figure 7.21 effects of feed rate, moisture content, clearance, thickness of the grinding disk and rotational speed on the broken kernels.

It can be seen from figure 7.21, broken kernels decreases from 18.50% to 10.30% by increasing the feed rate (15 kg/hr to 25 kg/hr); moisture content percent from (9 % d.b to 17 % d.b); the clearance (6 mm to 10 mm); the thickness of the grinding disk from (19 mm to 32 mm); and the rotational speed of the flywheel (400 rpm to 600 rpm).

Figure 7.22 shows an influence of feed rate and moisture content on the broken kernels. From figure 7.22 (a) it can be seen that broken kernels received at a feed rate of 15 kg/hr, 20 kg/hr and 25 kg/hr varies between 18.50 to 15.50%, 15.90 to 10.90 % and 11.40 to 16.70% respectively. The highest broken kernels obtained were 18.5 %, 17.9 %, & 17.50 at a feed rate of 15 kg/hr, 20 kg/hr and 25 kg/hr respectively. Whereas the lowest broken kernels obtained was 11.20 % for feed rate of 15 kg/hr, 10.80 % for feed rate of 20 kg/hr, & 10.30 % for feed rate of 25 kg/hr. The highest

broken kernels were observed 17.90 % at a feed rate of 20 kg/hr; whereas the broken kernels were observed 10.30% for feed rate of 25 kg/hr.

A value of broken kernels shows sinusoidal pattern and complex behavior with increase in feed rate. The trend of the increasing/decreasing the broken kernels with feed rate is found complex. But there is a significant variation in the broken kernels. At a feed rate of 25 kg/hr, percentage of broken kernels was significantly changed from 17.50 to 10.30 %. This means, lower kernel breakage is received at a feed rate of 25 kg/hr. The lower percentage of broken kernel at higher feed was because of low impact force was applied on charoli nut which leads to the lower kernel damage. The higher percentage of broken kernel at lower feed was because of charoli nut has gat higher residence time in deshelling unit due to which kernel get damaged. Furthermore, according to Taguchi analysis, feed rate has a significant impact on broken kernels, with contribution of 0.93 %.

(a)   (b)
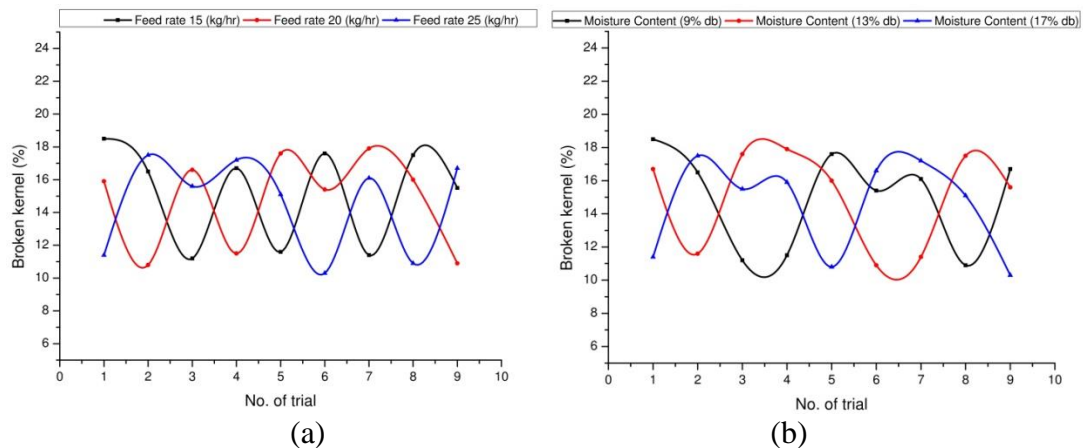
Figure 7.22 Influence of individual feed rate and moisture content on the broken kernels.

From figure 7.22 (b) it can be seen that broken kernels received at a moisture content percent of 9 (% d.b), 13 (% d.b) and 17 (% d.b) varies between 18.5 to 16.7 %, 16.7 to 15.60 % and 11.40 to 10.3 % respectively. The highest broken kernels obtained was 18.50%, 17.90%, & 17.50% at a moisture content percent of 9 (% d.b), 13 (% d.b) and 17 (% d.b) respectively. Whereas the lowest broken kernels obtained was 10.90 % for a moisture content percent of 9 (% d.b), 10.90 % for a moisture content percent of 13 (% d.b), & 10.3 % for a moisture content percent of 17 (% d.b). The highest broken kernels was observed 18.50 % at a moisture content percent of 9 (% d.b); whereas the

lowest broken kernels was observed 10.30% for a moisture content percent of 17 (% d.b).

The value of broken kernels shows sinusoidal pattern and complex behavior with increase in moisture content percent. The trend of the increasing/decreasing the broken kernels with moisture content % is found complex. But there is a significant variation in the broken kernels. The proportion of broken kernels decreased significantly as the moisture level increased. This might be due to the nut's flexible nature, which makes it less likely to break when it's wet. Mechanical damage might occur because of this change in the structure of the fruit. When the kernel is to be used in the future, a deshelling machine with little kernel breakage is desirable. In addition, a higher market price is demanded for a low kernel breaking rate. Furthermore, according to Taguchi analysis, moisture content percent has a significant impact on broken kernels, with contribution of 0.76 %.

Figure 7.23 shows the effect of clearance & thickness of the grinding disk on the broken kernels. From figure 7.23 (a) it can be seen that broken kernels obtained at a clearance of 6 mm, 8 mm and 10 mm varies between 18.5 to 16.1 %, 16.5 to 10.9 % and 11.2 to 16.7 % respectively. The highest broken kernels obtained were 18.5%, 17.6%, & 17.6% at clearance of 6 mm, 8 mm and 10 mm respectively. Whereas the lowest broken kernels obtained was 11.40% for clearance of 6 mm, 10.80% for clearance of 8 mm, & 10.30% for clearance of 10 mm. The highest broken kernels was observed 18.50 % at clearance of 6 mm; whereas the lowest broken kernels was observed 10.30% for clearance of 10 mm.

The value of broken kernels shows sinusoidal pattern and complex behavior with increase in clearance. The trend of the increasing/decreasing the broken kernels with clearance is found complex. But there is a significant variation in the broken kernels. At a clearance of 6mm, a larger proportion of broken kernels was found. As the moisture level drops, the nut dries out, and the fruit is crushed owing to the short clearance between axial dimensions and the fruit's axial dimensions, increasing the proportion of broken kernels. Furthermore, according to Taguchi analysis, clearance

has a significant impact on broken kernels, with second highest contribution of 1.27 %.
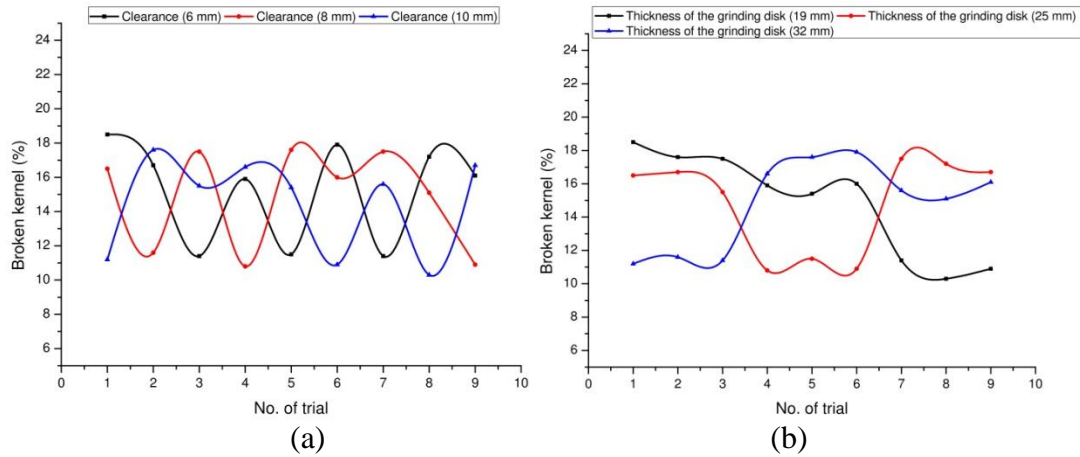
Figure 7.23 Influence of individual clearance and thickness of grinding disk on the broken kernels.

From figure 7.23 (b) it can be seen that broken kernels obtained at a thickness of grinding disk of 19 mm, 25 mm and 32 mm varies between 18.5 to 10.9 %, 16.5 to 16.7 % and 11.2 to 16.1% respectively. The highest broken kernels obtained were 18.50%, 17.50%, & 17.90% at disk thickness of 19 mm, 25 mm and 32 mm respectively. Whereas the lowest broken kernels obtained was 10.30% for disk thickness of 19 mm, 10.80% for disk thickness of 25 mm, & 11.20% for disk thickness of 32 mm. The highest broken kernels were observed 18.50 % at disk thickness of 25 mm; whereas the lowest broken kernels were observed 10.30% for disk thickness of 25 mm.

The value of broken kernels shows sinusoidal pattern and complex behavior with increase in thickness of grinding disk. The trend of the increasing/decreasing the broken kernels with clearance is found complex.. Furthermore, according to Taguchi analysis, disk thickness has not a significant impact on broken kernels, and have a least contribution of 0.0 %.

From figure 7.24 it can be seen that broken kernels obtained at a rotational speed of the flywheel of 400 rpm, 500 rpm and 600 rpm varies between 18.5 to 16.7 %, 16.5 to 16.10 % and 11.2 to 10.9% respectively. The highest broken kernels obtained were 18.50%, 16.70%, and 11.60% at rotational speed of 400 rpm, 500 rpm and 600 rpm

respectively. Whereas the lowest broken kernels obtained was 16.60% for rotational speed of 400 rpm, 15.10% for rotational speed of 500 rpm, & 10.30% for rotational speed of 600 rpm. The highest broken kernels were observed 18.50 % at rotational speed of 400 rpm; whereas the lowest broken kernels was observed 10.30% for rotational speed of 600 rpm.
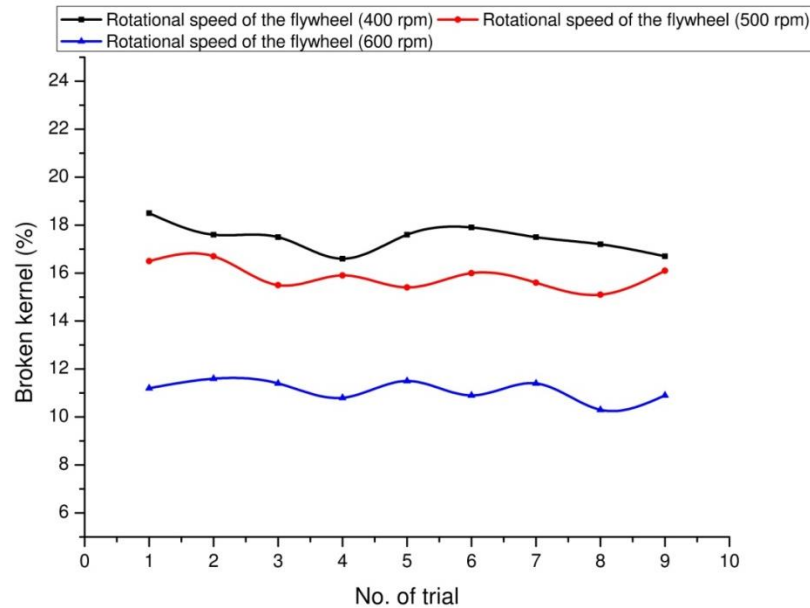
Figure 7.24 Influence of individual rotational speed of the flywheel on the broken kernels.

The value of broken kernels decreases significantly with increasing with the rotational speed of the flywheel. The trend of the decreasing the broken kernels with increasing rotational speed is found. By changing a rotational speed from 400 to 600 rpm, percentage of broken kernels was significantly reduced from 18.5 to 10.9 %. This indicates at higher rotational speed broken kernels is minimum as desired. The lower percentage of broken kernel at higher speed is was due to shorter residence time of Charoli nut at deshelling unit which avoids the breaking or damaging of the whole kernel at deshelling unit. Furthermore, according to Taguchi analysis, rotational speed of the flywheel has a significant impact on broken kernels, with highest contribution of 96.89 %.

Interaction effect of feed rate and clearance also have considered in study to find out its impact on the broken kernels. As per Taguchi analysis, Interaction effect of feed rate and clearance has a not a significant impact on broken kernels, and have a least

contribution of 0.02 % only. That means, though the feed rate and clearance have significant effect on broken kernels but their interactions doesn't have any significant contribution on broken kernels.

From the Taguchi analysis, it is noted that rotational speed of the flywheel with contribution of 96.89 %, clearance with contribution of 1.27 %, feed rate with contribution of 0.93 %, and moisture content percent with contribution of 0.76 % are the significantly affecting the broken kernels. Among these factors effect of rotational speed of the flywheel followed by clearance, feed rate and moisture content percent are highly significant both physically and statistically. The changes of the thickness of the grinding disk and interaction of feed rate and clearance have minimal impacts on broken kernels, both statistically and physically. Therefore, for maximum broken kernels, more attention needs to be focused on rotational speed of the flywheel followed by clearance, feed rate and moisture content percent.

7.3.4. Influence of various input parameters on the partially shelled / unshelled nuts :

Figure 7.25 shows the effect of feed rate, moisture content, clearance, thickness of the grinding disk and rotational speed of the flywheel on the partially shelled / unshelled nuts .
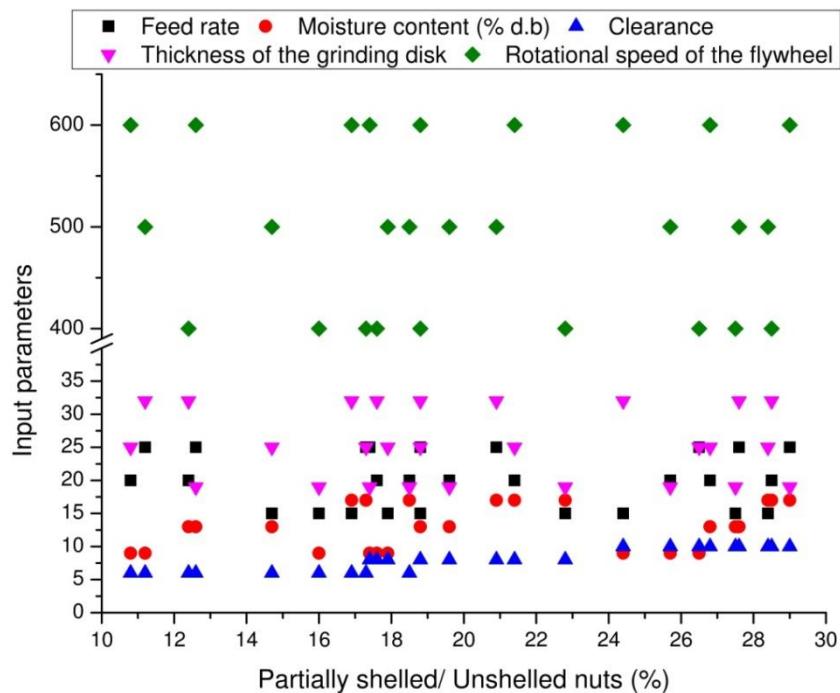
Figure 7.25 effects of feed rate, moisture content, clearance, thickness of the grinding disk and rotational speed on the partially shelled / unshelled nuts.

It can be seen from figure 7.25, partially shelled / unshelled nuts decreases from 29.00% to 10.80% by increasing the feed rate (15 kg/hr to 25 kg/hr); moisture content percent from (9 % d.b to 17 % d.b); the clearance (6 mm to 10 mm); the thickness of the grinding disk from (19 mm to 32 mm); and the rotational speed of the flywheel (400 rpm to 600 rpm).

Figure 7.26 shows an influence of feed rate and moisture content on the partially shelled / unshelled nuts. From figure 7.26 (a) it can be seen that partially shelled / unshelled nuts received at a feed rate of 15 kg/hr, 20 kg/hr and 25 kg/hr varies between 16.00 to 28.40%, 18.50 to 16.80 % and 12.60 to 26.50% respectively. The highest partially shelled / unshelled nuts obtained were 28.4 %, 28.50 %, & 29.00 at a feed rate of 15 kg/hr, 20 kg/hr and 25 kg/hr respectively. Whereas the lowest partially shelled / unshelled nuts obtained was 14.70 % for feed rate of 15 kg/hr, 10.80 % for feed rate of 20 kg/hr, & 11.20 % for feed rate of 25 kg/hr. The highest partially shelled / unshelled nuts were observed 28.50 % at a feed rate of 20 kg/hr; whereas the partially shelled / unshelled nuts were observed 10.80% for feed rate of 20 kg/hr.

A value of partially shelled / unshelled nuts shows sinusoidal pattern and complex behavior with increase in feed rate. The trend of the increasing/decreasing the partially shelled / unshelled nuts with feed rate is found complex. But there is a significant variation in the partially shelled / unshelled nuts. At a feed rate of 20 kg/hr, percentage of partially shelled / unshelled nuts was significantly changed from 28.50 to 10.80 %. This means, lower kernel breakage is received at a feed rate of 20 kg/hr. The higher partially shelled / unshelled nuts at higher feed was mainly due to the reduction in the residence time. The lower partially shelled / unshelled nuts at optimum feed was because charoli nut has got enough time to be impacted & get deshelled. But, according to Taguchi analysis, feed rate has a insignificant impact on partially shelled / unshelled nuts, with contribution of 0.33 %.

From figure 7.26 (b) it can be seen that partially shelled / unshelled nuts received at a moisture content percent of 9 (% d.b), 13 (% d.b) and 17 (% d.b) varies between 16.0 to 26.5 %, 14.7 to 27.60 % and 16.90 to 29.00 % respectively. The highest partially shelled / unshelled nuts obtained was 26.50%, 27.60%, & 29.00% at a moisture content percent of 9 (% d.b), 13 (% d.b) and 17 (% d.b) respectively. Whereas the lowest partially shelled / unshelled nuts obtained was 10.80 % for a moisture content percent of 9 (% d.b), 12.40 % for a moisture content percent of 13 (% d.b), & 16.9 % for a moisture content percent of 17 (% d.b). The highest partially shelled / unshelled nuts was observed 27.60 % at a moisture content percent of 13 (% d.b); whereas the lowest partially shelled / unshelled nuts was observed 10.80% for a moisture content percent of 9 (% d.b).
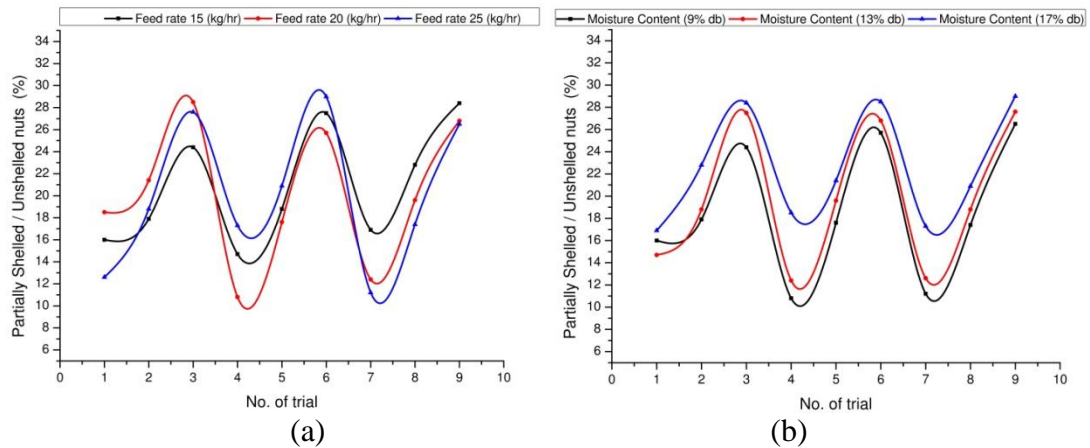
Figure 7.26 Influence of individual feed rate and moisture content on the partially shelled / unshelled nuts.

The value of partially shelled / unshelled nuts shows sinusoidal pattern and complex behavior with increase in moisture content. The trend of the increasing/decreasing the partially shelled / unshelled nuts with moisture content % is found complex. But there is a significant variation in the partially shelled / unshelled nuts. At a moisture content of 9 (%db), percentage of partially shelled / unshelled nuts was significantly changed from 26.50 to 10.80 %. This means, lower kernel breakage is received at a moisture content of 9 (%db). The Lowest partially shelled / unshelled nuts was noted at moisture content 9 % db. This be due to at lower moisture content nut becomes more brittle & susceptible to mechanical damage.

Furthermore, according to Taguchi analysis, moisture content percent has a significant impact on partially shelled / unshelled nuts, with second highest contribution of 9.04 %.

Figure 7.27 shows the effect of clearance & thickness of the grinding disk on the partially shelled / unshelled nuts. From figure 7.27 (a) it can be seen that partially shelled / unshelled nuts obtained at a clearance of 6 mm, 8 mm and 10 mm varies between 16.0 to 11.2 %, 17.9 to 17.4 % and 24.4 to 26.5 % respectively. The highest partially shelled / unshelled nuts obtained were 18.5%, 22.8%, & 29.0% at clearance of 6 mm, 8 mm and 10 mm respectively. Whereas the lowest partially shelled / unshelled nuts obtained was 10.80% for clearance of 6 mm, 17.40% for clearance of 8 mm, & 24.40% for clearance of 10 mm. The highest partially shelled / unshelled nuts

were observed 29.00 % at clearance of 10 mm; whereas the lowest partially shelled / unshelled nuts were observed 10.80% for clearance of 6 mm.

The value of partially shelled / unshelled nuts shows sinusoidal pattern and complex behavior with increase in feed rate. The trend of the increasing/decreasing the partially shelled / unshelled nuts with clearance is found complex. But there is a significant variation in the partially shelled / unshelled nuts. At a clearance of 6 mm, percentage of partially shelled / unshelled nuts was significantly changed from 18.50 to 10.80 %. This means, lower kernel breakage is received at a clearance of 6 mm. The highest percentage of partially shelled / unshelled nuts observed at clearance of 10mm whereas lowest is observed at 6mm. This is mainly because of optimum pressure created at this point of the clearance to split the nuts into kernel & shells Furthermore, according to Taguchi analysis, clearance has a significant impact on partially shelled / unshelled nuts, with highest contribution of 86.97 %.
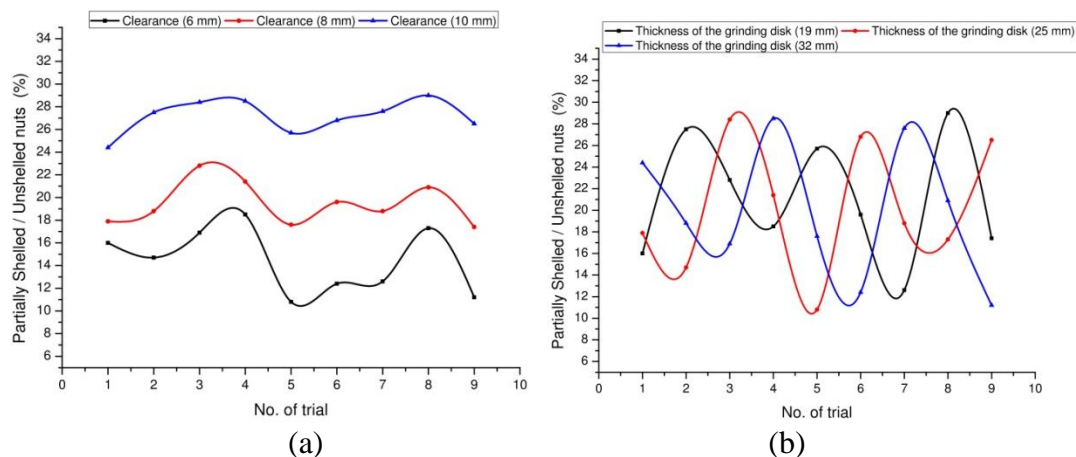
Figure 7.27 Influence of individual clearance and thickness of grinding disk on the partially shelled / unshelled nuts.

From figure 7.27 (b) it can be seen that partially shelled / unshelled nuts obtained at a thickness of grinding disk of 19 mm, 25 mm and 32 mm varies between 16.0 to 17.4 %, 17.9 to 26.5 % and 24.4 to 11.2% respectively. The highest partially shelled / unshelled nuts obtained were 29.00%, 28.40%, & 28.50% at disk thickness of 19 mm, 25 mm and 32 mm respectively. Whereas the lowest partially shelled / unshelled nuts obtained was 12.60% for disk thickness of 19 mm, 10.80% for disk thickness of 25 mm, & 11.20% for disk thickness of 32 mm. The highest partially shelled / unshelled

nuts were observed 29.0 % at disk thickness of 19 mm; whereas the lowest partially shelled / unshelled nuts were observed 10.80% for disk thickness of 25 mm.

The value of partially shelled / unshelled nuts shows sinusoidal pattern and complex behavior with increase in disk thickness. The trend of the increasing/decreasing the partially shelled / unshelled nuts with disk thickness is found complex. Furthermore, according to Taguchi analysis, disk thickness has not a significant impact on partially shelled / unshelled nuts, and have a least contribution of 0.78 %.
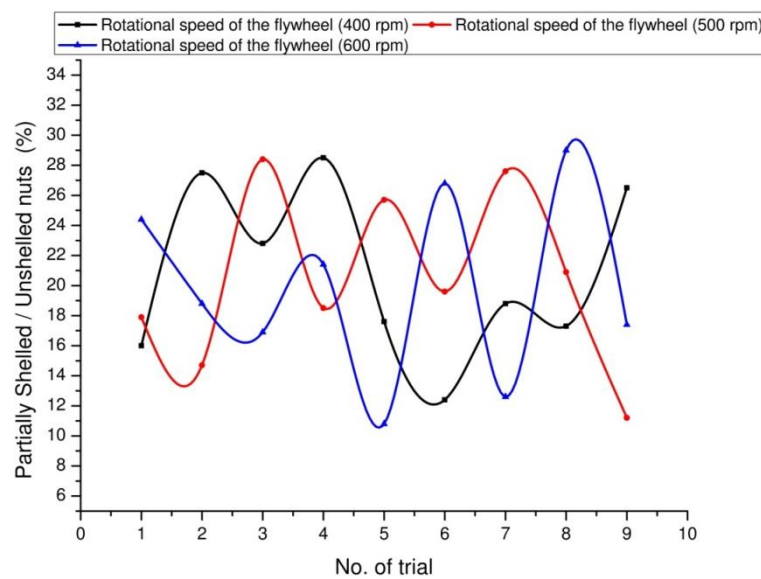
Figure 7.28 Influence of individual rotational speed of the flywheel on the partially shelled / unshelled nuts.

From figure 7.28 it can be seen that partially shelled / unshelled nuts obtained at a rotational speed of the flywheel of 400 rpm, 500 rpm and 600 rpm varies between 16.0 to 26.5 %, 17.9 to 11.20 % and 24.4 to 17.4% respectively. The highest partially shelled / unshelled nuts obtained were 28.50%, 28.40%, and 29.00% at rotational speed of 400 rpm, 500 rpm and 600 rpm respectively. Whereas the lowest partially shelled / unshelled nuts obtained was 12.40% for rotational speed of 400 rpm, 11.20% for rotational speed of 500 rpm, & 10.80% for rotational speed of 600 rpm. The highest partially shelled / unshelled nuts were observed 28.50 % at rotational speed of 400 rpm; whereas the lowest partially shelled / unshelled nuts were observed 10.80% for rotational speed of 600 rpm.

The value of partially shelled / unshelled nuts shows sinusoidal pattern and complex behavior with increase in rotational speed of the flywheel. The trend of the increasing/decreasing the partially shelled / unshelled nuts with rotational speed is found complex. Low impact force applied on nut leads to partially shelled / unshelled nuts at the outlet. Also lower residence time of nut in deshelling unit is reason for higher partially shelled / unshelled nuts. Furthermore, according to Taguchi analysis, rotational speed of the flywheel has not a significant impact on partially shelled / unshelled nuts, and have a least contribution of 0.6 %.

Interaction effect of feed rate and clearance also have considered in study to find out its impact on the partially shelled / unshelled nuts. As per Taguchi analysis, Interaction effect of feed rate and clearance has a not a significant impact on partially shelled / unshelled nuts, and have a least contribution of 0.98 % only. That means, though the clearance have significant effect on partially shelled / unshelled nuts but their interactions doesn't have any significant contribution on partially shelled / unshelled nuts .

From the Taguchi analysis, it is noted that clearance with contribution of 86.97 %, and moisture content percent with contribution of 9.04 % are the significantly affecting the partially shelled / unshelled nuts. Among these factors effect of clearance followed by clearance, moisture content percent are highly significant both physically and statistically. The changes of the feed rate, thickness of the grinding disk, rotational speed of the flywheel and interaction of feed rate and clearance have minimal impacts on partially shelled / unshelled nuts, both statistically and physically. Therefore, for minimum partially shelled / unshelled nuts, more attention needs to be focused on clearance followed moisture content percent.

7.3.5. Influence of various input parameters on the resistive torque

Figure 5.29 shows the effect of feed rate, moisture content, clearance, thickness of the grinding disk and rotational speed of the flywheel on the resistive torque.
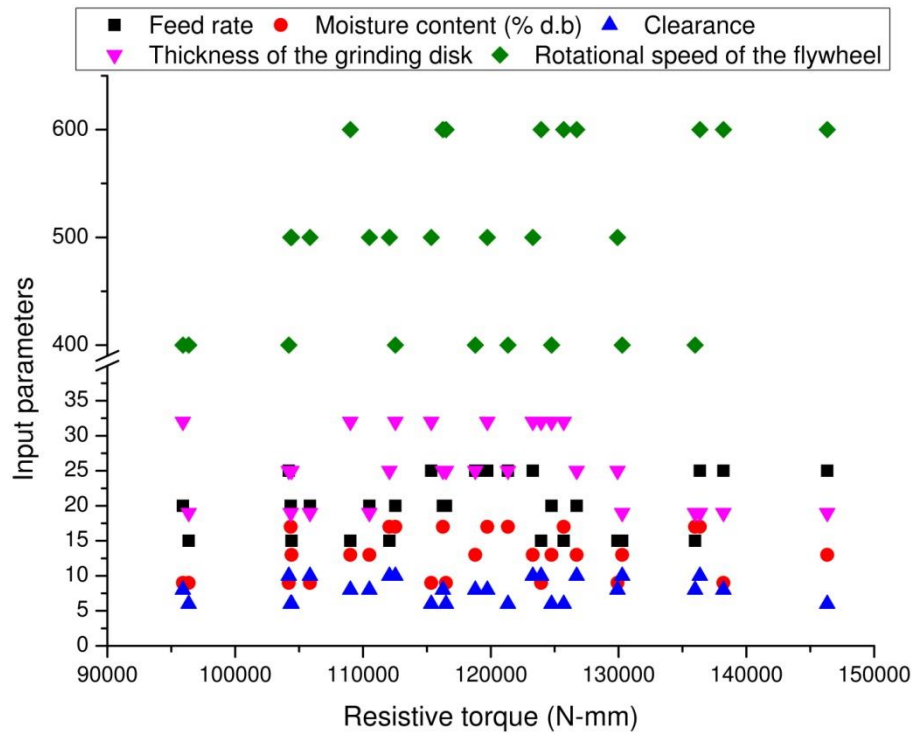
Figure 7.29 effects of feed rate, moisture content, clearance, thickness of the grinding disk and rotational speed on the resistive torque.

It can be seen from figure 7.29, resistive torque increases from 96364.48 to 146322.31 N-mm by increasing the feed rate (15 kg/hr to 25 kg/hr); moisture content percent from (9 % d.b to 17 % d.b); the clearance (6 mm to 10 mm); the thickness of the grinding disk from (19 mm to 32 mm); and the rotational speed of the flywheel (400 rpm to 600 rpm).

Figure 7.30 shows an influence of feed rate and moisture content on the resistive torque. From figure 7.30 (a) it can be seen that resistive torque received at a feed rate of 15 kg/hr, 20 kg/hr and 25 kg/hr varies between 96364.48 to 112077.33 N-mm, 104356.04 to 126730.54 N-mm, and 146322.31 to 104198.85 N-mm respectively. The highest resistive torque obtained were 135984.90, 126730.54, & 146322.31 N-mm at a feed rate of 15 kg/hr, 20 kg/hr and 25 kg/hr respectively. Whereas the lowest resistive torque obtained was 96364.49 N-mm for feed rate of 15 kg/hr, 95916.22 N-mm for feed rate of 20 kg/hr, & 104198.86 N-mm for feed rate of 25 kg/hr. The

highest resistive torque was observed 146322.31 N-mm at a feed rate of 25 kg/hr; whereas the resistive torque was observed 95916.22 N-mm for feed rate of 20 kg/hr.

A value of resistive torque shows sinusoidal pattern and complex behavior with increase in feed rate. The trend of the increasing/decreasing the resistive torque with feed rate is found complex. But there is a significant variation in the resistive torque. The higher entry of nuts inside the deshelling units due to high feed rate exerts maximum resistance from the machine. But, according to Taguchi analysis, feed rate has a insignificant impact on resistive torque, with contribution of 15.72 %.

(a)   (b)
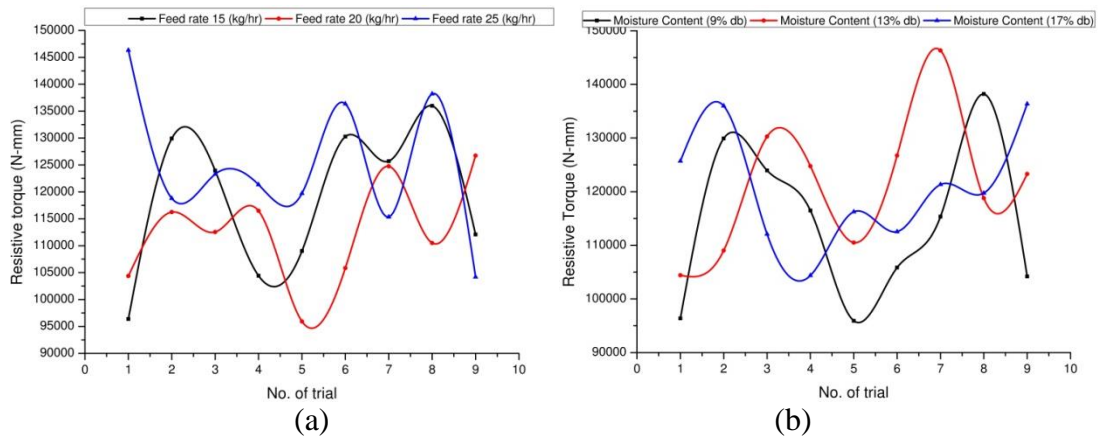
Figure 5.30 Influence of individual feed rate and moisture content on the resistive torque .

From figure 7.30 (b) it can be seen that resistive torque received at a moisture content percent of 9 (% d.b), 13 (% d.b) and 17 (% d.b) varies between 96364.48 to 104198.85 N-mm, 104410.36 to 123293.50 N-mm, and 125714.16 to 136359.53 N-mm, respectively. The highest resistive torque obtained was 138207.55, 146322.31, and 136359.538 N-mm at a moisture content percent of 9 (% d.b), 13 (% d.b) and 17 (% d.b) respectively. Whereas the lowest resistive torque obtained was 95916.216 N-mm for a moisture content percent of 9 (% d.b), 104410.36 N-mm for a moisture content percent of 13 (% d.b), & 104356.046 N-mm for a moisture content percent of 17 (% d.b). The highest resistive torque was observed 146322.31 N-mm at a moisture content percent of 17 (% d.b); whereas the lowest resistive torque was observed 95916.216 N-mm for a moisture content percent of 9 (% d.b).

The value of resistive torque shows sinusoidal pattern and complex behavior with increase in moisture content. The trend of the increasing/decreasing the resistive torque with moisture content % is found complex. But there is a significant variation in the resistive torque. Furthermore, according to Taguchi analysis, moisture content has an insignificant impact on resistive torque, with contribution of 6. 98 %.

Figure 7.31 shows the effect of clearance & thickness of the grinding disk on the resistive torque. From figure 7.31 (a) it can be seen that resistive torque obtained at a clearance of 6 mm, 8 mm and 10 mm varies between 96364.48 to 115339.06 N-mm, 129916.94 to 138207.54 N-mm, and 123945.45 to 104198.85 N-mm respectively. The highest resistive torque obtained were 146322.31, 138207.54, & 136359.53 N-mm at clearance of 6 mm, 8 mm and 10 mm respectively. Whereas the lowest resistive torque obtained was 96364.48 N-mm for clearance of 6 mm, 95916.21 N-mm for clearance of 8 mm, & 104198.85 N-mm for clearance of 10 mm. The highest resistive torque was observed 146322.31 N-mm at clearance of 6 mm; whereas the lowest resistive torque was observed 95916.21 N-mm for clearance of 8 mm.

The value of resistive torque shows sinusoidal pattern and complex behavior with increase in clearance. The trend of the increasing/decreasing the resistive torque with clearance is found complex. But there is a significant variation in the resistive torque. At a clearance of 6 mm, percentage of resistive torque was significantly changed from 18.50 to 10.80 %. This means, lower kernel breakage is received at a clearance of 6 mm. At a lower clearance, there is a maximum possibility of nuts in contact with a disc which creates the resistance for process. Therefore maximum resistive torque occurred at a clearance of 6mm. Furthermore, according to Taguchi analysis, clearance has an insignificant impact on resistive torque, with contribution of 6. 98 %.

From figure 7.31 (b) it can be seen that resistive torque obtained at a thickness of grinding disk of 19 mm, 25 mm and 32 mm varies between 96364.48 to 138207.54 N-mm, 129916.94 to 104198.85 N-mm,   and 123945.45 to 115339.06 N-mm respectively. The highest resistive torque obtained were 146322.31, 126730.54, &

125714.16 N-mm at disk thickness of 19 mm, 25 mm and 32 mm respectively. Whereas the lowest resistive torque obtained was 96364.48 N-mm for disk thickness of 19 mm, 104198.85 N-mm for disk thickness of 25 mm, & 95916.21 N-mm for disk thickness of 32 mm. The highest resistive torque was observed 146322.31 N-mm at disk thickness of 19 mm; whereas the lowest resistive torque was observed 95916.21 N-mm for disk thickness of 32 mm.
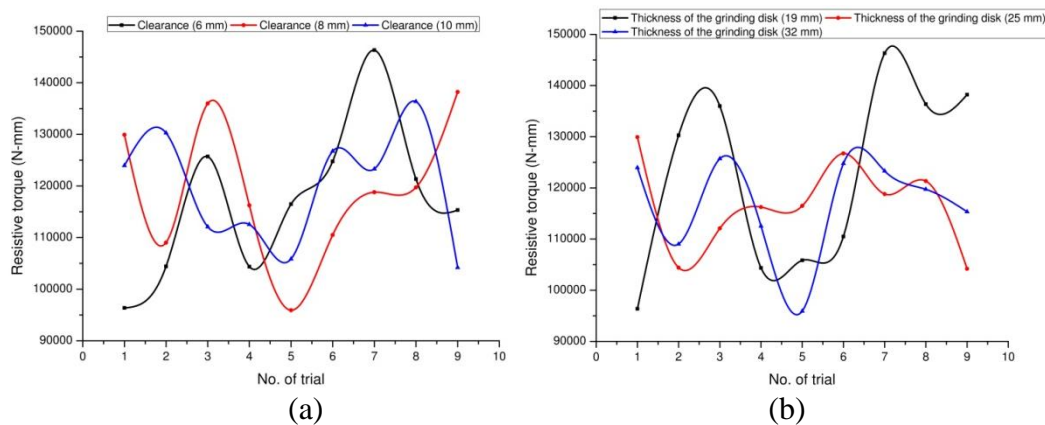
Figure 7.31 Influence of individual clearance and thickness of grinding disk on the resistive torque.

The value of resistive torque shows sinusoidal pattern and complex behavior with increase in disk thickness. The trend of the increasing/decreasing the resistive torque with disk thickness is found complex. Furthermore, according to Taguchi analysis, disk thickness has not a significant impact on resistive torque, and have a contribution of 5.04 %.

From figure 7.32 it can be seen that resistive torque obtained at a rotational speed of the flywheel of 400 rpm, 500 rpm and 600 rpm varies between 96364.48 to 104198.85 N-mm, 129916.94 to 115339.06 N-mm and 123945.45 to 138207.54 N-mm respectively. The highest resistive torque obtained was 135984.90 N-mm, 129916.94 N-mm, and 146322.31 N-mm at rotational speed of 400 rpm, 500 rpm and 600 rpm respectively. Whereas the lowest resistive torque obtained was 95916.21 N-mm for rotational speed of 400 rpm, 104356.04 N-mm for rotational speed of 500 rpm, & 109014.20 N-mm for rotational speed of 600 rpm. The highest resistive torque was observed 135984.90 N-mm at rotational speed of 400 rpm; whereas the lowest resistive torque were observed 104356.04 N-mm for rotational speed of 500 rpm.
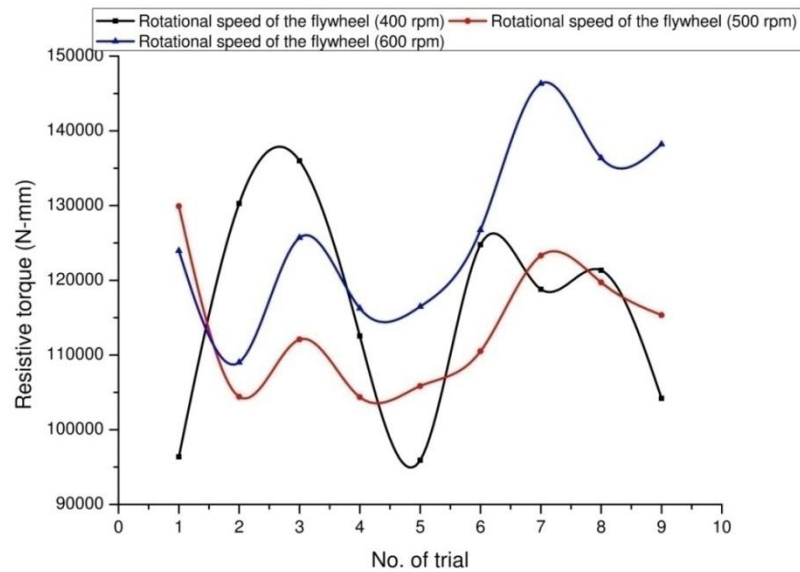
Figure 7.32 Influence of individual rotational speed of the flywheel on the resistive torque.

The value of resistive torque shows sinusoidal pattern and complex behavior with increase in rotational speed of the flywheel. The trend of the increasing/decreasing the resistive torque with rotational speed is found complex. Furthermore, according to Taguchi analysis, disk thickness has not a significant impact on resistive torque, and have a least contribution of 19.76 %.

Interaction effect of feed rate and clearance also have considered in study to find out its impact on the resistive torque. As per Taguchi analysis, Interaction effect of feed rate and clearance has a not a significant impact on resistive torque, and have a least contribution of 13.85 % only. That means, interactions doesn't have any significant contribution on resistive torque.

From the Taguchi analysis, it is noted that none of the input variable found significant or significantly affecting the resistive torque. This may be due to the extraneous variable like vibrations in the machines which have not considered as a variable for the study.

7.3.6. Influence of various input parameters on the processing time

Figure 7.33 shows the effect of feed rate, moisture content, clearance, thickness of the grinding disk and rotational speed of the flywheel on the processing time.
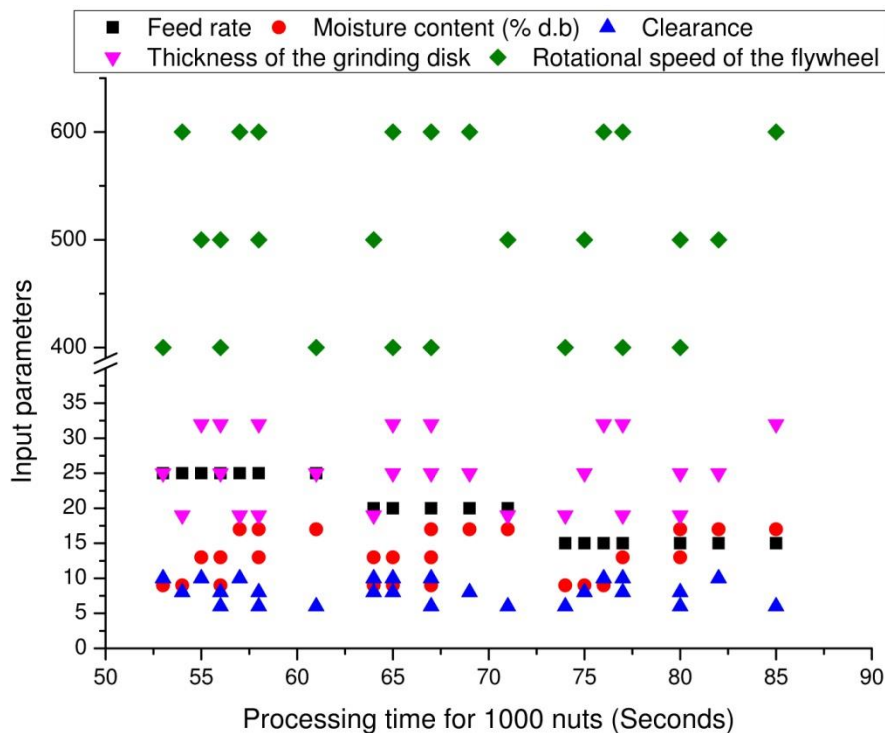
Figure 7.33 effects of feed rate, moisture content, clearance, thickness of the grinding disk and rotational speed on the processing time.

It can be seen from figure 7.33, processing time decreases from 85 Sec to 53 Sec by increasing the feed rate (15 kg/hr to 25 kg/hr); moisture content percent from (9 % d.b to 17 % d.b); the clearance (6 mm to 10 mm); the thickness of the grinding disk from (19 mm to 32 mm); and the rotational speed of the flywheel (400 rpm to 600 rpm).

Figure 7.34 shows an influence of feed rate and moisture content on the processing time. From figure 7.34 (a) it can be seen that processing time received at a feed rate of 15 kg/hr, 20 kg/hr and 25 kg/hr varies between 74 to 82 Sec, 71 to 65 Sec and 58 to 53 Sec respectively. The highest processing time obtained was 85 Sec, 71 Sec, & 61 Sec at a feed rate of 15 kg/hr, 20 kg/hr and 25 kg/hr respectively. Whereas the lowest processing time obtained was 74 Sec for feed rate of 15 kg/hr, 64 Sec for feed rate of

20 kg/hr, & 53 Sec for feed rate of 25 kg/hr. The highest processing time were observed 85 Sec at a feed rate of 15 kg/hr; whereas the processing time were observed 53 Sec for feed rate of 25 kg/hr.

A value of processing time clearly shows decrease in processing time with increase in feed rate. The trend of decreasing the processing time with feed rate is found consistently. But there is a significant variation in the processing time. At a feed rate of 25 kg/hr, percentage of processing time was significantly changed from 61 Sec to 53 Sec. This means, lower processing time is received at a feed rate of 25 kg/hr. Also, according to Taguchi analysis, feed rate has a significant impact on processing time, with highest contribution of 91.89 %.

(a)   (b)
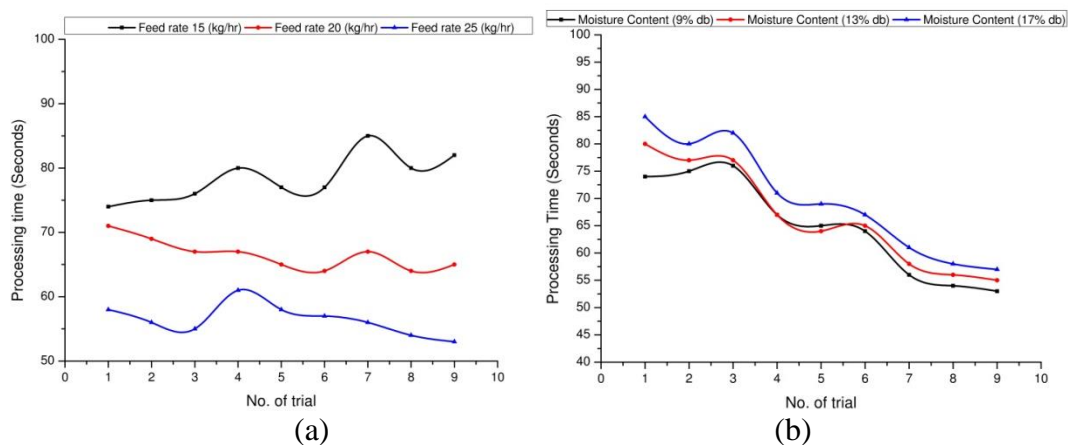
Figure 7.34 Influence of individual feed rate and moisture content on the processing time.

From figure 7.34 (b) it can be seen that processing time received at a moisture content percent of 9 (% d.b), 13 (% d.b) and 17 (% d.b) varies between 74 Sec to 53 Sec, 80 Sec to 55 Sec and 85 Sec to 57 Sec respectively. The highest processing time obtained was 76 Sec, 80 Sec, & 85 Sec at a moisture content percent of 9 (% d.b), 13 (% d.b) and 17 (% d.b) respectively. Whereas the lowest processing time obtained was 53 Sec for a moisture content percent of 9 (% d.b), 55 Sec for a moisture content percent of 13 (% d.b), & 57 Sec for a moisture content percent of 17 (% d.b). The highest processing time was observed 85 Sec at a moisture content percent of 17 (% d.b);

whereas the lowest processing time was observed 53 Sec for a moisture content percent of 9 (% d.b).

The value of processing time shows decrease in processing time with increase in feed rate. The trend of the increasing the processing time with moisture content % is found found consistently. But there is a significant variation in the processing time. At a moisture content of 9 (%db), percentage of processing time was significantly changed from 76 to 53 Sec. This means, lower processing time is received at a moisture content of 9 (%db). Furthermore, according to Taguchi analysis, moisture content percent has a significant impact on processing time, with second highest contribution of 5.15 %.

Figure 7.35 shows the effect of clearance & thickness of the grinding disk on the processing time. From figure 5.35 (a) it can be seen that processing time obtained at a clearance of 6 mm, 8 mm and 10 mm varies between 74 to 56 Sec, 75 to 54 Sec and 76 to 53 Sec respectively. The highest processing time obtained was 85 Sec, 80 Sec, & 82 Sec at clearance of 6 mm, 8 mm and 10 mm respectively. Whereas the lowest processing time obtained was 56 Sec for clearance of 6 mm, 54 Sec for clearance of 8 mm, & 53 Sec for clearance of 10 mm. The highest processing time were observed 85 Sec at clearance of 6 mm; whereas the lowest processing time was observed 53 Sec for clearance of 10 mm.

The value of processing time shows decrease in processing time with increase in clearance. The trend of decreasing the processing time with clearance is found consistently. But there is a significant variation in the processing time. At a clearance of 10 mm, processing time was significantly changed from 82 to 53 Sec. This means, lower processing time is received at a clearance of 10 mm. Furthermore, according to Taguchi analysis, clearance has a significant impact on processing time, with third highest contribution of 1.52 %.

From figure 7.35 (b) it can be seen that processing time obtained at a thickness of grinding disk of 19 mm, 25 mm and 32 mm varies between 74 to 54 Sec, 75 to 53

Sec and 76 to 56 Sec respectively. The highest processing time obtained was 80 Sec, 82 Sec, & 85 Sec at disk thickness of 19 mm, 25 mm and 32 mm respectively. Whereas the lowest processing time obtained was 54 Sec for disk thickness of 19 mm, 53 Sec for disk thickness of 25 mm, & 55 Sec for disk thickness of 32 mm. The highest processing time were observed 85 Sec at disk thickness of 32 mm; whereas the lowest processing time was observed 54 Sec for disk thickness of 19 mm.

| (a) | (b) |
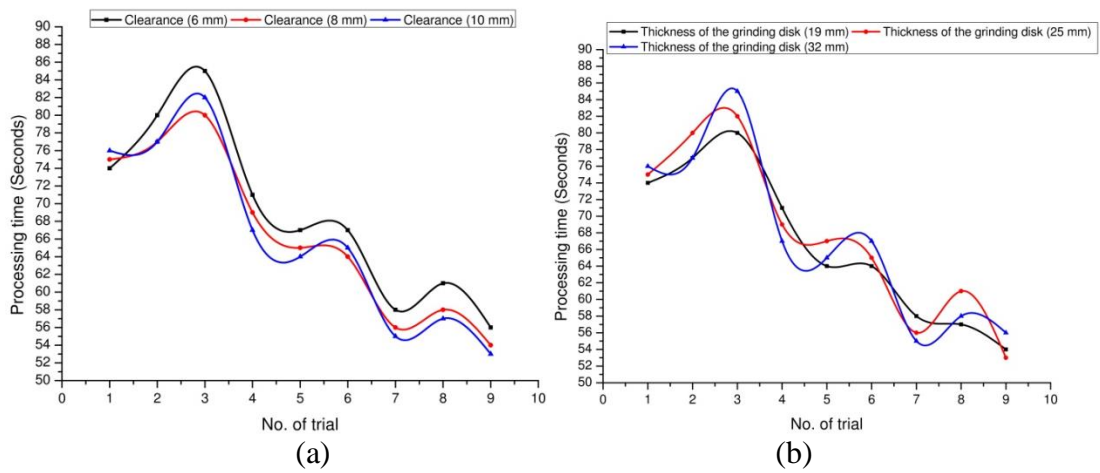
Figure 7.35 Influence of individual clearance and thickness of grinding disk on the processing time.

The value of processing time shows sinusoidal pattern and complex behavior with increase in disk thickness. The trend of the increasing/decreasing the processing time with disk thickness is found complex. Furthermore, according to Taguchi analysis, disk thickness has not a significant impact on processing time, and have a least contribution of 0.21 %.
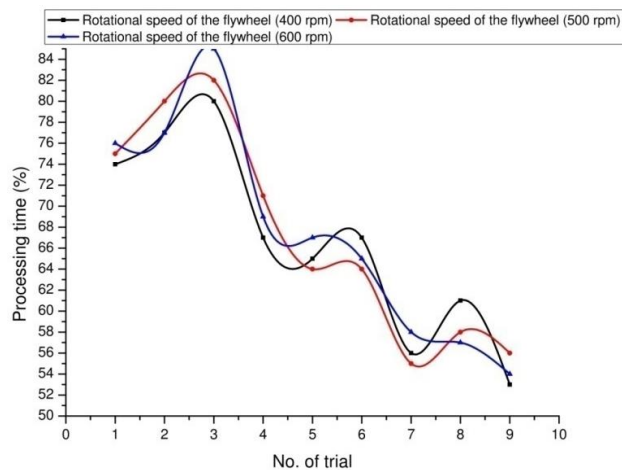
Figure 7.36 Influence of individual rotational speed of the flywheel on the processing time.

From figure 7.36 it can be seen that processing time obtained at a rotational speed of the flywheel of 400 rpm, 500 rpm and 600 rpm varies between 74 to 53 Sec, 75 to 56 Sec and 76 to 54 Sec respectively. The highest processing time obtained was 80 Sec, 82 Sec, and 85 Sec at rotational speed of 400 rpm, 500 rpm and 600 rpm respectively. Whereas the lowest processing time obtained was 53 Sec for rotational speed of 400 rpm, 55 Sec for rotational speed of 500 rpm, & 54 Sec for rotational speed of 600 rpm. The highest processing time were observed 85 Sec at rotational speed of 600 rpm; whereas the lowest processing time was observed 53 for rotational speed of 400 rpm.

The value of processing time shows sinusoidal pattern and complex behavior with increase in rotational speed of the flywheel. The trend of the increasing/decreasing the processing time with rotational speed is found complex. Furthermore, according to Taguchi analysis, disk thickness has not a significant impact on processing time, and have a least contribution of 0.15 %.

Interaction effect of feed rate and clearance also have considered in study to find out its impact on the processing time. As per Taguchi analysis, Interaction effect of feed rate and clearance has a not a significant impact on processing time, and have a least contribution of 0.19 % only. That means, though the clearance have significant effect on processing time but their interactions doesn't have any significant contribution on processing time.

From the Taguchi analysis, it is noted that feed rate with contribution of 91.89 %, moisture content percent with contribution of 5.15 % and clearance with contribution of 1.52 % are the significantly affecting the processing time. Among these factors effect of feed rate followed by moisture content percent and clearance are highly significant both physically and statistically. The changes of the thickness of the grinding disk, rotational speed of the flywheel and interaction of feed rate and clearance have minimal impacts on processing time, both statistically and physically. Therefore, for minimum processing time, more attention needs to be focused on feed rate followed by moisture content percent and clearance.

7.4 Effect of individual input parameters on the output parameters

7.4.1. Effect of feed rate on the output parameters

On the basis of performed experimentations and Taguchi analysis as given in chapter 4, feed rate plays more crucial role in the process of Charoli nut deshelling. Feed rate effects significantly as per experimentations and Taguchi analysis on deshelling efficiency (%),whole kernel recovery (%), broken kernels (%), and processing time (1000 nuts).

Table 7.13: Significant / insignificant parameters for feed rate

	Significant	Contribution	Insignificant
Feed rate	Processing time	91.89%	Partially shelled/ unshelled nuts
	Deshelling efficiency	30.23%	
	Whole kernel recovery	11.91%	Resistive torque
	Broken kernels	0.93%	

As per Taguchi analysis, feed rate contribution is highest in processing time (91.89%) followed by deshelling efficiency (30.23%), whole kernel recovery (11.91%), and broken kernels (0.93%). Feed rate contribution in case of partially shelled / unshelled nuts (%) and resistive torque is found as insignificant as compared to other factors.

7.4.2. Effect of moisture content percent on the output parameters

On the basis of performed experimentations and Taguchi analysis as given in chapter 4, moisture content percent is plays more crucial role in the process of Charoli nut deshelling. Moisture content percent effects significantly as per experimentations and Taguchi analysis on deshelling efficiency (%), whole kernel recovery (%), broken kernels (%), partially shelled / unshelled nuts (%) and processing time (1000 nuts).

Table 7.14: Significant / insignificant parameters for moisture content percent

	Significant	Contribution	Insignificant
Moisture content percent	Deshelling efficiency	25.77 %	Resistive torque
	Whole kernel recovery	10.25%	
	Partially shelled/unshelled nuts	9.04%	
	Processing time	5.15%	
	Broken kernels	0.76%	

As per Taguchi analysis, moisture content percent contribution is highest in deshelling efficiency (25.77 %), whole kernel recovery (10.25%), partially shelled / unshelled nuts (9.04%), processing time (5.15%) and broken kernels (0.76%). Moisture content percent contribution in case of resistive torque is found as insignificant as compared to other factors.

7.4.3. Effect of clearance on the output parameters:

On the basis of performed experimentations and Taguchi analysis as given in chapter 4, clearance is plays more crucial role in the process of Charoli nut deshelling. Clearance effects significantly as per experimentations and Taguchi analysis on deshelling efficiency (%), whole kernel recovery (%), broken kernels (%), and processing time (1000 nuts).

Table 7.15: Significant / insignificant parameters for clearance

	Significant	Contribution	Insignificant
Clearance	Partially shelled/unshelled nuts	86.97%	Resistive torque
	Deshelling efficiency	40.87%	
	Whole kernel recovery	16.05%	
	Broken kernels	1.27 %	
	Processing time	1.52 %	

As per Taguchi analysis, clearance contribution is highest in partially shelled / unshelled nuts (86.97%) followed by deshelling efficiency (40.87%), whole kernel recovery (16.05%), broken kernels (1.27 %), and processing time (1.52 %). Clearance

contribution in case resistive torque is found as insignificant as compared to other factors.

7.4.4. Effect of thickness of the grinding disk on the output parameters

On the basis of performed experimentations and Taguchi analysis as given in chapter 4, thickness of the grinding disk is not found too much significant in the process of Charoli nut deshelling.

Table 7.16: Significant / insignificant parameters for thickness of the grinding disk

	Significant	Contribution	Insignificant
Clearance	NIL	N.A	Deshelling efficiency
			Whole kernel recovery
			Broken kernels
			Partially shelled / unshelled nuts
			Resistive torque
			Processing time

Thickness of the grinding disk effects on the contribution as per experimentations and Taguchi analysis on deshelling efficiency (0.05%), whole kernel recovery (0.05%), broken kernels (0%), partially shelled / unshelled nuts (0.78%) and resistive torque (5.04%) and processing time (0.21%).

7.4.5. Effect of rotational speed of the flywheel on the output parameters

On the basis of performed experimentations and Taguchi analysis as given in chapter 4, rotational speed of the flywheel is plays more crucial role in the process of Charoli nut deshelling. Rotational speed of the flywheel effects significantly as per experimentations and Taguchi analysis on deshelling efficiency (%), whole kernel recovery (%), broken kernels (%), and processing time (1000 nuts).

Table 7.17: Significant / insignificant parameters for rotational speed of the flywheel

	Significant	Contribution	Insignificant
Rotational speed of the flywheel	Broken kernels	96.89%	Deshelling efficiency
			Partially shelled/unshelled nuts
	Whole kernel recovery	60.29%	Resistive torque
			Processing time

As per Taguchi analysis, rotational speed of the flywheel contribution is highest in broken kernels (96.89%) followed by whole kernel recovery (60.29%). Rotational speed of the flywheel contribution in case of deshelling efficiency, partially shelled / unshelled nuts (%), resistive torque and processing time is found as insignificant as compared to other factors.

7.5 CONFIRMATION OF EXPERIMENTS

The confirmation of experimentation is the final stage in any investigation for validating the results of the previous round of experimentation, especially when the optimal set of variables and levels wasn't included in the experimental plan. The optimal settings for the significant variables are determined, and a predetermined number of experiments are conducted under the given constraints. The results of the confirmation trials are done and compared to the expected predicted mathematical equation based model on the factors and levels investigated.

7.5.1 Result of confirmation of experiments (Taguchi method)

The confirmation experiment is an important step that is highly suggested in order to validate the experimental findings. The purpose of the confirmation experiment is to verify the conclusion made during the analysis phase. The deshelling efficiency, whole kernel recovery, broken kernels, partially shelled / unshelled nuts, resistive torque and processing time of the specified experiments was projected jointly within the 95 percent prediction interval using the software's point prediction capabilities. Six confirmation tests were carried out in order to validate the appropriateness of the developed model (Table 7.18). The confirmation experiments are performed by considering the optimum set of parameters and levels setting A_1, B_2, C_1, D_3, E_1;

A_1,B_2,C_1,D_3,E_3; A_3,B_3,C_3,D_1,E_3; A_2,B_1,C_1,D_3,E_3; A_2,B_1,C_1,D_2,E_2; and A_3,B_1,C_3,D_1,E_1 to predict the deshelling efficiency, whole kernel recovery, broken kernels, partially shelled / unshelled nuts, resistive torque and processing time. The previously constructed model is used to forecast the values and the related prediction interval. The anticipated and actual experimental values were compared, and the residual and percentage error were computed as shown in Table 7.18.

Table 7.18: Confirmation of experiments using the Taguchi method

Expt no. / Factors	A	B	C	D	E	Actual	Predicted	Residual	Error
	(ψ) (kg/hr)	(M_c) (% d.b)	(C_d) (mm)	(t) (mm)	(V_f) (rpm)				
1. for (η_d)	15	13	6	32	400	86.2	82.90	3.30	3.83%
2. for (η_w)	15	13	6	32	600	73.5	70.48	3.02	4.11%
3. for (η_b)	25	17	10	19	600	10.3	10.76	0.46	4.43%
4. for (η_u)	20	9	6	32	600	11.10	10.89	0.21	1.86%
5. for (Γ_r)	20	9	6	25	500	109582.74	114519.00	4937.74	4.13%
6. for (T_p)	25	9	10	19	400	49	51.00	2.00	3.76%

Where, (η_d) = Deshelling efficiency, (η_w) = Whole kernel recovery, (η_b) = Broken kernels, (η_u) = Partially Shelled / Unshelled nuts, (Γ_r) = Resistive Torque, and (T_p) = Processing time (1000 nuts),

Percentage error range for the response variable varied from 1.86 to 4.13 percent between the actual and projected value. The percentage error were obtained for deshelling efficiency (3.83%), whole kernel recovery (4.11%), broken kernels (4.43%), partially shelled / unshelled nuts (1.86%), resistive torque (4.13%), and processing time (3.76%). The empirical models created were pretty accurate, it may be stated. The confirmation run's actual results are all within the 95 percent prediction interval. The 95 percent prediction interval is the range of values into which may anticipate any specific number to fall 95% of the time.

7.5.2 Result of confirmation of experiments (TOPSIS)

The confirmation test for the optimal parameter setting with a selected level was conducted to evaluate the quality characteristics. From experiment run (Table 7.19)

shows the lowest closeness coefficient, indicating the optimal process parameter set up of A_1, B_1, C_1, D_1, E_1 has the best multiple performance characteristics among the 27 experiments, which can be compared with results of confirmation experiments for validation of results by using Taguchi TOPSIS.

Table 7.19: Confirmation of experiments (TOPSIS)

Sr. No	Response Charecteristics	Optimal Parameter Combination	Actual	Predicted	Residual	Error
1	Deshelling efficiency (η_d)		84.00	84.07	0.07	0.09
2	Whole kernel recovery (η_w)	A_1,	65.50	65.13	0.37	0.57
3	Broken kernels (η_b)	B_1,	18.50	18.94	0.44	2.39
4	Partially shelled / unshelled nuts (η_u)	C_1, D_1,	16.00	15.23	0.77	4.81
5	Resistive Torque (T_r)	E_1	96364.49	103693	7328.51	7.60
6	Processing time (T_p)		74.00	75.56	1.56	2.11

Percentage error range for the response variable varied from 0.09 to 7.60 percent between the actual and projected value. The percentage error were obtained for deshelling efficiency (0.09%), whole kernel recovery (0.57%), broken kernels (2.39%), partially shelled / unshelled nuts (4.81%), resistive torque (7.60%), and processing time (2.11%). The empirical models created were pretty accurate, it may be stated. The confirmation run's actual results are all within the 95 percent prediction interval. The 95 percent prediction interval is the range of values into which may anticipate any specific number to fall 95% of the time.

7.6 COST ECONOMICS OF CONVENTIONAL AND DEVELOPED CHAROLI NUT DESHELLER

Table 7.20 shows the comparison between the cost economics of conventional and developed charoli nut desheller

Particulars	Conventional method	Developed Charoli Desheller		
Machine Capacity /Chakki (kg/h)	1.80	15	20	25
Raw Charoli consumption/ day (kg)	14.4	120	160	200
Output of kernels (kg/h)	0.6	5.00	6.66	8.33
Whole kernel recover (Output x Avg. WKR) (kg/h)	0.198	3.2	4.26	5.33
Production/hour	Rs. 198	Rs. 3,200	Rs. 4,260	Rs. 5,330
Production/day (8 hours)	Rs. 1,584	Rs. 25,600	Rs. 34,080	Rs. 42, 460
Labour required	1	2	2	2
Labour charges	Rs. 500	Rs. 1000	Rs. 1000	Rs. 1000
Cost of Raw Charoli	Rs. 432	Rs. 3,600	Rs. 4,800	Rs. 6,000
Net Income/day	Rs. 652	Rs. 21,000	Rs. 28,280	Rs. 35, 460

Comparison between the cost economics of conventional and developed charoli nut desheller clearly shows the developed Charoli nut desheller have capacity to increase the income of the tribal/ rural people from Rs. 652 to Rs. 21,000, Rs. 28,280 or Rs. 35, 460 per day. This will be the motivating factor to tribal/ rural people to shift towards the mechanization rather than the conventional charoli nut deshelling method.

CHAPTER - 8
CONCLUSIONS AND FUTURE SCOPE

8.1 Conclusions

The machine for the deshelling of Charoli nut has been developed and tested successfully. The developed data will provide the optimised scheme of parameters so that deshelling efficiency and whole kernel recovery can be increased. The current machine is vigorous in structure and can be controlled by semi-skilled/skilled/unskilled personnel. The machine has provided with two circular adjustable disk, so, this machine can simply process any size Charoli nut. Because Charoli nuts are in great demand in the market, this machine is especially beneficial in rural and tribal regions. So, with the assistance of a constructed machine, tribal/rural/low-profiled individuals can establish their own Charoli deshelling firm and can send final product direct to the market. This machine will increase employment and livelihood opportunities for rural/tribal peoples by allowing them to become entrepreneurs. Since this machine is operating by human powered flywheel motor (HPFM), it does not need electricity to operate, this machine is really helpful in remote places in which there is no access to electricity. and where there are tremendous problems of availability of electricity viz. load shading. Some other conclusions which can be made from the present study is given below,

1. A machine for deshelling Charoli nuts has successfully built and tested that may be operated by semi-skilled, skilled, or unskilled workers. Tribal/rural/low-profiled peoples can start their own Charoli deshelling business and sell the finished product directly to the market which will empower rural/tribal people to become entrepreneurs, increasing job and income options.

2. The optimum set of variable values, economic health and acceptability, and cheap cost of manufacturing will facilitate rural and tribal persons in establishing small-scale industries.

3. The data in this study was gathered through various experiments. As a result, the current study has clearly reflects the degree of interaction of numerous independent

factors. This is only feasible because of the method used in this research. The percentage error of estimate for the anticipated / calculated values of the dependent parameters is considered to be significantly low. This gives authenticity to the developed mathematical models and ANN.

4. The patterns for the performance of the models shown by graphs, effect assessment, and Taguchi analysis were discovered to be complimentary. These tendencies have been shown to be genuinely warranted by certain conceivable phenomena physics.

5. The dependent term values acquired from experiment results, mathematical model, and ANN are analyzed. Based on the percent error data, it has been determined that the mathematical models may be effectively employed to compute dependent terms for a specified set of independent terms. The data may be used by Indian companies to calculate responses and estimate the power of a human-driven Charoli nut deshelling machine powered by HPFM.

6. At the most of the places Charoli nuts are deshelled with the help of hammer and stones, however, the current machine powered by HPFM can be driven by legs, which have been shown to be superior than arm muscles in terms of power and energy needs, the processing time of operation and the deshelling efficiency in the less operating time.

7. The maximum deshelling efficiency upto 84 % is obtained by experimentation. Clearance is the most influencing parameter with contribution of 40.87 %, feed rate with contribution of 30.23 %, and moisture content percent with contribution of 25.77 %. These three parameters have highly significant impact on deshelling efficiency both physically and statistically. Therefore, for maximum efficiency, more attention needs to be focused on clearance followed by feed rate and moisture content percent.

8. The maximum whole kernel recovery upto 71 % is obtained by experimentation. Rotational speed of the flywheel with contribution of 60.29 % is the most influencing parameter for deshelling efficiency, followed by clearance with contribution of 16.05 %, feed rate with contribution of 11.91 %, and moisture content percent with contribution of 10.25 % are the significantly affecting the whole kernel recovery.

Among these factors effect of rotational speed of the flywheel followed by clearance, feed rate and moisture content percent are highly significant both physically and statistically. Therefore, for maximum whole kernel recovery, more attention needs to be focused on rotational speed of the flywheel followed by clearance, feed rate and moisture content percent.

9. Minimal broken kernels values of 10.3 % is obtained for experimentation. Rotational speed of the flywheel (PC=96.89 %) is the highly significant parameter followed by clearance (PC=1.27 %), feed rate (PC=0.93%), and moisture content percent (PC=0.76%). Therefore, for reducing the broken kernels, more attention needs to be focused on rotational speed of the flywheel followed by clearance, feed rate and moisture content percent.

10. The minimum partially shelled / unshelled nuts of 10.8 % are obtained by experimentation. Clearance with contribution of 86.97 %, and moisture content percent with contribution of 9.04 % is the significantly affecting parameters on the partially shelled / unshelled nuts. Among these factors effect of clearance followed by moisture content percent are highly significant both physically and statistically. Therefore, for minimum partially shelled / unshelled nuts, more attention needs to be focused on clearance followed moisture content percent.

11. Minimum resistive torque of 95916 N-mm is experienced by experimentation. From the Taguchi analysis, it is noted that none of the input variable found significant or significantly affecting the resistive torque. This may be due to the extraneous variable like vibrations in the machines which have not considered as a variable for the study.

12. Minimum processing time of 53 seconds is obtained by experimentation. Feed rate (PC=91.89 %), moisture content percent (PC=5.15 %) and clearance (PC=1.52 %) are the significantly affecting the processing time. Among these factors effect of feed rate followed by moisture content percent and clearance are highly significant both physically and statistically. Therefore, for minimum processing time, more attention needs to be focused on feed rate followed by moisture content percent and clearance.

13. Feed rate contribution is highest in processing time (91.89%) followed by deshelling efficiency (30.23%), whole kernel recovery (11.91%), and broken kernels (0.93%). Feed rate contribution in case of partially shelled / unshelled nuts (%) and resistive torque is found as insignificant as compared to other factors

14. Moisture content percent contribution is highest in deshelling efficiency (25.77%), whole kernel recovery (10.25%), partially shelled / unshelled nuts (9.04%), processing time (5.15%) and broken kernels (0.76%). Moisture content percent contribution in case of resistive torque is found as insignificant as compared to other factors.

15. Clearance contribution is highest in partially shelled / unshelled nuts (86.97%) followed by deshelling efficiency (40.87%), whole kernel recovery (16.05%), broken kernels (1.27 %), and processing time (1.52 %).

16. Thickness of the grinding disk is not found too much significant in the process of Charoli nut deshelling.

17. Rotational speed of the flywheel contribution is highest in broken kernels (96.89%) followed by whole kernel recovery (60.29%).

18. Recommended optimum set of parameters and levels setting as per SN ratio plot for maximum deshelling efficiency is at A_1,B_2,C_1,D_3,E_1 i.e. at feed rate 15 kg/hr, moisture content 13 % d.b., clearance 6 mm, thickness of the grinding disk 32 mm and rotational speed of the flywheel 400 rpm. Deshelling efficiency obtained at this optimum set of parameters and levels 86.2% with percentage error of 3.83% between actual and predicted value.

19. Recommended optimum set of parameters and levels setting as per SN ratio plot for maximum whole kernel recovery is at A_1,B_2,C_1,D_3,E_3 i.e. at feed rate 15 kg/hr, moisture content 13 % d.b., clearance 6 mm, thickness of the grinding disk 32 mm and rotational speed of the flywheel 600 rpm. Whole kernel recovery obtained at this optimum set of parameters and levels 73.5% with percentage error of 4.11% between actual and predicted value.

20. Recommended optimum set of parameters and levels setting as per SN ratio plot for lowest broken kernels is at A_3,B_3,C_3,D_1,E_3 i.e. at feed rate 25 kg/hr, moisture content 17% d.b., clearance 10 mm, thickness of the grinding disk 19 mm and rotational speed of the flywheel 600 rpm. Broken kernels obtained at this optimum set of parameters and levels 10.3% with percentage error of 4.43% between actual and predicted value.

21. Recommended optimum set of parameters and levels setting as per SN ratio plot for lowest percentage of partially shelled/unshelled nuts is at A_2,B_1,C_1,D_3,E_3 i.e. at feed rate 20 kg/hr, moisture content 9 % d.b., clearance 6 mm, thickness of the grinding disk 32 mm and rotational speed of the flywheel 600 rpm. Partially shelled/unshelled nuts obtained at this optimum set of parameters and levels 11.10% with percentage error of 1.86 % between actual and predicted value.

22. Recommended optimum set of parameters and levels setting as per SN ratio plot for lowest resistive torque is at A_1,B_2,C_1,D_3,E_1 i.e. at feed rate 15 kg/hr, moisture content 13 % d.b., clearance 6 mm, thickness of the grinding disk 32 mm and rotational speed of the flywheel 400 rpm. Lowest resistive torque obtained at this optimum set of parameters and levels 119456.74 N-mm with percentage error of 4.13 % between actual and predicted value.

23. Recommended optimum set of parameters and levels setting as per SN ratio plot for lowest processing time is at A_1,B_2,C_1,D_3,E_1 i.e. at feed rate 15 kg/hr, moisture content 13 % d.b., clearance 6 mm, thickness of the grinding disk 32 mm and rotational speed of the flywheel 400 rpm. Lowest processing time obtained at this optimum set of parameters and levels 53 seconds with percentage error of 3.76 % between actual and predicted value.

24. Recommended optimum set of parameters and levels setting as per TOPSIS for higher deshelling efficiency, higher whole kernel recovery, minimum broken kernels, minimum percentage of partially shelled/unshelled nuts, minimum resistive torque and minimum processing time is at A_1, B_1, C_1, D_1, E_1 i.e. at feed rate 15 kg/hr, moisture content 9 % d.b., clearance 6 mm, thickness of the grinding disk 19 mm and

rotational speed of the flywheel 400 rpm. The recorded output is 84.00%, 65.50%, 18.50%, 16.00%, 96364.49 N-mm and 74 seconds for deshelling efficiency, whole kernel recovery, broken kernels, percentage of partially shelled/unshelled nuts, resistive torque and processing time respectively.

8.2 Limitations and Future scope

During the process of research work and exhaustive study of literature, few thrust areas are identified for possible future development to be treated as future scope. The proposals for the future work are listed below:

1. Only the Charoli nut, which has a hard shell, can be successfully deshelled with the help of the suggested study activity. The scope of the study might be expanded to include the development of a generalised machine that is capable of deshelling tough nuts such as almonds, walnuts, cashews, and charoli simultaneously.

2. In current work only one type of the disk was utililised for the deshelling of the nut. Morever, few other types of disk like wooden disk, metallic plate disk and casted disk may be used to find out the impact on the output parameters.

3. In current work only plane surface disks was utililised for the deshelling of the nut. Morever, disks having varying angle can also be used to find out the impact on the output parameters.

4. Current Charoli desheller is operated human powered and have limitations of 25 kg/hr, hence for the more output, motorized Charoli desheller can be made to compare the performance with the present machine.

5. In the work that has been done thus far, just an analysis of machine performance has been carried out, but machine vibrations have not been taken into account. Including machine vibrations in the work process allows for more work to be done.

6. It is important to do research on the resistance of kernels to shear and compressive forces. This is due to the fact that many types of hard shell nuts each have their own

unique set of physical traits and properties. Additionally, the breaking properties of Charoli nuts are distinct from one another, and it is to be anticipated that the kernels' physical qualities will likewise be distinct from one another.

7. The fact that the Charoli nut desheller may also be used for deshelling charoli nuts is one of the many benefits offered by this tool. It is possible to significantly cut down on both time and labour by making use of the labour cost for deshelling. As a result, it is strongly suggested that the performance be assessed on a continuing basis in order to make progress.

8. In spite of the fact that tribal and rural peoples might increase their revenue by deshelling charoli nuts, there is a possibility that doing so for the purpose of direct sale would create difficulties for tribal and rural peoples' marketing efforts. This is due to the fact that purchasers may have a tendency to provide lower prices to individual farmers when the farmers are selling modest quantities of Charoli nuts as opposed to doing so via cooperatives.

Bibliography

[1] Bhatnagar, P. and Bhausar, K.N. 1988. Economic Potential of Buchnanialanzan in Madhya Pradesh. VanikiSandesh, 12(4): 16- 20.

[2] Hiwale, S. (2015). Chironji (Buchanania lanzan Spreng.). In Sustainable Horticulture in Semiarid Dry Lands (pp. 247–253). Springer, New Delhi. https://doi.org/10.1007/978–81–322–2244–6_17

[3] Singh D, Nath K, Sharma YK (2007) Response of wheat seed germination and seedling growth under copper stress. J Environ Biol 28:409–414

[4] Ansari MKA, Oztetik E, Ahmad A, Umar S, Iqbal M, Owens G (2013) Identification of the phytoremediation potential of Indian mustard genotypes for copper, evaluated from a hydroponic experiment. Clean: Soil Air Water 41:789–796

[5] Brun LA, Maillet J, Richarte J, Herrmann P, Remy JC (1998) Relationships between extractable copper, soil properties and copper uptake by wild plants in vineyard soils. Environ Pollut 102:151–161

[6] Oommachan M, Masih SK, Shrivastava JL (1989): Ethnobotanical studies in certain forest areas of Madhya Pradesh. Trop Forestry 5: 182–196.

[7] Pradhan RC, Naik SN, Bhatnagar N, Vijay VK. Moisture-dependent physical properties of jatropha fruit. Indus Crops Prod 2009;29:341–7

[8] Chauhan PS et al. Chirongi: a promising tree fruits of dry subtropics. Hort Flora Res Spectrum 2012; 1(3):375-379.

[9] Shelare, S. D., Kumar, R., & Khope P. B. (2021). ASSESSMENT OF PHYSICAL, FRICTIONAL AND AERODYNAMIC PROPERTIES OF CHAROLI (Buchanania Lanzan Spreng) NUT AS POTENTIALS FOR DEVELOPMENT OF PROCESSING MACHINES. Carpathian Journal of Food Science and Technology, 174–191. doi:10.34302/crpjfst/2021.13.2.16.

[10] Hemavathy, J., & Prabhakar, J. V. (1988). Lipid composition of chironji (Buchanania lanzan) kernel. Journal of Food Composition and Analysis, 1(4), 366–370. doi:10.1016/0889-1575(88)90037-3

[11] Kumar, J., Vengaiah, P. C., Srivastav, P. P., and Bhowmick, P. K. (2012). Chironji nut (Buchananialanzan) processing, present practices and

scope. Indian Journal of Traditional Knowledge, 11(1), 202–204. https://doi.org/10.5935/1806–6690.20150001

[12]   Banerjee A, Jain M (1988) Investigation on BuchananialanzanSpreng, seed oil. Fitoterapia 59:406

[13]   Bhatnagar P, Jain S. Collection, processing and marketing of Buchanania lanzan (Chironji) in Chhindwara District. Vaniki Sandesh. 2002; 26(3):11-15.

[14]   Sharma A. Scientific harvesting for quality seed collection of Buchanania lanzan Spreng. For its conservation and sustainable management-case study of Chhindwara, Madhya Pradesh, India. Int J Bio-Sci Bio-Technol. 2012; 4(1):65-74.

[15]   Singh Jagdish, Banerjee SK, Francis Alfred. Vegetaive propagation of Buchanania lanzan Spreng. Root cuttings. Indian Forester. 2002; 128(6):700-704.

[16]   Shende, S. and Rai, M. 2005. Multiple shoot formation and plant regeneration of a commercially-useful tropical plant, Buchanania lanzan (Spreng). Plant Biotechnology, 22(1): 59–61.

[17]   Prasad, S. (2020). Chironji (Buchanania lanzan): A Retreating Valuable Resource of Central India. International Journal of Bioresource Science, 7(1). doi:10.30954/2347-9655.01.2020.1

[18]   Das, D. and Agrawal, V.S. 1991. "Fruits drug plants of India", Kalyani Publishers, New Delhi, pp. 250.

[19]   Zeven, A.C., and de Wet, J.M.J. (1982). Dictionary of Cultivated Plants and Their Regions of Diversity: Excluding Most Ornamentals, Forest Trees and Lower Plants (Wageningen, The Netherlands: Centre for Agricultural Publishing and Documentation (Pudoc)), pp.263.

[20]   Zhang, J.-L., Zhu, J.-J., and Cao, K.-F. (2007). Seasonal variation in photosynthesis in six woody species with different leaf phenology in a valley savannain southwestern China. Trees (Berl.) 21 (6), 631–643 https://doi.org/10.1007/s00468-007-0156-9.

[21]   Singh, S., Singh, A.K., Joshi, H.K., Kanak, L., Sisodia, P.S., and Bagle, B.G. (2010). Floral biology studies in Bhuchanania under semi-arid ecosystem of western India. Indian J. Hortic. 67 (2), 161–168.

[22]   Patel K, Sarnaik D, Asati B, Tirkey T. 2004. Studies on variability, heritability and genetic advance in brinjal (Solanum melongena L.). Agric Sci Digest. 24: 256-259.

[23]   Mehta SK, Mukherjee S, Jaiprakash B. Preliminary phytochemical investigation on leaves of Buchanania lanzan (Chironji). Int J Pharm Sci Rev Res 2010;3(2):55-9.

[24]   Patsnaik AK, Kodati D, Pareta SK, Patra KC, Harwansh RK. Analgesic and anti-inflammatory activities of Buchanania lanzan Spreg. roots. Res J Pharm Biol Chem Sci 2011;2(1):419-25.

[25]   Livelihood Manual Integrated Watershed Management Programme (IWMP) (2012), Gujarat State Watershed Management Agency Commission rate of Rural Development Government of Gujarat. https://ruraldev.gujarat.gov.in/writereaddata/images/pdf/gswma/manuals/livelihood-manual-draft-3.pdf

[26]   Bandyopadhyay, A., &Banerjee, S. (2014). Buchanania lanzan spreng: A veritable storehouse of phytomedicine. Asian Journal Pharm Clinical Research, 8, 18–22.

[27]   Kumar, J., Prabhakar, P.K., Srivastav, P.P., & Bhowmick, P.K. (2016). Moisture Dependent Physical Properties of Chironji (BuchananiaLanzan)Nut. Journal of Agricultural Engineering, 53, 45-54.

[28]   Deshmukh, Shilpa D., Mohini M. Dange, I. L. Pardeshi, and P. A. Borkar. 2017. "Physical Properties of Chironji Nut (Buchanania Lanzan L .) as Potential for Development of Processing Machines." 04(01):6–10.

[29]   Ghafari, A., G. R. Chegini, J. Khazaei, and K. Vahdati. 2011. Design , Construction and Performance Evaluation of the Walnut Cracking Machine. International Journal of Nuts and Related Sciences, 2 (1): 11–16.

[30]   Khope, P. B., A. Meshram. 2017. Literature Review on Design & Development of Portable Charoli Desheller. International Journal for Scientific Research & Development. 5 (05): 433–34

[31]   Singh, Ranjan Kumar, Joydip Mandal, and Bikash Das. 2018. "Study on Present Practices of Chironji Nut (Buchanania Lanzan) Processing in Chotanagpur Plateau Region." (7):4680–84.

[32]   Oluwole, F. A., M. B. Oumarou, and G. M. Ngala. 2016. Dynamics of Centrifugal Impact Nut Cracker. International Journal of Research Studies in Science, Engineering and Technology. 3 (1): 15–21

[33]   Chavoshgoli, Es., Sh. Abdollahpour, and H. Ghasemzadeh. 2019. Designing, fabrication and evaluation of threshing unit edible sunflower. Agricultural Engineering International: CIGR Journal, 21(2): 52–58.

[34]   Manjunath, B. A., K. S. Ahmed, and L. K. Sreepathi. 2016. Design and Fabrication of Pongamia Pinnata Decorticator. Journal of Mechanical Engineering   and   Automation.   6   (5):   1–7. https://doi.org/10.5923/c.jmea.201601.01.

[35]   Pandey, M., 2006. Present Status and Future Requirement of Farm Equipment for Crop Production. Status of Farm Mechanization nn India. 95: 69–113.

[36]   Karthickumar, P., N. K. Pandian, P. Rajkumar, A. Surendrakumar, and M. Balakrishnan. 2015. Development and evaluation of a continuous type tamarind deseeder. Agricultural Engineering. 2: 49-59.

[37]   Adewumi, B. A., and A B. Fatusin. 2006. Design, Fabrication and Testing of an Impact-Type Hand Operated Cocoa Pod Breaker. Agricultural Engineering International: CIGR Journal,VIII: 1–12.

[38]   Kumar, C.S., R. C. Pradhan, and S. Mishra. 2017. Fabrication, Performance Evaluation and Optimization of Sal (Shorea Robusta) Seed Decorticator. Journal of Food Process Engineering 40 (3): 1–10. https://doi.org/10.1111/jfpe.12468.

[39]   Lim, B. Y., R. Shamsudin, B. T. Hang, T. Baharudin, and R. Yunus. 2014. The Performance of a Jatropha Fruit Shelling Machine and the Future Improvement. Universal Journal of Applied Science 2 (7): 233–36. https://doi.org/10.13189/ujas.2014.020703.

[40]   Galedar, M. N., S. S. Mohtasebi, A. Tabatabaeefar, A. Jafari, and H. Fadaei. 2009. "Mechanical Behavior of Pistachio Nut and Its Kernel under

Compression Loading." Journal of Food Engineering 95 (3): 499–504. https://doi.org/10.1016/j.jfoodeng.2009.06.009

[41]   Ojolo, S., A. Ogundare, A. Adesina, and O. Ibhadode. 2018. Development of almond seed extractor for whole kernel recovery. Agricultural Engineering International: CIGR Journal, 20(4): 195–201

[42]   Nwakuba, N. R., P. K. Ejesu, and V. C. Okafor. 2017. A mathematical model for predicting the drying rate of cocoa bean (Theobroma cacao L.) in a hot air dryer. Agricultural Engineering International: CIGR Journal, 19(3): 195–202.

[43]   Lim, B. Y., R. Shamsudin, B. T. Hang, T. Baharudin, and R. Yunus. 2014. The Performance of a Jatropha Fruit Shelling Machine and the Future Improvement. Universal Journal of Applied Science 2 (7): 233–36. https://doi.org/10.13189/ujas.2014.020703.

[44]   Kilanko, O., S. J. Ojolo, A. O. Inegbenebor, T. A. Ilori, R. O. Leramo, P. O. Babalola, and S. O. Oyedepo. 2018. Design and Performance Evaluation of Centrifugal Cashew Nut Sheller for Improving the Whole Kernel Recovery. Agricultural Engineering International: CIGR Journal 20 (1): 162–70.

[45]   Sharma, R., D. S. Sogi, and D. C. Saxena. 2009. Dehulling Performance and Textural Characteristics of Unshelled and Shelled Sunflower (Helianthus Annuus L.) Seeds. Journal of Food Engineering 92 (1): 1–7. https://doi.org/10.1016/j.jfoodeng.2008.10.013.

[46]   Antia, O. O., W. Olosunde, and A. Offiong. 2014. Determination of Optimum Moisture Content of Palm Nut Cracking for Efficient Production of Whole Kernel. Nigerian Journal of Technological Development, 11 (2): 27–30

[47]   Jekayinfa, S. O., and A. I. Bamgboye. 2006. Estimating Energy Requirement in Cashew (Anacardium Occidentale L.) Nut Processing Operations. Energy 31 (8–9): 1305–1320. https://doi.org/10.1016/j.energy.2005.07.001.

[48]   Maghsoudi, H., M. H. Khoshtaghaza, and S. Minaei. 2010. Selected Geometric Characteristics, Density, and Mechanical Properties of Unsplit Pistachio Nut. International Journal of Food Properties 13 (2): 394–403. https://doi.org/10.1080/10942910802571745

[49]   Romuli, S., S. Karaj, and J. Müller. 2015. Influence of Physical Properties of Jatropha Curcas L. Seeds on Shelling Performance Using a Modified Disc Mill. Industrial Crops and Products 77: 1053–1562. https://doi.org/10.1016/j.indcrop.2015.10.014.

[50]   Oluwole, F. A., M. B. Oumarou, and G. M. Ngala. 2016. Dynamics of Centrifugal Impact Nut Cracker. International Journal of Research Studies in Science, Engineering and Technology. 3 (1): 15–21.

[51]   Olaoye, J. O., and O. B. Aturu. 2018. Effect of Seed Variety, Operating Speed and Moisture Content on the Shelling Efficiency of a Mechanized Centrifugal Melon Shelling and Cleaning Machine. ASABE Annual International Meeting,: 1–9. https://doi.org/10.13031/aim.201800093.

[52]   Jahanbakhshi, A., B. Ghamari, and K. Heidarbeigi. 2016.   Effect of engine rotation speed and gear ratio on the acoustic emission of John   Deere   1055I   combine   harvester. Agricultural   Engineering International: CIGR Journal, 18(3):106-112

[53]   Srivastava, A. K., E. G. Carroll, P. R. Roger, and D. R. Buckmaster. 2006. Machinery Selection and Management. Machinery Selection and Management. Chapter 15 in Engineering Principles of Agricultural Machines, 2nd Ed., 525-552. St. Joseph, Michigan: ASABE. 10 (1930): 525.

[54]   Hasantabar Amiji, S., S. R. Mousavi Seyedi, D. Kalantari. 2019. Design, construction and evaluation of a seed pod husker and testing with soybean and mung bean. Agricultural Engineering International: CIGR Journal, 21(1): 90–99.

[55]   Tang, G. P., T. Liang, and F. Munchmeyer. 1982. A Variable Deformation Macadamia Nut Cracker. Transactions of the ASAE. 25 (6): 1506–11. https://doi.org/10.13031/2013.33755.

[56]   Fadele, O. K., and A. K. Aremu. 2018. Optimization of Shelling Efficiency of a Moringa Oleifera Seed Shelling Machine Based on Seed Sizes. Industrial   Crops   and   Products   112:   775–82. https://doi.org/10.1016/j.indcrop.2018.01.011.

[57]   Pradhan, R. C., V. Meda, S. N. Naik, and L. Tabil. 2010. Physical Properties of Canadian Grown Flaxseed in Relation to Its Processing.

International Journal of Food Properties, 13:4, 732-743. https://doi.org/10.1080/10942910902818137.

[58]   Ikubanni, P.P., C.A. Komolafe, O.O. Agboola, and C.O. Osueke. 2017. Moringa Seed Dehulling Machine: A New Conceptual Design. Journal of Production Engineering. 20: 2–7. http://doi.org/10.24867/JPE-2017-02-073.

[59]   Too, D. and G. E. Landwer. 2003. "Factors Affecting Performance in Human Powered Vehicles: A Biomechanical Model." Human Power (54):14–16.

[60]   Pradhan, Rama Chandra, Venkatesh Meda, Satya Narayan Naik, and Lope Tabil. 2010. "Physical Properties of Canadian Grown Flaxseed in Relation to Its Processing." International Journal of Food Properties 13(4):732–43

[61]   Singh, S. P. and Pratap Singh. 2010. "Hand Operated Maize Dehusker-Sheller for Farm Women." Agric Engg Today 34(June 2012):152–54.

[62]   Ojolo, S. J., O. Damisa, J. I. Orisaleye, and C. Ogbonnaya. 2010. "Design and Development of Cashew Nut Shelling Machine." Journal of Engineering, Design and Technology 8(2):146–57

[63]   JOSHUA OLANREWAJU OLAOYE, TIMOTHY ADESOYE ADEKANYE. 2018. "Properties Influencing Cracking and Separation of Palm Nuts in a Mechanical Cracker Cum Separator." Croatian Journal of Food Science and Technology 10(1):42–50.

[64]   Chengmao, Cao, Sun Si, Ding Ran, Li Bing, and Wang Shuo. 2017. "Experimental Study on Mechanical Characteristics of Nut Rupturing under Impact Loading." International Journal of Agricultural and Biological Engineering 10(1):53–60

[65]   Wilson, David Gordon and John Furber. 1986. "UNDERSTANDING PEDAL POWER." Technical Reviewers John Furber Lawrence M. Halls Lauren Howard, VITA, 1–18

[66]   Singh, K. P., I. L. Pardeshi, M. Kumar, K. Srinivas, and A. K. Srivastva. 2008. "Optimisation of Machine Parameters of a Pedal-Operated Paddy Thresher Using RSM." 100:591–600.

[67]   Ajao, Kajogbola R., Kadiri Mustapha, Modupe R. Mahamood, and Muritala O. Iyanda. 2010. "Design and Development of a Pedal-Powered Soap Mixer." 3(1):2–5

[68]   Wu, Jodie. 2009. "Bicycle-Powered Attachments: Designing for Developing Countries" Massachusetts Institute of Technology, : 3-35

[69]   Zakiuddin, K. S. and J. P. Modak. 2010. "Formulation of Data Based Ann Model for the Human Powered Fodder - Chopper." Journal of Theoretical and Applied Information Technology 15(2):79–85.

[70]   Tiwari, P. S., L. P. Gite, M. M. Pandey, and A. K. Shrivastava. 2011. "Pedal Power for Occupational Activities: Effect of Power Output and Pedalling Rate on Physiological Responses." International Journal of Industrial Ergonomics 41(3):261–67.

[71]   Hussain, H. A., M. Sohail Pervez, Naushad Alam, and Atul P. Ganorkar. n.d. "Design and Development of Bicycle Integrated Pipe Bending Machine." 2014:24–28.

[72]   Waweru, A. (2016). Design of a Bicycle Peddle Operated Grain Mill. Jomo Kenyatta University of Agriculture and Technology.

[73]   Modak, J. P. and A. R. Bapat. 1994. "Formulation of a Generalized Experimental Model for a Manually Driven Flywheel Motor and Its Optimization." Applied Ergonomics 25(2):119–22

[74]   Modak, J. P. and A. R. Bapat. 1994. "Formulation of a Generalized Experimental Model for a Manually Driven Flywheel Motor and Its Optimization." Applied Ergonomics 25(2):119–22

[75]   Zakiuddin, K. S. and J. P. Modak. 2012. "Post Harvest Crop Processing Machine." Agricultural Engineering International: CIGR Journal 14(3):99–104

[76]   Dhale, A. D. and J. P. Modak. 2012. "Formulation of Experimental Data Based Model for Oil Press Using Human Powered Flywheel Motor as Energy Source." Agricultural Engineering International: CIGR Journal 14(3):218–29

[77]   Zakiuddin, K. S. and J. P. Modak. 2012. "Post Harvest Crop Processing Machine." Agricultural Engineering International: CIGR Journal 14(3):99–104.

[78]   Khope, P. B. and J. P. Modak. 2013. "Establishing empirical relationship to predict the chaff cutting phenomenon energized by human powered flywheel motor (hpfm)." IOSR Journal of Agriculture and Veterinary Science, 3(2), 35–39. doi:10.9790/2380-0323539

[79]   Khope, P. B. and J. P. Modak. 2013. "Development And Performance Evaluation Of A Human Powered Flywheel Motor Operated Forge Cutter." International Journal of Scientific & Technology Research, 2(3), 146-149. doi: 10.1.1.300.7337

[80]   Bhatkulkar, H. S. and J. P. Modak. 2014. "Design & Development of Nursery Fertilizer Mixer Energized by Human Powered Flywheel Motor." (5):69–73.

[81]   Sonkhaskar, Y. M., Swapnil S. Asati, and Abhinav M. Purohit. 2015. "Human Powered Flywheel Motor Driven Process Units : A Review." 10944–49.

[82]   Undirwade, S. K., M. P. Singh, and C. N. Sakhale. 2015. "Experimental Investigation of Processing Time , Number of Slivers and Resistive Torque Required for Human Powered Bamboo Sliver Cutting Operation." 14:33–51.

[83]   Undirwade, S. K., M. P. Singh, and C. N. Sakhale. 2015. "Experimental Investigation of Processing Time, Number of Slivers and Resistive Torque Required for Human Powered Bamboo Sliver Cutting Operation." Journal of Bamboo and Rattan 14(1–4):33–51

[84]   Chandak, Pawan A., Arati Lende, and Jayant Modak. 2018. "Modeling of Human Power Flywheel Motor through Artificial Neural Network- A Novel Approach." Procedia Computer Science 125(2009):77–84

[85]   Undirwade, Siddharth K. 2018. "Development and Optimization of Experimental Data based Models for Bamboo Sliver Cutting by using Human Powered Flywheel Motor." International Journal of Mechanical and Production Engineering Research and Development , 8(1):1007–20

[86]   Oluwole, F. A., A. T. Abdulrahim, and M. B. Oumarou. 2007. "Development and Performance Evaluation of Impact Bambara Groundnut Sheller." Int. Agrophysics 21:269–74

[87]   Atiku, A. A., N. A. Aviara, and M. A. Haque. 2004. "Performance Evaluation of a Bambara Ground Nut Sheller." Agricultural Engineering International VI:1–18.

[88]   Oluwole, F. A., A. T. Abdulrahim, and M. B. Oumarou. 2007. "Development and Performance Evaluation of Impact Bambara Groundnut Sheller." Int. Agrophysics 21:269–74

[89]   Ogunsina, B. S., O. A. Koya, and O. O. Adeosun. 2008. "Deformation and Fracture of Dika Nut (Irvingia Gabonensis) under Uni-Axial Compressive Loading." Energy 249–53.

[90]   Sharifian, Faroogh, Allaeddin Rahmani Didar, and Mohammadali Haddad Derafshi. 2017. "Design of a Walnut Cracking Machine Based on Acquired Mechanical Properties Design of a Walnut Cracking Machine Based on Acquired Mechanical Properties." 10th International Congress on Mechanization and Energy in Agriculture "14-17 October 2008, Antalya-Turkiye: 826-831.

[91]   Jarimopas, Bundit, Suttiporn Niamhom, and Anupun Terdwongworakul. 2009. "Development and Testing of a Husking Machine for Dry Betel Nut (Areca Catechu Linn.)." Biosystems Engineering 102(1):83–89.

[92]   Wesley, B. John, R. Swamy, B. Hari Babu, and T. Yellamanda Reddy. 2010. "MODIFICATION OF GROUNDNUT THRESHER FOR DECORTICATING GROUNDNUT PODS AND CASTOR." 30(1):23–25

[93]   Ojolo, S. J., O. Damisa, J. I. Orisaleye, and C. Ogbonnaya. 2010. "Design and Development of Cashew Nut Shelling Machine." Journal of Engineering, Design and Technology 8(2):146–57

[94]   Ishola, Tajudeen Abiodun, Kayode Carroll Oni, Azmi Yahya, and Mohammed Shu. 2011. "Development and Testing of a Prosopis Africana Pod Thresher." 5(5):759–67

[95]   TING, Richard P., Ed Vidona CASAS, Engelbert K. PERALTA, and Jessie C. ELAURIA. 2012. "Design, Fabrication, and Optimization of Jatropha Sheller." An International Journal of Optimization and Control: Theories & Applications (IJOCTA) 2(2):113–27

[96]   Kumar, T. V. Arun, Lokesh, and T. N. Sandeep. 2012. "Development of Mango Stone Decorticator." International Journal of Agricultural Engineering 5(2):215–19.

[97]   Kareem, I., O. K. Owolarafe, and O. A. Ajayi. 2012. "Development of a Kolanut Peeling Device." Journal of Food Science and Technology 51(10):2769–75.

[98]   Lim, Bo Yuan, Rosnah Shamsudin, B. T. Hang Tuah Baharudin, and Robiah Yunus. 2014. "The Performance of a Jatropha Fruit Shelling Machine and the Future Improvement." 2(7):233–36

[99]   Ojolo, Sunday, Adebayo Ogundare, and Abiola Adegbiji. 2015. "Development of a Variable Size Nut Cracker." (October).

[100]   C. Misra, M. Geller, P. Shah, C. Sioutas, and P. Solomon, "DEVELOPMENT AND EVALUATION OF A CONTINUOUS TYPE TAMARIND DESEEDER," Sci. J. Agric. Eng., vol. 2, no. 2, pp. 49–59, 2001, [Online].   Available: http://www.usc.edu/dept/civil_eng/aerosol/papers/JAWMA51()1309-1317.pdf

[101]   Aremu, A. K., Adeniyi, A. O., & Fadele, O. K. (2015). Development and Performance of a Jatropha Seed Shelling Machine Based on Seed Moisture Content. Journal of Biosystems Engineering, 40(2), 137–144. doi:10.5307/jbe.2015.40.2.137

[102]   Sobowale, S. S., J. A. Adebiyi, and O. A. Adebo. 2016. "Design and Performance Evaluation of a Melon Sheller." Journal of Food Process Engineering 39(6):676–82.

[103]   Anon, 2015. Performance Study of a Jatropha Curcas L. Fruit Shelling Machine for Kernel Recovery in Biodiesel Production. Applied Engineering and Agriculture, pp.755–765. Available at: http://dx.doi.org/10.13031/aea.31.11211.

[104]   Manjunath, B.A., Ahmed, K.S., & Sreepathi, L.K. (2016). Design and Fabrication of Pongamia Pinnata Decorticator. Journal of Mechanical Engineering and Automation, 6, 1-7.

[105]   Pradeep, N. and D. Sasikala. 2016. "Design and Development of Smart Cashew Nut Shelling , Inspection & Grading Machine." Journal of Mechanical Engineering and Automation, 9(4):3142–46

[106]   Ibrahim, M. G., A. A. Shehu, S. M. Dauda, and D. Ahmad. 2016. "Design, Fabrication and Testing of Shea Nut Shelling Machine." International Food Research Journal 23(December):S71–79

[107]   Shashi Kumar, C., Pradhan, R. C., & Mishra, S. (2016). Fabrication, performance evaluation and optimization of Sal (shorea robusta) seed decorticator. Journal of Food Process Engineering, 40(3), e12468. doi:10.1111/jfpe.12468

[108]   Fadele, O. K. and A. K. Aremu. 2016. "Design, Construction and Performance Evaluation of a Moringa Oleifera Seed Shelling Machine." Engineering in Agriculture, Environment and Food 9(3):250–56.

[109]   Math, R. G., G. Ramesh, A. Nagender, and A. Satyanarayana. 2016. "Design and Development of Annatto (Bixa Orellana L.) Seed Separator Machine." Journal of Food Science and Technology 53(1):703–11.

[110]   Chengmao, Cao, Sun Si, Ding Ran, Li Bing, and Wang Shuo. 2017. "Experimental Study on Mechanical Characteristics of Nut Rupturing under Impact Loading." International Journal of Agricultural and Biological Engineering 10(1):53–60

[111]   Ogunsina, B. S., O. A. Koya, and O. O. Adeosun. 2008. "Deformation and Fracture of Dika Nut (Irvingia Gabonensis) under Uni-Axial Compressive Loading." Energy 249–53.

[112]   Adejugbe, I., O. Oyegunwa, D. Iliya, J. Aigbogun, A. Oyelami, and S. Olusunle. 2017. "Design and Development of an Improved Palm Kernel Shelling Machine and Separator." Physical Science International Journal 14(3):1–9.

[113]   Ajav, E. A. and M. A. Mankinde. 2015. "Design, Construction and Performance Evaluation of an Àmàlà Making Machine." Nigerian Food Journal 33(1):73–82.

[114]   Kilanko, O., S. J. Ojolo, A. O. Inegbenebor, T. A. Ilori, R. O. Leramo, P. O. Babalola, S. O. Oyedepo. 2018. Design and performance evaluation of centrifugal cashew nut sheller for improving the whole kernel recovery. Agricultural Engineering International: CIGR Journal, 20(1): 162–170.

[115]   ASAE, 1982. Standard S352. Moisture measurement–grain and seeds. Agricultural Engineers Year Book. ASAE, St. Joseph, MI, p. 345

[116]   Bajpai, A., Kumar, Y., Singh, H., Prabhakar, P. K., and Meghwal, M. (2019). Effect of moisture content on the engineering properties of Jamun (Syzgium cuminii) seed. Journal of Food Process Engineering, (November), 1–8. https://doi.org/10.1111/jfpe.13325

[117]   Galus, S., and Lenart, A. (2019). Optical, mechanical, and moisture sorption properties of whey protein edible films. Journal of Food Process Engineering, 42(6), 1–10. https://doi.org/10.1111/jfpe.13245

[118]   Igbozulike, A. O., and Amamgbo, N. (2019). Effect of Moisture Content on Physical Properties of Fluted Pumpkin Seeds. Journal of Biosystems Engineering, 44(2), 69–76. https://doi.org/10.1007/s42853–019–00015–z

[119]   Kacal, M., and Koyuncu, M. A. (2017). Cracking characteristics and kernel extraction quality of hazelnuts: Effects of compression speed and positions. International Journal of Food Properties, 20(2), 1664–1674. https://doi.org/10.1080/10942912.2017.1352600

[120]   Galedar, M. N., Tabatabaeefar, A., Jafari, A., Sharifi, A., Mohtasebi, S. S., and Fadaei, H. (2010). Moisture dependent geometric and mechanical properties of wild pistachio (Pistacia vera L.) nut and kernel. International Journal of Food Properties, 13(6), 1323–1338. https://doi.org/10.1080/10942910903062099

[121]   Moradi, M., Mousavi Khaneghah, A., Parvaresh, M., and Balanian, H. (2019). Development and validation of mathematical modeling for terminal

velocity of cantaloupe. Journal of Food Process Engineering, 42(3), 1–8. https://doi.org/10.1111/jfpe.13000

[122]   Jahanbakhshi, A., Abbaspour–Gilandeh, Y., Ghamari, B., and Heidarbeigi, K. (2019). Assessment of physical, mechanical, and hydrodynamic properties in reducing postharvest losses of cantaloupe (Cucumis melo var. Cantaloupensis). Journal of Food Process Engineering, 42(5), 1–8. https://doi.org/10.1111/jfpe.13091

[123]   Arjun, S., Girish, G., Nagaraju, V. D., and Sridhar, B. S. (2017). Physico– fracture characteristics of Makhana (Euryale ferox)seeds. International Journal of Food Properties, 20(2), 1204–1209. https://doi.org/10.1080/10942912.2016.1214843

[124]   Malik M.A. and Saini C.S., 2016. Engineering properties of sun– flower seed: Effect of dehulling and moisture content. Cogent Food Agric., 2(1), 1145783, 1–11.

[125]   Pathak, S. S., Pradhan, R. C., & Mishra, S. (2019). Physical characterization and mass modeling of dried Terminalia chebula fruit. Journal of Food Process Engineering, 42(3), e12992. doi:10.1111/jfpe.12992

[126]   Mohsenin, N. N. (1980). Physical properties of plants and animal materials. New York, NY: Gordon and Breach Science Publishers.

[127]   Coskuner, Y., and Karababa, E. (2007). Physical properties of coriander seeds (Coriandrum sativum L.). Journal of Food Engineering, 80, 408–416. https://doi.org/10.1016/j.jfoodeng.2006.02.042

[128]   Singh, S. S., Abdullah, S., Pradhan, R. C., and Mishra, S. (2019). Physical, chemical, textural, and thermal properties of cashew apple fruit. Journal of Food Process Engineering, 42(5), 1–10. https://doi.org/10.1111/jfpe.13094

[129]   Garnayak, D. K., Pradhan, R. C., Naik, S. N., and Bhatnagar, N. (2008). Mois– ture–dependent physical properties of Jatropha seed (Jatropha curcas L.). Industrial Crops and Products, 27(1), 123–129. https://doi.org/10.1016/j.indcrop.2007.09.001

[130]   Izli N., Unal H., and Sincik M., (2009). Physical and mechanical properties of rapeseed at different moisture content. Int. Agrophys., 23, 137–145

[131]   Sacilik, K., Öztürk, R., and Keskin, R. (2003). Some physical properties of hemp seed. Biosystems Engineering, 86(2), 191–198. https://doi.org/ 10.1016/S1537–5110(03)00130–2

[132]   Ghosh, P., Pradhan, R. C., Mishra, S., Patel, A. S., and Kar, A. (2017). Physico– chemical and nutritional characterization of Jamun (Syzygium cuminii). Current Research in Nutrition and Food Science Journal, 5(1), 25–35. https://doi.org/10.12944/CRNFSJ.5.1.04

[133]   Pradhan, R. C., Naik, S. N., Bhatnagar, N., and Swain, S. K. (2008). Moisture– dependent physical properties of Karanja (Pongamia pinnata) kernel. Industrial Crops and Products, 28(2), 155–161. https://doi.org/10. 1016/j.indcrop.2008.02.006

[134]   Kashaninejad, M; Mortazavi, A; Safekordi, A; Tabil, L.G. (2005). Some physical properties of pistachio (Pistacia vera L.) nut and its kernel. Journal of Food Engineering, 72 (1), 30–38.

[135]   Mwithiga, G. and Sifuna, M.M., 2006. Effect of moisture content on the physical properties of three varieties of sorghum seeds. Journal of Food Engineering 75: 480–486

[136]   Kilickan, A., Üçer, N., and Yalçin, I. (2010). Some physical properties of spinach (Spinacia oleracea L.) seed. African Journal of Biotechnology, 9(5), 648–655. https://doi.org/10.5897/AJB09.1616.

[137]   Chowdhury, M.M.I.; Sarker, R.I.; Bala, B.K.; Hossain, M.A. (2001). Physical Properties of Gram as a Function of Moisture Content. Int. J. Food Proper., 4, 297–310.

[138]   Konak, M, Çarman K, Aydin C. (2002). Physical Properties of Chickpea Grains. Biosystems Engineering, 82(1): 73–78.

[139]   Aviara, N. A., Ibrahim, E. B. and Onuoha, L. N. (2014) 'Physical properties of Brachystegia Eurycoma seeds as affected by moisture content', International Journal of Agricultural and Biological Engineering, 7(1), pp. 84–93. doi: 10.3965/j.ijabe.20140701.010.

[140]   Obi, O. F., Ijere, N. C., and Okechukwu, M. E. (2018). Determination of physical and aerodynamic characteristics of African olive (Canarium Schweinfurthii) nut. Agricultural Engineering International: CIGR Journal, 20(3), 172–179.

[141]   Mansouri, A., Mirzabe, A. H., and Ráufi, A. (2017). Physical properties and mathematical modeling of melon (Cucumis melo L.) seeds and kernels. Journal of the Saudi Society of Agricultural Sciences, 16(3), 218–226. https://doi.org/10.1016/j.jssas.2015.07.001

[142]   Mirzabe, A. H., Kakolaki, M. B., Abouali, B., and Sadin, R. (2017). Eval– uation of some physical properties of cucumber (Cucumis sativus L.) seeds and kernels based on image processing. Information Processing in Agriculture, 4,300–315. https://doi.org/10.1016/j. inpa.2017.07.001

[143]   Tabatabaeefar, A. (2003). Moisture dependent physical property of wheat. International Agro Physics, 17(4), 207–212.

[144]   Mirzabe, A. H., Khazaei, J., Chegini, G. R., andGholami, O. (2013). Some physical properties of almond nut and kernel and modeling dimensional properties. Agricultural Engineering International: CIGR Journal, 15(2), 256–265.

[145]   Khodabakhshian, R., Emadi, B. and Abbaspour Fard, M. H. (2010). Gravimetrical properties of sunflower seeds and kernels. World Applied Sciences Journal 8(1): 119–128

[146]   Gezer, I; Haciseferogullari, H; Demir, F. (2002). Some physical properties of hacihaliloglu apricot pit and its kernel. Journal of Food Engineering, 56, 49–57.

[147]   Unal R, Dean EB. Taguchi approach to design optimization for quality and cost: an overview. In: Proceedings of the International Society of Parametric Analyst 13th Annual, May 21–24; 1991.

[148]   M.S. Phadke, Quality Engineering Using Robust Design, Prentice-Hall, New Jersey, 1989

[149]   Ross PJ (1988) Taguchi technique for quality engineering. McGraw-Hill Book Company, New York, pp 45–48

[150]   A. Kaphle, P. Hari, Enhancement in power conversion efficiency of silicon solar cells with cobalt doped ZnO nanoparticle thin film layers, Thin Solid Films 657 (2018) 76–87, https://doi.org/10.1016/j.tsf.2018.05.014.

[151]   Z.L. Tseng, C.H. Chiang, C.G. Wu, Surface engineering of ZnO thin film for high efficiency planar perovskite solar cells, Sci. Rep. 5 (2015) 13211, https://doi.org/ 10.1038/srep13211.

[152]   Y. Liu, J. Zhu, L. Cai, Z. Yao, C. Duan, Z. Zhao, C. Zhao, W. Mai, Solution-processed high-quality Cu2O thin films as hole transport layers for pushing the conversion efficiency limit of Cu2O/Si heterojunction solar cells, Sol. RRL. 4 (2020) 1–8, https://doi.org/10.1002/solr.201900339.

[153]   J.H. Lee, Y.W. Noh, I.S. Jin, S.H. Park, J.W. Jung, Facile surface engineering of nickel oxide thin film for enhanced power conversion efficiency of planar heterojunction perovskite solar cells, ACS Sustain. Chem. Eng. 7 (2019) 15495–15503, https://doi.org/10.1021/acssuschemeng.9b03148.

[154]   G. Shen, H. Dong, Q. Cai, X. Wen, X. Xu, C. Mu, A facile route for preparing nickel (ii) oxide thin films for high-performance inverted perovskite solar cells, Sustain. Energy Fuels 4 (2020) 3597–3603, https://doi.org/10.1039/d0se00200c.

[155]   P. Sawicka-Chudy, M. Sibiński, E. Rybak-Wilusz, M. Cholewa, G. Wisz, R. Yavorskyi, Review of the development of copper oxides with titanium dioxide thin-film solar cells, AIP Adv. 10 (2020), 010701, https://doi.org/10.1063/ 1.5125433

[156]   Štreimikienė, D. (2013). Assessment of Energy Technologies In Electricity And Transport Sectors Based On Carbon Intensity And Costs. Technological and Economic Development of Economy, 19(4), 606–620. doi:10.3846/20294913.2013.837113

[157]   Z. Yue, A method for group decision-making based on determining weights of decision makers using TOPSIS, Applied Mathematical Modelling 35(4) (2011) 1926–1936.

[158]   M. Ravanshadnia, H. Rajaie, Semi-ideal bidding via a fuzzy TOPSIS project evaluation framework in risky environments, Journal of Civil Engineering and Management 19 (Supplement 1) (2013) S106–S115.

[159]   M. Li, L. Jin and J. Wang, A new MCDM method combining QFD with TOPSIS for knowledge management system selection from the user's perspective in intuitionistic fuzzy environment, Applied Soft Computing 21 (2014) 28–37.

[160]   H. Samadi, S. Nazari-Shirkouhi and A. Keramati, Identifying and analyzing risks and responses for risk management in information technology outsourcing projects under fuzzy environment, International Journal of Information Technology&Decision Making 13(6) (2014) 1283–1323